The Dissertation Committee for Andrew Timothy Nelson Certifies that this is the approved version of the following Dissertation:

Synthesis, SAR Library, and Chemical Biology Probes of PAHSAs, a Family of Natural Product Lipids with Anti-Diabetic Activity

Committee:

Jennifer S. Brodbelt, Supervisor

Dionicio R. Siegel, Co-Supervisor

Eric V. Anslyn

Hung-Wen Liu

Synthesis, SAR Library, and Chemical Biology Probes of PAHSAs, a Family of Natural Product Lipids with Anti-Diabetic Activity

by

Andrew Timothy Nelson

Dissertation

Presented to the Faculty of the Graduate School of

The University of Texas at Austin

in Partial Fulfillment

of the Requirements

for the Degree of

Doctor of Philosophy

The University of Texas at Austin

August 2018

Abstract

Synthesis, SAR Library, and Chemical Biology Probes of PAHSAs, a Family of Natural Product Lipids with Anti-Diabetic Activity

Andrew Timothy Nelson, PhD

The University of Texas at Austin, 2018

Supervisor: Jennifer S. Brodbelt

Co-Supervisor: Dionicio R. Siegel

Nearly one in ten Americans has type 2 diabetes mellitus (T2DM), a major source of morbidity, mortality, and healthcare costs. Most patients with diabetes are treated with medicines which may have adverse side effects. The prevalence of this disease necessitates the addition of new, safer compounds to the anti-diabetic arsenal. The recently reported Fatty Acid esters of Hydroxy Fatty Acids (FAHFAs) included eight Palmitic Acid esters of Hydroxy Stearic Acid (PAHSA) regioisomers, which may provide a new avenue for treatment of T2DM. In particular, 5- and 9-PAHSA increased insulin secretion, improved blood sugar, and decreased adipose tissue inflammation in diabetic mice. While this activity is encouraging, much remains unknown about PAHSAs, including the influence of chemical connectivity on their activity. Furthermore, the molecular targets of PAHSAs have not been fully elucidated. Until these questions are answered, there can be no hope of treating T2DM with an optimized PAHSA analog, nor means to rationally upregulate *de novo* PAHSA synthesis. This resulted in a scalable total synthesis of racemic 5- and 9-PAHSA, both enantiomers of 9-PAHSA, and preparation of a 30 membered library of

PAHSA analogs to probe structure activity relationships. Furthermore, 6 chemical biology probes have been prepared to determine in an unbiased manner the molecular targets of PAHSAs and their metabolism.

Table of Contents

List of Tables

List of Figures

Chapter 1: Type 2 Diabetes in the United States and Fatty Acid-Hydroxy Fatty Acids (FAHFAs), a Novel Family of Anti-Diabetic Lipids

1. Type 2 Diabetes in the United States of America

1.1 Epidemiology and Economics

In the United States type 2 diabetes mellitus (T2DM) is a common and costly disease. 9.3% of Americans are afflicted with this malady and the prevalence is rising.[1] In 2017, T2DM accounted for $327 billion dollars in health care expenditures in the US, or 25% of all health care costs.[2] Far greater than the financial burden of T2DM is the human toll.

1.2 Mortality and Morbidity

A diagnosis of T2DM is associated with a loss of life at all ages, with an earlier age of onset resulting in more life-years lost; those diagnosed with T2D at age 20 are anticipated to lose 20 years from their lifespan while those diagnosed at 60 are expected to give up the ghost 4.5 years prematurely.[3]

In addition to the loss of life, T2DM is a significant cause of morbidity in the US, where it is the leading cause of kidney failure, extremity amputation, and adult blindness.[1] T2DM also increases the likelihood of heart attack and stroke.[4] Furthermore, elderly patients diagnosed with T2DM have a significantly greater risk of cognitive decline compared with their non-diabetic counterparts.[5]

All of these medical problems stem from the damage to blood vessels caused by chronically elevated blood sugar. However, maintenance of normal blood glucose will be discussed before the pathophysiology of T2DM.

1.3 Glucose Homeostasis

Normal blood glucose levels range between 70 to 120 mg/dL and it is vital to maintain blood sugar within this range.[6] Low blood sugar (hypoglycemia) results in neurological deficits and, ultimately, death due to the reliance of the central nervous system on glucose as an energy source.[6] Though lacking in dentition, the brain has a "sweet tooth;" the brain is only 2% of the human body mass, yet consumes 20% of the glucose.[7]

Blood glucose declines as a result of normal activity, so something must be done to replenish the body's sugar supply. As humans lack the enzymatic machinery to photosynthesize carbohydrates, neuroregulatory signals drive the individual to eat.[6]

The consumption, digestion, and absorption of carbohydrates has been well studied.[8] Much of the dietary glucose in carbohydrate-rich food is tied up as the dimer (maltose), trimer (maltotriose), oligosaccharides, a straight-chain polymer (amylose), or a branched-chain polymer (amylopectin). The latter two are commonly referred to as starch.

After consumption, the above-mentioned di-, tri-, oligo-, and poly-saccharides must be broken down to individual glucose monomers to be absorbed. The enzymes responsible for the complete hydrolysis of polysaccharides to glucose include salivary amylase and pancreatic amylase, glucoamylase, isomaltase, and sucrase. Once liberated, glucose monomers are transferred from the lumen of the gut into the enterocytes of the small intestine by the sodium-glucose co-tranporter 1 (SGLT1). Glucose then exits from the enterocytes into the bloodstream by way of the glucose transporter 2 (GLUT2), leading to an increase in blood glucose.

Insulin is required to return blood sugar to normal levels and there are three primary mechanisms leading to increased release of insulin from the pancreas into the blood.

First, glucose itself may stimulate insulin release. Glucose exits the circulation into the β-cells of the pancreas through GLUT2. The increase in cytosolic glucose initiates a

cascade of cellular events, ultimately leading to depolarization of the β-cells and exocytosis of insulin into the bloodstream.[9]

Second, glucose-dependent insulinotropic polypeptide (GIP) also stimulates insulin secretion by the pancreas.[10-12] As its name suggests, GIP is a polypeptide hormone. After eating, a high osmolarity of glucose in the duodenum of the small intestine causes K cells in the duodenum and jejunum to release GIP into the general circulation. The GIP receptor is a seven-transmembrane-spanning receptor protein located on β-cells of the pancreas. Docking of GIP in its receptor ultimately leads to increased insulin secretion.

Third, glucagon-like peptide-1 (GLP1) also promotes insulin secretion.[10, 11] In response to a meal, L-cells in the ileum of the small intestine and the large intestine secrete the peptide GLP-1 into the serum. The GLP-1 receptor is also located on the surface of pancreatic β-cells and the ligand/receptor interaction augments release of insulin.

GIP and GLP-1 are known as incretins and have a number of shared characteristics. Both are released by enteroendocrine cells in the gut, increase insulin secretion, and are polypeptides. GIP and GLP-1 are also both rapidly degraded by dipeptidyl peptidase-4 (DPP4). This physiology will be revisited while discussing T2DM treatment.

To recapitulate, consumption of dietary carbohydrates leads to elevated serum glucose levels and the release of insulin from β-cells of the pancreas by glucose itself and the incretins GIP and GLP-1.

Circulating insulin helps return elevated blood glucose to normal levels by acting on the insulin receptor, which is abundant on the surface of fat, muscle, and liver. After insulin docks in its insulin receptor, a series of cellular events results in the translocation of glucose transporter 4 (GLUT4) from vesicles within the cell to the surface of the cellular membrane, permitting glucose to flow down its concentration gradient into the cell while concomitantly lowering serum glucose levels.[13]

The importance of adipose GLUT4 in glucose homeostasis cannot be overemphasized.[14] GLUT4 is downregulated in the fat of overweight and/or diabetic humans.[15, 16] Furthermore, studies with genetically modified mice showed that knocking out GLUT4 specifically in fat cells was sufficient to induce insulin resistance, both in the organism and liver and muscle tissues.[17] On the other hand, mice with adipocyte specific GLUT4 overexpression (AG4OX mice), are protected from diabetes and will be discussed further later.

In summary, to return elevated blood glucose levels to their normal range, there are two critical steps: release of insulin by the β-cells of the pancreas and uptake of glucose by peripheral tissues like muscle and fat, which make up two-thirds of the body mass.[9] The two hallmarks of T2DM, and the cause of chronic hyperglycemia, are dysfunction of pancreatic β-cells and a dampened response to insulin in the periphery.[6, 9]

1.4 T2DM Pathophysiology

The single greatest risk factor in T2DM is obesity; over 80% of individuals diagnosed with T2DM have a body mass index (BMI) in excess of 30.[9] Increase in body weight is associated with increased serum free fatty acids,[18] a state of low grade inflammation,[19] and oxidative stress.[20] Free fatty acids,[21, 22] inflammation,[23, 24] and oxidative stress[25, 26] all contribute to peripheral insulin resistance and impaired insulin secretion by β-cells. This dual-edged sword of diminished insulin secretion and decreased insulin uptake by fat and muscle leads to higher concentrations of sugar in the blood. Two of the most well understood mechanisms of hyperglycemia induced angiopathy include advanced glycation end products (AGE)[27] and activation of protein kinase C (PKC).[28]

AGEs are formed non-enzymatically when sugars or their degradation products form covalent bonds to proteins.[27] Mechanistically, this starts when the aldehyde of glucose

1 forms a Schiff base **2** with the terminal amino group of a peptide, or with the free amine group of an internal lysine. (Figure 1) Tautomerization of **2** gives enol-enamine **3**, which may tautomerize back to the starting material **2** or irreversibly form the AGE aminoketone **4** by the Amadori rearrangement. AGEs like **4** then stimulate the receptor of advanced glycation end products (RAGE), which leads to the release of cytokines, reactive oxygen species, and growth factors vascular endothelial growth factor (VEGF) and transforming growth factor β (TGFβ), ultimately causing the vascular damage responsible for the end organ damage in T2DM.

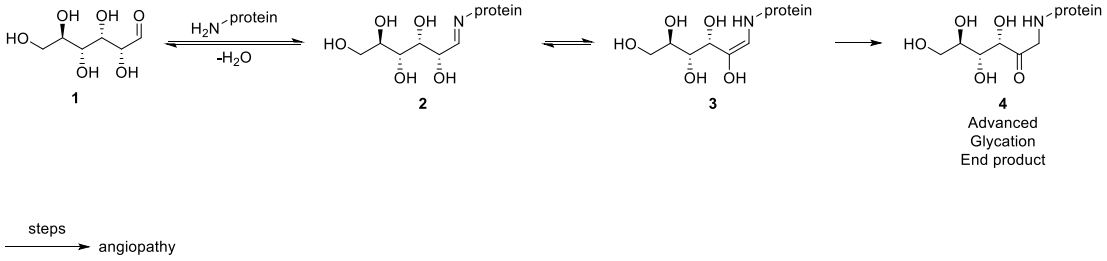

Figure 1. Formation of advanced glycation end products from glucose

Another mechanism whereby hyperglycemia results in vascular damage is the activation of PKC by the secondary messenger diacylglycerol (DAG)[28] **8**. According to this model, excess glucose in the cell is converted by glycolysis to acetyl CoA **5**, which is used as the feedstock to synthesize fatty acids **6**. The latter are appended to glycerol-3-phosphate **7**, another product of glucose metabolism, yielding DAG **8** after loss of phosphate. DAG then activates PKC, which, like AGE and RAGE, leads to an increase in the production of VEGF and TGFβ. In addition, protein plasminogen activator inhibitor-1 (PAI-1) is also synthesized. These factors ultimately lead to blood vessel destruction and the comorbidities commonly observed in patients with T2DM.

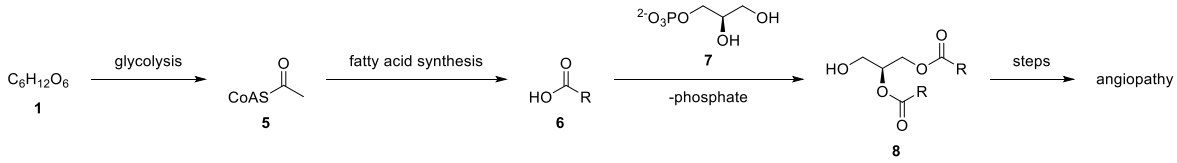

Figure 2. Conversion of glucose to DAG, a potent activator of PKC.

1.5 T2DM Treatment

Lifestyle changes (exercise, diet, and weight loss) are recommended for patients newly diagnosed with T2DM. Most patients, however, will ultimately need multi-drug therapy.[29] Unfortunately, many anti-diabetic drugs have adverse side effects. As mentioned above, GLP-1 augments insulin secretion and DPP4 degrades GLP-1, suggesting that GLP-1 agonists and DPP4 inhibitors would be viable pharmacological targets. The FDA has approved a number GLP-1 agonists and DPP4 inhibitors; unfortunately, the drugs in these two classes have been linked to an increased risk of acute pancreatitis.[30, 31] Thiazoladinediones, another class of medicine used to treat T2DM, have been associated with cardiovascular risks.[32, 33] These adverse effects underscore the need to develop novel agents for the treatment of T2DM. Luckily, a new family of lipids with anti-diabetic activity has recently been discovered and they are called Fatty Acid-Hydroxy Fatty Acids (FAHFAs).[34]

2. FAHFAs

2.1 Foundation

The groundwork for the discovery of FAHFAs was laid over 20 years before the initial report on FAHFAs was released in October of 2014. In 1993 the Kahn lab[35] selectively overexpressed the GLUT4 receptor in murine adipocytes. Phenotypically, these Adipocyte specific Glucose transporter OverExpresser (AG4OX) mice were overweight

with a 2-3-fold increase in body lipid, but the same amount of body protein compared to their wild type (WT) counterparts. Most notably, these overweight AG4OX mice showed improved glucose tolerance, with basal (ie, without insulin) glucose transport increased 20-34-fold and insulin-stimulated glucose transport increased 2-4 fold compared to WT. Mechanistically, the improved glucose tolerance and glucose uptake in AG4OX mice was attributed to the 6-9-fold increase in the GLUT4 receptor in white adipose tissue (WAT) and a 3-5-fold increase in the GLUT4 receptor in brown adipose tissue (BAT). An overweight mouse with improved glucose tolerance was an incredible finding as elevated body weight is normally correlated with increased risk of T2DM in humans; 80% of individuals diagnosed with T2DM are obese.

In 1995 the Kahn lab[36] built on the previous report and used a radioactive uniformly labelled 14C-glucose tracer to follow how glucose was being used in AG4OX mice. Surprisingly, a comparison between AG4OX adipocytes and WT adipocytes revealed that *de novo* fatty acid synthesis is markedly elevated in AG4OX adipocytes; fatty acid synthesis was increased 31-fold in absence of insulin and 21-fold in the presence of insulin in AG4OX fat cells, compared to their wild type counterparts. This raises an interesting question: is there a difference in the composition of the lipids that makes these fat, overweight mice healthier?

2.2 FAHFA Discovery

Working in collaboration, the Kahn and Saghatelian labs[34] employed an untargeted lipidomic screen, comparing lipids in AG4OX and WT mice. This anylysis revealed the presence of a new family of lipids that were elevated 16-18-fold in AG4OX compared to WT mice. Further analysis resulted in the discovery that these lipids were fatty acids (FAs) condensed to the secondary alcohol of hydroxyfatty acids (HFAs) via an ester linkage.

Thus, these new lipids were dubbed FAHFAs. For example (Figure 3), oleic acid (OA) **9** condenses with 5-hydroxypalmitic acid (5-HPA) **10** to yield 5-oleic acid-hydoxypalmitic acid (5-OAHPA) **11**. While 5-oleic acid-hydroxypalmitic acid is not true to IUPACs "5-(oleolyoxy)hexadecenoic acid," we feel the nomenclature proposed by the authors is clearer.

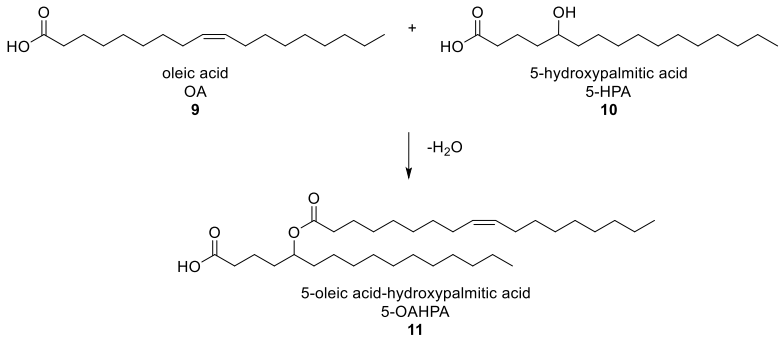

Figure 3. Synthesis of 5-oleic acid-hydroxypalmitic acid from oleic acid and 5-hydroxypalmitic acid.

In the initial report, 16 families were discovered: palmitic acid (PA), palmitoleic acid (PO), stearic acid (SA), and oleic acid (OA) crossed with hydroxypalmitic acid (HPA), hydroxypalmitoleic acid (HPO), hydroxystearic acid (HSA), and hydroxyoleic acid (HOA) in all possible combinations. (Table 1)

	HPA	HPO	HSA	HOA
PA	PAHPA	PAHPO	PAHSA	PAHOA
PO	POHPA	POHPO	POHSA	POHOA
SA	SAHPA	SAHPO	SAHSA	SAHOA
OA	OAHPA	OAHPO	OAHSA	OAHOA

Table 1. The 16 FAHFA Families Discovered by Yore *et al*.

Of the sixteen families, palmitic acid-hydroxystearic acids (PAHSAs) were the most upregulated in the adipose tissue of AG4OX mice. Yore *et al* found that the PAHSA family included 8 regioisomers, with the ester located at carbon 5, 7, 8, 9, 10, 11, 12, and 13). (A subsequent study by Kuda and co-workers found 6-PAHSA, increasing the number to 9 regioisomers). Of the PAHSA regioisomers, 5- and 9-PAHSA stood out as 5-PAHSA **12** was the regioisomer most downregulated in the serum and fat of insulin resistant mice while 9-PAHSA **13** was the most upregulated in AG4OX mice (Figure 4).

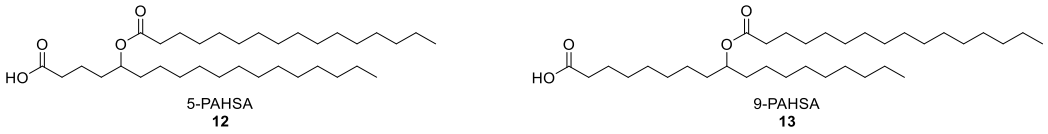

Figure 4. 5- and 9-PAHSA, the most notable PAHSA regioisomers with the greatest change in concentration.

In mice, acute gavage with 5- and 9-PAHSA gavage led to increased serum concentration, improved glycemia, improved glucose tolerance, increased GLP-1 secretion, increased insulin, and decreased inflammation.

In vitro studies with human pancreatic β-cells showed that PAHSAs augmented insulin secretion, while PAHSA treated stc-1 enteroendocrine cells increased glp-1 secretion in a dose dependent manner. Furthermore, PAHSA treatment increased 3T3-L1 adipocyte specific insulin-stimulated glucose transport by enhancing GLUT4 translocation. It is noteworthy that neither palmitic acid, nor 9-HSA showed this activity. Mechanistically, gpr120 (aka free fatty acid receptor 4, FFAR4) was determined to be the target of PAHSAs, with both 5- and 9-PAHSA activating gpr120 in a dose-dependent manner. Previous work by Oh and co-workers showed that gpr120 stimulation increases GLUT4 translocation.

Most importantly, PAHSAs were found in humans and that serum and fat concentration were higher in insulin sensitive individuals than in their insulin resistant counterparts. These data suggest that PAHSAs play an important role in human glucose homeostasis. It is also noteworthy that Yore *et al* also found FAHFAs in food.

2.3 Developments Since the Initial Report

Since the initial FAHFA report in 2014, a number of monographs have appeared, expanding the FAHFA literature. This work may be divided into 5 fields: 1) FAHFAs and inflammation, 2) FAHFA hydrolases, 3) FAHFAs in unexpected places, 4) FAHFA analysis, and 5) FAHFA synthesis (the subject of chapter 2),

2.3.1 FAHFAs and Inflammation

As mentioned above, the anti-inflammatory activity is of particular importance as the development of insulin resistance and T2DM are associated with chronic low grade inflmmation. Since the initial findings by Yore *et al*, two groups have shared additional reports on the anti-inflammatory activity of FAHFAs.

Lee and co-workers[37] explored the utility of PAHSAs in a murine model of ulcerative colitis (UC). UC is a chronic colonic inflammatory condition and is commonly modeled in mice with dextran sulfate sodium (DSS). In their study, Lee *et al* found that pretreatment with a combination of 5- and 9-PAHSA followed by the DSS insult decreased weight loss and improved colitis score when compared to mice treated with vehicle. Furthermore, they observed in the PAHSA treatment group a dampening of T cell activation and a decrease in pro-inflammatory cytokines and chemokines compared with the control group. Mechanistically, they concluded that gpr120 was partially responsible

for these effects, further supporting the conclusions Yore *et al* drew with respect to gpr120 functioning as a FAHFA target.

Subsequently, Kuda *et* al[38] discovered a new FAHFA, 13-docosahexaenoic acid-hydroxylinoleic acid (13-DHAHLA) **14**, with more potent anti-inflammatory activity than 9-PAHSA in a LPS-stimulated RAW264.7 macrophage model. In addition to 13-DHAHLA, the group also found two additional new FAHFAs, 9-DHAHLA **15** and 14-docosohexaenoic acid-hydroxydocosohexaenoic acid (14-DHADHA) **16**, in the serum and fat of humans and mice that received supplemental DHA and eicocospentaenoic acid (EPA). (Figure 5) Surprisingly, no FAHFAs with EPA, nor HEPA were disclosed.

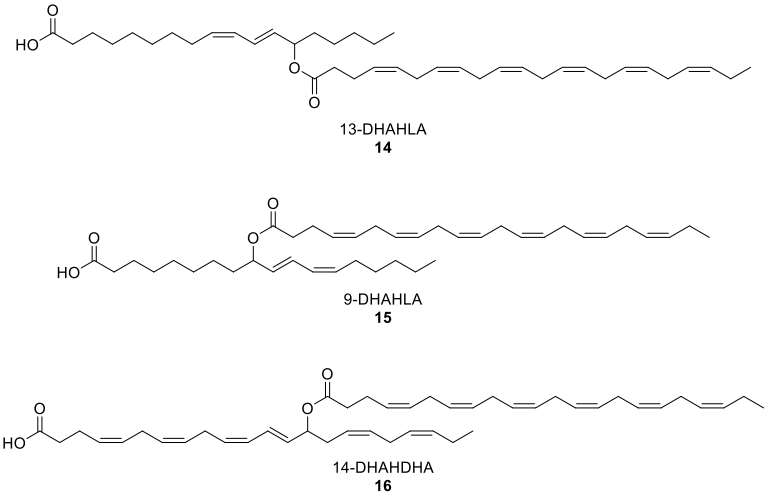

Figure 5. Three new FAHFAs found in mice and humans who received supplemental DHA an EPA.

2.3.2 FAHFA Hydrolases

In the years following the discovery, little has been learned about FAHFA metabolism. A specific enzyme responsible for the acylation of HFAs remains elusive, but three FAHFA hydrolases have been reported.

Parsons and co-workers[39] used activity-based protein profiling (ABPP) to discover the first two FAHFA specific hydrolazes. Pulldown experiments and proteomic analysis identified androgen-induced gene 1 protein (AIG1) and androgen-dependent TFPI-regulating protein (ADTRP) as potential FAHFA hydrolases. The Saghatelian and Cravatt labs found that AIG1 and ADTRP were threonine hydrolases that preferentially targeted the ester bond of FAHFAs. Mutation studies proved the key residues were thr48/his134 and thr47/his131 for AIG1 and ADTRP, respectively. The hydrolytic activity of the two enzymes was tested against a broad lipid library that included FAHFAs (5-, 9-, and 12-PAHSA; 5-, 9-, 12-, and 13-POHSA; 5-, 9-, 12-, and 13-SAHSA; and 5-, 9-, 12-, and 13-OAHSA), triacylglycerol, diacylglycerol, monoacylglycerol, cholesterol ester, phoshatidylserine, phosphatidylcholine, phosphatidylethanolamine, phosphatidylinositiol, phosphatidylglycerol, phosphatidic acid, and lysophospholipids. AIG1 and ADTRP selectively hydrolyzed FAHFA over other members of the library; furthermore, the rate of FAHFA hydrolysis was regioselective with the hydrolysis rate increasing as the ester position was located further from the carboxylic acid head of the FAHFA.

Later in 2016, Kolar and co-workers[40] discovered a 3rd FAHFA-specific hydrolase, carboxyl ester lipase (CEL). In contrast with the previous report on AIG1 and ADTRP, which used ABPP to find the enzymes of interest, Kolar and colleagues investigated tissue lysates (pancreas, spleen, brain, kidney, liver, brown adipose tissue, perigonadal white adipose tissue, and subcutaneous white adipose tissue) for their ability to hydrolyze 9-PAHSA. Pancreatic tissue was by far the most active, with the rate of hydrolysis over an order of magnitude higher than the next most active tissue screened. The pancreatic proteome was then divided into membrane and soluble fractions, with the membrane portion containing most of the hydrolytic activity. Screening the pancreatic membrane with inhibitors suggested that the enzyme of interest was a serine hydrolase, narrowing the likely

targets to CEL, pancreatic lipase (PNLIP), and pancreatic lipase-related protein 2 (PNLIPRP2). Sodium taurocholate augments the hydrolytic activity of CEL while dampening the activity of PNLIP and PNLIPRP2. Addition of sodium taurocholate to the pancreatic membrane fraction increased the rate with which 9-PAHSA was hydrolyzed, confirming that CEL was the culprit. HEK293T cells were transfected with CEL and the cell lysate was screened for hydrolytic activity with the same 31 compound lipid library that was used with AIG1 and ADTRP. Surprisingly, CEL hydrolyzed FAHFAs at nearly double the rate of AIG1 or ADTRP and with the same regioselective preference for FAHFAs with the ester bond further from the carboxylic acid. Humans with maternity-onset diabetes of the young type 8 (MODY8) are known to have a mutated CEL enzyme and the MODY8 varient of CEL was twice as active as the human wild type variant. The influence the MODY8 CEL variant has on patient FAHFA levels merits further exploration.

2.3.3 FAHFAs in unexpected places

Yore *et al* first found FAHFAs in mice and men. Subsequent studies have found FAHFA in marsupials, microbes, and milk. Two groups have even found FAHFAs incorporated into triacylglycerols (TAGs).

McLean and co-workers[41] were the first to observe FAHFAs in TAGs. While analyzing the lipid content of the paracloacal glands of the brushtail possum, a marsupial native to Australia, they found 150 TAG-FAHFAs. The other acyl groups appended to the glycerol backbone were medium chain fatty acids (C7 to C9) while the FAHFA moiety contained between 33-36 carbons and 2-3 degrees of saturation. Position of the FAHFA ester and olefins was not discussed, nor the position of the acyl groups on the glyceride backbone. It is noteworthy that other fat depots in the abdomen and around the kidney had

a lipid distribution similar to mammals and did not include any TAG-FAHFAs. The authors suspected that these different lipids stored in the paracloacal glands function as a semiochemicals, permitting olfactory communication between animals.

Subsequently, Kajikawa and colleagues[42] of the Fukuzawa lab found FAHFA TAGs in a genetically modified strain of the microalgal diatom *Chatoceros gracilis*. The Fukuzawa lab was attempting to synthesize the industrially important hydroxyfatty acid ricinoleic acid in a carbon neutral manner. To achieve this end, they introduced the gene fatty acid hydratase (FAH) from the fungus *Claviceps purpurea* into the diatom *C. gracilis*. FAH is the enzyme that converts oleic acid to ricinoleic acid via a homoallylic oxidation at C12. Under photosynthetic, chemoautotrophic conditions, up to 11% of the lipid content of genetically modified *C gracilis* contained ricinoleic acid. 70% of the ricinoleic acid were FAHFA triglycerides, either as ricinoleic acid-hydroxyoleic acid (RAHOA) TAG **17**, with a free-hydroxyl group, or PAHOA, or POHOA **18**. (Figure 6) The FAHFAs were located uniquely at the C1/3 position of the triglyceride backbone with myristic acid, PA, or PO at the other two positions of glycerol.

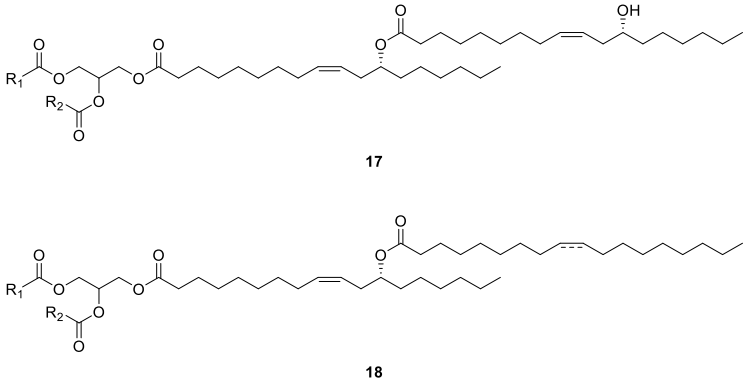

Figure 6. Two types of FAHFA TAGs discovered in a genetically modified strain of *C gracilis.*

Most interestingly, FAHFAs were found in human milk. In 2018, Brezinova and coworkers[43] investigated breast milk for the presence of FAHFAs. The first sample was acquired at 72 hours after birth and FAHFAs were still present 9 months after birth. All known FAHFAs were present, with a markedly higher concentrations of 5-PAHSA in milk compared to 5-PAHSA levels previously observed in sera and other tissues. Surprisingly, total PAHSA levels and 5-PAHSA levels were higher in the breast milk of lean mothers than in obese mothers. Furthermore, chiral chromatography revealed that R-5-PAHSA was the major enantiomer, which is consistent with our findings that R-9-PAHSA was the major enantiomer in AG4OX mice.[44] It was also noteworthy that they observed 13-DHAHLA in a mother who was taking omega-3 fatty acid supplements. Brezinova and colleagues supported their human studies with mouse work. Murine milk also contained elevated 5 PAHSA concentrations compared to other tissues and serum. Furthermore, gavage with 5 PAHSA at increasing doses (5, 10, 20 mg/kg) led to proportional increases in serum levels, suggesting that 5-PAHSA is absorbed from the GI tract into the serum of the newborn. The role 5-PAHSA plays in the development of the newborn remains to be determined.

2.3.4 FAHFA Analysis

While the original LC-MS method allowed for the discovery of FAHFAs, there have been some important contributions in FAHFA analysis, permitting automatic annotation, quicker run time, and heightened sensitivity.

Ma and colleagues[45] developed a freely available, *in silico* MS/MS library, allowing for rapid, automatic annotation. Their library contained predicted fragmentation for over 1,000 possible FAHFAs. Furthermore, they validated their method by applying it to a complex mixture of lipids extracted from egg yolk, where they discovered 4 new FAHFA oleaic acid-hydroxy linoleic acid (OAHLA), linoleic acid-hydroxyoleic acid (LAHOA),

linoleic acid-hydroxylinoleic acid (LAHLA), and alpha-linolenic acid-hydroxyoleic acid (ALAHOA), though the regioisomers were not specified.

López-Bascón and coworkers[46] contributed an automated workflow for automated solid phase extraction (SPE) and LC-MS analysis of FAHFA levels in serum. In addition to the convenience of automation, their method also cut down the time to only 25 minutes per sample, with 20 minutes for analysis and 5 minutes to re-equilibrate the column between injections. While this seems to be an advantage over the 90-minute run time described by Zhang *et al*,[47] the Lopez-Bascon separates FAHFA families, but not regioisomers. Their analysis showed that FAHFA family serum concentrations vary based on BMI and glycemic state; normoglycemic individuals had higher POHPO levels than their prediabetic counterparts and diabetics had higher PAHPA concentrations than their prediabetic counterparts; POHPA levels were elevated in normal weight individuals than in those who were overweight.

Zhu *et al*[48] combined strong anion exchange-solid phase extraction with chemical labelling and ultra high performance liquid chromatography/mass spectrometry to give the lengthy acronym SAX-SPE-CL-UHPLC/MS. Impressively, chemical labelling of FAHFAs **19** with 2-dimethylaminoethylamine **20** and 2-chloromethylpyridinium iodide **21** gave the corresponding amide **22** with 10- to 100-fold in detection sensitivity by MS. (Figure 7)

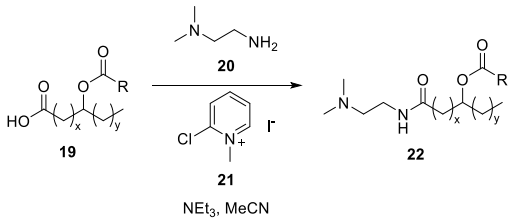

Figure 7. Zhu and colleagues chemical labelling of FAHFAs for improved MS sensitivity.

This is a major improvement for a class of molecules that are present at low concentrations in serum and tissue. It is also noteworthy that their chromatographic method allowed for separation of regioisomers in only 20 minutes. With this method in hand, they discovered that 9- and 13-PAHSA and 12- and 13-SAHSA were decreased in the serum of breast cancer patients compared to healthy controls. This raises interesting questions about a potential link between FAHFAs and cancer.

Chapter 2: PAHSA and SAR Library Synthesis*

2.1 FAHFA Prior Syntheses

When we initiated our FAHFA research program, there were only two reported synthetic routes to FAHFAs. The Yore[34] synthesis of 5-PAHSA **12** began with the addition of pent-4-en-1-ylmagnesium bromide **24** to tetradecanal **23**, providing olefin-alcohol **25**. The secondary alcohol of **25** was acylated with palmitic anhydride, affording olefin-ester **26**. The synthesis concluded with an ozonolyis and Pinnick oxidation to yield 5-PAHSA **12**. Drawbacks to this route include the modest overall yield, the expensive aldehyde starting material, and poor atom economy in the acylation step. Furthermore, the experimental was poorly written, with identical characterization data for different compounds (**12** and **26**) and the oxidant in the Pinnick oxidation written as sodium hypochlorite (NaOCl), rather than sodium chlorite ($NaClO_2$)

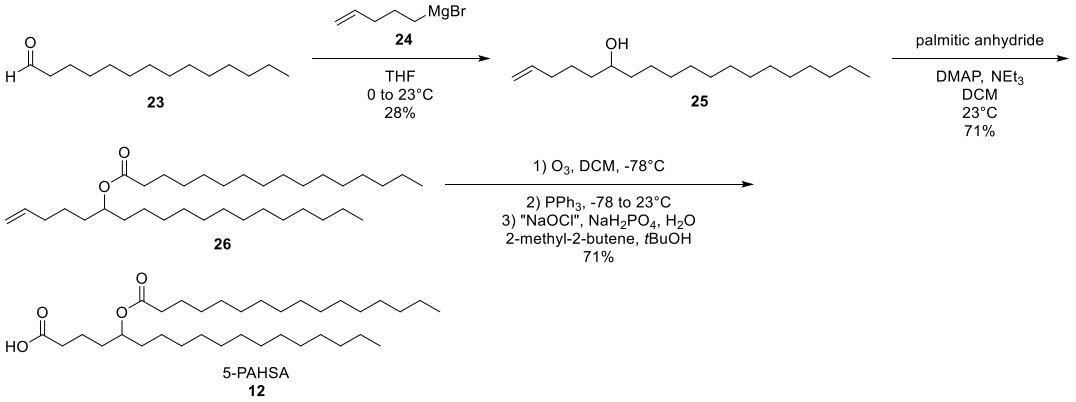

Figure 8. Synthesis of 5-PAHSA originally reported by Yore and co-workers.

* Some of the contents of this chapter was based on Nelson, A.T.; Kolar, M.J.; Chu, Q.; Syed, I.; Kahn, B.B.; Saghatelian, A.; Siegel, D. Stereochemistry of Endogenous Palmitic Acid Ester of 9-Hydroxystearic Acid and Relevance of Absolute Configuration to Regulation. *J. Am. Chem. Soc.* **2017**, *139*, 4943-4947. Nelson and Kolar contributed equally to this work. Nelson developed the hypothesis for the project, planned and executed the synthesis, characterized all compounds, and co-wrote the manuscript.

The other previously described FAHFA synthesis was in a 2015 patent.[49] (Figure 9) In the first step nonane-1,9-diol **27** was monoprotected as THP ether **28** with PPTS and THP. The primary alcohol of **28** was oxidized with PCC to aldehyde **29**. Addition of nonylmagnesium bromide to the aldehyde of **29** gave secondary alcohol **30**, which was acylated with acetic anhydride, giving THP-acetate **31**. Doubly protected **31** was converted to 9-HSA **35** by a four step sequence involving removal of the THP group with PPTS and ethanol, oxidation of the primary alcohol **32** to the aldehyde **33** with PCC, then oxidation of the aldehyde to the carboxylic acid **34** under Pinnick's condition, and, finally, cleavage of the acetate of **34** with lithium hydroxide, yielding 9-HSA **35**. The carboxylic acid of 9-HSA **35** was protected with alpha-bromoketone **36** and dicyclohexylamine, yielding ester-alcohol **37**. The secondary alcohol of **37** was acylated with palmitoyl chloride and DMAP; subsequent chemoselective ester cleavage with zinc and acetic acid gave 9-PAHSA **13**. The synthesis suffers from a high step count, low yield (<1 %), multiple protecting group manipulations, and stoichiometric chromium in two steps.

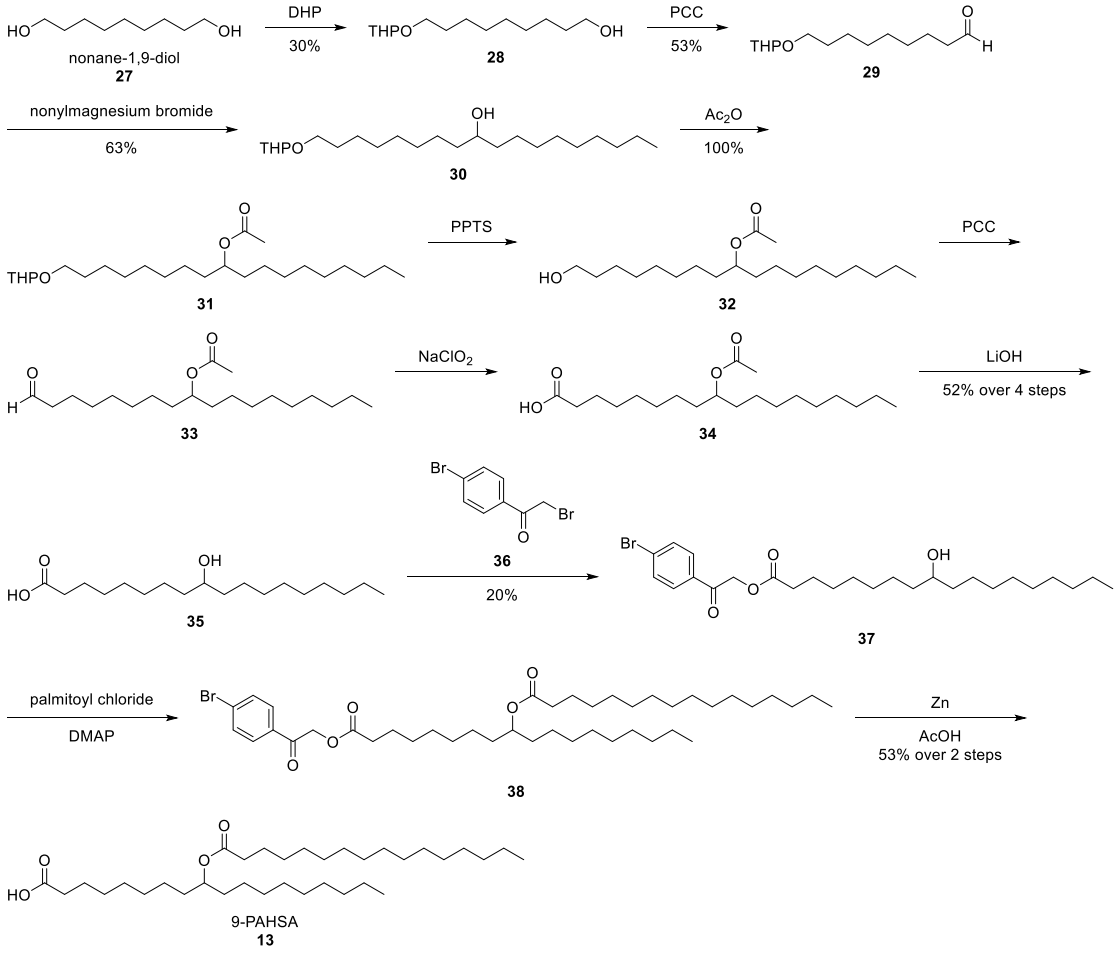

Figure 9. The second reported FAHFA synthesis.

Concurrent with our work on the synthesis of FAHFAs, Balas and coworkers[50] developed a synthesis of PAHPA and OAHPA regioisomers. (Figure 10) First, commercial olefin-alcohol **39** was protected as the corresponding TBS ether **40**, whose terminal olefin was oxidized to epoxide **41** with *m*CPBA. The authors noted that reversing the order of protection/oxidation steps gave lower yields. The terminal epoxide of **41** was opened with lithium acetylide **42** and boron trifluoride-diethyl etherate, yielding homopropargylic alcohol **43**. The alkyne of **43** was exhaustively reduced in good yield to alcohol **44** with hydrogen and Rosenmund's catalyst. Surprisingly, when palladium on carbon was used in

lieu of Rosenmund's catalyst, yields were markedly lower. The secondary alcohol of **44** was then esterified under the conditions of Steglich, affording ester **45**. The silyl group was deprotected with TBAF to give primary alcohol **46**. The synthesis was concluded with a Jones oxidation of primary alcohol **46** to the corresponding carboxlyic acid **47**. This route was also used to synthesize 5-PAHPA, 5- and 9-OAHPA, and 10-OAHSA.

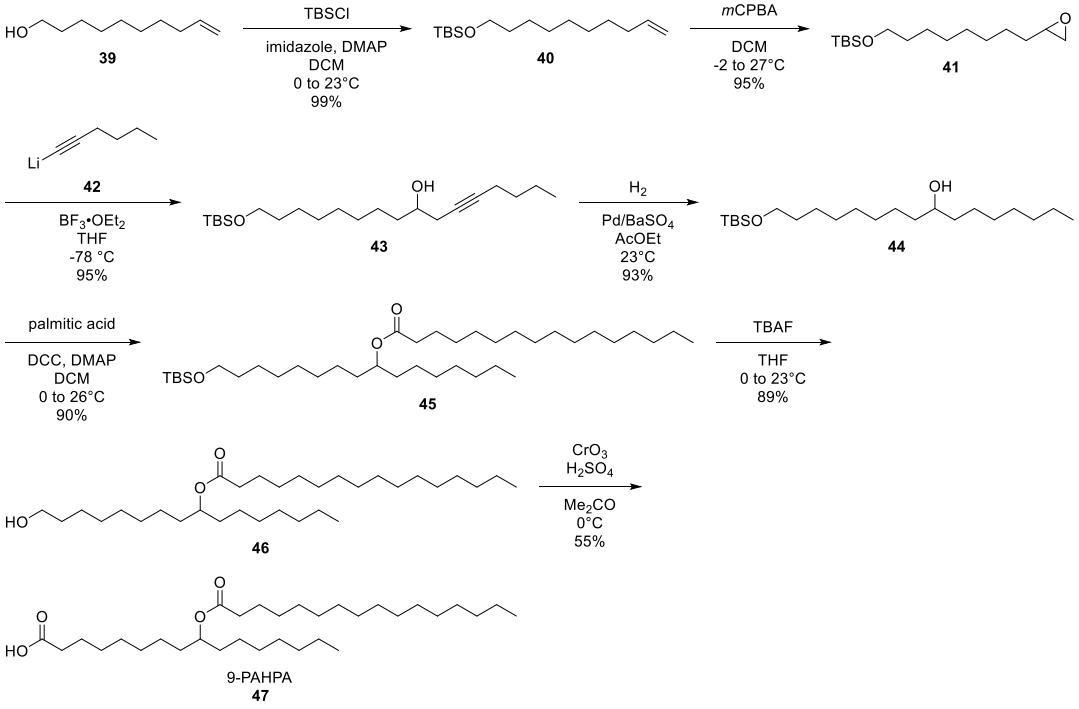

Figure 10. The Balas acetylide approach to 9-PAHPA.

Balas and colleagues also prepared 7-PAHPA, PAHSA, OAHPA, and OAHSA in a similar, though not identical, manner. (Figure 11) The left fragment was prepared by protecting the primary alcohol **48** as TBS ether **49**. The two pieces were connected when the lithium acetylide **50** added to the terminal epoxide of **51**, yielding homopropargylic alcohol **52**. The end game for the 7-series was identical to the final steps in Figure 10 with exhaustive reduction to **53**, Steglich esterification to **54**, silyl deprotcation to **55**, and Jones oxidation completing the synthesis of 7-PAHSA **56**.

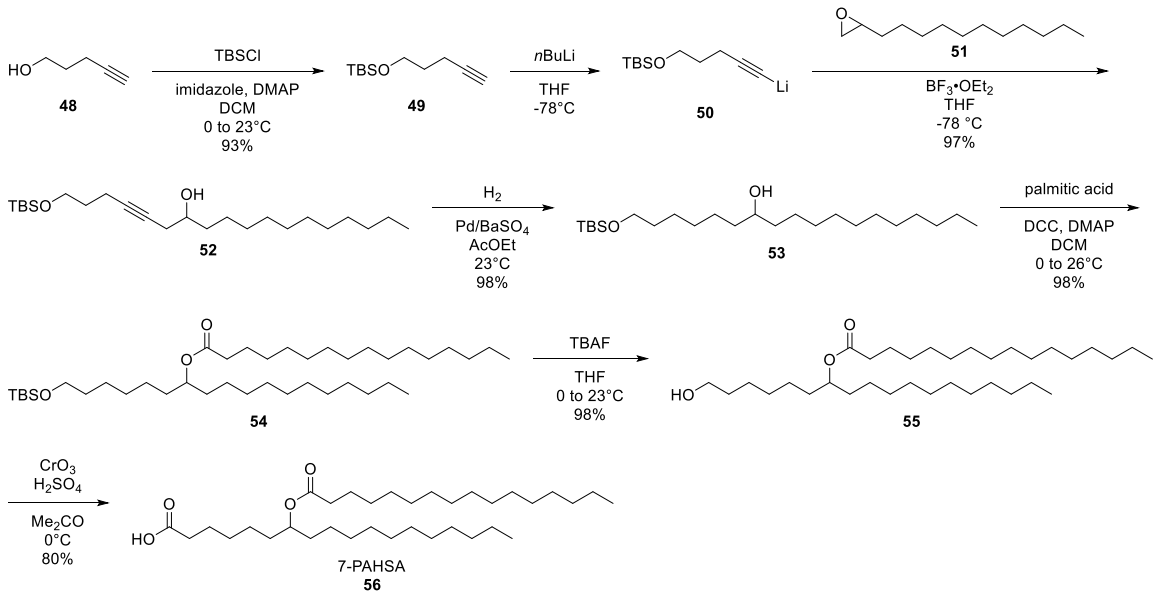

Figure 11. The Balas acetylide approach to 7-PAHSA.

While the route of Balas co-workers resulted in the synthesis of a number of new FAHFAs, there are some limitations, including utilization of super-stoichiometric quantitites of toxic chromium in the final step, and small scale.

Also concurrent with our work, Kuda and coworkers[38] reported a synthesis of 13-DHAHLA **14**. (Figure 12) Their synthesis begins with a soybean lipooxygenase catalyzed conversion of linoleic acid to 13-HODE **57**. Steglich esterification of **57** with DHA yielded 13-DHAHLA **14** after purification via HPLC. Surprisingly, the experimental procedures mentioned neither reaction scale, nor yield.

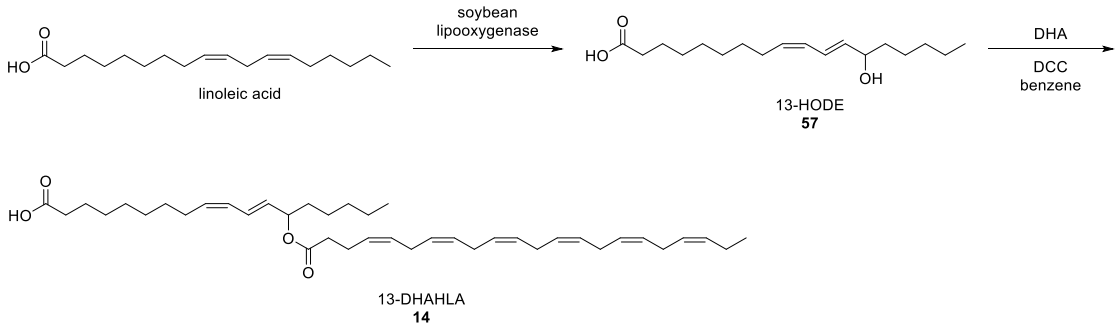

Figure 12. Kuda and co-workers synthesis of 13-DHAHLA.

2.1 SCALABLE SYNTHESIS OF 5- AND 9-PAHSA

We sought to develop a concise, scalable synthesis that avoided using toxic metals as we needed multiple grams of 5- and 9-PAHSA for *in vitro* and *in vivo* studies. Owing to the prohibitive expense of tetradecanal, our synthesis of 5-PAHSA began with the oxidation of 1-tetradecanol **58** to tetradecanal **23**. Oxidation with TEMPO and DAIB at ambient temperature under the conditions of De Mico and coworkers[51] resulted in clean and complete conversion of decanol to decanal. Other conditions explored included tempo with NCS[52] or trichloroisocyanuric acid[53] as terminal oxidant, both of which had a more tedious workup and gave a product of lower purity. The Parikh-Doering[54] and Swern[55] oxidations, while effective, were disagreeable due to the smelly dimethyl sulfide evolved. Crude aldehyde **23** was used directly in the next step, where addition of Grignard **24** afforded olefin-alcohol **25**. The secondary alcohol of **25** was acylated to ester **26** in good yield with commercial palmitoyl chloride in lieu of palmitic anhydride, improving the atom economy of this step.

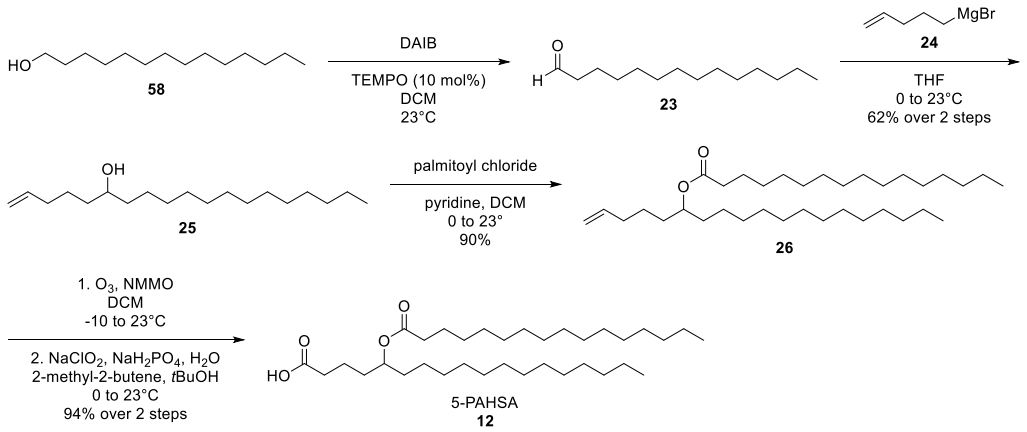

Figure 13. Our synthesis of racemic 5-PAHSA.

The ozonolysis of the terminal olefin of **26** proved non-trivial. The ozonolytic conditions reported by the Drussault lab[56] with NMMO as an additive were singular in their ability to fully suppress formation of the secondary ozonide. According to the Criegee mechanism[57] (Figure 14), ozonolysis begins with a 1,3 dipolar cycloaddition of ozone with olefin **59**, forming secondary ozonide **60**. Decomposition gives formaldehyde **61** and carbonyl oxide **62**. Another 1,3 dipolar cycloaddition yields secondary ozonide **63**. These species are known to be shock-sensitive and potentially explosive and should be avoided, particularly when working on scale.

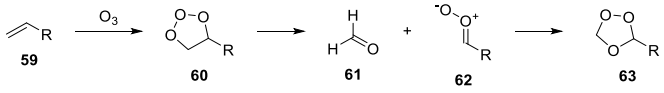

Figure 14. The Criegee mechanism of ozonolyis.

The Drussault lab[56] proposes that NMMO **64** adds into carbonyl oxide **62**, forming a tetrahedral intermediate **65**, which decomposes to aldehyde **66**, NMO **67**, and oxygen. (Figure 15) Conveniently, aqueous workup removed all NMO and the crude aldehyde was used without further purification.

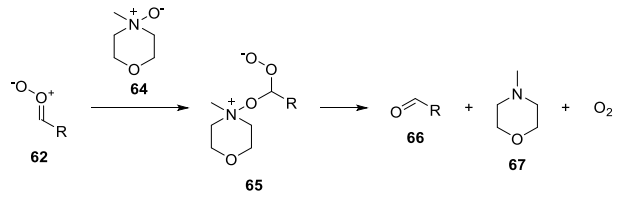

Figure 15. Prevention of secondary ozonide formation with NMMO as per Drussault.

Other methods for the ozonlysis of **26** were explored, including formic acid with hydrogen peroxide,[58] quenching with dimethyl sulfide[59] or triphenylphosphine,[60] with pyridine as an additive,[61] and running the reaction in wet acetone[62] or acetonitrile.[63] All of these other methods formed notable quantities of secondary ozonide. These data are summarized in Table 2.

Ozone + Reactant	Solvent	Temp (°C)	Product:2° Ozonide
NMMO, then $NaClO_2$	DCM	0	100:0 (94% yield)
PPh_3 (2 eq)	DCM:MeOH (80:20)	0	95:5
$NaClO_2$	Acetone:water	0	93:7
$NaClO_2$	Acetonitrile:water	0	90:10
Me_2S (40 eq)	DCM	-78	86:14
Pyridine	DCM	-78	85:15
Formic acid, H_2O_2	Formic acid	Reflux	79:21

Table 2. Conditions explored for the ozonolysis of terminal alkene **26**.

With a safe method to cleave **26** on decagram scale, the synthesis of 5-PAHSA was concluded with Pinnick oxidation of the crude aldehyde to 5-PAHSA **12**. The final step reaction has been successfully cacrried out to afford over 20 g of final product in a single batch in good overall yield.

9-PAHSA was synthesized in an analogous manner, (Figure 16) using 1-decanol **68** as the starting alcohol and non-8-en-1-ylmagnesium bromide **70** as the Grignard reagent. We found it was important to use freshly prepared decanal **69** rather than commercial decanal; even new bottles of decanal gave a more complex mixture after addition of non-8-en-1-ylmagnesium bromide **70**. The olefin-alcohol **71** was then acylated with palmitoyl chloride to give olefin-ester **72**, which was oxidized under the optimized conditions to yield 9-PAHSA **13** in 4 steps and good overall yield.

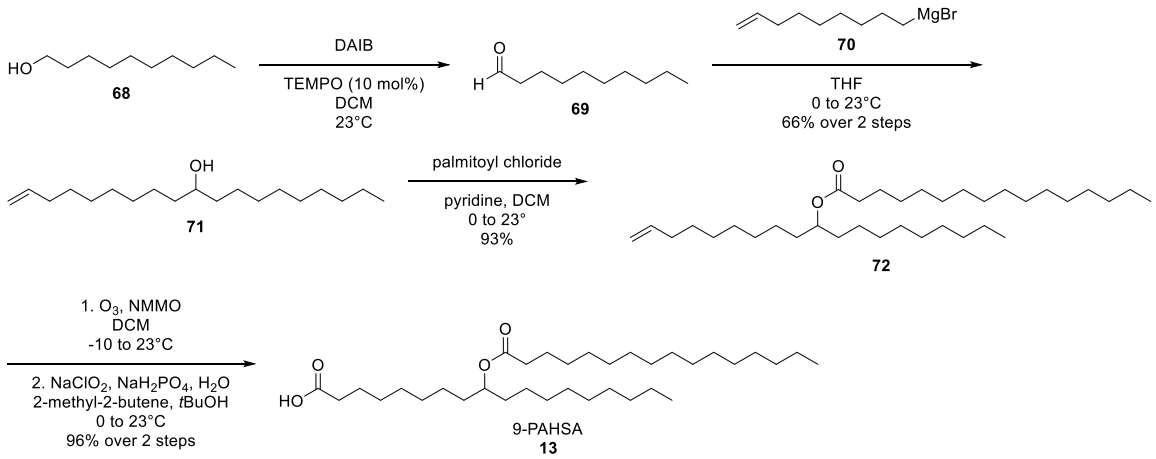

Figure 16. Our racemic synthesis of 9-PAHSA.

2.1.1 Biological Studies With 5- and 9-PAHSA

With decagrams of 5- and 9-PAHSA in hand, we have been able to conduct a number of *in vivo* and *in vitro* studies. Two of these have been published.

In the first study, Vijayakumar and colleagues[64] explored the effects of 9-PAHSA in the context of adipocyte specific knockout of carbohydrate response element binding protein mice (AdChREBP KO). In humans, lower levels of ChREBP in adipocytes and decreased *de novo* lipogenesis are linked to insulin resistance. To further explore this phenomenon, we selectively knocked out ChREBP in adipocytes in mice, generating

AdChREBP KO mice. Compared to controls, AdChREBP KO mice were insulin resistant and the liver, muscle, and adipose tissue showed attenuated insulin action. AdChREBP KO adipocytes had similar GLUT4 levels to WT mice, but GLUT4 translocation and exocytosis were blunted. Furthermore, AdChREBP KO adipose tissue showed more inflammation and serum had lower PAHSA concentrations, compared to WT controls. Incredibly, AdChREBP KO mice supplemented with 9-PAHSA saw a complete reversal of the previously observed insulin resistance, adipose tissue inflammation, impaired glucose transport, and GLUT4 transport.

In the second report, Syed *et al*,[65] we investigated the chronic effects of 5- and 9-PAHSA administration *via* minipump over several months. This is in contrast with the Yore report which only studied the acute effects of 5- and 9-PAHSA on glucose homeostasis. Chronic PAHSA administration to chow fed mice increased serum and fat tissue PAHSA levels, improved glucose tolerance and insulin sensitivity, and augmented insulin and GLP-1 secretion, compared with control mice. PAHSA treated mice also had reduced inflammation in adipose tissue, with decreased in pro-inflammatory macrophages and no change in anti-inflammatory macrophages. Mechanistically, gpr40 (free fatty acid receptor 1, FFAR1) was reported for the first time to play an important role in PAHSA activity. Hek293 cells transfected with murine gpr40 were used to show that 9-PAHSA activates gpr40 in a dose-dependent manner; furthermore, blockade of gpr40 genetically (siRNA) and pharmacologically (gw1100) attenuated agonism of 9-PAHSA at this receptor, confirming that gpr40 is a target of 9-PAHSA. It is worth noting that gpr40/FFAR1 is considered a promising target for the treatment of T2DM.

2.2 SYNTHESIS OF ENANTIOPURE 9-PAHSA

While these animal studies with racemic 5- and 9-PAHSA provided exciting results, an outstanding question remained: what is the stereochemistry of endogenously produced 9-PAHSA? In order to answer this question, we needed to synthesize enantiopure standards. (Figure 17) In our synthesis,[44] we chose a chiral pool approach, employing inexpensive S-(+)- and R-(-) epichlorohydrin as the source of chirality for R- and S-9-PAHSA, respectively. The synthesis of R-9-PAHSA began with copper catalyzed addition of 7-oectenylmagneisum bromide **74** into the unsubstituted end of S-(+)-epichlorohydrin, giving chlorohydrin **73**. An intramolecular Williamson ether synthesis followed converted chlorohydrin **73** to terminal epoxide **76** via a 3-*exo*-tet cyclization, which is favored according to Baldwin's rules.[66] Octylmagnesium chloride was added with catalytic copper iodide, yielding secondary alcohol **71**. Relay of chirality was confirmed by derivatization as the corresponding S-9-acetylmandelate ester; the diastereomeric ratio proved to be greater that 99:1, with no trace of racemization. The synthesis terminates using the same steps mentioned above. Alcohol **71** was acylated with palmitoyl chloride to give ester **72**, which was subjected to ozonolysis and Pinnick oxidation, yielding enantiopure R-9-PAHSA **R-13** in 55% yield. S-9-PAHSA **S-13** was synthesized in 61% overall yield in an analogous manner starting with R-(-)-epichlorohydrin **R-73** in lieu of S-(+)-epichlorohydrin **S-73**.

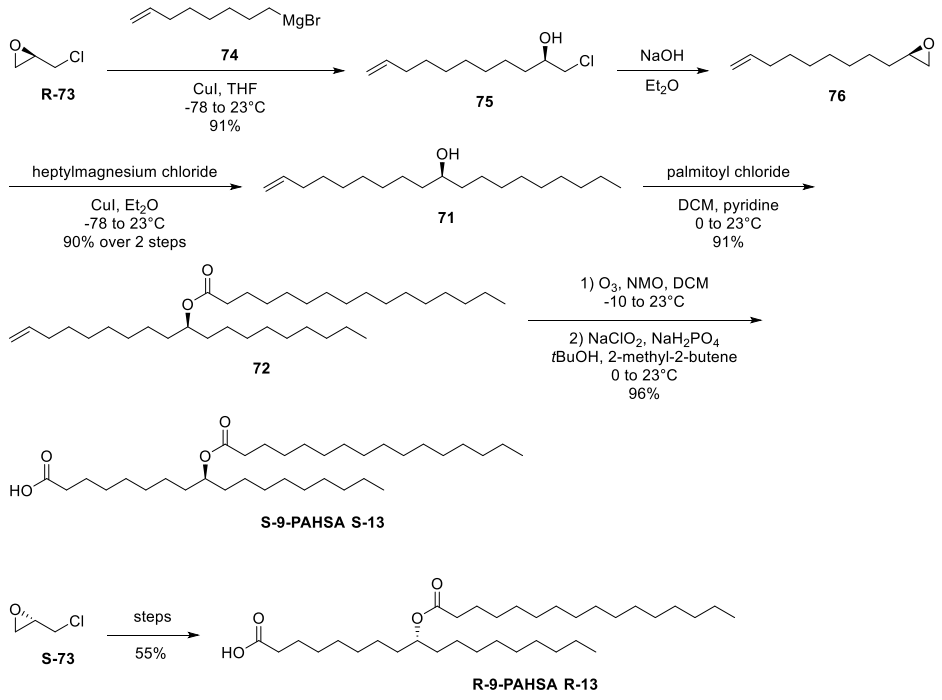

Figure 17. Our synthesis of enantiopure S- and R-9-PAHSA.

Some of the R- and S-9-PAHSA were saponified to R- and S-9-hydroxystearic acid, respectively, with potassium hydroxide. (Figure 18) It should be noted that previous efforts to resolve 9-HSA enzymatically only provided 9-HSA modest optical purity (54% ee).

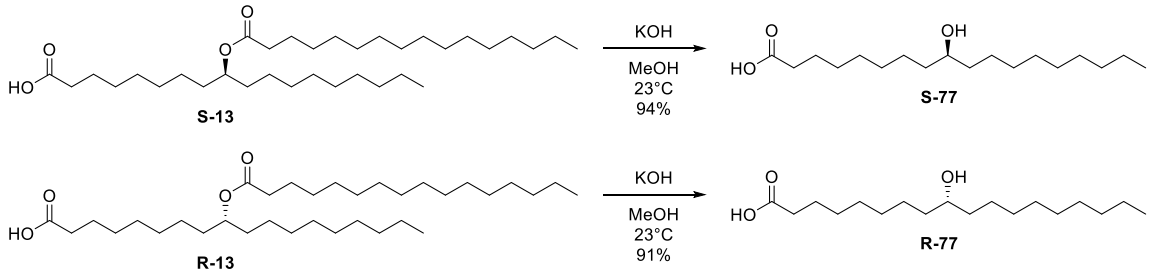

Figure 18. Synthesis of enantiopure S- and R-9-HSA by saponifying 9-PAHSA.

2.2.1 Biological Testing with Enantiopure 9-PAHSA

With enantiopure 9-PAHSA in hand a number of analytical methods to resolve the enantiomers were explored. (Figure 19) First, derivatization of 9-PAHSA as the

corresponding methyl ester **78** followed by chiral GC resolution failed, likely owing to the large molecular weight. Secondly, we used S-1-phenylethan-1-amine to prepare amide **79**. The diastereomers formed would not separate under any of the liquid chromatographic conditions explored, nor was any splitting observed in the 1H NMR spectrum; in both cases, this was likely due to the distance between the two chiral centers.

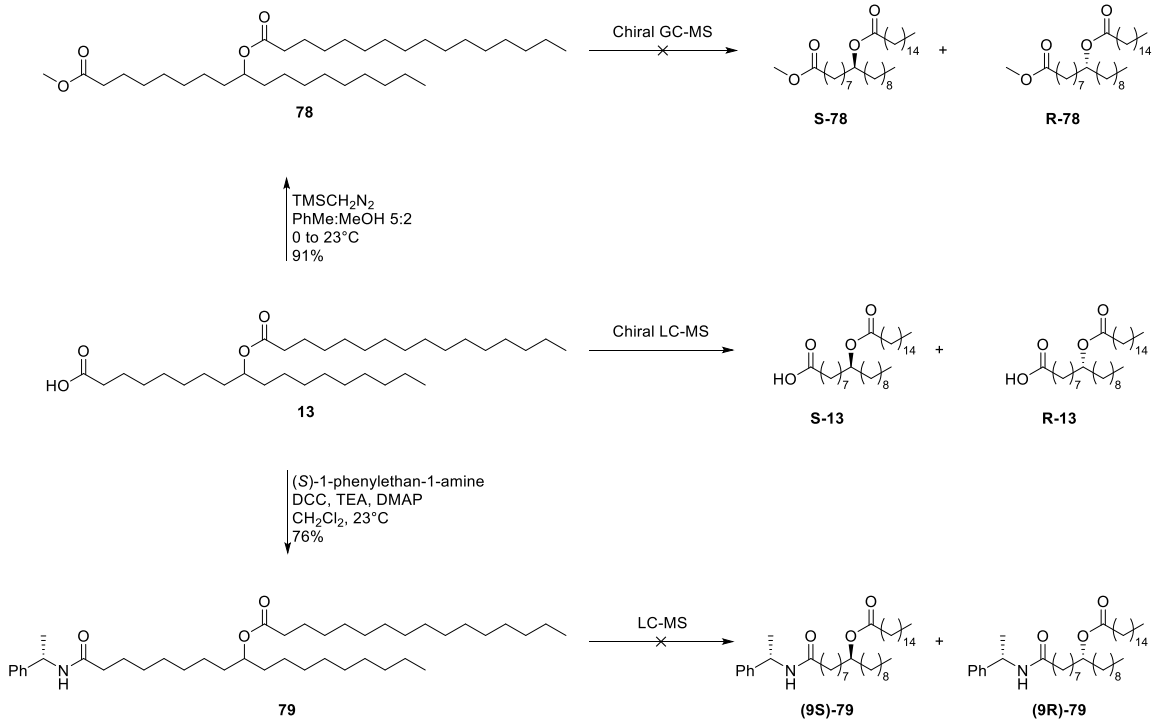

Figure 19. Efforts towards the resolution of 9-PAHSA and its derivatives.

Having exhausted the resources at our disposal to separate the enantiomers/diasteriomers, we turned to the chiral screening service offered by Phenomenex (Torrance, CA). We provided rac- and R-9-PAHSA and, after screening 6 chiral columns (cellulose-1, -2, -3, and -4, and amylose-1, and -2) and 3 solvent systems (water/acetonitrile, hexane/ethanol, and methanol/isopropanol), they found that the Lux 5 um cellulose-3 column with methanol/isopropanol/trifluoroacetic acid (90:10:0.1)

successfully resolved the enantiomers. One drawback of this solvent system is that TFA is not compatible with our LC-MS, thus we had to further optimize the solvent conditions.

We found that methanol/water/formic acid (96:4:0.1) provided separation of the enantiomers, with S-9-PAHSA eluting first at 17.4 min and R-9-PAHSA eluting at 20.2 min. Regrettably, the formic acid led to a 25-fold decrease in sensitivity. Thus, to determine the endogenous stereoisomer of 9-PAHSA, we used perigonadal gonadal white adipose tissue from AG4OX mice as this lipid depot boasts the highest concentrations of 9-PAHSA of all tissues sampled.

The Kahn lab generously donated AG4OX pgwat. After Bligh Dyer extraction and separation of neutral lipids with a solid phase exstraction cartridge, we resolved the enantiomers using our optimized conditions via chiral LC-MS. The data show R-9-PAHSA is the major enantiomer of 9-PAHSA in AG4OX. (Figure 20)

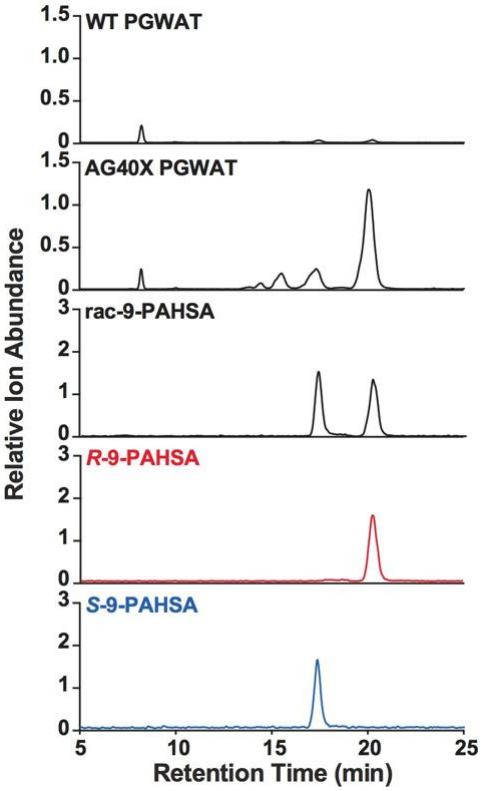

Figure 20. Resolution of 9-PAHSA enantiomers and abundance in AG4OX PGWAT

At first glance, it would appear that there are also appreciable amounts of S-9-PAHSA, however, further studies showed that R-10-PAHSA co-elutes with S-9-PAHSA under these conditions

In addition to showing that R-9-PAHSA is the predominant enantiomer found in AG4OX mice, we also discovered two of the mechanisms for this phenomenon. 9-PAHSA is synthesized by condensing 9-hydroxystearic acid with palmitic acid and hydrolysis of 9-PAHSA yields 9-HSA and PA. In previous studies, CEL was the most potent of the 3 FAHFA hydrolases that have been discovered. When 9-PAHSA was incubated with pancreatic lysate (Figure 21A) or HEK293T transfected with CEL (Figure 21B), S-9-

PAHSA was selectively hydrolyzed in preference to R-9-PAHSA, explaining, in part, a reason for the predominance of r-9-PAHSA in AG4OX mice.

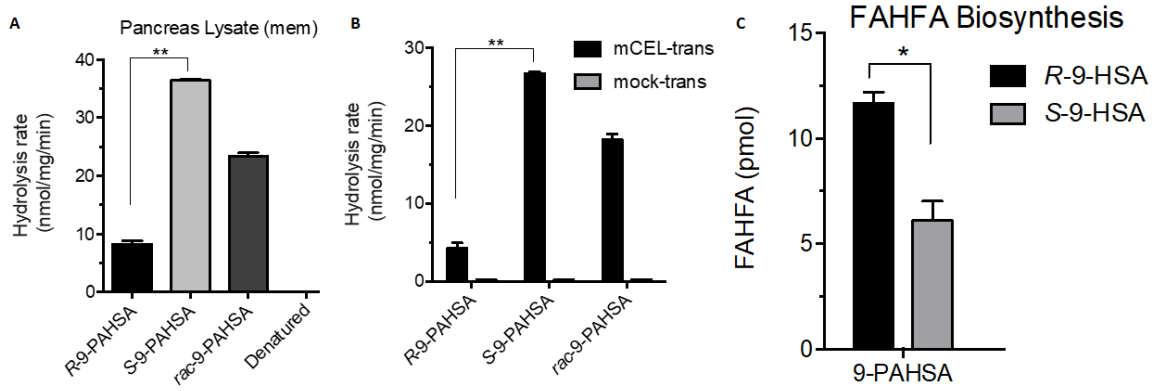

Figure 21. Asymmetric hydrolysis of 9-PAHSA and acylation of 9-HSA. A) Pancreatic lysate hydrolyses *S*-9-PAHSA more rapidly than *R*-9-PAHSA. B) HEK293T cells transfected with CEL hydrolyses *S*-9-PAHSA more rapidly than *R*-9-PAHSA. C) HEK293T cells preferentially acylate *R*-9-HSA compared with *S*-9-HSA

As mentioned previously, 9-PAHSA may be biosynthesized via condensation of 9-HSA with palmitic acid. The enzyme responsible for this activity remains unknown, but a previous report showed that 17 carbon hydroxyheptadecanoic acid was acylated in cells to form the corresopnding FAHFA. In a similar manner, we incubated HEK293T cells with either R-9-hsa or S-9-HSA, then analyzed the cells for 9-PAHSA. We found nearly twice as much 9-PAHSA when cells were incubated with R-9-HSA than S-9-HSA. (Figure 21C) These data suggest that FAHFAs are formed stereoselectively by an enzymatic process. In summary, R-9-PAHSA is the major enantiomer in mice for at least two reasons: 1) S-9-PAHSA is preferentially hydrolyzed by CEL and 2) R-9-HSA is selectively acylated by an as yet undiscovered enzyme.

2.3 PAHSA SAR LIBRARY

FAHFAs have a wealth of promising biological activity, however the relationship between FAHFA structure and activity (SAR) has never been logically examined. A few of the previously mentioned studies provided insight into the parameters worth exploring. Our work with showed that the stereochemistry of 9-PAHSA and 9-HSA effects its cellular processing.[44] The work by Parsons[39] and Kolar[40] showed that FAHFA are regioselectively hydrolyzed. Finally, Kuda and coworkers[38] discovered a highly unsaturated FAHFA with more potent anti-inflammatory activity than fully saturated 9-PAHSA. With this work in mind we devised a 30-member FAHFA library based on the PAHSA scaffold that would probe the importance of stereochemistry, regiochemistry, and saturation/unsaturation. As FAHFAs only contain one stereocenter, both the S and R enantiomers were selected. To test the influence of regiochemistry, we chose the 5-, 9-, and 13-regioisomers as they are the first, middle, and last regioisomers of the PAHSAs. Finally, the ester will be varied from palmitic acid (16:0) to oleic acid (18:1), linoleic acid (18:2), alpha-linolenic acid (18:3, omega-3), and gamma-linolenic acid (18:3, omega-6). The parameters of the FAHFA library are summarized in Table 3.

Stereoisomers	S	R				2
Regioisomers	5-	9-	13-			3
Unsaturation	PA	OA	LA	ALA	GLA	5
						= 30

Table 3. Summary of FAHFA SAR parameters under investigation in this chemical library.

Our synthesis of 9-PAHSA provided highly enantioenriched material on multigram scale, however, one of the major drawbacks in the context of this chemical library was the ozonolysis at the end of the route. Performing such an oxidation at the end of the synthesis

precluded the preparation of any FAHFA analogues containing any olefins. Thus, we elected to end the synthesis by chemoselectively saponifying a methyl ester in the presence of an ester formed with a secondary alcohol.

2.3.1 Synthesis of the 5-series

The synthesis of the 5-series began with the protection of the primary alcohol of commerical 3-bromo-1-propanol **80** as the corresponding TBS ether **81**. (Figure 22) Treatment of **81** with magnesium gave a Grignard, which added to R-(-)-epichlorohydrin under copper catalysis, forming chlorohydrin **82**. The chlorohydrin **82** was treated with sodium hydroxide to give epoxide **83**, which was used directly in the next step without purification. Addition of dodecylmagnesium bromide with catalytic copper (I) bromide yielded **84**, which had the complete carbon skeleton of the hydroxystearic acid backbone. The silyl ether of **84** was deprotected with TBAF, affording diol **85**. Following a procedure from Hansen and colleagues,[67] diol **85** was converted directly to lactone **86**, presumably through chemoselective oxidation of the primary alcohol to the corresponding aldehyde, formation of the six-membered lactol, then oxidation of the lactol to lactone **86**. The latter was opened to methyl 5-hydroxystearate **87** with methanol and triethylamine in almost quantitative yield using conditions previously reported by Nicolau and co-workers.

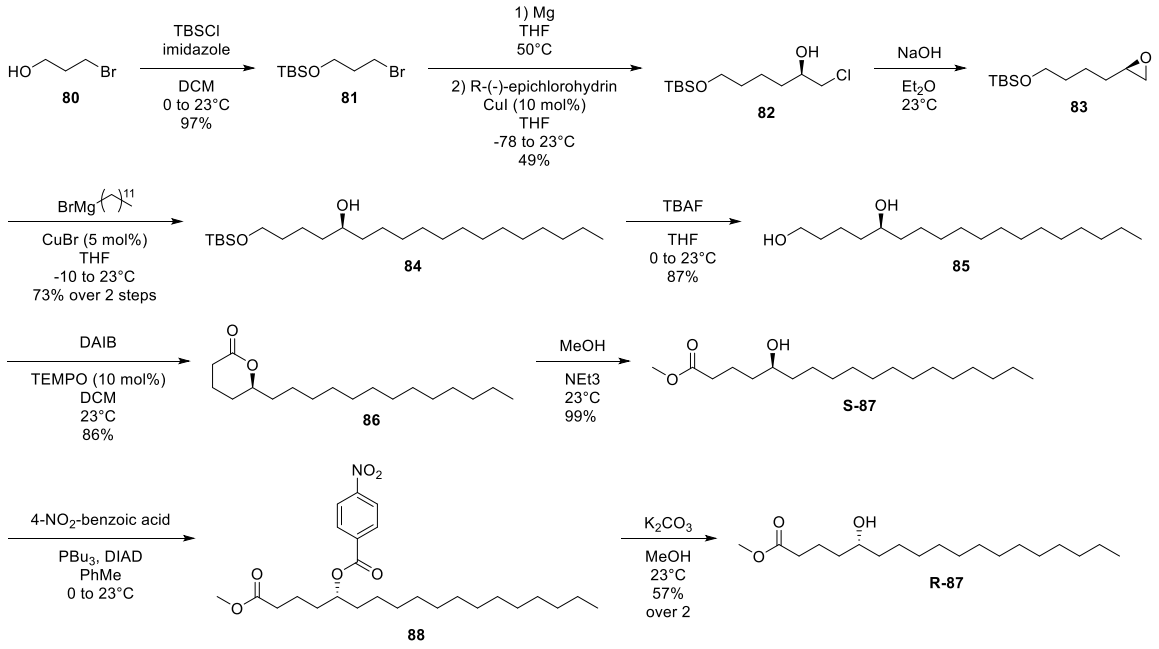

Figure 22. Synthesis of both antipodes of methyl 5-hydroxystearate.

Surprisingly, attempts to open the lactone with excess sodium methoxide (3 eq) in methanol exclusively gave 5-hydroxystearic acid, whether using ACS grade (Fisher) or anhydrous methanol (Alfa Aesar), commercial sodium methoxide or sodium methoxide in methanol prepared from freshly cut sodium metal. Furthermore, catalytic sodium methoxide (30 mol%) gave a disappointing mixture of unreacted lactone **86**, methyl 5-hydroxystearate **87**, and 5-hydroxystearic acid.

In order to access the other antipode of **87** without repeating the first 7 steps of the synthesis with S-(+)-epichlorohydrin, we attempted to invert the stereocenter of **S-87** with the Martin and Dodge[68, 69] variation of the Mitsunobu reaction. In the Organic Syntheses report,[69] THF was used as the solvent. When replicating these conditions, we found that the ee% of the product had eroded markedly. By switching to benzene, the hydrocarbon solvent used in the original report,[68] we found that the final product had cleanly inverted with no sign of the other enantiomer. This is a powerful reminder of the importance of

solvent effects on reaction outcomes. In addition to modifying the solvent, we also found that using tributylphosphine in lieu of triphenyl phosphine facilitated the workup.

The 4-nitrobenzoate ester of **88** was selectively methanolized with potassium carbonate in methanol to afford methyl 5-hydroxystearate **R-87** along with some of the lactone **86**. Attempts to effect this same transformation with triethylamine as the base failed to go to completion, even when employing a large excess (21 eq) of base.

With both enantiomers of methyl 5-hydroxystearate in hand, we attempted to esterify the secondary alcohol with the appropriate acid chloride and pyridine under the conditions employed in the synthesis of 9-PAHSA. The acid chlorides were synthesized from the appropriate acid with oxalyl chloride in DCM. Analysis of the crude (1H NMR) showed clean and complete conversion to the acid chloride. The yield of the esterification reaction was good for the palmitic acid chloride, but yields decreased as the degree of unsaturation increased, necessitating the development of an alternative process.

The Yamaguchi esterification and the Steglich eseterification were explored. Neither DCC, nor EDC, nor benzoyl chloride, nor toluoyl chloride worked as well as 2,4,6-trichlorobenzoyl chloride. Furthermore, 1.25 eq of the acid partner was optimal in our hands.

Diesters **89-93** were synthesized in good yield with our optimized conditions. (Figures 23 and 24). Subsequent chemoselective saponification provided both enantiomers of 5-PAHSA **94**, -OAHSA **95**, -LAHSA **96**, -ALAHSA **97**, and -GLAHSA **98**. Unlike with the 9- and 13-series FAHFAs, saponification of the 5-series went with more modest yield due to formation of the lactone **86**. And 5-hydroxystearic acid. In all his elegant work on ring closure, Baldwin never commented on any ring greater than 7-members.[66, 70-72] Even so, we hypothesize the methyl ester of 5-PAHSA is first saponified at the methyl ester, giving the corresponding carboxylate. An 8-*exo*-trig would engage the other ester, forming

a mixed anhydride. This could subsequently hydrolyze to 5-hydroxystearic acid, or the alkoxide could engage via a favored 6-*exo*-trig to form the lactone.

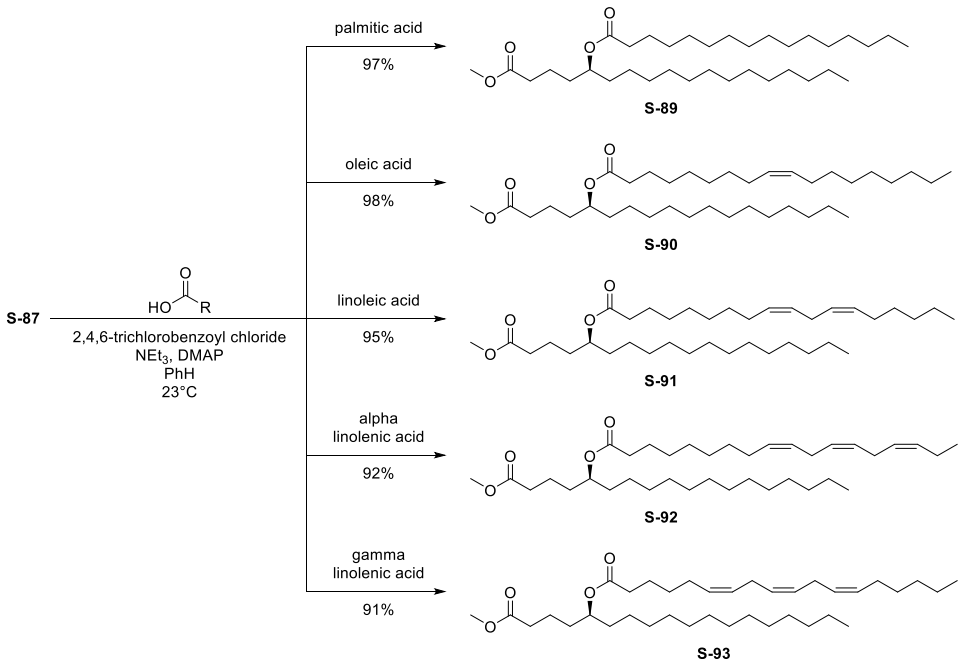

Figure 23 Mitsunobu esterification of the S-5-series.

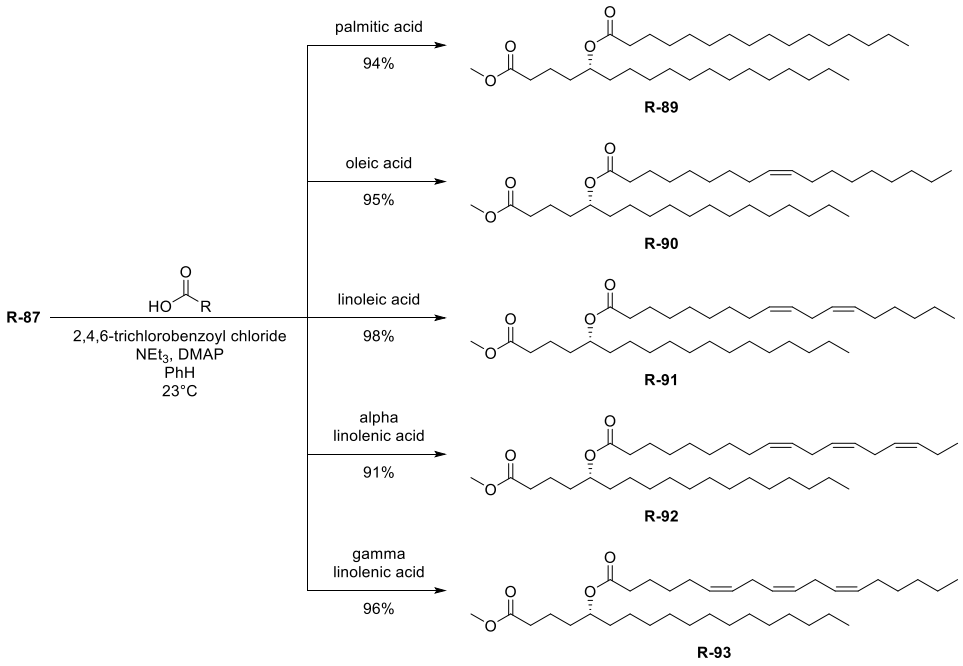

Figure 24 Mitsunobu esterification of the R-5-series.

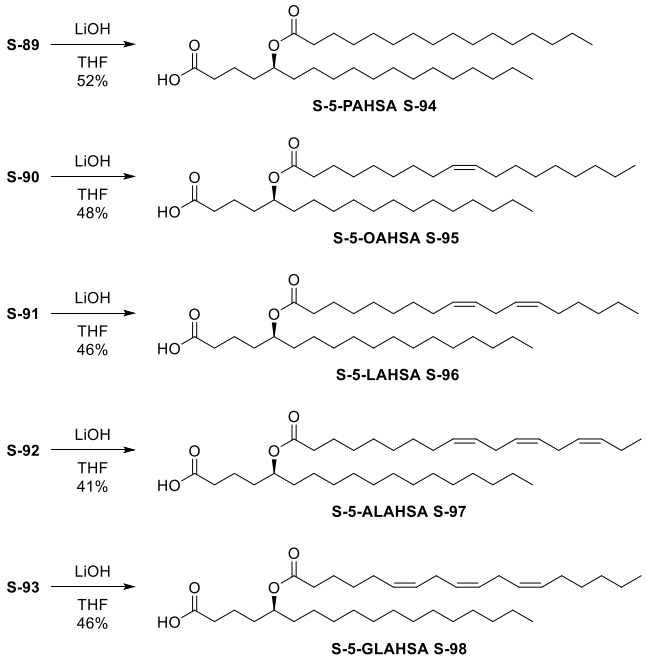

Figure 25. Chemoselective saponification of the S-5-series.

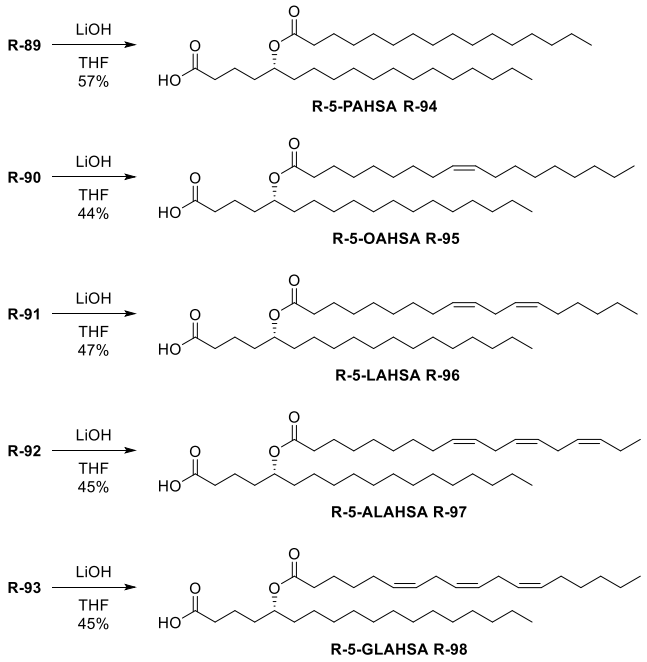

Figure 26. Chemoselective saponification of the R-5-series.

2.3.2 Synthesis of the 9-Series

The synthesis the 9-series members of the FAHFA library debuted with the conversion of commercial 1,7-heptanediol **99** to bromoalcohol **100**; refluxing the diol with 48% HBr in toluene with a Dean-Stark trap gave the desired product in 72% yield. The primary alcohol of **100** was protected as the TBS ether **101**. Treatment with magnesium gave the corresponding Grignard, which added to the unsubstituted end of *R*-(-)-epichlorohydrin with the assistance of catalytic copper iodide, yielding chlorohydrin **102**. Sodium hydroxide in dry ether converted the chlorohydrin **102** to epoxide **41**. Surprisingly, two attempts to open the epoxide with octylmagnesium bromide and copper iodide in THF were unsuccessful, sparking a literature search. The epoxide opening protocol of Alam and coworkers[73] was modified, substituting copper (I) bromide or copper (I) chloride and using organomagnesium bromide in place of organomagnesium chloride. This variation provided

the secondary alcohol **44** in good yield. The silyl ether was deprotected with TBAF, yielding diol **103**. There are a number of reports where catalytic TEMPO preferentially oxidizes primary alcohols over secondary alcohols; DIAD,[51] NCS,[52] and trichlorocyanuric acid[53] have all been used as the terminal oxidant. In our hands, DIAD gave the crude aldehyde in higher yield and purity. Two more telescoped procedures followed: Pinnick oxidation of the crude aldehyde and Fisher-Speier esterification gave methyl ester **S-104** in 74% yield over 3 steps.

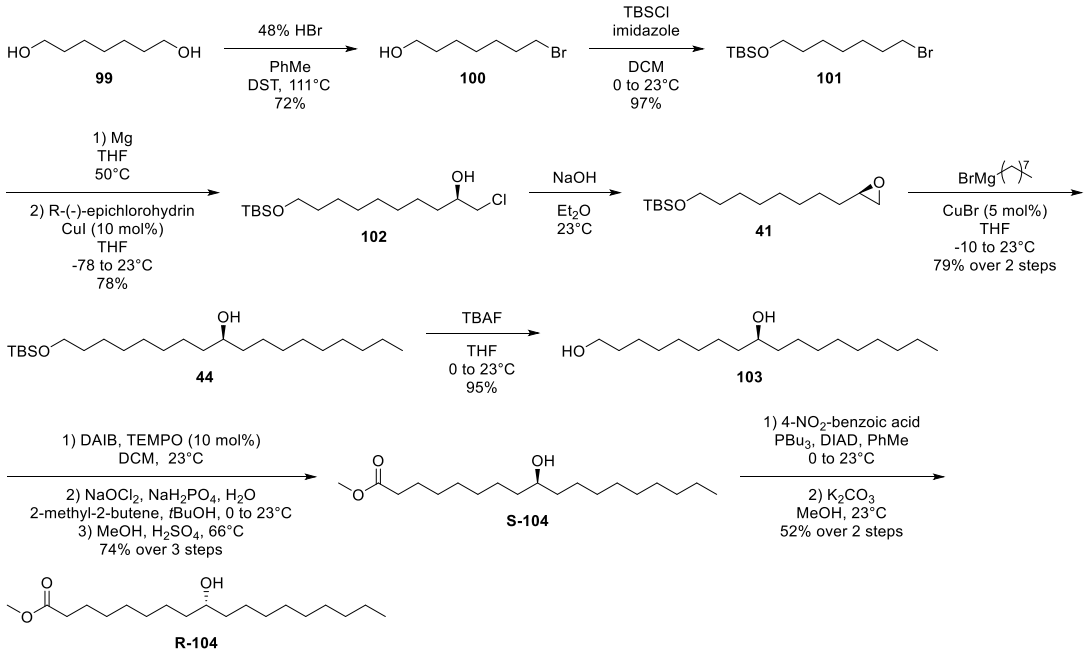

Figure 27 Synthesis of both enantiomers of methyl 9-hydroxystearate.

As for the 5-series, methyl ester **104** was converted into both antipodes of diesters **105-109** (Figures 28 and 29) with our optimized Yamaguchi esterification conditions. The methyl ester was then chemoselectively cleaved to yield the final products, S- and R-PAHSA **110**, -OAHSA **111**, LAHSA **112**, ALAHSA **113**, GLAHSA **114**. (Figures 30 and 31)

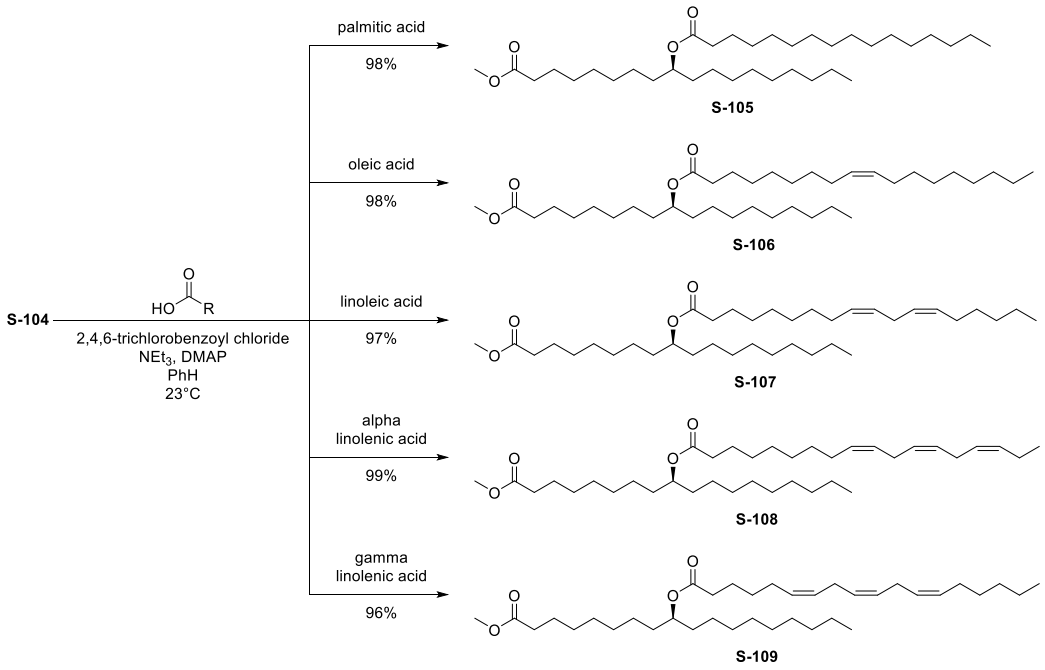

Figure 28. Mitsunobu esterification of the S-9-series.

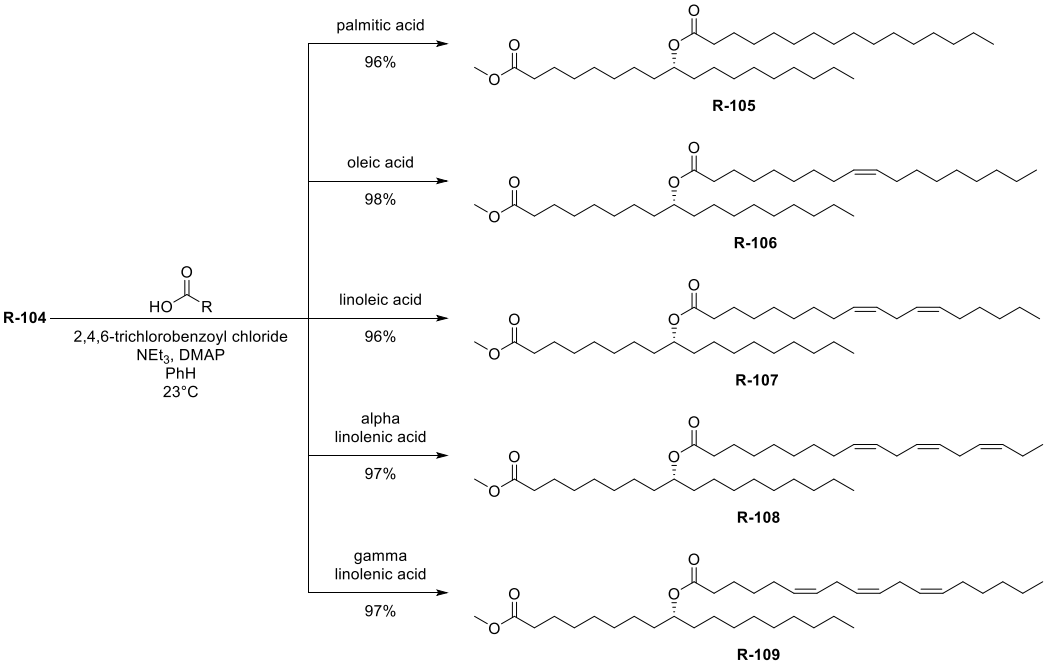

Figure 29. Mitsunobu esterification of the R-9-series.

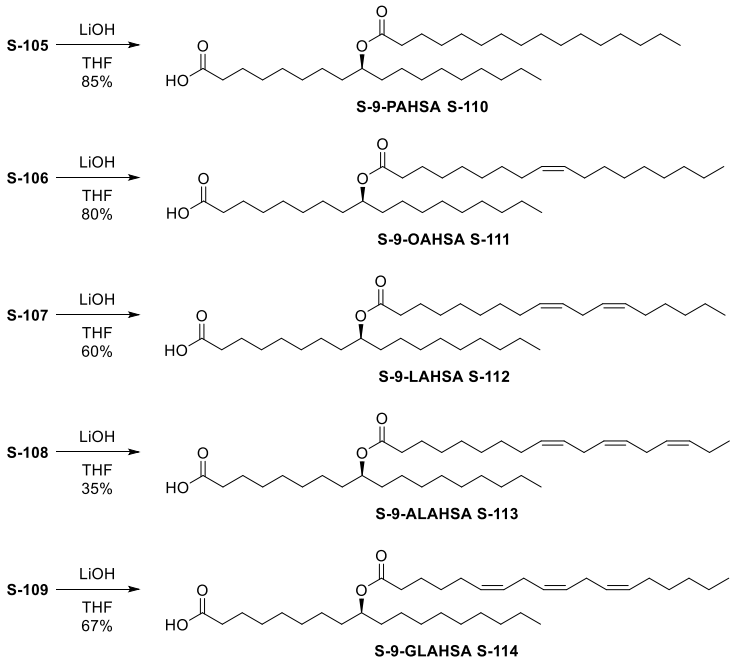

Figure 30. Chemoselective saponification of the S-9-series.

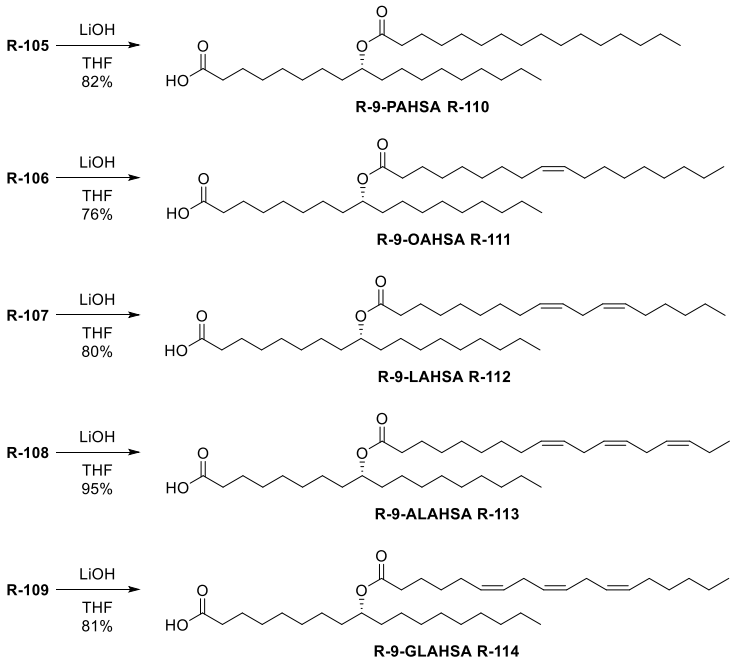

Figure 31. Chemoselective saponification of the R-9-series.

2.3.2 Synthesis of the 13-Series

The conditions developed for the synthesis of the 9-series of the FAHFA library were applied without complication to members of the 13-series. (Figure 32) Commercial 11-bromoundecan-1-ol **115** was protected as tbs ether **116**, which was converted to the corresponding Grignard and added to R-(-)-epichlorohydrin, yielding chlorohydrin **117**. Formation of epoxide **118** with sodium hydroxide was followed by copper (I) catalyzed, regioselective epoxide opening with butylmagnesium bromide, yielding alcohol **119**. Silyl deprotection to **120** and, oxidation and Fisher-Speier esterification gave methyl ester **S-121**, whose stereocenter was inverted as before.

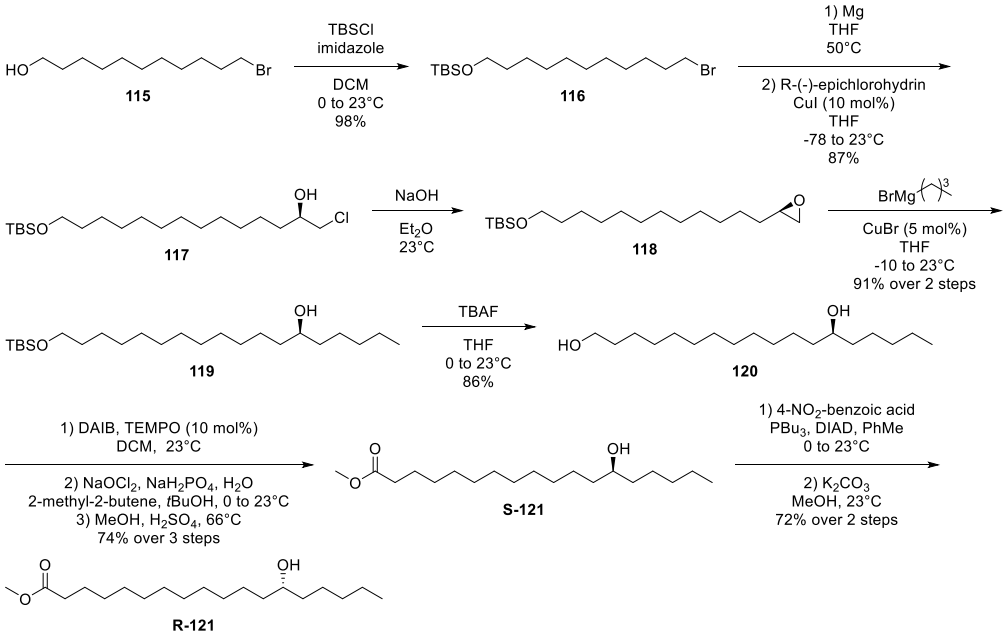

Figure 32. Synthesis of the key methyl ester intermediates in the 13-series.

The two antipodes of methyl 13-hydroxystearate **121** were converted to their diesters **122-126** (Figures 33 and 34), before the final round of saponification necessary to complete the 13-series (**127-131**, Figures 35 and 36) of the FAHFA SAR library.

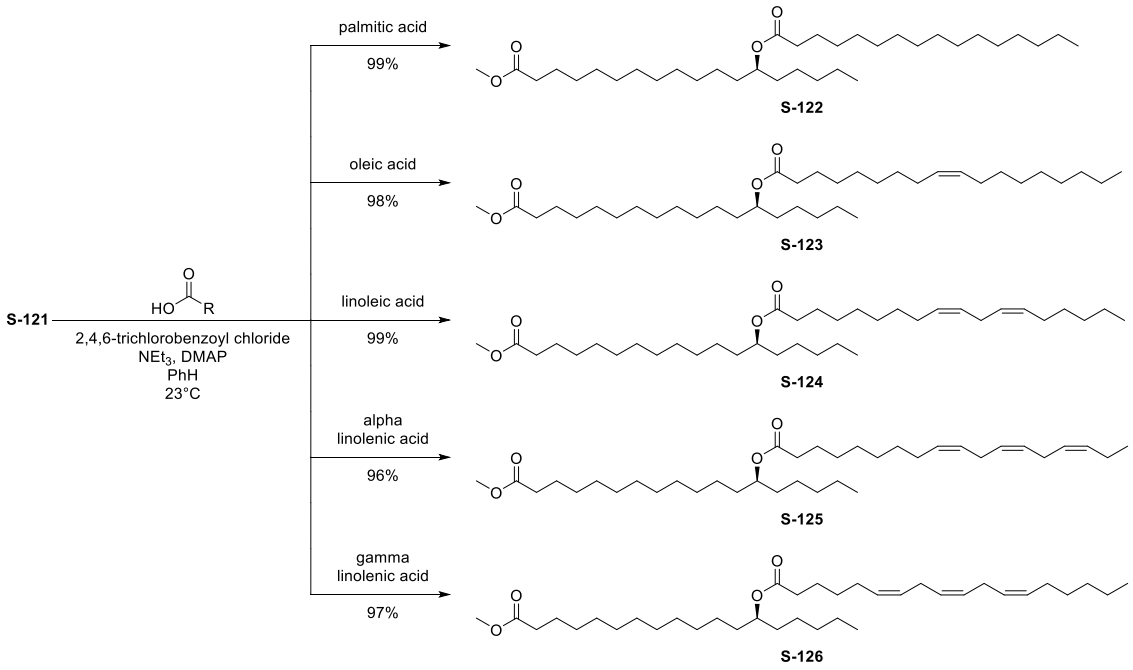

Figure 33. Mitsunobu esterification of the S-13-series.

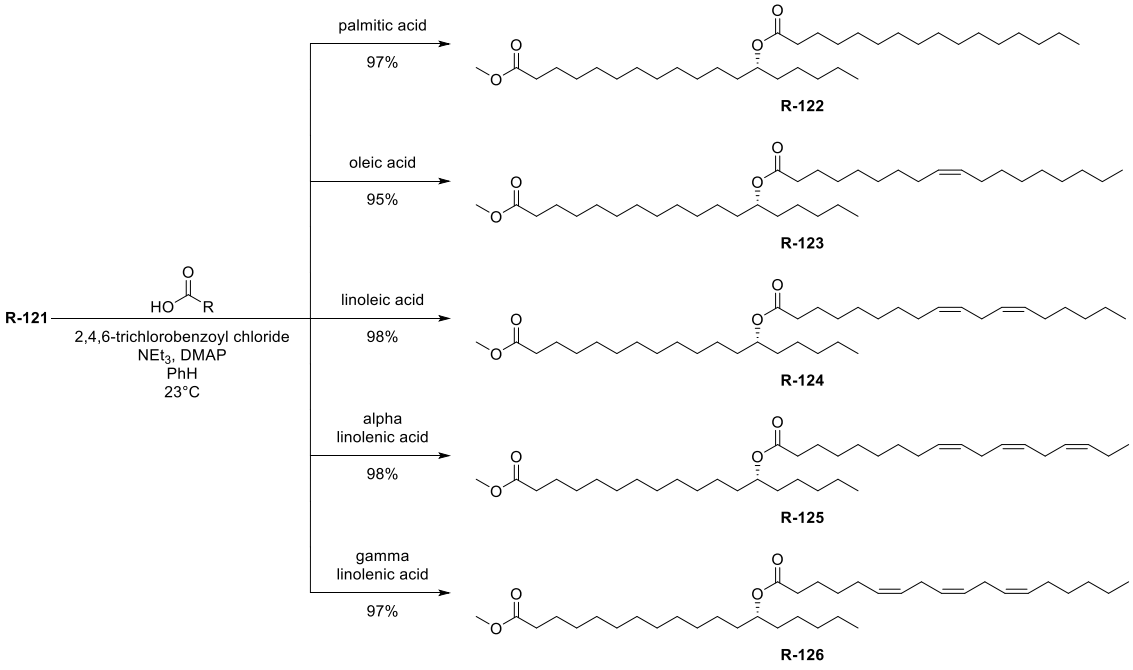

Figure 34 Mitsunobu esterification of the R-13-series.

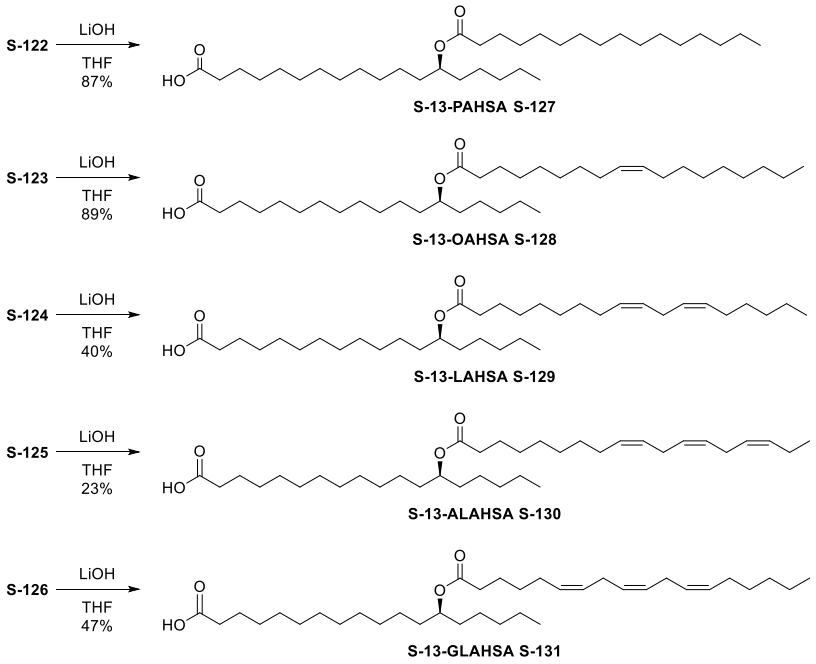

Figure 35. Chemoselective saponification of the S-13-series.

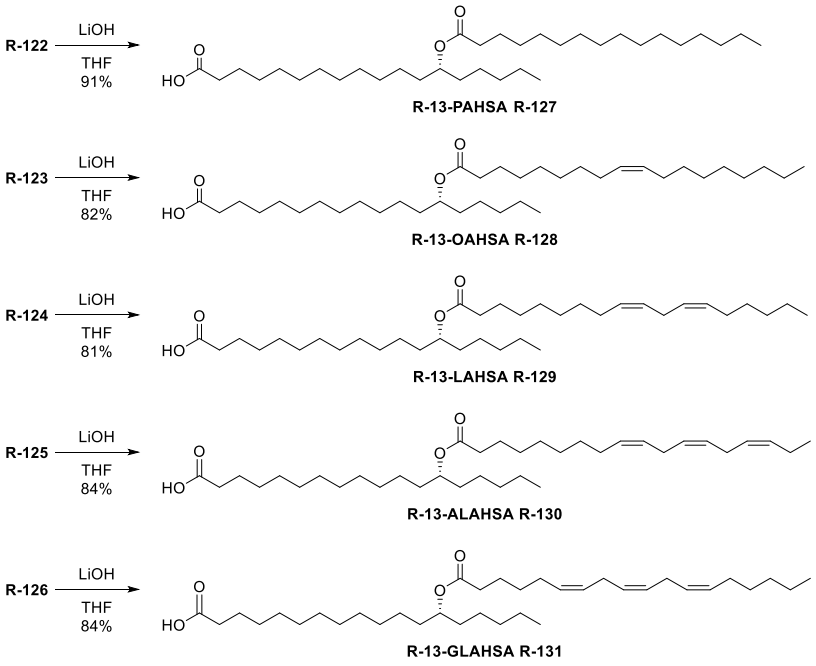

Figure 36. Chemoselective saponification of the R-13-series.

With this 30-member library in hand, we will now be able to probe systematically the structure activity relationships of FAHFA for the first time. The information gained from these studies will show the importance of stereochemistry, regiochemistry, and unsaturation in FAHFA biology. Furthermore, this will also lay the foundation for future FAHFA optimization.

Chapter 3: PAHSA Probes for Chemical Biology

FAHFAs are a recently discovered family of natural product lipids with promising anti-diabetic and anti-inflammatory activity. Any time a novel small molecule with interesting *in vivo* and *in vitro* activity is discovered, two important questions should be asked: 1) what are the molecular targets of this small molecule and 2) how is it modified in cells/organisms?

3.1 Bifunctional 9-PAHSA Probe

To date gpr40 and gpr120 have been identified as FAHFA targets, but these discoveries were based on biological activity and structural similarity to known agonists. We wished to determine in an unbiased manner the proteins with which FAHFAs interact. Thankfully, The Haberkant and Cravatt labs laid the foundation for our work in this field.

Haberkant and co-workers[74] synthesized a bifunctional palmitic acid probe **136** that contained both a diazirine and terminal alkyne in order to investigate palmitate/protein interactions. The synthesis of the probe begins with addition of Grignard **133** into acid chloride **132**, which provides **134** with the complete carbon skeleton for the probe (Figure 37). The methyl ester and silyl protecting group were both cleaved with potassium hydroxide in methanol to afford **135**. The ketone of **135** was converted into the diazarine **136** in the usual 3 step sequence of ammonia, hydroxylamine-O-sulfonic acid, and iodine.

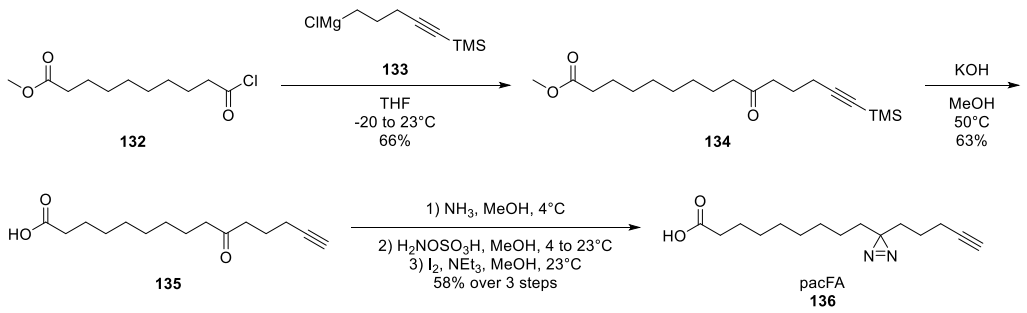

Figure 37. Haberkant and colleagues synthesis of pacFA, a bifunctional palmitic acid probe.

With the bifunctional probe in hand, they sought to determine what proteins interacted with their palmitic acid surrogate. The probe could form covalent adducts with proteins in one of two ways (Figure 38). In the absence of light, some proteins were acylated with the probe, giving species **137**. Alternatively, irradiation with UV light caused the diazirine to decompose into a carbene, which rapidly formed a covalent bond with nearby proteins as conjugate **138**.

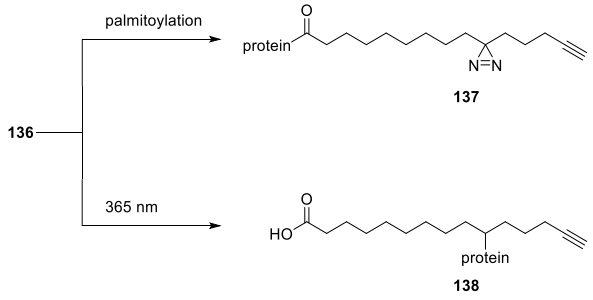

Figure 38. PacFA may form covalent bonds with protein through enzymatic acylation at the carboxylic acid or the carbene generated from the diazirene.

Acyl-alkyne **137** was then subjected to copper catalyzed cyclization with biotin-fluorescin to form adduct **139**, which was primed for visualization. The alkyne was also "clicked" to biotin azide, giving species **140** for proteomics. (Figure 39)

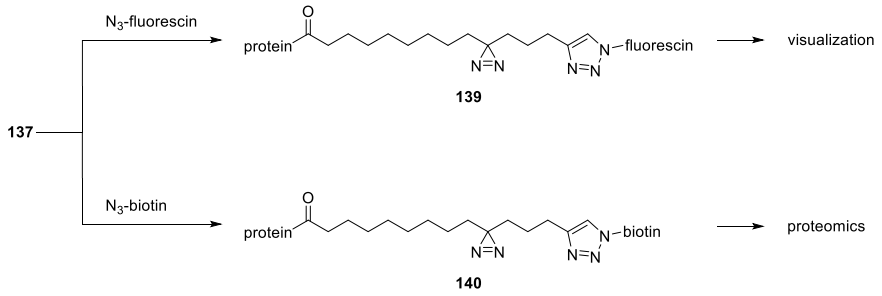

Figure 39. Processing of acyl adducts of pacFA.

In another experiment, the cells incubated with the probe were irradiated with light to convert the diazirine of **136** into an unstable carbene that rapidly formed covalent attachments to nearby proteins, yielding **138**. As before, the free alkyne of **138** provided a useful handle for the Huisgen reaction with biotin azide and fluorescin azide, permitting proteomic analysis and visualization, respectively, of probe-protein adducts **141** and **142**.

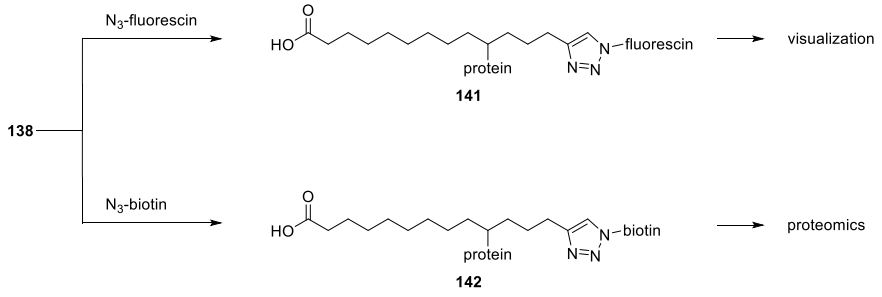

Figure 40. Processing of proteins appended to pacFA from diazirine-derived carbene.

This method allowed Haberkant and coworkers to elucidate 185 protein targets that were acylated and 253 that formed adducts after irradiation with light. In addition to the cellular work, they also found that their probe was effective *in vivo* with model organism *C. elegans*.

The Cravatt lab[75] similarly used a bifunctional cholesterol mimic **149** to investigate cholesterol-protein interactions. (Figure 41) Hulce and co-workers start with a chemoselective potassium chromate mediated oxidation of the secondary alcohol at C6 of

hyodeoxycholic acid **143** to the corresponding ketone **144**. Treatment of **144** with methanol and hydrochloric acid converts the carboxylic acid to the corresponding methyl ester, while also epimerizing the proton at C5 to give ester **145**. The secondary alcohol of **145** was converted to the corresponding mesylate **146**. Substitution of mesylate **146** with acetate went cleanly with inversion of stereochemistry at C3, yielding **147**. Both of the esters of **147** were saponified with lithium hydroxide, revealing the secondary alcohol and carboxylic acid of **148**. The synthesis of bifunctional probe 149 ends with conversion of the ketone at C6 to a diazirine and Steglich esterification of 5-hexyn-1-ol to the carboxylic acid to append the requisite alkyne.

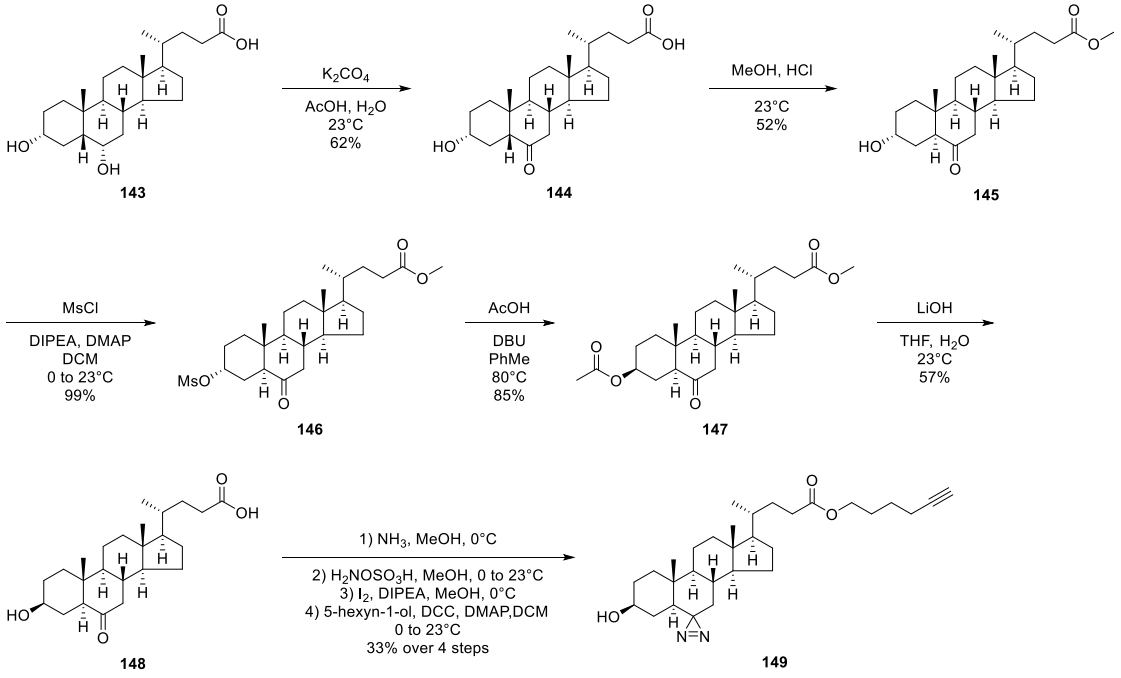

Figure 41. The Cravatt synthesis of a bifunctional diazirine-alkyne cholesterol probe from hyodeoxycholic acid.

The probe **149** was then incubated with HeLa cells and irradiated with 365 nm UV light to generate a carbene, which formed covalent adduct **150** with nearby proteins (Figure 42). Similar to the Haberkant report, the free alkyne was then "clicked" to functionalized

azides for visualization and proteomics. For the visualization studies, the Cravatt lab used a rhodamide functionalized azide in place of the fluorescin azide selected by the Haberkant lab. With their cholesterol probe, Hulce *et al* identified 265 likely cholesterol-protein targets. Some of these protein interactions were known, validating the method, while other proteins had theretofore unknown interactions with cholesterol.

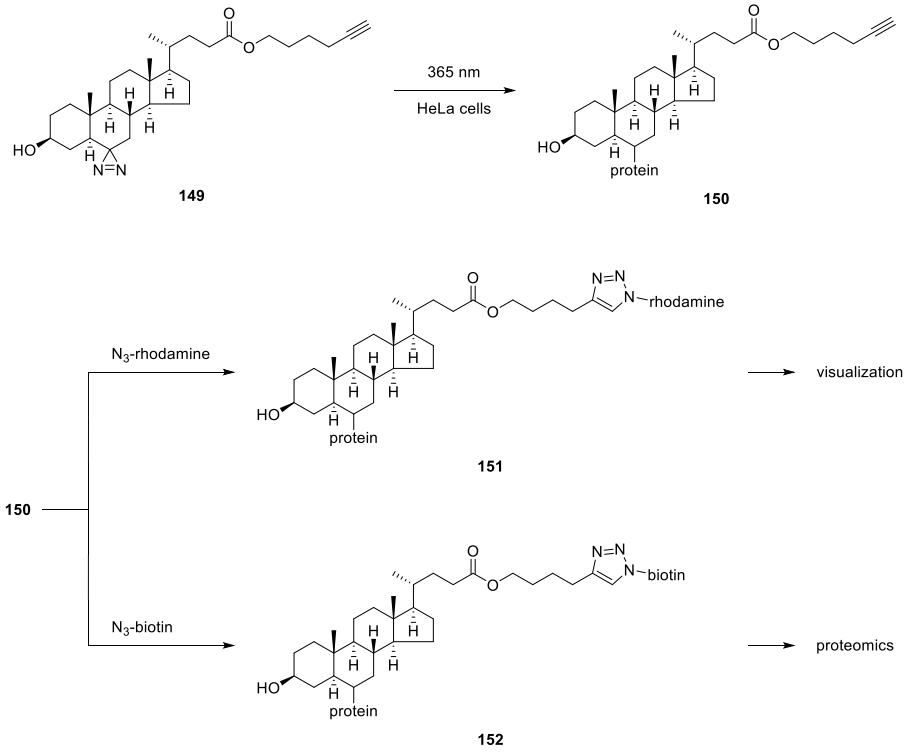

Figure 42. Cravatt's covalent capture of proteins with a bifunctional cholesterol and subsequent processing.

Taking our cues from these two outstanding examples of chemical biology, we designed our own bifunctional probes **153** based on 9-PAHSA (Figure 43), the most well studied of the FAHFAs. As in the above examples, our probe contains a photoreactive diazirine and a terminal alkyne. In light of what we have learned about FAHFA hydrolysis, we thought it essential to place the diazirine and alkyne moieties on different parts of the molecule, so that only proteins that interact with intact FAHFA would be pulled down. The

diazirine was placed on the fatty acid portion and the alkyne positioned on the HFA for ease of synthesis.

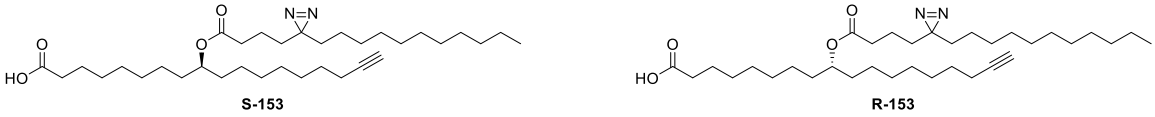

Figure 43. 9-PAHSA inspired bifunctional diazirine-alkyne probe.

The synthesis began with copper catalyzed addition of Grignard **154** to epoxide **41**, which was also used to synthesize the 9-series members of the FAHFA library. (Figure 44) The two silyl protecting groups were deprotected with TBAF, yielding diol **156**. Gratifyingly, the previously developed chemoselective oxidation, Pinnick oxidation, and Fisher-Speier esterification were effective on this substrate, giving methyl ester **S-159**. The antipode **R-159** was again synthesized using the Martin-Dodge variant of the Mitsunobu reaction, followed by chemoselective ester cleavage.

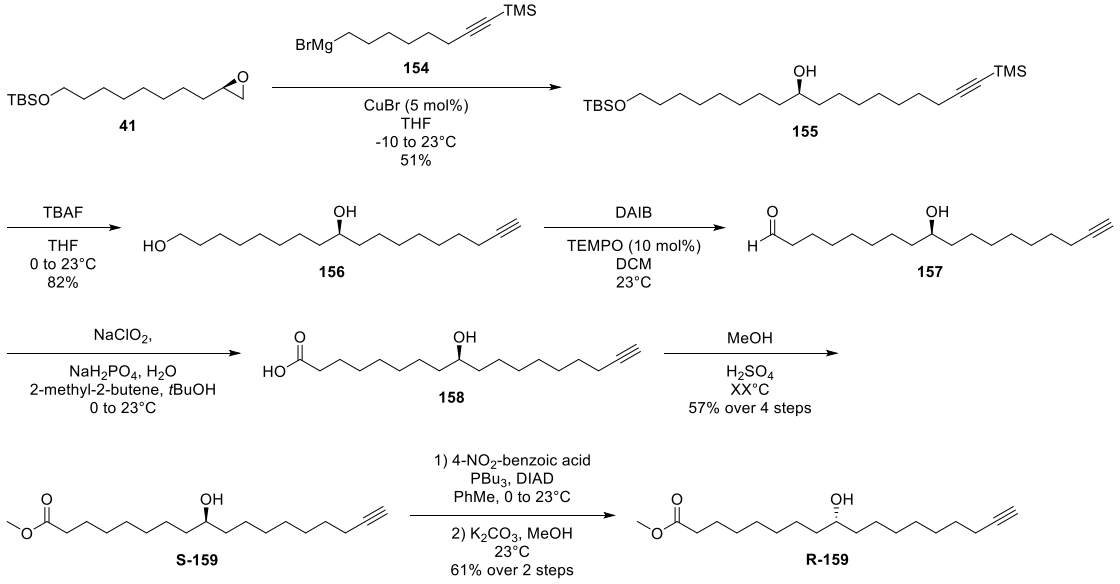

Figure 44. Synthesis of the alkyne-hydroxyfatty acid backbone of the 9-PAHSA probe.

The diazirine moiety was synthesized from commercially available acid chloride **160**. (Figure 45) Addition of undecylmagnesium bromide under copper catalysis to acid chloride **160** gave keto-ester **161**, which was previously synthesized with toxic cadmium.[76] Saponification with potassium hydroxide gave known keto-acid **162**.[77] The ketone of **162** was converted to diazirine **163** by the usual sequence. More recent methods using liquid ammonia were ineffective in our hands.

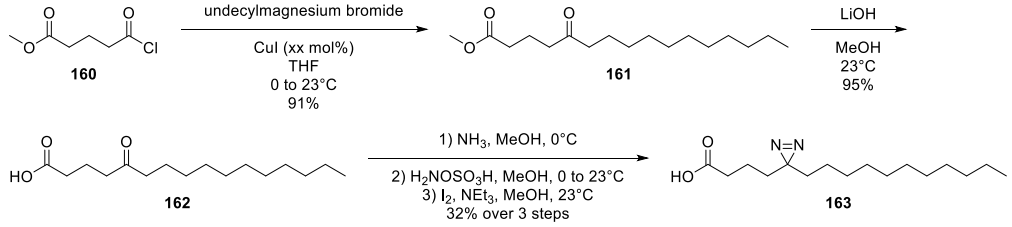

Figure 45. Synthesis of the diazirine moiety of the 9-PAHSA probe.

Diazirine-acid **163** was then appended to the secondary alcohol of **S-159** via Steglich esterification with EDCI, giving the penultimate product **S-160**. Chemoselective cleavage of the methyl ester with lithium hydroxide in THF gave the desired bifunctional probe **S-153**. The same reactions were carried out in similar yield for the antipode **R-153**.

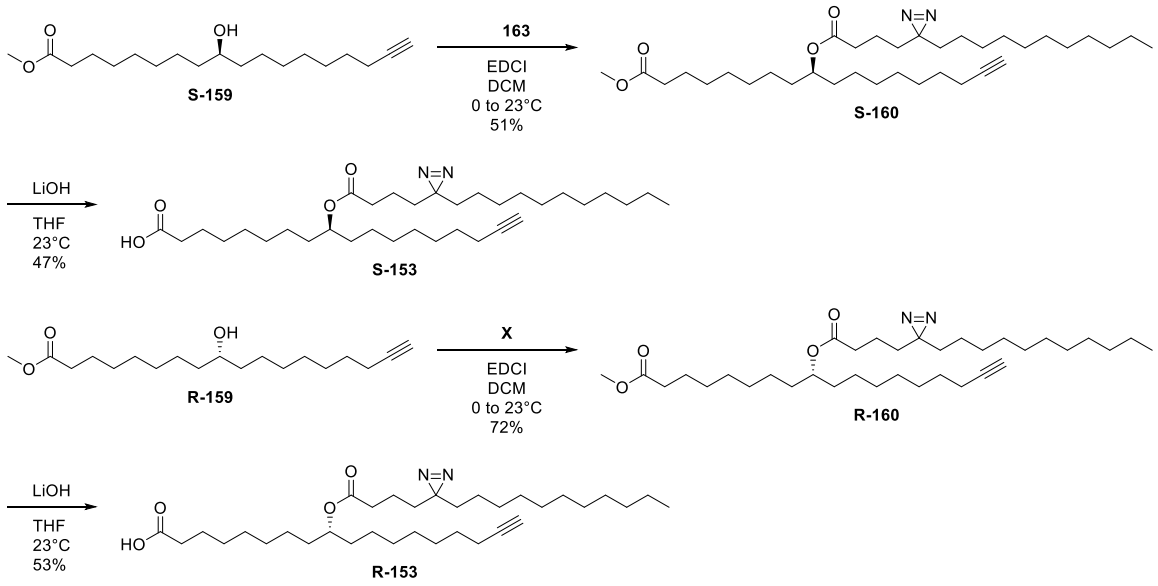

Figure 46. Endgame of the 9-PAHSA diazirine-alkyne probe.

Experiments are presently underway to determine the proteins with which 9-PAHSA derived probe **S/R-153** interacts. As the structure is similar to the natural product, the probe should allow us to determine in an unbiased manner the targets of 9-PAHSA, while also confirming the known interactions with gpr40 and gpr120. The results will be reported in due course.

3.2 Cobalt Catch-and-Release of alkynyl-9-PAHSA

While the bifunctional probe **153** will be a useful tool to determine the proteins with which 9-PAHSA interacts, it will be of limited value in the determination of the cellular and organismal metabolism of 9-PAHSA and 9-HSA. The data suggests that FAHFAs are enzymatically hydrolyzed to form HFAs and that HFAs are enzymatically acylated to form FAHFAs. It is easy to imagine many other possibilities, such as extension, beta oxidation, acylation, elimination of the secondary alcohol. How can we determine in an impartial manner the ways in which cells/organisms metabolize 9-PAHSA and 9-HSA?

Luckily, the labs of Brown and Turner have developed an ingenious solution to this problem. They found it was possible to "catch-and-release" alkynyl fatty acids that were incubated with cells. (Figure 47) First, lipids, including alkynyl lipids **161**, were extracted from the cell medium, then treated with Co2(CO)8, forming organocobalt species **162**. A silica supported phosphine resin **163** then displaced one of the carbonyl ligands from **163**, forming complex **164**. The solid support was then washed, removing compounds that did not contain any alkynes. Finally, complex **164** was treated with iron (III) nitrate, restoring alkyne **165**.

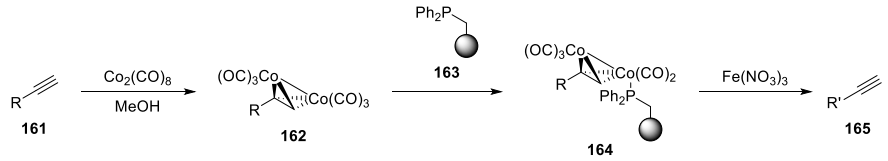

Figure 47. Cobalt "Catch-and-Release" approach to enriching samples.

Brown and Turner have validated this method with alkynyl palmitic acid surrogate **166**. (Figure 48) Probe **166** was incubated with RAW264.7 cells and, after lipid extraction and cobalt catch-and-release, analysis revealed that the majority of **166** was incorporated into phosphatidylcholine at position 1 **167**, position 2 **168**, or both 1 and 2 **169**. Furthermore, **166** was also elongated by 2 carbons, yielding alkynyl stearic acid **170**.

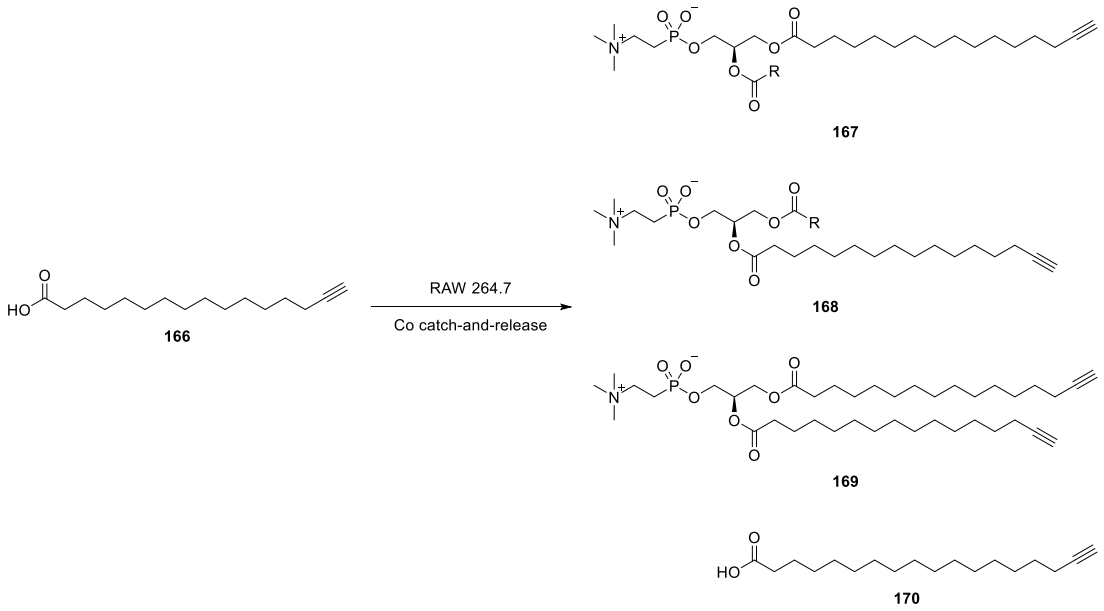

Figure 48. RAW264.7 cells incorporate palmitic acid surrogate into phosphatidylcholine lipids and elongate it by 2 carbons.

This clever work by Brown and Turner shows that, even with terminal alkyne in place, cells process fatty acids comparably to their native counterparts. With this in mind we have prepared both antipodes of a 9-HSA alkynyl derivative **158**. (Figure 49) Saponification of **159** with lithium hydroxide gave the products in good yield.

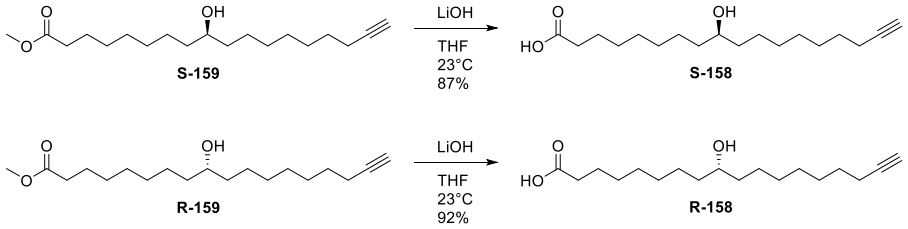

Figure 49. Synthesis of both enantiomers of 9-hydroxystearic acid probe for cobalt catch-and-release.

In addition, we also synthesized alkynal 9-PAHSA in order to investigate its metabolism. The secondary alcohol of **159** was acylated with palmitoyl chloride, yielding

diester **171**, which was chemoselectively saponified with lithium hydroxide to the desired alkyne derivative **172**.

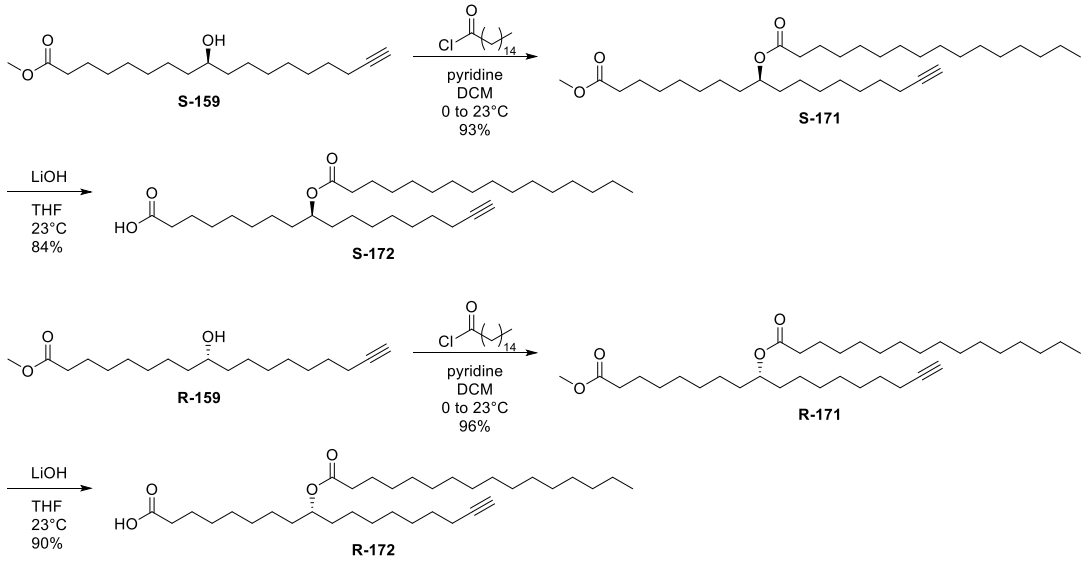

Figure 50. Synthesis of alkynyl 9-PAHSA for cobalt catch-and-release.

To recapitulate, we have synthesized both a bifunctional diazirine-alkyne derivative of 9-PAHSA and an alkynyl variant of 9-PAHSA. The former will allow us to determine in an unbiased manner the small molecule-protein interactions in which 9-PAHSA participates; the latter will provide an unprejudiced view of the small molecule modification that 9-PAHSA experiences. The results of this experimentation will be reported in due course.

Experimental Section

General Information

All reactions were performed in flame- or oven-dried glassware sealed with rubber septa and under nitrogen atmosphere, unless otherwise indicated. Air- and/or moisture-sensitive liquids or solutions were transferred by cannula or syringe. Organic solutions were concentrated by rotary evaporator at 30 millibar with the water bath heated to not more than 40°C, unless specified otherwise. Tetrahydrofuran (THF), diethyl ether (Et2O), and dichloromethane (DCM) were purified with a Pure-Solve MD-5 Solvent Purification System (Innovative Technology). Thin-layer chromatography (TLC) was performed using 0.2 mm commercial silica gel plates (silica gel 60, F254, EMD Chemicals) and visualized with a UV lamp (short and long wave) and/or aqueous potassium permanganate (KMnO4) stain. Optical rotations were measured on a JASCO P-2000 polarimeter. Melting points were measured with a MEL-TEMP apparatus without correction. Nuclear Magnetic Resonance (NMR) spectra were recorded on a Varian 600 MHz (1H at 600 MHz, 13C at 151 MHz). All spectra were taken in CDCl3 with shifts reported in parts per million (ppm) referenced to protium or carbon of the solvent (7.26 or 77.16, respectively). Coupling constants are reported in Hertz (Hz). Data for 1H-NMR are reported as follows: chemical shift (ppm, reference to protium; s = single, d = doublet, t = triplet, q = quartet, dd = doublet of doublets, ddd = doublet of doublet of doublets, m = multiplet, coupling constant (Hz), and integration). High Resolution Mass Spectra (HRMS) were acquired on an Agilent 6230 High Resolution time-of-flight mass spectrometer and reported as m/z for the molecular ion [M+Na]+, [M+H]+, [M-H]+, or [M-Cl]+.

Synthesis of Racemic 5- and 9-PAHSA

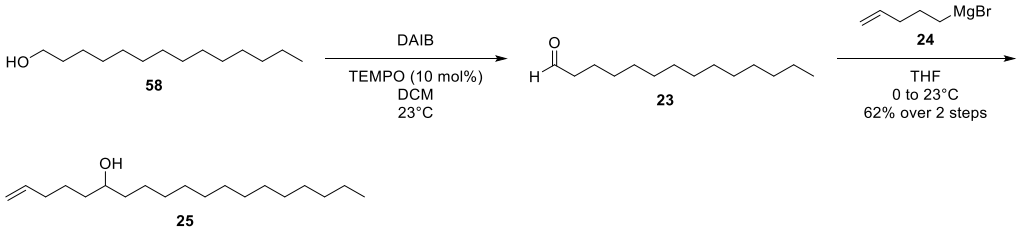

nonadec-1-en-6-ol **25**

A 250 mL round-bottom flask equipped with stir bar was charged sequentially with tetradecanol (21.44 g, 100 mmol, 1 eq), DCM (100 mL, 1 M), TEMPO (1.56 g, 10.0 mmol, 0.1 eq), and DAIB (35.4 g, 110 mmol, 1.1 eq), giving a clear, orange solution. The reaction was monitored by TLC. Upon completion the reaction was quenched with sat aq sodium thiosulfate (100 mL) and DI water (50 mL), extracted with ethyl acetate (100 mL x 3). Organics were combined and washed with sat aq sodium bicarbonate (50 mL x 3) and brine (50 mL), dried (sodium sulfate), filtered, concentrated, and used in the next step without further purification.

A 500 mL dry round-bottom flask under nitrogen atmosphere and equipped with stir bar was charged with tetradecanal (100 mmol, 1 eq) and dissolved in dry THF (200 mL, 0.5M). Stirring was initiated, giving a clear solution. The reaction vessel was cooled in an ice water bath before adding a solution pent-4-enylmagnesium bromide **24** (228 mL, 0.527 M, 120 mmol, 1.2 eq) dropwise via syringe pump over 60 minutes.

The Grignard **24** was prepared as follows: a 500 mL round-bottom flask was equipped with stir bar and magnesium turnings (18.23 g, 750 mmol, 3.75 eq). The reaction vessel was flame-dried under vacuum, cooled to ambient temperature, flushed with nitrogen, and sealed with a rubber septum. Dry THF (200 mL, 1 M) was added via syringe. Stirring was initiated, giving a heterogeneous mixture of solvent and turnings. A solution of DIBAL in toluene (6.25 mL, 1.2 M, 7.50 mmol, 0.0375 eq) was added by syringe and

the reaction was aged for 5 min. The reaction vessel was then warmed to 35°C in an oil bath before adding dropwise via syringe pump over 200 minutes 5-bromo-1-pentene (23.7 mL, 200 mmol, 1 eq). After addition was complete, the reaction was warmed to 50°C, then cooled to ambient temperature. The Grignard was titrated according to the method of Paquette (Synthetic Communication. 1994, 24, 2503-2506) and the concentration was 0.527 M.

The reaction was allowed to warm to ambient temperature overnight, quenched with saturate aqueous ammonium chloride (100 mL). The mixture was transferred to a separatory funnel and extracted with a mixture of ethyl ether:hexanes (50:50, 200 mL x 3). Combined organics were washed with brine (100 mL), dried (sodium sulfate), filtered, and concentrated to give a crude solid. The residue was purified by silica gel column chromatography, eluting with hexanes:EtOAc (95:5 to 90:10) to yield alcohol 25 (17.52 g, 62%) as a white solid.

Rf = 0.35 (silica gel, 90:10 hexanes:EtOAc, KMnO4); MP (°C): 42-43; 1H-NMR (600 MHz, CDCl3): δ 5.81 (m, 1H), 5.04 – 4.98 (m, 1H), 4.98 – 4.93 (m, 1H), 3.59 (s, 1H), 2.12 – 2.02 (m, 2H), 1.59 – 1.21 (m, 29H), 0.88 (t, J = 7.0 Hz, 3H); 13C-NMR (151 MHz, CDCl3): δ 138.91, 114.71, 72.01, 37.69, 37.03, 33.89, 32.07, 29.85, 29.84, 29.82, 29.81, 29.80, 29.78, 29.77, 29.51, 25.80, 25.08, 22.84, 14.26; IR (film, cm-1): 911, 1467, 2849, 2916, 2956, 3327; HRMS (APCI) calc. for C19H37O [M-H]+: 281.2839, obs. 281.2841.

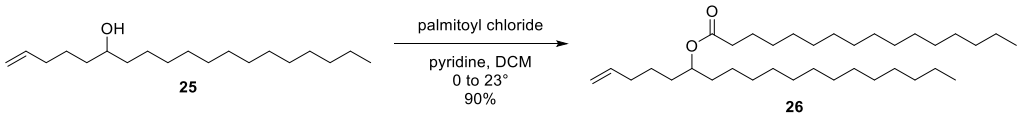

A dry 1000 mL round-bottom flask equipped with stir, under nitrogen atmosphere, and sealed with a rubber septum was charged with alcohol 25 (17.52 g, 62.0 mmol, 1 eq) and dry dichloromethane (374 mL, 0.17 M). Stirring was initiated, giving a clear solution. Dry pyridine (25.1 mL, 310 mmol, 5 eq) was added dropwise via syringe. The reaction vessel was submerged in an ice water bath and aged 30 minutes. Palmitoyl chloride (20.7 mL, 68.2 mmol, 1.1 eq) was added dropwise via syringe. The reaction was allowed to warm to ambient temperature and stirred overnight. The reaction was quenched with deionized water (100 mL) and stirred vigorously for 30 minutes. The biphasic mixture was transferred to a separatory funnel. The layers were partitioned and separated. The organic layer was saved while the aqueous layer was extracted with dichloromethane (150 mL x 2). Organics were combined and washed with 0.5 M aqueous hydrochloric acid (100 mL), saturate aqueous sodium bicarbonate (100 mL), and brine (100 mL), dried (sodium sulfate), filtered, and concentrated. The crude product was purified by silica column chromatography, eluting with hexanes:EtOAc (100:0 to 95:5) to give 26 (29.1 g, 90%) as a clear oil.

Clear oil. Yield = 90%; Rf = 0.52 (silica gel, 95:5 hexanes:EtOAc, KMnO4); 1H-NMR (600 MHz, CDCl3): 1H NMR (600 MHz, CDCl3) δ 5.78 (m, 1H), 5.00 (dd, J = 17.1, 1.6 Hz, 1H), 4.95 (dd, J = 10.1, 0.7 Hz, 1H), 4.92 – 4.84 (m, 1H), 2.28 (t, J = 7.5 Hz, 2H), 2.07 – 2.00 (m, 2H), 1.65 – 1.57 (m, 2H), 1.57 – 1.21 (m, 52H), 0.88 (t, J = 7.0 Hz, 6H); 13C-NMR (151 MHz, CDCl3): δ 173.84, 138.67, 114.82, 73.99, 34.88, 34.32, 33.73, 33.71, 32.08, 29.85, 29.84, 29.83, 29.81, 29.78, 29.74, 29.70, 29.68, 29.66, 29.52, 29.46,

29.35, 25.46, 25.34, 24.74, 22.84, 14.26; IR (film, cm-1): 1466, 1735, 2853, 2924; HRMS (ESI) calc. for C35H68O2Na [M+Na]+: 543.5112, obs. 543.5095.

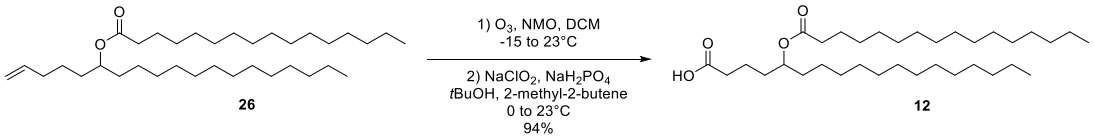

4-methylmorpholine N-oxide monohydrate (20.3 g, 150 mmol, 3 eq) was dehydrated by heating at 90°C under high vacuum overnight. Following the ozonolysis conditions of Drussault, a 500 mL round-bottom flask was charged with olefin X (26.0 g, 50 mmol, 1 eq), the anhydrous 4-methyl N-oxide prepared above, and dry DCM (333 mL, 0.15M). Stirring was initiated, affording a clear solution. The reaction vessel was submerged in an ice-acetone bath and cooled to approximately -10°C for 15 minutes before bubbling in a mixture of ozone/oxygen. Conversion was complete within 15 minutes. The ozone generator was turned off and oxygen was bubbled through the solution for an additional 5 minutes. The reaction vessel was allowed to warm to ambient temperature and aged for 1 hour. The reaction was concentrated and the residue was dissolved in ethyl acetate (300 mL) and washed with water (100 mL) and brine (50 mL x 2), dried (sodium sulfate), filtered, and concentrated. The crude material was used in the next step without further purification.

A 250 mL round-bottom flask equipped with stir bar and addition funnel was charged with the crude material above and dissolved in 2-methyl-2-butene (53 mL, 500 mmol, 10 eq) and tert-butanol (250 mL, 0.2 M). Stirring was initiated, affording a clear solution. The reaction vessel was cooled in an ice-water bath for 30 minutes before adding an aqueous solution of sodium phosphate monobasic monohydrate (27.6 g, 200 mmol, 4 eq) and sodium chlorite (technical grade, 80%, 22.6 g, 200 mmol, 4 eq) in deionized water (125 mL) dropwise via addition funnel. The reaction was allowed to warm to ambient temperature and stirred overnight.

Peroxide test strips revealed the presence of peroxides. After adding an aqueous solution of sodium bisulfite (31.2 g, 300 mmol, 6 eq) in deionized water (125 mL) dropwise via addition funnel and aging 30 minutes, peroxides were absent. 2-methyl-2-butene and tert-butanol were removed by rotavap with water bath at 50°C. The residual aqueous layer was extracted with hexanes:ethyl acetate (50:50, 100 mL x 3). Combined organics were washed with brine (100 mL), dried (sodium sulfate), filtered, and concentrated. The crude product was purified by silica column chromatography, eluting with hexanes:EtOAc (90:10 to 70:30) to yield X (25.3 g. 94%) as a white solid.

Rf = 0.29 (silica gel, 80:20 hexanes:EtOAc, KMnO4); MP: (°C) 34; 1H-NMR (600 MHz, CDCl3): δ 4.89 – 4.83 (m, 1H), 2.34 (t, J = 7.5 Hz, 2H), 2.27 (t, J = 7.5 Hz, 2H), 1.65 – 1.58 (m, 4H), 1.50 (m, J = 4.8 Hz, 4H), 1.27 (m, J = 22.8 Hz, 46H), 0.88 (t, J = 6.8 Hz, 6H); 13C-NMR (151 MHz, CDCl3): δ 179.05, 173.91, 74.17, 34.90, 34.31, 34.28, 33.97, 32.08, 32.05, 29.85, 29.82, 29.81, 29.78, 29.71, 29.69, 29.67, 29.51, 29.46, 29.46, 29.35, 29.27, 29.12, 25.47, 25.40, 25.34, 24.78, 22.84, 22.83, 14.26, 14.25; IR (film, cm-1): 1466, 1635, 1711, 1733, 2854, 2925, 3427; HRMS (ESI) calc. for C34H66O4Na [M+Na]+: 561.4853, obs. 561.4855.

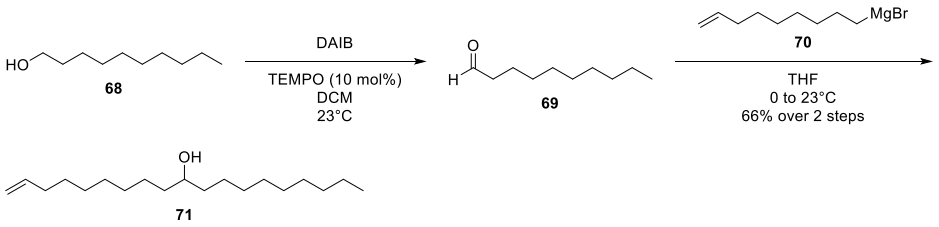

A 250 mL round-bottom flask equipped with stir bar was charged sequentially with decanol (19.07 mL, 100 mmol, 1 eq), DCM (100 mL, 1 M), TEMPO (1.56 g, 10.0 mmol, 0.1 eq), and DAIB (35.4 g, 110 mmol, 1.1 eq), giving a clear, orange solution. The reaction was monitored by TLC. Upon completion the reaction was quenched with sat aq sodium thiosulfate (100 mL) and DI water (50 mL), extracted with ethyl acetate (100 mL x 3). Organics were combined and washed with sat aq sodium bicarbonate (50 mL x 3) and brine (50 mL), dried (sodium sulfate), filtered, concentrated, and used in the next step without further purification.

A 500 mL dry round-bottom flask under nitrogen atmosphere and equipped with stir bar was charged with decanal (100 mmol, 1 eq) and dissolved in dry THF (200 mL, 0.5M). Stirring was initiated, giving a clear solution. The reaction vessel was cooled in an ice water bath before adding a solution non-8-enylmagnesium bromide X (239 mL, 0.502 M, 120 mmol, 1.2 eq) dropwise via syringe pump over 60 minutes.

The Grignard 70 was prepared as follows: a 500 mL round-bottom flask was equipped with stir bar and magnesium turnings (18.23 g, 750 mmol, 3.75 eq). The reaction vessel was flame-dried under vacuum, cooled to ambient temperature, flushed with nitrogen, and sealed with a rubber septum. Dry THF (200 mL, 1 M) was added via syringe. Stirring was initiated, giving a heterogeneous mixture of solvent and turnings. A solution of DIBAL in toluene (6.25 mL, 1.2 M, 7.50 mmol, 0.0375 eq) was added by syringe and the reaction was aged for 5 min. The reaction vessel was then warmed to 35°C in an oil bath before adding dropwise via syringe pump over 200 minutes 9-bromo-1-nonene (37.1

mL, 200 mmol, 1 eq). After addition was complete, the reaction was warmed to 50°C, then cooled to ambient temperature. The Grignard was titrated according to the method of Paquette (Synthetic Communication. 1994, 24, 2503-2506) and the concentration was 0.502 M.

The reaction was allowed to warm to ambient temperature overnight, quenched with saturate aqueous ammonium chloride (100 mL). The mixture was transferred to a separatory funnel and extracted with a mixture of ethyl ether:hexanes (50:50, 200 mL x 3). Combined organics were washed with brine (100 mL), dried (sodium sulfate), filtered, and concentrated to give a crude solid. The residue was purified by silica gel column chromatography, eluting with hexanes:EtOAc (95:5 to 90:10) to yield alcohol X (18.65 g, 66%) as a white solid.

nonadec-1-en-10-ol **71**

Rf = 0.41 (silica gel, 90:10 hexanes:EtOAc, KMnO4); MP (°C): 51-52; 1H-NMR (600 MHz, CDCl3) δ 5.80 (m, 1H), 4.98 (dd, J = 17.1, 1.6 Hz, 1H), 4.92 (d, J = 10.2 Hz, 1H), 3.59 – 3.54 (m, 1H), 2.03 (q, J = 7.1 Hz, 2H), 1.48 – 1.20 (m, 29H), 0.87 (t, J = 7.0 Hz, 3H); 13C-NMR (151 MHz, CDCl3): δ 139.30, 114.25, 72.11, 37.64, 37.61, 33.92, 32.03, 29.86, 29.79, 29.78, 29.72, 29.60, 29.46, 29.22, 29.05, 25.80, 25.78, 22.81, 14.23; IR (film, cm-1): 650, 735, 909, 994, 1466, 2854, 2926, 3373; HRMS (APCI) calc. for C19H37O [M-H]+: 281.2839, obs. 281.2843.

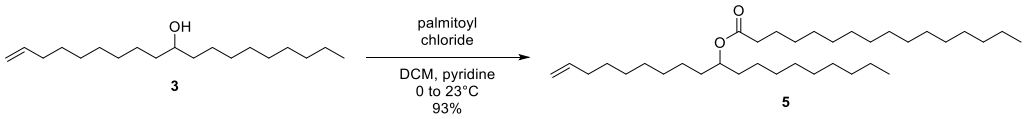

A dry 1000 mL round-bottom flask equipped with stir, under nitrogen atmosphere, and sealed with a rubber septum was charged with alcohol X (18.21 g, 64.5 mmol, 1 eq) and dry dichloromethane (388 mL, 0.17 M). Stirring was initiated, giving a clear solution. Dry pyridine (26.1 mL, 322 mmol, 5 eq) was added dropwise via syringe. The reaction vessel was submerged in an ice water bath and aged 30 minutes. Palmitoyl chloride (21.5 mL, 70.9 mmol, 1.1 eq) was added dropwise via syringe. The reaction was allowed to warm to ambient temperature and stirred overnight. The reaction was quenched with deionized water (100 mL) and stirred vigorously for 30 minutes. The biphasic mixture was transferred to a separatory funnel. The layers were partitioned and separated. The organic layer was saved while the aqueous layer was extracted with dichloromethane (150 mL x 2). Organics were combined and washed with 0.5 M aqueous hydrochloric acid (100 mL), saturate aqueous sodium bicarbonate (100 mL), and brine (100 mL), dried (sodium sulfate), filtered, and concentrated. The crude product was purified by silica column chromatography, eluting with hexanes:EtOAc (100:0 to 95:5) to give X (31.2 g, 93%) as a clear oil.

nonadec-1-en-10-yl palmitate 5

Rf = 0.58 (silica gel, 95:5 hexanes:EtOAc, KMnO4); 1H-NMR (600 MHz, CDCl3): δ 5.80 (m, 1H), 4.98 (dd, J = 17.1, 1.4 Hz, 1H), 4.92 (d, J = 10.2 Hz, 1H), 4.89 – 4.84 (m, 1H), 2.27 (t, J = 7.5 Hz, 2H), 2.03 (q, J = 7.1 Hz, 2H), 1.65 – 1.58 (m, 2H), 1.50 (m, J = 5.0 Hz, 4H), 1.43 – 1.20 (m, 48H), 0.88 (t, J = 7.0 Hz, 6H); 13C-NMR (151 MHz, CDCl3): δ 173.80, 139.27, 114.27, 74.16, 34.89, 34.32, 34.31, 33.93, 32.08, 32.05, 29.85, 29.84, 29.82, 29.81, 29.78, 29.71, 29.69, 29.67, 29.62, 29.53, 29.51, 29.47, 29.35, 29.19, 29.05,

25.47, 25.45, 25.34, 22.84, 22.83, 14.25, 14.24; IR (film, cm-1) 909, 1176, 1466, 1734, 2854, 2925; HRMS (APCI) calc. for C35H69O2 [M+H]+: 521.5292, obs. 521.5292.

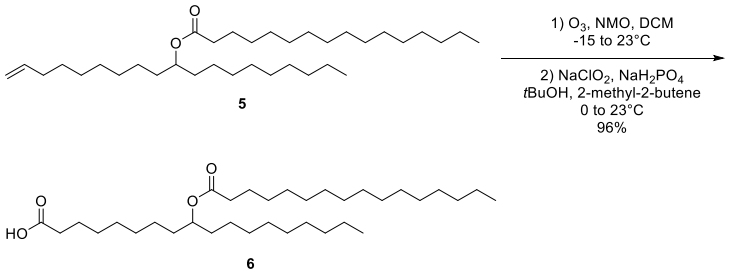

4-methylmorpholine N-oxide monohydrate (20.3 g, 150 mmol, 3 eq) was dehydrated by heating at 90°C under high vacuum overnight. Following the ozonolysis conditions of Drussault, a 500 mL round-bottom flask was charged with olefin X (26.0 g, 50 mmol, 1 eq), the anhydrous 4-methyl N-oxide prepared above, and dry DCM (333 mL, 0.15M). Stirring was initiated, affording a clear solution. The reaction vessel was submerged in an ice-acetone bath and cooled to approximately -10°C for 15 minutes before bubbling in a mixture of ozone/oxygen. Conversion was complete within 15 minutes. The ozone generator was turned off and oxygen was bubbled through the solution for an additional 5 minutes. The reaction vessel was allowed to warm to ambient temperature and aged for 1 hour. The reaction was concentrated and the residue was dissolved in ethyl acetate (300 mL) and washed with water (100 mL) and brine (50 mL x 2), dried (sodium sulfate), filtered, and concentrated. The crude material was used in the next step without further purification.

A 250 mL round-bottom flask equipped with stir bar and addition funnel was charged with the crude material above and dissolved in 2-methyl-2-butene (53 mL, 500 mmol, 10 eq) and tert-butanol (250 mL, 0.2 M). Stirring was initiated, affording a clear solution. The reaction vessel was cooled in an ice-water bath for 30 minutes before adding an aqueous solution of sodium phosphate monobasic monohydrate (27.6 g, 200 mmol, 4 eq) and sodium chlorite (technical grade, 80%, 22.6 g, 200 mmol, 4 eq) in deionized water

(125 mL) dropwise via addition funnel. The reaction was allowed to warm to ambient temperature and stirred overnight.

Peroxide test strips revealed the presence of peroxides. After adding an aqueous solution of sodium bisulfite (31.2 g, 300 mmol, 6 eq) in deionized water (125 mL) dropwise via addition funnel and aging 30 minutes, peroxides were absent. 2-methyl-2-butene and tert-butanol were removed by rotavap with water bath at 50°C. The residual aqueous layer was extracted with hexanes:ethyl acetate (50:50, 100 mL x 3). Combined organics were washed with brine (100 mL), dried (sodium sulfate), filtered, and concentrated. The crude product was purified by silica column chromatography, eluting with hexanes:EtOAc (90:10 to 70:30) to yield X (25.6 g. 95%) as a white solid.

9-PAHSA 6

Rf = 0.29 (silica gel, 80:20 hexanes:EtOAc, KMnO4); MP: (°C) 34; 1H-NMR (600 MHz, CDCl3): δ 4.89 – 4.83 (m, 1H), 2.34 (t, J = 7.5 Hz, 2H), 2.27 (t, J = 7.5 Hz, 2H), 1.65 – 1.58 (m, 4H), 1.50 (m, J = 4.8 Hz, 4H), 1.27 (m, J = 22.8 Hz, 46H), 0.88 (t, J = 6.8 Hz, 6H); 13C-NMR (151 MHz, CDCl3): δ 179.05, 173.91, 74.17, 34.90, 34.31, 34.28, 33.97, 32.08, 32.05, 29.85, 29.82, 29.81, 29.78, 29.71, 29.69, 29.67, 29.51, 29.46, 29.46, 29.35, 29.27, 29.12, 25.47, 25.40, 25.34, 24.78, 22.84, 22.83, 14.26, 14.25; IR (film, cm-1): 1466, 1635, 1711, 1733, 2854, 2925, 3427; HRMS (ESI) calc. for C34H66O4Na [M+Na]+: 561.4853, obs. 561.4855.

Synthesis of Enantiopure 9-PAHSA and 9-HAS

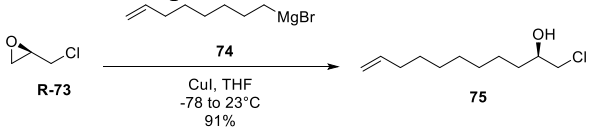

A 250 mL round-bottom flask equipped with stir bar and charged with magnesium turnings (2.96 g, 122 mmol, 3.75 eq) was flame dried under vacuum, cooled to ambient temperature, flushed with nitrogen, and sealed with a rubber septum. Dry THF (66 mL, 2/3 total volume) was added by syringe. Stirring was initiated, affording a heterogeneous mixture of clear solvent and metal turnings. A solution of DIBAL in toluene (0.27 mL, 1.2 M, 0.32 mmol, 0.01 eq) was added via syringe to activate the magnesium turnings. The reaction vessel was submerged in an oil bath, warmed to 35°C, and aged for 5 minutes before adding 8-bromo-1-octene (8.16 mL, 48.6 mmol, 1.5 eq) dropwise over 30 minutes by syringe pump. The reaction turned increasingly brown over the course of addition and the temperature rose to 41°C. After addition was complete, the vessel was warmed to 50°C before being allowed to cool to ambient temperature. The reaction was stirred for an additional 2 hours. A second 250 mL round-bottom flask equipped with stir bar and charged with copper (I) iodide (0.62 g, 3.24 mmol, 0.10 eq) was flame dried under vacuum, cooled to ambient temperature, flushed with nitrogen, sealed with a rubber septum, and maintained under a nitrogen atmosphere. Dry THF (33 mL, 1/3 total volume) and S-(-)-epichlorohydrin 4 (2.54 mL, 32.4 mmol, 1 eq) were added by syringe, giving a white, opaque mixture. The reaction vessel was submerged in a dry ice-acetone bath and cooled for 15 minutes. The Grignard reagent prepared above was drawn up in a syringe and added dropwise via syringe pump over 1 hour to the cooled mixture of S-(-)-epichlorohydrin 4. The reaction was allowed to warm to ambient temperature overnight and the color changed to a deep, dark blue. The reaction was carefully quenched with 100 mL saturated aqueous ammonium chloride. The mixture was stirred vigorously until the color changed to a

brilliant, royal blue. The mixture was transferred to a separatory funnel and extracted with a mixture of ethyl ether:hexanes (50:50, 50 mL x 3). Combined organics were washed with saturated aqueous ammonium chloride (50 mL x 2), brine (50 mL), dried (sodium sulfate), filtered, and concentrated to give a crude, slightly yellow oil. The residue was purified by silica gel column chromatography, eluting with hexanes:EtOAc (95:5 to 90:10) to afford S-5 (6.11 g, 92%) as a clear oil.

S-1-chloroundec-10-en-2-ol 5

Rf = 0.29 (silica gel, 90:10 hexanes:EtOAc, KMnO4); 1H-NMR (600 MHz, CDCl3): δ 5.81 (m, 1H), 5.02 – 4.96 (m, 1H), 4.95 – 4.90 (m, 1H), 3.83 – 3.77 (m, 1H), 3.63 (dd, J = 11.1, 3.2 Hz, 1H), 3.47 (dd, J = 11.1, 7.2 Hz, 1H), 2.13 (d, J = 4.9 Hz, 1H), 2.04 (q, J = 14.4, 7.0 Hz, 2H), 1.57 – 1.26 (m, 13H); 13C-NMR (151 MHz, CDCl3): δ 139.30, 114.33, 71.61, 50.76, 34.37, 33.91, 29.58, 29.47, 29.15, 29.02, 25.65; IR (film, cm-1): 3377; HRMS (APCI) calc. for C11H21O [M-Cl]+: 169.1587, obs. 169.1584.

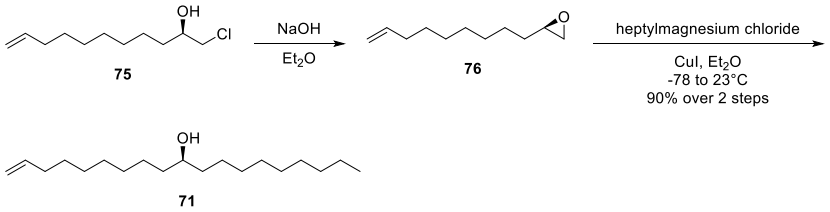

75 76 71

A 100 mL round-bottom flask equipped with an egg-shaped stir bar was charged with chlorohydrin 5 (5.61 g, 27.4 mmol, 1 eq) and dissolved in dry ether (55 mL, 0.5M). Stirring was initiated, giving a clear solution. Freshly crushed sodium hydroxide (6.58 g, 164 mmol, 6 eq) was added in one portion, affording a heterogeneous mixture. The reaction was stirred vigorously (1200 rpm) and monitored by aliquot 1H-NMR. Conversion was complete within 3 hours. The mixture was vacuum filtered into a dry flask containing 4Å mole sieves, rinsing the filter cake with dry ether (25 mL x 3). The vessel was sealed with a rubber septum and spurged with nitrogen. After aging over sieves for 3 hours, crude epoxide 6 was used without purification.

A 500 mL round-bottom flask charged with magnesium turnings (4.01 g, 165 mmol, 1 eq) and equipped with a stir bar and reflux condenser. The ensemble was flame dried under vacuum, cooled to ambient temperature, flushed with nitrogen, sealed with a rubber septum, and maintained under a nitrogen atmosphere. Dry ether (82.5 mL, 1/2 total volume) was added via syringe. Stirring was initiated, giving a heterogeneous mixture of solvent and turnings. A solution of DIBAL in toluene (1.38 mL, 1.2 M, 1.65 mmol, 0.01 eq) was added by syringe and the reaction was aged for 5 min. A clear solution of 1-chlorooctane (28.0 mL, 165 mmol, 1 eq) in dry ether (82.5 mL, 1/2 total volume) was added dropwise and the reaction was heated to reflux for 3 hours. The reaction yellowed slightly over the course of the reflux and grew increasingly opaque. Most of the magnesium turnings were consumed. The reaction was allowed to cool to ambient temperature.

Stirring was arrested and the supernatant solution of 1-octylmagnesium chloride was titrated as 0.52 M using the method of Love and Jones.

A 500 mL round-bottom flask equipped with stir bar and charged with copper (I) iodide (0.522 g, 2.75 mmol, 0.1 eq) was flame dried under vacuum, cooled to ambient temperature, flushed with nitrogen, and sealed with a rubber septum. The ethereal solution of epoxide 5 was vacuum filtered into the reaction vessel to remove the molecular sieves. Stirring was initiated, affording an opaque mixture. A dry addition funnel was attached and the reaction was cooled in a dry ice-acetone bath for 30 minutes. The ethereal solution of 1-octylmagnesium chloride (79 mL, 0.52 M, 41.3 mmol, 1.5 eq) prepared above was transferred via cannula to the addition funnel and added dropwise over 1 hour. The reaction mixture was allowed to warm to ambient temperature overnight and the color changed to a deep, dark blue. The reaction was carefully quenched with 200 mL saturated aqueous ammonium chloride. The mixture was stirred vigorously until the color changed to a brilliant, royal blue. The mixture was transferred to a separatory funnel and extracted with a mixture of ethyl ether:hexanes (50:50, 100 mL x 3). Combined organics were washed with saturated aqueous ammonium chloride (50 mL x 2), brine (50 mL), dried (sodium sulfate), filtered, and concentrated to give a crude solid. The residue was purified by silica gel column chromatography, eluting with hexanes:EtOAc (95:5 to 90:10) to yield R-7 (5.45 g, 70%) as a white solid.

R-nonadec-1-en-10-ol 7

Rf = 0.41 (silica gel, 90:10 hexanes:EtOAc, $KMnO_4$); MP (°C): 51-52; 1H-NMR (600 MHz, $CDCl_3$) δ 5.80 (m, 1H), 4.98 (dd, J = 17.1, 1.6 Hz, 1H), 4.92 (d, J = 10.2 Hz, 1H), 3.59 – 3.54 (m, 1H), 2.03 (q, J = 7.1 Hz, 2H), 1.48 – 1.20 (m, 29H), 0.87 (t, J = 7.0 Hz, 3H); 13C-NMR (151 MHz, $CDCl_3$): δ 139.30, 114.25, 72.11, 37.64, 37.61, 33.92,

32.03, 29.86, 29.79, 29.78, 29.72, 29.60, 29.46, 29.22, 29.05, 25.80, 25.78, 22.81, 14.23; IR (film, cm-1): 3373; HRMS (APCI) calc. for C19H37O [M-H]+: 281.2839, obs. 281.2843.

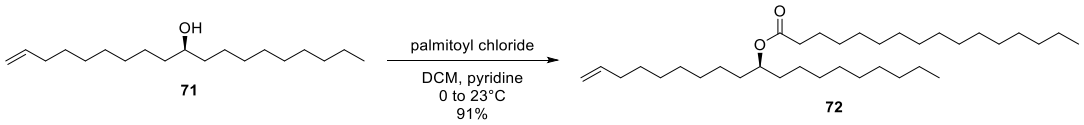

A dry 250 mL round-bottom flask equipped with stir bar, under nitrogen atmosphere, and sealed with a rubber septum was charged with alcohol 7 (4.45 g, 15.8 mmol, 1 eq) and dry dichloromethane (95 mL). Stirring was initiated, giving a clear solution. Dry pyridine (6.37 mL, 79 mmol, 5 eq) was added dropwise via syringe. The reaction vessel was submerged in an ice water bath and aged 15 minutes. Palmitoyl chloride (5.26 mL, 17.3 mmol, 1.1 eq) was added dropwise via syringe. The reaction was allowed to warm to ambient temperature and stirred overnight. The reaction was quenched with deionized water (100 mL) and stirred vigorously for 30 minutes. The biphasic mixture was transferred to a separatory funnel. The layers were partitioned and separated. The organic layer was saved while the aqueous layer was extracted with dichloromethane (150 mL x 2). Organics were combined and washed with 0.5 M aqueous hydrochloric acid (100 mL), saturate aqueous sodium bicarbonate (100 mL), and brine (100 mL), dried (sodium sulfate), filtered, and concentrated. The crude product was purified by silica column chromatography, eluting with hexanes:EtOAc (100:0 to 95:5) to give 8 (7.46 g, 91%) as a yellow oil.

R-nonadec-1-en-10-yl palmitate 8

Rf = 0.58 (silica gel, 95:5 hexanes:EtOAc, KMnO4); 1H-NMR (600 MHz, CDCl3): δ 5.80 (m, 1H), 4.98 (dd, J = 17.1, 1.4 Hz, 1H), 4.92 (d, J = 10.2 Hz, 1H), 4.89 – 4.84 (m, 1H), 2.27 (t, J = 7.5 Hz, 2H), 2.03 (q, J = 7.1 Hz, 2H), 1.65 – 1.58 (m, 2H), 1.50 (m, J = 5.0 Hz, 4H), 1.43 – 1.20 (m, 48H), 0.88 (t, J = 7.0 Hz, 6H); 13C-NMR (151 MHz, CDCl3): δ 173.80, 139.27, 114.27, 74.16, 34.89, 34.32, 34.31, 33.93, 32.08, 32.05, 29.85, 29.84, 29.82, 29.81, 29.78, 29.71, 29.69, 29.67, 29.62, 29.53, 29.51, 29.47, 29.35, 29.19, 29.05,

25.47, 25.45, 25.34, 22.84, 22.83, 14.25, 14.24; IR (film, cm-1) 1734; HRMS (APCI) calc. for C35H69O2 [M+H]+: 521.5292, obs. 521.5292.

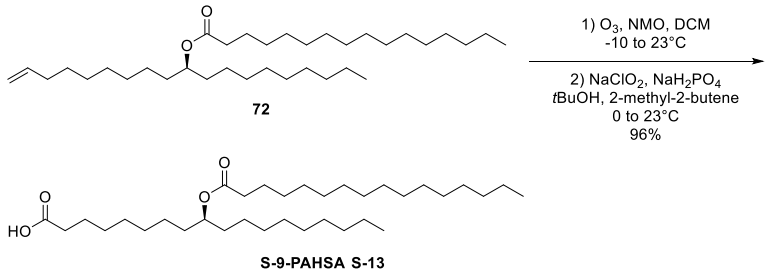

4-methylmorpholine N-oxide monohydrate (4.05 g, 30.0 mmol, 3 eq) was dehydrated by heating at 90°C under high vacuum overnight. A 250 mL round-bottom flask equipped with stir bar was charged with olefin 8 (5.21 g, 10.0 mmol, 1 eq), the anhydrous 4-methyl N-oxide prepared above, and dry DCM (67 mL). Stirring was initiated, affording a clear solution. The reaction vessel was submerged in an ice-acetone bath and cooled to -10°C for 15 minutes before bubbling in a mixture of ozone/oxygen. Conversion was complete within 7 minutes. The ozone generator was turned off and oxygen was bubbled through the solution for an additional 5 minutes. The reaction vessel was allowed to warm to ambient temperature and aged for 1 hour. The reaction was concentrated and the residue was dissolved in ethyl acetate (150 mL) and washed with water (100 mL) and brine (50 mL x 2), dried (sodium sulfate), filtered, and concentrated. The crude material was used in the next step without further purification.

A 250 mL round-bottom flask equipped with stir bar and addition funnel was charged with the crude material above and dissolved in 2-methyl-2-butene (10.6 mL) and tert-butanol (50 mL). Stirring was initiated, affording a clear solution. The reaction vessel was cooled in an ice-water bath for 15 minutes before adding an aqueous solution of sodium phosphate monobasic monohydrate (5.52 g, 40.0 mmol, 4 eq) and sodium chlorite (technical grade, 80%, 4.52 g, 40.0 mmol, 4 eq) in deionized water (25 mL) dropwise via addition funnel. The reaction was allowed to warm to ambient temperature and stirred overnight.

Peroxide test strips revealed the presence of peroxides. After adding an aqueous solution of sodium bisulfite (6.24 g, 60.0 mmol, 6 eq) in deionized water (25 mL) dropwise via addition funnel and aging 30 minutes, peroxides were absent. 2-methyl-2-butene and tert-butanol were removed by rotavap with water bath at 50°C. The residual aqueous layer was extracted with hexanes:ethyl acetate (50:50, 100 mL x 3). Combined organics were washed with brine (100 mL), dried (sodium sulfate), filtered, and concentrated. The crude product was purified by silica column chromatography, eluting with hexanes:EtOAc (90:10 to 70:30) to yield (1-R) (5.17 g. 96%) as an oil.

R-9-PAHSA (1-R)

Rf = 0.29 (silica gel, 80:20 hexanes:EtOAc, KMnO4); [α]23D 0.1000 (range: -0.1160 to 0.3040) (c 1.00, CHCl3); 1H-NMR (600 MHz, CDCl3): δ 4.89 – 4.83 (m, 1H), 2.34 (t, J = 7.5 Hz, 2H), 2.27 (t, J = 7.5 Hz, 2H), 1.65 – 1.58 (m, 4H), 1.50 (m, J = 4.8 Hz, 4H), 1.27 (m, J = 22.8 Hz, 46H), 0.88 (t, J = 6.8 Hz, 6H); 13C-NMR (151 MHz, CDCl3): δ 179.05, 173.91, 74.17, 34.90, 34.31, 34.28, 33.97, 32.08, 32.05, 29.85, 29.82, 29.81, 29.78, 29.71, 29.69, 29.67, 29.51, 29.46, 29.46, 29.35, 29.27, 29.12, 25.47, 25.40, 25.34, 24.78, 22.84, 22.83, 14.26, 14.25; IR (film, cm-1): 1711, 1733, 3427; HRMS (ESI) calc. for C34H66O4Na [M+Na]+: 561.4853, obs. 561.4855.

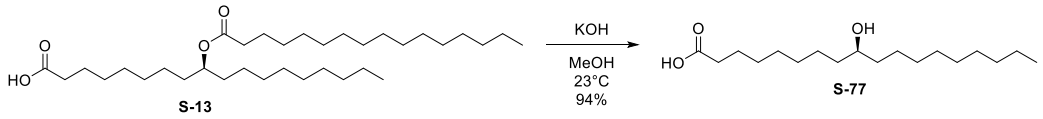

A 25 mL round-bottom flask equipped with stir bar was charged with S-9-PAHSA S-1, dissolved in methanol (4 mL) and a few drops of hexanes. A solution of potassium hydroxide in methanol (4 mL, 10% w/v, 400 mg, 7.13 mmol, 15.5 eq) was added dropwise and the reaction was stirred at ambient temperature for 1 hour, then heated to 40°C and stirred overnight. The reaction was cooled to ambient temperature, then ice cubes were added followed by ice-cold 6M HCl until litmus paper turned red. The product was extracted with ethyl acetate (25 mL x 3) and combined organics were washed with brine (25 mL), dried (sodium sulfate), filtered, and concentrated. The residue was purified by flash chromatography, eluting with hexanes:ethyl acetate (90:10 to 50:50) to yield S-77 (126 mg, 91%) as a white solid. Spectra were in agreement with those previously reported.[78]

General Procedures for FAHFA Library Synthesis and Chemical Biology Probes

A) TBS protection of primary alcohols

A round bottom flask equipped with stir bar was charged with primary alcohol (1 eq) and dissolved in DCM (0.5 M), giving a clear, colorless solution. The solution was cooled in an ice water bath for 30 minutes before adding TBSCl (1.04 eq) in one portion, giving a clear, colorless solution. The reaction was aged for an additional 30 minutes at 0C before adding imidazole (1.1 eq) in one portion, affording an opaque, white heterogeneous mixture. The slurry was stirred for 12 hours before quenching with saturated aqueous ammonium chloride and deionized water. The biphasic mixture was transferred to a separatory funnel, extracted with ether (x 3). Combined organics were washed with brine, dried (sodium sulfate), filtered, and concentrated. The crude residue was purified by column chromatography, eluting with hexanes:ethyl acetate (99:1 to 95:5).

B) Grignard Formation

A round bottom flask charged with stir bar and magnesium turnings (2.5 eq) was flame dried under vacuum, cooled to ambeint temperature, flushed with nitrogen, sealed with a rubber septum, and maintained under a nitrogen atmosphere. THF (1 M) was added via cannula. A solution of DIBAL (1.2 M in toluene, 0.025 eq) was added dropwise via syringe. The vessel was placed in an oil bath and warmed to 35 C for 15 minutes. Bromide (1 eq) was added NEAT via syringe pump (1 mmol/min), changing the color from clear to brown. After addition of of the bromide, the bath was heated to 50 C, then cooled to ambient temperature and used directly.

C) Grignard Addition to epichlorohydrin

A round bottom flask equipped with stir bar addition funnel was charged with copper iodide (10 mol%), flame dried under vacuum, cooled to ambeint temperature, flushed with nitrogen, sealed with arubber septum, and maintained under a nitrogen

atmosphere. THF (0.5 M) and S-(+)-epichlorohydrin (1 eq) were added via cannula and syringe, respectively, giving an opaque, pink slurry. The apparatus was placed in a bath of dry ice-acetone and cooled for 30 minutes. The addition funnel was charged with Grignard via cannula. The Grignard (1.5 eq) was then added dropwise, changing color to a deep, dark blue. The vessel was allowed to warm to ambient temperature overnight. The reaction was carefully quenched dropwise with saturated aqueous ammonium chloride, then diluted with ethyl ether:hexanes (50:50). The heterogeneous mixture was stirred vigorously until the aqueous layer turned a brilliant, royal blue. The mixture was transferred to a separatory funnel and extracted with with ethyl ether:hexanes (50:50, x 3). Combined organics were washed with saturated aqueous ammonium chloride (x 2), brine, dried (sodium sulfate), filtered, and concentrated. The crude residue was purified by column chromatography, eluting with hexanes:ethyl acetate (90:10 to 80:20).

D) Intramolecular Williamson Ether Synthesis

A round bottom flask equipped with stir bar was charged with chlorohydrin (1 eq), ethyl ether (0.5 M), and sodium hydroxide (6 eq) and sealed. The heterogenous mixture was vigorously stirred (>1000 rpm) and monitored via aliquot NMR. Upon completion (usually within 4 hours), the heterogeneous mixture was filtered with a Buchner funnel, washing the filter cake with ethyl ether. The filtrate was transferred to a separatory funnel, washed with water and brine, dried (sodium sulfate), filtered, and concentrated before being used directly in the next step without further purification.

E) Epoxide Opening

A round bottom flask equipped with stir bar was charged with copper bromide (5 mol%), flame dried under vacuum, cooled to ambeint temperature, flushed with nitrogen, sealed with arubber septum, and maintained under a nitrogen atmosphere. Grignard (1.5 eq) was added via syringe, giving a dark, opaque mixture. The vessel was placed in a bath

(70:30, water:methanol and dry ice) and cooled for thirty minutes after the cooling bath had formed a slurry/solid. A solution of epoxide (1 eq) in THF (1 M) was added dropwise via syringe pump (1 mL/min). The vessel was allowed to warm to ambient temperature overnight. The reaction was carefully quenched dropwise with saturated aqueous ammonium chloride, then diluted with ethyl ether:hexanes (50:50). The heterogeneous mixture was stirred vigorously until the aqueous layer turned a brilliant, royal blue. The mixture was transferred to a separatory funnel and extracted with with ethyl ether:hexanes (50:50, x 3). Combined organics were washed with saturated aqueous ammonium chloride (x 2), brine, dried (sodium sulfate), filtered, and concentrated. The crude residue was purified by column chromatography, eluting with hexanes:ethyl acetate (90:10 to 80:20).

F) Silyl ether deprotection

Taking no precaution to maintain a dry, inert atmosphere, a round bottom flask equipped with stir bar was charged with silyl ether (1 eq) and THF (0.5 M). The vessel was placed in an ice-water bath and cooled for 30 minutes. A solution of TBAF in THF (1.5 eq/silyl ether) was added dropwise via syringe. Upon completion (TLC control), the reaction was quenched with ice cold 2 M hydrochloric acid. The mixture was transferred to a separatory funnel and extracted with ethyl acetate (x 3). Combined organics were washed with saturated aqueous sodium bicarbonate and brine, dried (sodium sulfate), filtered, and concentrated. The crude residue was purified by column chromatography, eluting with hexanes:ethyl acetate (80:20 to 60:40).

G) TEMPO catalyzed oxidation of primary alcohols to aldehydes

Taking no precaution to maintain a dry, inert atmosphere, a round bottom flask equipped with stir bar was charged with diol (1 eq) and DCM (0.1 M), affording a clear solution. TEMPO (10 mol%) was added in one portion, giving a clear, red-orange solution. DAIB (1.5 eq) was then added in one portion. Upon completion (TLC control), the reaction

was quenched with saturated aqueous sodium thiosulfate (NB! The aqueous sodium thiosulfate layer was more dense than the organic DCM layer). The mixture was transferred to a separatory funnel and extracted with ethyl acetate (x 3). Combined organics were washed with saturated aqueous sodium bicarbonate (x 3), brine, dried (sodium sulfate), filtered, and concentrated. The crude aldehyde residue was used in the next step without further purification.

H) Pinnick Oxidation

Taking no precaution to maintain a dry, inert atmosphere, a round bottom flask equipped with stir bar was charged with crude aldehyde (1 eq), 2-methyl-2-butene (10 eq), tert-butanol (0.1 M), giving a clear solution. The vessel was placed in an ice-water bath and cooled for 15 minutes. An aqueous solution of sodium chlorite (80% technical grade, 4 eq) and sodium phosphate monobasic monohydrate (4 eq) was added dropwise. The biphasic mixture was vigorously stirred (>1000 rpm) in an effort to render the melange homogenous. Upon complete (TLC control), test strips revealed the presence of peroxides. The vessel was recooled in an ice-water bath for 15 minutes before adding dropwise an aqueous solution of sodium bisulfite (6 eq). Within 30 minutes the peroxides had been consumed. The 2-methyl-2-butene and tert-butanol were removed in vacuo with the heating bath at 50 C. The mixture was diluted with brine and ethyl acetate before transfer to a separatory funnel. The mixture was extracted with ethyl acetate (x 3), dried (sodium sulfate), filtered, and concentrated. The crude carboxylic acid was used in the next step without further purification.

I) Fisher-Speier Esterification

A round bottom flask equipped with stir bar and reflux condensor was charged with cude carboxylic acid (1 eq) and methanol (40 eq). The apparatus was sealed with a rubber septum and spurged with nitrogen for 5 minutes. Concentrated sulfuric acid (1 eq) was

added dropwise via syringe before placing the reaction vessel in an oil bath and heating to reflux. Upon completion (TLC control), the reaction was cooled to ambient temperature and carefully quenched by adding solid sodium bicarbonate (4 eq) in portions. The mixture was gravity filtered and the filter cake washed with methanol. The filtrate was concentrated and the residue was dissolved in water and ethyl acetate before transfer toa separatory funnel. The mixture was extracted with ethyl acetate (x 3). Combined organics were washed with brine, dried (sodium sulfate), filtered, and concentrated. The crude residue was purified by column chromatography, eluting with hexanes:ethyl acetate (85:15 to 70:30).

J) Mitsunobu Reaction

A round bottom flask equipped with stir bar was sequentially charged with secondary alcohol (1 eq), 4-nitrobenzoic acid (4 eq), benzene (0.1 M), and tributyl phosphine (4 eq). The vessel was placed in an ice-water bath and cooled for 30 minutes before adding dropwise via syringe diisopropylazadicarboxylate (4 eq). The reaction was allowed to warm to ambient temperature ovenight and diluted with hexanes. The mixture was transferred to a separatory funnel and washed with 2 M sodium hydroxide (x 3) and brine, dried (sodium sulfate), filterted, and concentrated. The residue was filtered through a plug of silica, eluting with hexanes:ethyl acetate (95:5). After concentrating the solvent in vacuo, the residue was used in the next step without further purification.

K) Chemoselective Cleavage of Aryl Ester

A round bottom flask equipped with stir bar was charged with diester (1 eq) and methanol (x M). Solid potassium carbonate (1 eq) was added in one portion. Upon completion (TLC control) the solvent was removed in vacuo. The residue was dissolved in ethyl acetate and brine with acetic acid (2 eq). The mixture was transferred toa separatory funnel and extracted with ethyl aceteate (x 3). Combined organics were washed with brine,

dried (sodium sulfate), filtered, and concentratated. The crude residue was filtered through a plug of silica, eluting with hexanes:ethyl acetate (95:5). Solvent was removed in vacuo and used in the next step without further purification.

L) Yamaguchi Esterification

A round bottom flask equipped with stir bar was charged with methyl hydroxystearate (1 eq), carboxylic acid (1.25 eq), and benzene (0.1 M). After dissolution, 2,4,6-trichlorobenzoyl chloride (1.25 eq) was added dropwise via syringe and the reaction aged 15 minutes. Triethylamine (6.25 eq) was added dropwise via syringe, followed by DMAP (12.5 mol%) in one portion. The reaction was allowed to stir overnight, diluted with hexanes and transferred to a separatory funnel. The organic layer was washe with aqueous hydrochloric acid (2 M), brine, dried (sodium sulfate), filtered, and concentrated. The residue was purified by column chromatography, eluting with hexanes:ethyl acetate (95:5 to 90:10).

M) Chemoselective Saponification of Methyl Esters

A round bottom flask equipped with stir bar was charged with methyl ester (1 eq) and dissolved in THF (0.1 M). Aqueous lithium hydroxide (1 M, 2 eq) was added dropwise via syringe. Upon completion (TLC control), the reaction was diluted with ethyl acetate and brine with acetic acid (3 eq). The mixture was transferred to a separatory funnel and extracted with ethyl acetate (x 3). Combined organics were dried (sodium sulfate), filtered, and concentrated. The residue was purified by column chromatography, eluting with hexanes:ethyl acetate:acetic acid (95:5:1 to 90:10:1).

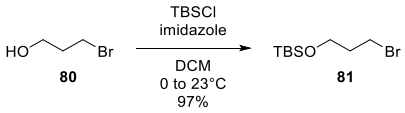

Following General Procedure A for the TBS protection of primary alcohols, primary alcohol **80** gave TBS protected **81** as a clear, colorless oil. Spectra were in agreement with those previously reported.[79]

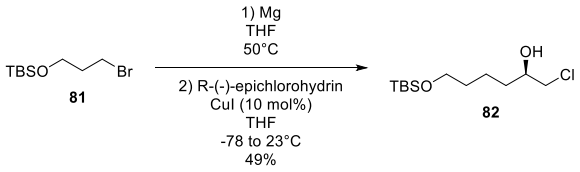

Following General Procedures B and C for the formation of Grignards and their addition to epichlorohydrin, bromide **81** gave chlorohydrin **82** as a clear, colorless oil.

Rf = 0.18 (silica gel, 90:10, hexanes:ethyl acetate)

1H NMR (600 MHz, CDCl3) δ 3.82 – 3.76 (m, J = 6.9, 3.8 Hz, 1H), 3.63 – 3.59 (m, 3H), 3.46 (dd, J = 11.1, 7.0 Hz, 1H), 1.57 – 1.36 (m, 6H), 0.87 (s, 9 H), 0.03 (s, 6H).

13C NMR (151 MHz, CDCl3) δ 71.49, 63.05, 50.55, 34.01, 32.60, 26.07, 22.01, 18.46, -5.18.

HR-ESI-TOFMS calc. for [C12 H28 Cl O2 Si]+: 267.1542, obs. 267.1542

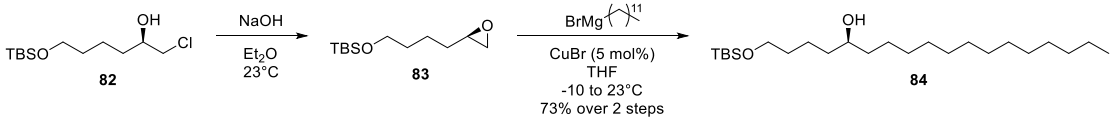

Following General Procedures D, B, and E for the intramolecular Williamson ether synthesis, Grignard formation, and epoxide opening, respectively, **82** gave **84** as a white solid.

Rf = 0.38 (silica gel, 90:10, hexanes:ethyl acetate)

1H NMR (600 MHz, CDCl3) δ 3.65 – 3.55 (m, 3H), 1.58 – 1.21 (m, 32H), 0.90 – 0.86 (m, 12H), 0.05 (s, 6H).

13C NMR (151 MHz, CDCl3) δ 72.04, 63.30, 37.60, 37.29, 32.90, 32.07, 29.82, 29.51, 26.13, 26.11, 25.79, 22.85, 22.05, 18.52, 14.29, -5.11, -5.14.

HRMS: HR-ESI-TOFMS calc. for [C24 H53 O2 Si]+ : 401.3809 obs. 401.3808

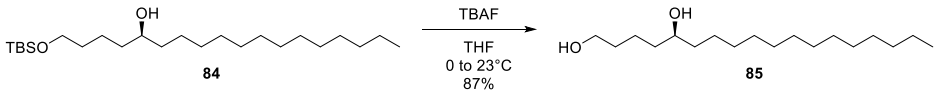

Following General Procedure F for silyl ether deprotection, **84** gave **85** as a white solid.

Rf = 0.09 (silica gel, 70:30, hexanes:ethyl acetate)

1H NMR (600 MHz, CDCl3) δ 3.66 (t, J = 6.5 Hz, 2H), 3.64 – 3.58 (m, 1H), 1.65 – 1.22 (m, 36H), 0.88 (t, J = 7.0 Hz, 3H).

13C NMR (151 MHz, CDCl3) δ 72.04, 63.01, 37.69, 37.16, 32.78, 32.07, 29.84, 29.82, 29.81, 29.80, 29.78, 29.76, 29.51, 25.81, 22.84, 21.97, 14.29.

HRMS: HR-ESI-TOFMS calc. for [C18 H37 O2]-: 285.2799 obs. 285.2797

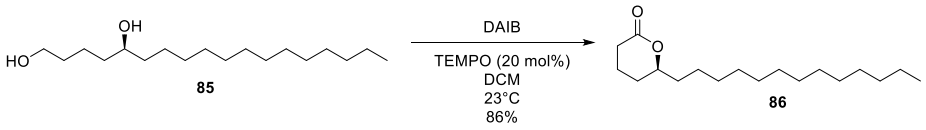

Taking no precaution to maintain a dry, inert atmosphere, a round bottom flask equipped with stir bar was charged with diol **86** (2.86 g, 10 mmol, 1 eq), DCM (100 mL, 0.1 M), TEMPO (0.31 g, 2.0 mmol, 20 mol%), and DAIB (10.2 g, 31.6 mmol, 3.16 eq). Upon complete (TLC control), the reaction was quenched with saturated aqueous sodium thiosulfate (NB! The aqueous sodium thiosulfate layer was more dense than the organic DCM layer). The mixture was transferred to a separatory funnel and extracted with ethyl acetate (x 3). Combined organics were washed with saturated aqueous sodium bicarbonate (x 3), brine, dried (sodium sulfate), filtered, and concentrated. The residue was purified by column chromatography, eluting with hexanes:ethyl acetate (90:10 to 80:20), giving lactone **88** as a fragrant, slightly yellow solid. Spectra were in agreement with those previously reported.[80]

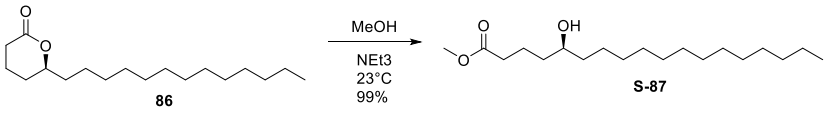

Taking no precaution to maintain a dry, inert atmosphere, a round bottom flask equipped with stir bar was charged with lactone **86** (1 eq), methanol (0.1 M), and triethylamine (3 eq). Upon completion (TLC control), volatiles were removed in vacuo, yielding analytically pure methyl hydroxystearate **87**.

Rf = 0.26 (silica gel, 80:20, hexanes:ethyl acetate)

1H NMR (599 MHz, CDCl3) δ 3.68 (s, 3H), 3.63 – 3.56 (m, 1H), 2.35 (t, J = 7.4 Hz, 2H), 1.83 – 1.22 (m, 42H), 0.88 (t, J = 7.0 Hz, 3H).

HRMS: HR-ESI-TOFMS calc. for [C19 H38 O3 Na]+ : 337.2713 obs. 337.2711

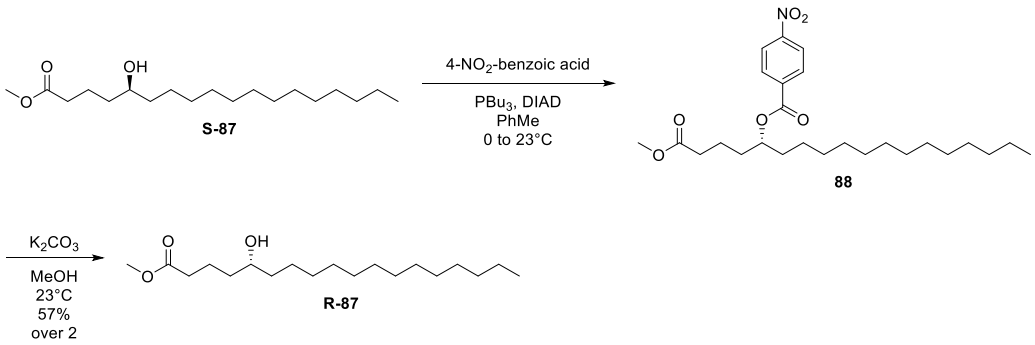

Following General Procedures J and K for the Mitsunobu reaction, and chemoselective saponification of aryl esters, respectively, **S-87** gave **R-87**.

Rf = 0.26 (silica gel, 80:20, hexanes:ethyl acetate)

1H NMR (599 MHz, CDCl3) δ 3.68 (s, 3H), 3.63 – 3.56 (m, 1H), 2.35 (t, J = 7.4 Hz, 2H), 1.83 – 1.22 (m, 42H), 0.88 (t, J = 7.0 Hz, 3H).

HRMS: HR-ESI-TOFMS calc. for [C19 H38 O3 Na]+ : 337.2713 obs. 337.2711

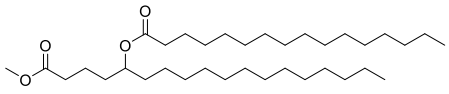

89

Following General Procedure L for the Yamaguchi esterification, **87** gave **89** as a white solid.

Rf = 0.51 (silica gel, 90:10, hexanes:ethyl acetate)

1H NMR (600 MHz, CDCl3) δ 4.91 – 4.84 (m, 1H), 3.66 (s, 3H), 2.31 (td, J = 7.4, 3.0 Hz, 2H), 2.28 (t, J = 7.5 Hz, 2H), 1.69 – 1.45 (m, 12H), 1.33 – 1.21 (m, 47H), 0.88 (t, J = 7.0 Hz, 6H).

13C NMR (151 MHz, CDCl3) δ 173.99, 173.85, 73.52, 51.69, 34.81, 34.18, 33.91, 33.59, 32.07, 29.85, 29.81, 29.78, 29.73, 29.69, 29.65, 29.52, 29.45, 29.34, 25.42, 25.28, 22.85, 20.84, 14.28.

HRMS: HR-ESI-TOFMS calc. for [C35 H68 O4 Na]+: 575.5010 obs. 575.5006

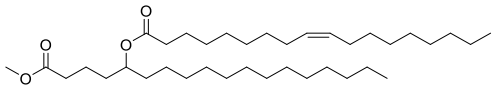

90

Following General Procedure L for the Yamaguchi esterification, **87** gave **90** as an oil.

Rf = 0.54 (silica gel, 90:10, hexanes:ethyl acetate)

1H NMR (600 MHz, CDCl3) δ 5.44 – 5.29 (m, 2H), 4.93 – 4.84 (m, J = 5.8 Hz, 2H), 3.66 (s, 3H), 2.36 – 2.23 (m, 4H), 2.11 – 1.92 (m, 4H), 1.72 – 1.43 (m, 9H), 1.43 – 1.18 (m, 45H), 0.87 (t, J = 6.8 Hz, 6H).

13C NMR (151 MHz, CDCl3) δ 173.81, 130.13, 129.89, 73.53, 51.69, 34.79, 34.17, 33.90, 33.58, 32.07, 32.05, 29.91, 29.85, 29.83, 29.80, 29.73, 29.69, 29.67, 29.64, 29.52, 29.47, 29.35, 29.31, 29.28, 27.36, 27.31, 25.43, 25.26, 22.84, 20.84, 14.28.

HRMS: HR-ESI-TOFMS calc. for [C37 H70 O4 Na]+ : 601.5166 obs. 601.5159

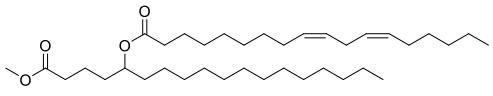

91

Rf = 0.50 (silica gel, 90:10, hexanes:ethyl acetate)

Following General Procedure L for the Yamaguchi esterification, **87** gave **91** as an oil.

1H NMR (600 MHz, CDCl3) δ 5.43 – 5.28 (m, 4H), 4.91 – 4.83 (m, J = 11.9, 5.9 Hz, 1H), 3.66 (s, 3H), 2.77 (t, J = 6.7 Hz, 2H), 2.35 – 2.25 (m, 4H), 2.04 (q, J = 6.9 Hz, 4H), 1.69 – 1.45 (m, 9H), 1.38 – 1.21 (m, 38H), 0.88 (q, J = 6.5 Hz, 6H).

13C NMR (151 MHz, CDCl3) δ 173.98, 173.80, 130.36, 130.19, 128.16, 128.03, 73.54, 51.69, 34.79, 34.17, 33.90, 33.58, 32.07, 31.66, 29.84, 29.82, 29.80, 29.76, 29.73, 29.69, 29.64, 29.51, 29.49, 29.35, 29.30, 29.29, 27.33, 25.76, 25.42, 25.25, 22.84, 22.72, 20.84, 14.28, 14.23.

HRMS: HR-ESI-TOFMS calc. for [C37 H68 O4 Na]+ : 599.5010 obs. 599.5008

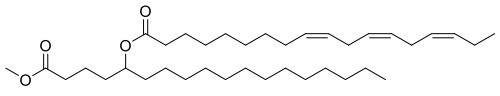

92

Following General Procedure L for the Yamaguchi esterification, **87** gave **92** as an oil.

Rf = 0.48 (silica gel, 90:10, hexanes:ethyl acetate)

1H NMR (600 MHz, CDCl3) δ 5.42 – 5.28 (m, 6H), 4.90 – 4.85 (m, 1H), 3.66 (s, 3H), 2.80 (s, 4H), 2.35 – 2.24 (m, J = 19.8, 16.5, 8.4 Hz, 4H), 2.12 – 2.01 (m, 4H), 1.70 – 1.45 (m, 8H), 1.38 – 1.18 (m, 32H), 0.97 (t, J = 7.5 Hz, 3H), 0.87 (t, J = 6.9 Hz, 3H).

13C NMR (151 MHz, CDCl3) δ 173.97, 173.79, 132.09, 130.41, 128.41, 128.38, 127.84, 127.23, 73.54, 51.68, 34.78, 34.17, 33.90, 33.57, 32.07, 29.84, 29.82, 29.80, 29.73, 29.69, 29.64, 29.51, 29.35, 29.30, 29.28, 27.35, 25.74, 25.66, 25.42, 25.24, 22.84, 20.84, 20.69, 14.43, 14.28.

HRMS: HR-ESI-TOFMS calc. for [C37 H66 O4 Na]+: 597.4853 obs. 597.4850

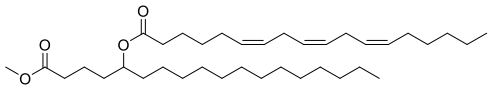

93

Following General Procedure L for the Yamaguchi esterification, **87** gave **93** as an oil.

Rf = 0.48 (silica gel, 90:10, hexanes:ethyl acetate)

1H NMR (600 MHz, CDCl3) δ 5.43 – 5.30 (m, 6H), 4.88 (dd, J = 11.9, 5.9 Hz, 1H), 3.66 (s, 3H), 2.80 (t, J = 5.7 Hz, 4H), 2.35 – 2.26 (m, 4H), 2.07 (dq, J = 21.0, 7.0 Hz, 4H), 1.69 – 1.19 (m, 42H), 0.88 (q, J = 6.6 Hz, 6H).

13C NMR (151 MHz, CDCl3) δ 173.96, 173.61, 130.58, 129.77, 128.53, 128.31, 128.21, 127.71, 73.60, 51.69, 34.65, 34.17, 33.89, 33.57, 32.07, 31.65, 29.84, 29.82, 29.80, 29.73, 29.69, 29.64, 29.51, 29.47, 29.27, 27.35, 27.02, 25.76, 25.75, 25.43, 24.86, 22.84, 22.72, 20.83, 14.28, 14.23.

HRMS: HR-ESI-TOFMS calc. for [C37 H66 O4 Na]+ : 597.4853 obs. 597.4848

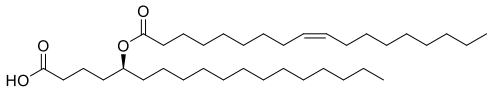

S-5-OAHSA S-95

Following General Procedure M for the chemoselective saponification of methyl esters, **90** gave **95** as a clear, slightly yellow oil.

Rf = 0.34 (silica gel, 70:30, hexanes:ethyl acetate)

1H NMR (600 MHz, CDCl3) δ 5.44 – 5.33 (m, 2H), 4.91 (s, 1H), 2.31 (t, J = 7.4 Hz, 2H), 2.03 (d, J = 5.8 Hz, 3H), 1.73 – 1.20 (m, 58H), 0.91 (t, J = 6.8 Hz, 6H).

13C NMR (151 MHz, CDCl3) δ 173.88, 130.13, 129.90, 73.53, 34.79, 34.19, 33.53, 32.08, 32.06, 29.92, 29.85, 29.83, 29.81, 29.74, 29.70, 29.68, 29.65, 29.52, 29.48, 29.35, 29.31, 29.29, 27.36, 27.32, 25.44, 25.26, 22.85, 14.29.

HRMS: HR-ESI-TOFMS calc. for [C36 H67 O4]-: 563.5045 obs. 563.5045

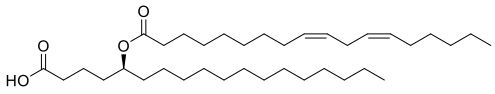

S-5-LAHSA S-96

Following General Procedure M for the chemoselective saponification of methyl esters, **91** gave **96** as a clear, slightly yellow oil.

Rf = 0.34 (silica gel, 80:20, hexanes:ethyl acetate)

1H NMR (600 MHz, CDCl3) δ 5.41 – 5.28 (m, 4H), 4.93 – 4.84 (m, 1H), 2.77 (t, J = 6.8 Hz, 2H), 2.28 (t, J = 7.5 Hz, 2H), 2.04 (q, J = 7.0 Hz, 4H), 1.76 – 1.13 (m, 49H), 0.88 (q, J = 6.5 Hz, 6H).

13C NMR (151 MHz, CDCl3) δ 173.88, 130.36, 130.20, 128.16, 128.04, 73.56, 34.79, 34.18, 33.57, 32.07, 31.67, 29.85, 29.83, 29.81, 29.76, 29.74, 29.70, 29.65, 29.52, 29.50, 29.36, 29.31, 29.30, 27.34, 25.76, 25.44, 25.25, 22.85, 22.73, 14.29, 14.24.

HRMS: HR-ESI-TOFMS calc. for [C36 H65 O4]-: 561.4888 obs. 561.4886

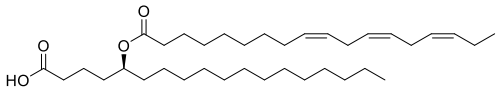

S-5-ALAHSA S-97

Following General Procedure M for the chemoselective saponification of methyl esters, **92** gave **97** as a clear, slightly yellow oil.

Rf = 0.34 (silica gel, 80:20, hexanes:ethyl acetate)

HRMS: HR-ESI-TOFMS calc. for [C36 H63 O4]-: 559.4732 obs. 559.4729

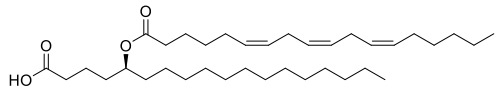

S-5-GLAHSA S-98

Following General Procedure M for the chemoselective saponification of methyl esters, **93** gave **98** as a clear, slightly yellow oil.

Rf = 0.34 (silica gel, 80:20, hexanes:ethyl acetate)

1H NMR (600 MHz, CDCl3) δ 5.45 – 5.23 (m, 6H), 4.92 – 4.84 (m, 1H), 2.81 (t, J = 6.0 Hz, 4H), 2.43 – 2.31 (m, 2H), 2.28 (t, J = 7.5 Hz, 2H), 2.07 (tt, J = 13.7, 6.9 Hz, 4H), 1.72 – 1.17 (m, 49H), 0.97 (t, 3H), 0.88 (t, J = 7.0 Hz, 3H).

13C NMR (151 MHz, CDCl3) δ 173.91, 132.10, 130.42, 128.42, 128.39, 127.84, 127.24, 73.62, 34.80, 34.18, 33.59, 32.08, 29.86, 29.84, 29.81, 29.75, 29.71, 29.66, 29.52, 29.36, 29.31, 29.30, 27.36, 25.75, 25.66, 25.45, 25.25, 22.85, 20.70, 14.44, 14.29.

HRMS: HR-ESI-TOFMS calc. for [C36 H63 O4]-: 559.4732 obs. 559.4729

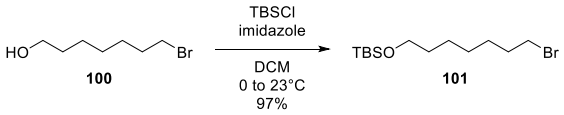

Following General Procedure A for the TBS protection of primary alcohols, primary alcohol **100** gave TBS protected **101** as a clear, colorless oil. Spectra were in agreement with those previously reported.[81]

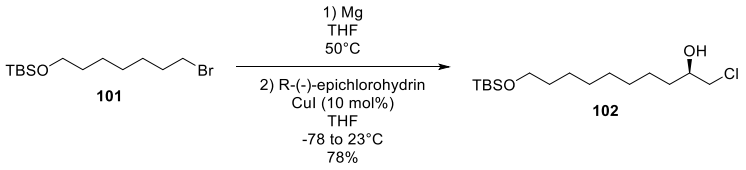

Following General Procedures B and C for the formation of Grignards and their addition to epichlorohydrin, bromide **101** gave chlorohydrin **102** as a clear, colorless oil.

Rf = 0.30 (silica gel, 90:10, hexanes:ethyl acetate)

1H NMR (600 MHz, CDCl3) δ 3.82 – 3.77 (m, 1H), 3.64 (dd, J = 11.1, 3.2 Hz, 1H), 3.59 (t, J = 6.6 Hz, 2H), 3.48 (dt, J = 11.1, 5.4 Hz, 1H), 1.57 – 1.26 (m, 14H), 0.89 (s, 9H), 0.04 (s, 6H).

13C NMR (151 MHz, CDCl3) δ 71.58, 63.44, 50.76, 34.34, 32.98, 29.61, 29.58, 29.47, 26.13, 26.12, 25.90, 25.65, -5.11.

HRMS: HR-ESI-TOFMS calc. for [C16 H36 Cl O2 Si]+: 323.2168 obs. 323.2170

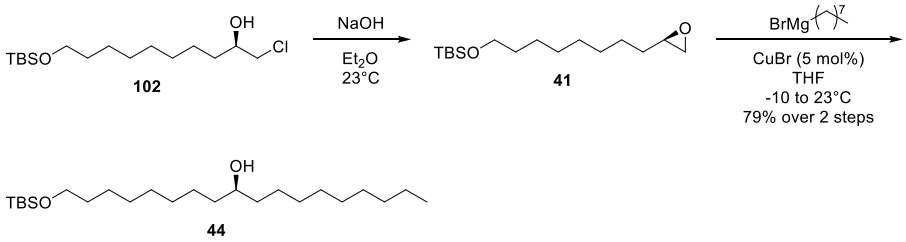

Following General Procedures D, B, and E for the intramolecular Williamson ether synthesis, Grignard formation, and epoxide opening, respectively, **102** gave **44** as a white solid.

Rf = 0.38 (silica gel, 90:10, hexanes:ethyl acetate)

1H NMR (600 MHz, CDCl3) δ 3.61 – 3.55 (m, 3H), 1.53 – 1.21 (m, 31H), 0.92 – 0.85 (m, 12H), 0.04 (s, 6H).

13C NMR (151 MHz, CDCl3) δ 72.10, 63.44, 37.61, 37.59, 32.99, 32.03, 29.86, 29.79, 29.78, 29.74, 29.72, 29.52, 29.47, 26.12, 26.11, 25.91, 25.80, 25.78, 22.82, 18.50, 14.26, -5.13, -5.13, -5.14, -5.14.

HRMS: HR-ESI-TOFMS calc. for [C24 H53 O2 Si]+: 401.3809 obs. 401.3806

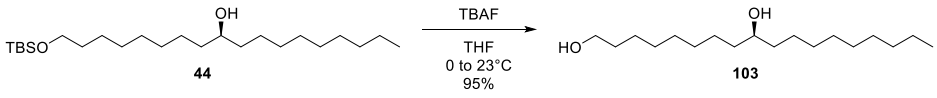

Following General Procedure F for silyl ether deprotection, **44** gave **103** as a white solid. Spectra were in agreement with those previously reported.[82]

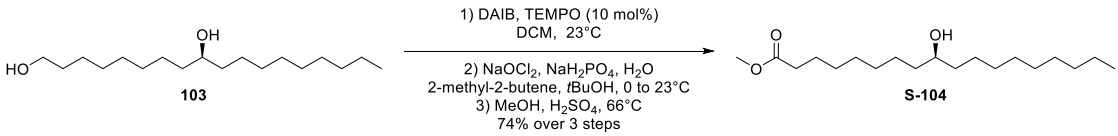

Following General Procedures G, H, and I for the chemoselective oxidation of primary alcohols to aldehydes, Pinnick oxidation, and Fisher-Speier esterification, respectively, **103** gave **104** as a white solid. Specta were in agreement with those previously reported.[83]

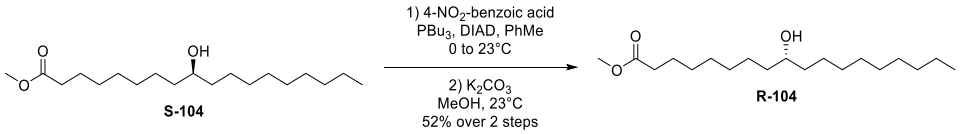

Following General Procedures J and K for the Mitsunobu reaction, and chemoselective saponification of aryl esters, respectively, **S-104** gave R-**104**. Specta were in agreement with those previously reported.[83]

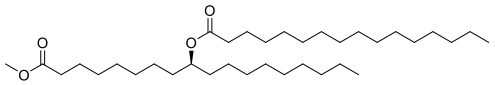

S-105

Following General Procedure L for the Yamaguchi esterification, **104** gave **105** as a white solid.

Rf = 0.49 (silica gel, 90:10, hexanes:ethyl acetate)

1H NMR (600 MHz, CDCl3) δ 4.82 – 4.75 (m, 1H), 3.60 (s, 3H), 2.25 – 2.17 (m, 4H), 1.57 – 1.13 (m, 57H), 0.81 (t, J = 6.8 Hz, 6H).

13C NMR (151 MHz, CDCl3) δ 174.46, 173.90, 74.14, 51.61, 34.88, 34.29, 34.27, 34.21, 32.07, 32.04, 29.85, 29.81, 29.78, 29.71, 29.69, 29.67, 29.52, 29.48, 29.47, 29.34, 29.30, 29.20, 25.46, 25.41, 25.33, 25.05, 22.84, 22.83, 14.28.

HRMS: HR-ESI-TOFMS calc. for [C35 H68 O4 Na]+: 575.5010 obs. 575.5007

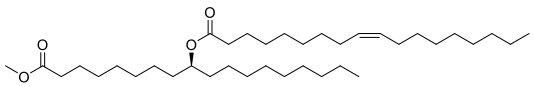

S-106

Following General Procedure L for the Yamaguchi esterification, **104** gave **106** as an oil.

Rf = 0.49 (silica gel, 90:10, hexanes:ethyl acetate)

1H NMR (600 MHz, CDCl3) δ 5.39 – 5.30 (m, 2H), 4.88 – 4.83 (m, 1H), 3.66 (s, 3H), 2.28 (dt, J = 12.6, 7.6 Hz, 4H), 2.06 – 1.97 (m, 4H), 1.64 – 1.19 (m, 52H), 0.90 – 0.85 (m, 6H).

13C NMR (151 MHz, CDCl3) δ 174.46, 173.87, 130.13, 129.90, 74.16, 51.62, 34.86, 34.29, 34.27, 34.22, 32.05, 32.04, 29.91, 29.85, 29.70, 29.68, 29.47, 29.36, 29.31, 29.29, 29.21, 27.36, 27.31, 25.46, 25.41, 25.31, 25.05, 22.83, 14.28.

HRMS: HR-ESI-TOFMS calc. for [C37 H70 O4 Na]+: 601.5166 obs. 601.5163

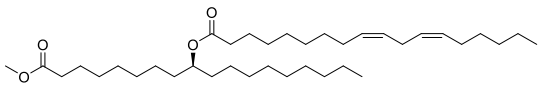

S-107

Following General Procedure L for the Yamaguchi esterification, **104** gave **107** as an oil.

Rf = 0.51 (silica gel, 90:10, hexanes:ethyl acetate)

1H NMR (600 MHz, CDCl3) δ 5.42 – 5.28 (m, 4H), 4.89 – 4.82 (m, 1H), 3.66 (s, 3H), 2.77 (t, J = 6.7 Hz, 2H), 2.33 – 2.23 (m, 4H), 2.04 (q, J = 6.9 Hz, 4H), 1.66 – 1.18 (m, 48H), 0.88 (q, J = 6.9 Hz, 6H).

13C NMR (151 MHz, CDCl3) δ 174.46, 173.85, 130.36, 130.20, 128.16, 128.04, 74.17, 51.62, 34.86, 34.29, 34.26, 34.21, 32.04, 31.67, 29.76, 29.70, 29.68, 29.49, 29.48, 29.46, 29.36, 29.30, 29.20, 27.34, 25.76, 25.46, 25.41, 25.30, 25.05, 22.83, 22.73, 14.28, 14.24.

HRMS: HR-ESI-TOFMS calc. for [C37 H68 O4 Na]+: 599.5010 obs. 599.5007

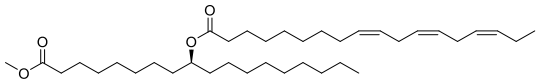

Following General Procedure L for the Yamaguchi esterification, **104** gave **108** as an oil.

Rf = 0.51 (silica gel, 90:10, hexanes:ethyl acetate)

1H NMR (600 MHz, CDCl3) δ 5.42 – 5.28 (m, 6H), 4.90 – 4.80 (m, 1H), 3.66 (s, 3H), 2.80 (s, 4H), 2.28 (dt, J = 12.0, 7.6 Hz, 4H), 2.12 – 2.00 (m, 4H), 1.65 – 1.18 (m, 42H), 0.97 (t, J = 7.5 Hz, 3H), 0.87 (t, J = 6.9 Hz, 3H).

13C NMR (151 MHz, CDCl3) δ 174.46, 173.85, 132.10, 130.42, 128.41, 128.38, 127.84, 127.24, 74.16, 51.62, 34.86, 34.29, 34.26, 34.21, 32.04, 29.85, 29.74, 29.70, 29.68, 29.48, 29.46, 29.36, 29.30, 29.20, 27.35, 25.74, 25.66, 25.46, 25.41, 25.30, 25.05, 22.83, 20.69, 14.44, 14.28.

HRMS: HR-ESI-TOFMS calc. for [C37 H66 O4 Na]+: 597.4853 obs. 597.4848

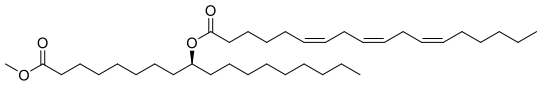

S-109

Following General Procedure L for the Yamaguchi esterification, **104** gave **109** as an oil.

Rf = 0.51 (silica gel, 90:10, hexanes:ethyl acetate)

HRMS: HR-ESI-TOFMS calc. for [C37 H66 O4 Na]+: 597.4853 obs. 597.4848

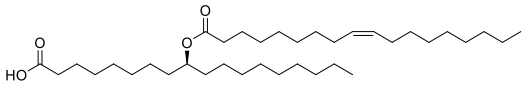

S-9-OAHSA S-111

Following General Procedure M for the chemoselective saponification of methyl esters, **106** gave **111** as a clear, slightly yellow oil.

Rf = 0.34 (silica gel, 80:20, hexanes:ethyl acetate)

1H NMR (600 MHz, CDCl3) δ 5.34 (d, J = 1.5 Hz, 2H), 4.90 – 4.82 (m, 1H), 2.34 (t, J = 7.1 Hz, 2H), 2.27 (t, J = 7.1 Hz, 2H), 2.00 (d, J = 5.8 Hz, 4H), 1.67 – 1.18 (m, 65H), 0.87 (t, J = 6.9 Hz, 6H).

13C NMR (151 MHz, CDCl3) δ 173.93, 130.13, 129.89, 74.18, 34.87, 34.29, 34.25, 32.04, 29.91, 29.85, 29.70, 29.69, 29.47, 29.44, 29.36, 29.31, 29.29, 29.27, 29.11, 27.36, 27.31, 25.47, 25.40, 25.31, 24.79, 22.83, 14.28.

HRMS: HR-ESI-TOFMS] calc. for [C36 H67 O4]-: 563.5045 obs. 563.5043

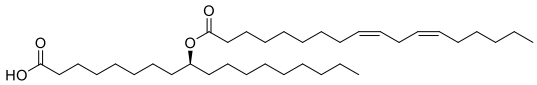

S-9-LAHSA S-112

Following General Procedure M for the chemoselective saponification of methyl esters, **107** gave **112** as a clear, slightly yellow oil.

Rf = 0.34 (silica gel, 80:20, hexanes:ethyl acetate)

1H NMR (600 MHz, CDCl3) δ 5.42 – 5.29 (m, 4H), 4.90 – 4.82 (m, 1H), 2.77 (t, J = 6.8 Hz, 2H), 2.35 (t, J = 6.6 Hz, 2H), 2.28 (dd, J = 16.8, 9.4 Hz, 2H), 2.04 (q, J = 6.9 Hz, 4H), 1.65 – 1.18 (m, 48H), 0.88 (q, J = 7.0 Hz, 6H).

1H NMR (600 MHz, CDCl3) δ 5.42 – 5.29 (m, 4H), 4.90 – 4.82 (m, 1H), 2.77 (t, J = 6.8 Hz, 2H), 2.35 (t, J = 6.6 Hz, 2H), 2.28 (dd, J = 16.8, 9.4 Hz, 2H), 2.04 (q, J = 6.9 Hz, 4H), 1.65 – 1.18 (m, 48H), 0.88 (q, J = 7.0 Hz, 6H).

HRMS: HR-ESI-TOFMS calc. for [C36 H65 O4]-: 561.4888 obs. 561.4886

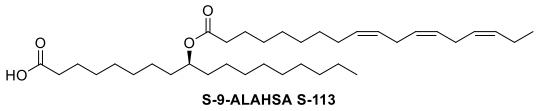

S-9-ALAHSA S-113

Following General Procedure M for the chemoselective saponification of methyl esters, **108** gave **113** as a clear, slightly yellow oil.

Rf = 0.34 (silica gel, 80:20, hexanes:ethyl acetate)

1H NMR (600 MHz, CDCl3) δ 5.44 – 5.27 (m, 6H), 4.89 – 4.82 (m, 1H), 2.80 (s, 4H), 2.35 (t, J = 6.9 Hz, 2H), 2.28 (dd, J = 17.0, 9.5 Hz, 2H), 2.12 – 2.00 (m, 4H), 1.66 – 1.19 (m, 43H), 0.97 (t, J = 7.5 Hz, 3H), 0.87 (t, J = 7.0 Hz, 3H).

13C NMR (151 MHz, CDCl3) δ 173.90, 132.10, 130.42, 128.42, 128.39, 127.84, 127.24, 34.86, 34.29, 34.25, 32.04, 29.74, 29.71, 29.68, 29.47, 29.44, 29.36, 29.31, 29.30, 29.27, 29.11, 27.35, 25.75, 25.66, 25.47, 25.40, 25.30, 24.79, 22.83, 20.70, 14.44, 14.28.

HRMS: HR-ESI-TOFMS calc. for [C36 H63 O4]-: 559.4732 obs. 559.4730

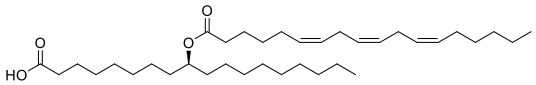

S-9-GLAHSA S-114

Following General Procedure M for the chemoselective saponification of methyl esters, **109** gave **114** as a clear, slightly yellow oil.

Rf = 0.34 (silica gel, 80:20, hexanes:ethyl acetate)

1H NMR (600 MHz, CDCl3) δ 5.43 – 5.30 (m, 6H), 4.89 – 4.83 (m, 1H), 2.84 – 2.77 (m, 4H), 2.35 (dd, J = 14.1, 6.7 Hz, 2H), 2.29 (t, J = 7.5 Hz, 2H), 2.11 – 2.02 (m, 4H), 1.68 – 1.20 (m, 41H), 0.88 (q, J = 7.1 Hz, 6H).

13C NMR (151 MHz, CDCl3) δ 173.71, 130.59, 129.80, 128.53, 128.30, 128.22, 127.72, 74.24, 34.72, 34.28, 34.25, 32.04, 31.66, 29.70, 29.69, 29.68, 29.47, 29.46, 29.45, 29.27, 29.11, 27.35, 27.03, 25.76, 25.75, 25.47, 25.41, 24.91, 24.77, 22.83, 22.73, 14.28, 14.24.

HRMS: HR-ESI-TOFMS calc. for [C36 H63 O4]-: 559.4732 obs. 559.4729

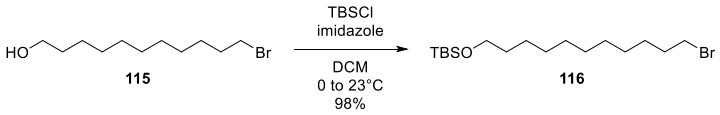

Following General Procedure A for the TBS protection of primary alcohols, primary alcohol **115** gave TBS protected **116** as a clear, colorless oil. Spectra were agreement with those previously reported.[84]

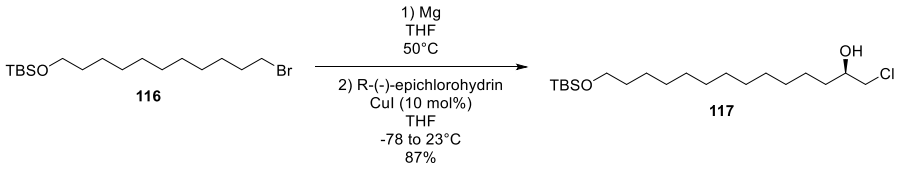

Following General Procedures B and C for the formation of Grignards and their addition to epichlorohydrin, bromide **116** gave chlorohydrin **117** as a clear, colorless oil.

Rf = 0.32 (silica gel, 90:10, hexanes:ethyl acetate)

1H NMR (600 MHz, CDCl3) δ 3.80 (ddd, J = 12.5, 7.5, 3.3 Hz, 1H), 3.66 – 3.62 (m, 1H), 3.59 (t, J = 6.7 Hz, 2H), 3.50 – 3.45 (m, 1H), 1.58 – 1.23 (m, 27H), 0.89 (s, 9H), 0.04 (s, 6H).

13C NMR (151 MHz, CDCl3) δ 71.59, 63.50, 50.78, 34.35, 33.03, 29.77, 29.75, 29.73, 29.69, 29.64, 29.59, 26.13, 25.94, 25.67, -5.11.

HRMS: HR-ESI-TOFMS calc. for [C20 H44 Cl O2 Si]+: 379.2794 obs. 379.2791

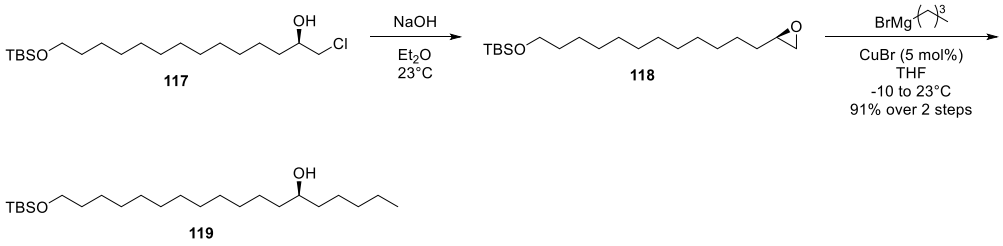

Following General Procedures D, B, and E for the intramolecular Williamson ether synthesis, Grignard formation, and epoxide opening, respectively, **117** gave **119** as a white solid.

Rf = 0.38 (silica gel, 90:10, hexanes:ethyl acetate)

1H NMR (600 MHz, CDCl3) δ 3.63 – 3.55 (m, 3H), 1.58 – 1.22 (m, 36H), 0.089 (s, 12H), 0.04 (s, 6H).

13C NMR (151 MHz, CDCl3) δ 72.19, 63.51, 37.63, 37.58, 33.03, 32.06, 29.86, 29.78, 29.75, 29.60, 26.14, 25.94, 25.81, 25.48, 22.81, 14.22, -5.11.

HRMS: HR-ESI-TOFMS calc. for [C24 H53 O2 Si]+: 401.3809 obs. 401.3805

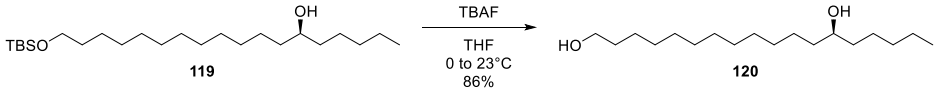

Following General Procedure F for silyl ether deprotection, **119** gave **120** as a white solid.

Rf = 0.31 (silica gel, 70:30, hexanes:ethyl acetate)

1H NMR (600 MHz, CDCl3) δ 3.65 (t, J = 8.7, 4.7 Hz, 2H), 3.63 – 3.56 (m, 1H), 1.61 – 1.23 (m, 35H), 0.90 (t, J = 9.3, 4.6 Hz, 3H).

13C NMR (151 MHz, CDCl3) δ 72.19, 63.26, 37.62, 37.59, 32.94, 32.06, 29.84, 29.75, 29.72, 29.70, 29.56, 25.86, 25.80, 25.48, 22.81, 14.22.

HRMS: HR-ESI-TOFMS calc. for [C18 H37 O2]-: 285.2799 obs. 285.2796

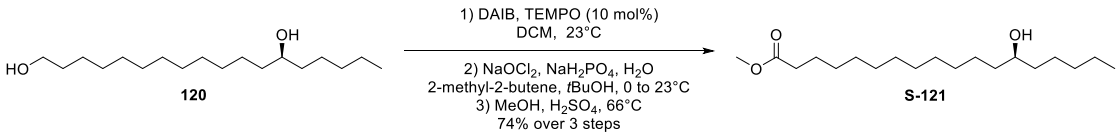

Following General Procedures G, H, and I for the chemoselective oxidation of primary alcohols to aldehydes, Pinnick oxidation, and Fisher-Speier esterification, respectively, **120** gave **121** as a white solid. Specta were in agreement with those previously reported.[85]

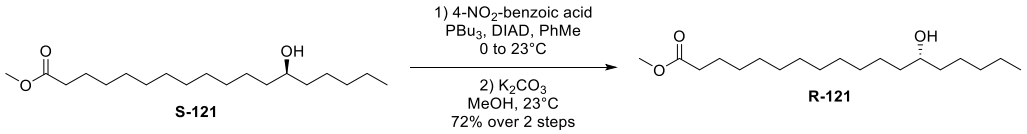

Following General Procedures J and K for the Mitsunobu reaction, and chemoselective saponification of aryl esters, respectively, **S-121** gave **R-121**. Spectra were in agreement with those previously reported.[85]

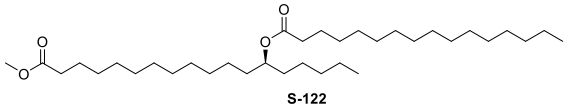

S-122

Following General Procedure L for the Yamaguchi esterification, **121** gave **122** as an oil.

Rf = 0.51 (silica gel, 90:10, hexanes:ethyl acetate)

1H NMR (600 MHz, CDCl3) δ 4.89 – 4.83 (m, 1H), 3.66 (s, 3H), 2.29 (dt, J = 14.6, 7.5 Hz, 4H), 1.65 – 1.19 (m, 62H), 0.87 (t, J = 6.5 Hz, 6H).

1H NMR (600 MHz, CDCl3) δ 4.89 – 4.83 (m, 1H), 3.66 (s, 3H), 2.29 (dt, J = 14.6, 7.5 Hz, 4H), 1.65 – 1.19 (m, 62H), 0.87 (t, J = 6.5 Hz, 6H).

HRMS HR-ESI-TOFMS calc. for [C35 H68 O4 Na]+: 575.5010 obs. 575.5005

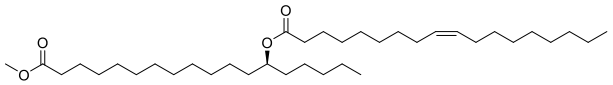

S-123

Following General Procedure L for the Yamaguchi esterification, **121** gave **123** as an oil.

Rf = 0.51 (silica gel, 90:10, hexanes:ethyl acetate)

1H NMR (600 MHz, CDCl3) δ 5.37 – 5.31 (m, 2H), 4.90 – 4.83 (m, 1H), 3.66 (s, 3H), 2.33 – 2.24 (m, 4H), 2.03 – 1.98 (m, 4H), 1.65 – 1.19 (m, 55H), 0.87 (t, J = 6.1 Hz, 6H).

13C NMR (151 MHz, CDCl3) δ 174.53, 173.87, 130.12, 129.90, 74.22, 51.61, 34.87, 34.30, 34.26, 34.24, 32.05, 31.86, 29.91, 29.85, 29.70, 29.69, 29.67, 29.59, 29.47, 29.41, 29.36, 29.30, 29.29, 27.36, 27.31, 25.48, 25.31, 25.13, 25.10, 22.84, 22.71, 14.28, 14.17.

HRMS: HR-ESI-TOFMS calc. for [C37 H70 O4 Na]+: 601.5166 obs. 601.5159

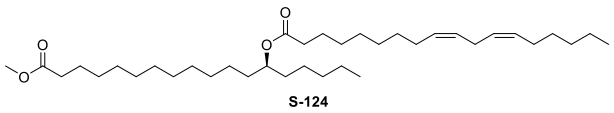

S-124

Following General Procedure L for the Yamaguchi esterification, **121** gave **124** as an oil.

Rf = 0.51 (silica gel, 90:10, hexanes:ethyl acetate)

1H NMR (600 MHz, CDCl3) δ 5.40 – 5.32 (m, 4H), 4.86 (p, J = 6.2 Hz, 1H), 3.66 (s, 3H), 2.77 (t, J = 6.7 Hz, 2H), 2.32 – 2.25 (m, 4H), 2.04 (t, J = 7.0 Hz, 4H), 1.65 – 1.19 (m, 49H), 0.88 (q, J = 7.0 Hz, 6H).

13C NMR (151 MHz, CDCl3) δ 174.52, 173.86, 130.36, 130.20, 128.15, 128.04, 74.22, 51.61, 34.87, 34.30, 34.26, 34.24, 31.86, 31.67, 29.75, 29.70, 29.69, 29.59, 29.49, 29.41, 29.36, 29.30, 27.34, 25.76, 25.48, 25.31, 25.13, 25.10, 22.73, 22.71, 14.24, 14.17.

HRMS: HR-ESI-TOFMS calc. for [C37 H68 O4 Na]+ : 599.5010 obs. 599.5003

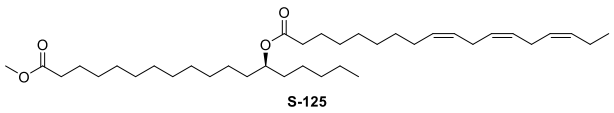

S-125

Following General Procedure L for the Yamaguchi esterification, **121** gave **125** as an oil.

Rf = 0.49 (silica gel, 90:10, hexanes:ethyl acetate)

1H NMR (600 MHz, CDCl3) δ 5.41 – 5.29 (m, 6H), 4.86 (p, J = 6.1 Hz, 1H), 3.66 (s, 3H), 2.80 (s, 4H), 2.32 – 2.25 (m, 4H), 2.10 – 2.02 (m, 4H), 1.65 – 1.19 (m, 43H), 0.97 (t, J = 7.5 Hz, 3H), 0.87 (t, J = 6.5 Hz, 3H).

13C NMR (151 MHz, CDCl3) δ 174.53, 173.86, 132.10, 130.42, 128.41, 128.39, 127.84, 127.24, 74.23, 51.62, 34.87, 34.30, 34.26, 34.24, 31.86, 29.74, 29.69, 29.59, 29.41, 29.36, 29.30, 27.35, 25.75, 25.66, 25.48, 25.31, 25.13, 25.10, 22.71, 20.69, 14.44, 14.17.

HRMS: HR-ESI-TOFMS calc. for [C37 H66 O4 Na]+ : 597.4853 obs. 597.4851

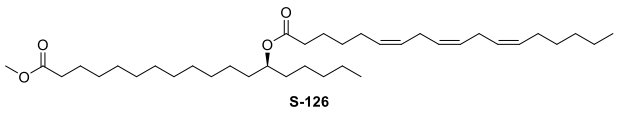

S-126

Following General Procedure L for the Yamaguchi esterification, **121** gave **126** as an oil.

Rf = 0.46 (silica gel, 90:10, hexanes:ethyl acetate)

1H NMR (600 MHz, CDCl3) δ 5.41 – 5.28 (m, 6H), 4.86 (p, J = 6.1 Hz, 1H), 3.66 (s, 3H), 2.80 (t, J = 5.8 Hz, 4H), 2.33 – 2.26 (m, 4H), 2.12 – 2.03 (m, 4H), 1.68 – 1.19 (m, 41H), 0.88 (dd, J = 14.6, 7.0 Hz, 6H).

13C NMR (151 MHz, CDCl3) δ 174.52, 173.67, 130.58, 129.80, 128.52, 128.29, 128.22, 127.72, 74.28, 51.61, 34.73, 34.29, 34.26, 34.23, 31.85, 31.66, 29.70, 29.69, 29.59, 29.47, 29.41, 29.29, 29.27, 27.35, 27.03, 25.75, 25.48, 25.13, 25.10, 24.92, 22.72, 22.70, 14.23, 14.17.

HRMS: HR-ESI-TOFMS calc. for [C37 H66 O4 Na]+: 597.4853 obs. 597.4852

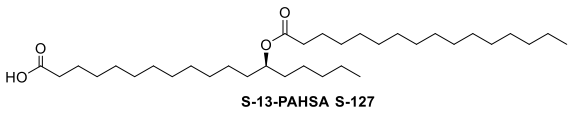

S-13-PAHSA S-127

Following General Procedure M for the chemoselective saponification of methyl esters, **122** gave **127** as a white solid.

Rf = 0.30 (silica gel, 80:20, hexanes:ethyl acetate)

1H NMR (600 MHz, CDCl3) δ 4.90 – 4.83 (m, 1H), 2.34 (t, J = 7.5 Hz, 2H), 2.27 (t, J = 7.5 Hz, 2H), 1.66 – 1.18 (m, 61H), 0.87 (td, J = 6.9, 1.6 Hz, 6H).

HRMS: HR-ESI-TOFMS calc. for [C34 H65 O4]-: 537.4888 obs. 537.4877

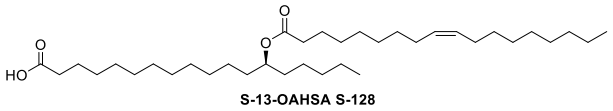

S-13-OAHSA S-128

Following General Procedure M for the chemoselective saponification of methyl esters, **123** gave **128** as a clear, slightly yellow oil.

Rf = 0.30 (silica gel, 80:20, hexanes:ethyl acetate)

1H NMR (600 MHz, CDCl3) δ 5.40 – 5.30 (m, 2H), 4.91 – 4.82 (m, 1H), 2.34 (t, J = 7.3 Hz, 2H), 2.27 (t, J = 7.4 Hz, 2H), 2.04 – 1.96 (m, 4H), 1.62 (dd, J = 14.2, 7.1 Hz, 4H), 1.49 (s, 4H), 1.27 (dd, J = 21.0, 8.8 Hz, 46H), 0.87 (t, J = 6.1 Hz, 6H).

13C NMR (151 MHz, CDCl3) δ 173.94, 130.13, 129.90, 74.25, 34.88, 34.30, 34.24, 32.05, 31.86, 29.91, 29.85, 29.67, 29.55, 29.47, 29.36, 29.30, 29.29, 29.18, 27.36, 27.31, 25.47, 25.31, 25.13, 24.82, 22.84, 22.71, 14.28, 14.17.

HRMS: HR-ESI-TOFMS calc. for [C36 H67 O4]-: 563.5045 obs. 563.5043

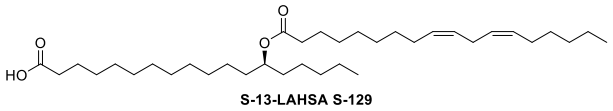

S-13-LAHSA S-129

Following General Procedure M for the chemoselective saponification of methyl esters, **124** gave **129** as a clear, slightly yellow oil.

Rf = 0.30 (silica gel, 80:20, hexanes:ethyl acetate)

1H NMR (600 MHz, CDCl3) δ 5.44 – 5.26 (m, 4H), 4.89 – 4.83 (m, 1H), 2.76 (t, J = 6.6 Hz, 2H), 2.34 (t, J = 7.0 Hz, 2H), 2.27 (t, J = 7.3 Hz, 2H), 2.08 – 2.00 (m, 4H), 1.66 – 1.16 (m, 50H), 0.87 (dd, J = 13.7, 6.7 Hz, 6H).

13C NMR (151 MHz, CDCl3) δ 179.98, 173.94, 130.34, 130.18, 128.15, 128.03, 74.26, 34.87, 34.29, 34.23, 34.18, 31.85, 31.66, 29.75, 29.67, 29.56, 29.49, 29.37, 29.35, 29.29, 29.19, 27.33, 25.75, 25.46, 25.30, 25.12, 24.82, 22.72, 22.70, 14.23, 14.16.

HRMS: HR-ESI-TOFMS calc. for [C36H65O4]-: 561.4888 obs. 561.4874

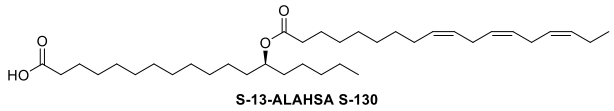

S-13-ALAHSA S-130

Following General Procedure M for the chemoselective saponification of methyl esters, **125** gave **130** as a clear, slightly yellow oil.

Rf = 0.30 (silica gel, 80:20, hexanes:ethyl acetate)

1H NMR (600 MHz, CDCl3) δ 5.42 – 5.28 (m, 6H), 4.90 – 4.84 (m, 1H), 2.80 (s, 4H), 2.35 (t, J = 7.5 Hz, 2H), 2.28 (t, J = 7.5 Hz, 2H), 2.11 – 2.02 (m, 4H), 1.67 – 1.20 (m, 44H), 0.97 (t, J = 7.5 Hz, 3H), 0.87 (t, J = 6.9 Hz, 3H).

13C NMR (151 MHz, CDCl3) δ 179.55, 173.84, 131.97, 130.30, 128.29, 128.26, 127.72, 127.12, 74.16, 34.75, 34.17, 34.12, 33.99, 31.74, 31.73, 29.61, 29.56, 29.44, 29.25, 29.23, 29.18, 29.17, 29.07, 27.23, 25.62, 25.54, 25.35, 25.18, 25.00, 24.70, 22.58, 20.57, 14.31, 14.05.

HRMS: HR-ESI-TOFMS calc. for [C36H63O4]-: 559.4732 obs. 559.4718

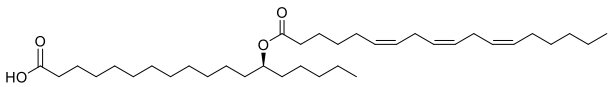

S-13-GLAHSA S-131

Following General Procedure M for the chemoselective saponification of methyl esters, **126** gave **131** as a clear, slightly yellow oil.

Rf = 0.30 (silica gel, 80:20, hexanes:ethyl acetate)

1H NMR (600 MHz, CDCl3) δ 5.45 – 5.28 (m, 6H), 4.92 – 4.81 (m, 1H), 2.86 – 2.76 (m, 4H), 2.34 (t, J = 7.5 Hz, 2H), 2.29 (t, J = 7.5 Hz, 2H), 2.12 – 2.02 (m, 4H), 1.68 – 1.20 (m, 41H), 0.88 (dd, J = 15.3, 7.0 Hz, 6H).

13C NMR (151 MHz, CDCl3) δ 173.73, 130.59, 129.80, 128.52, 128.29, 128.23, 127.72, 74.32, 34.74, 34.29, 34.23, 31.86, 31.66, 29.67, 29.55, 29.47, 29.36, 29.27, 29.18, 27.36, 27.03, 25.76, 25.75, 25.48, 25.13, 24.93, 24.83, 22.73, 22.71, 14.24, 14.18.

HRMS: HR-ESI-TOFMS calc. for [C36H63O4]-: 559.4732 obs. 559.4717

Appendix A: Catalog of Spectra

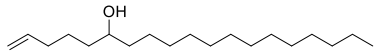
OH

25

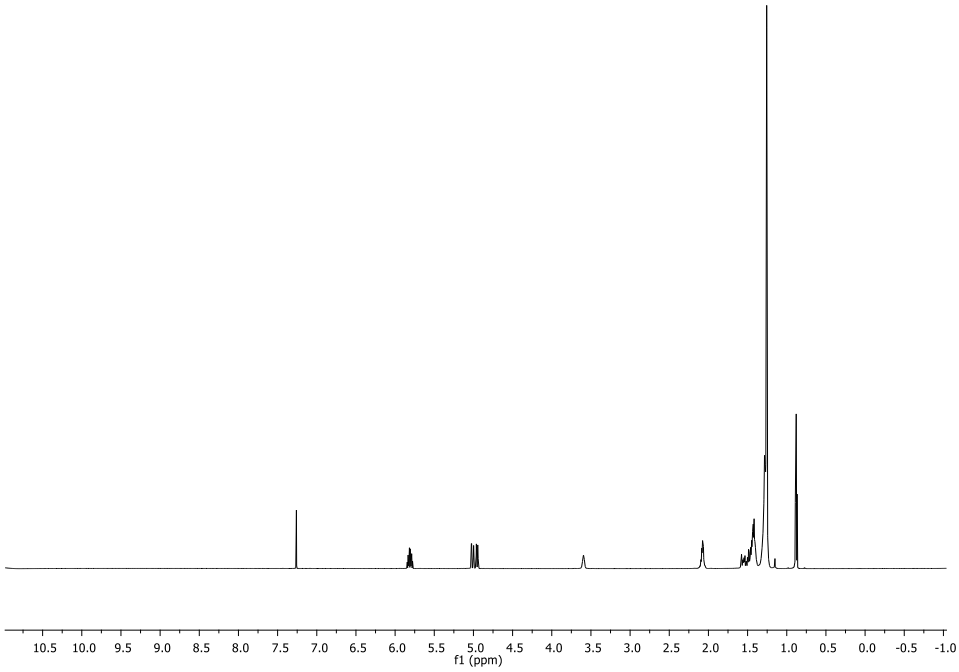
10.5 10.0 9.5 9.0 8.5 8.0 7.5 7.0 6.5 6.0 5.5 5.0 4.5 4.0 3.5 3.0 2.5 2.0 1.5 1.0 0.5 0.0 -0.5 -1.0
f1 (ppm)

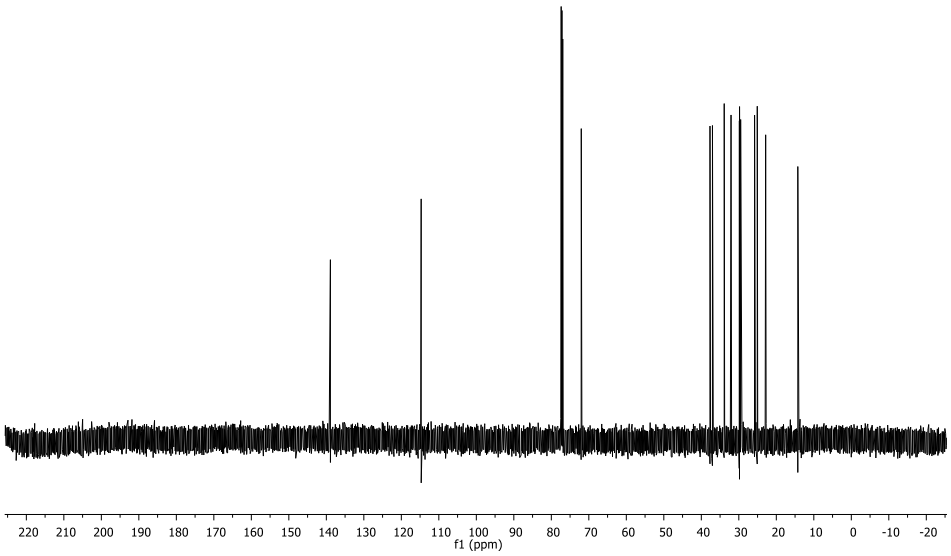
220 210 200 190 180 170 160 150 140 130 120 110 100 90 80 70 60 50 40 30 20 10 0 -10 -20
f1 (ppm)

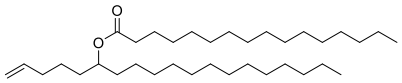

26

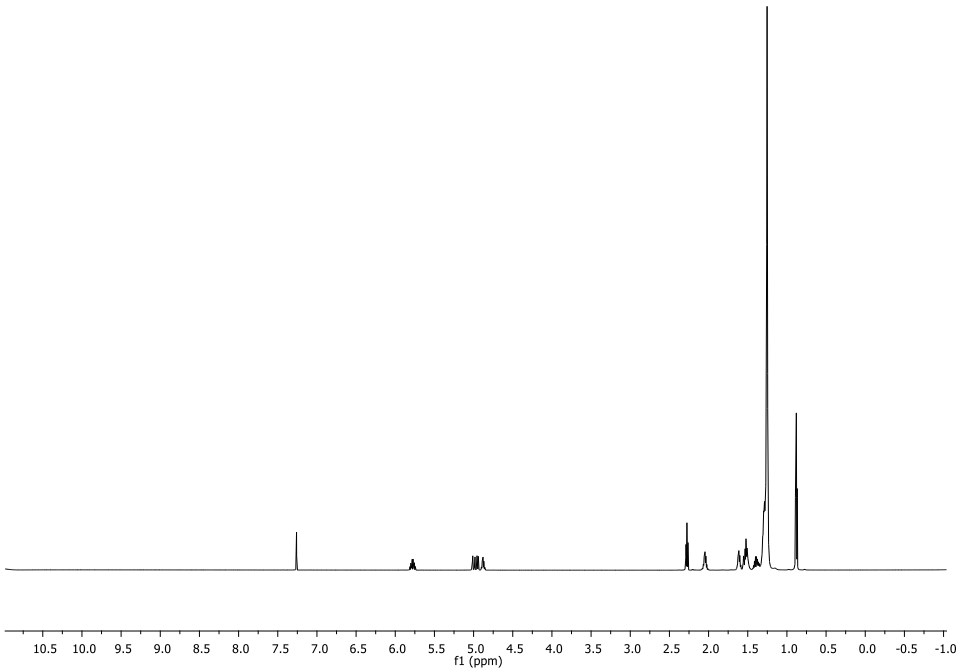
10.5 10.0 9.5 9.0 8.5 8.0 7.5 7.0 6.5 6.0 5.5 5.0 4.5 4.0 3.5 3.0 2.5 2.0 1.5 1.0 0.5 0.0 -0.5 -1.0
f1 (ppm)

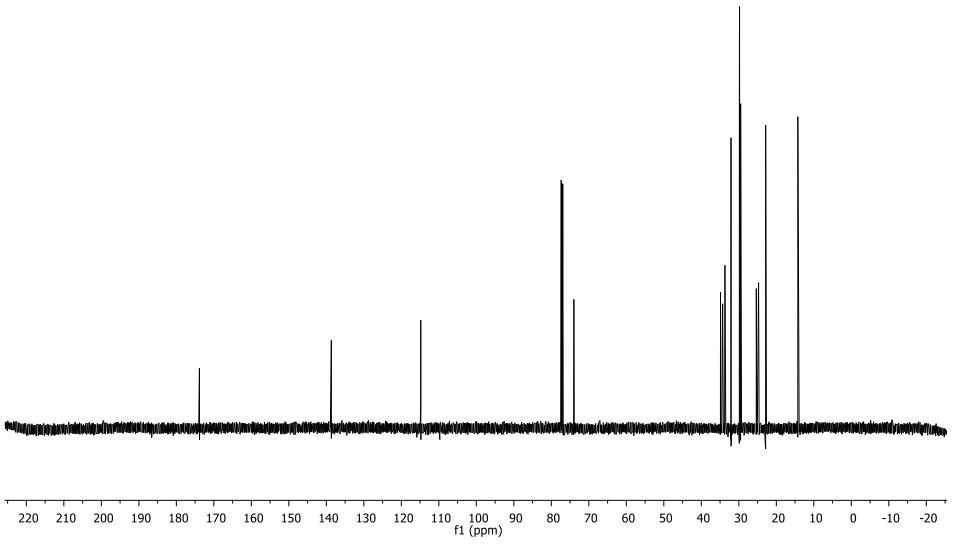
220 210 200 190 180 170 160 150 140 130 120 110 100 90 80 70 60 50 40 30 20 10 0 -10 -20
f1 (ppm)

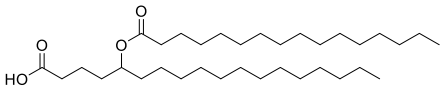
O
O
O
HO

5-PAHSA **12**

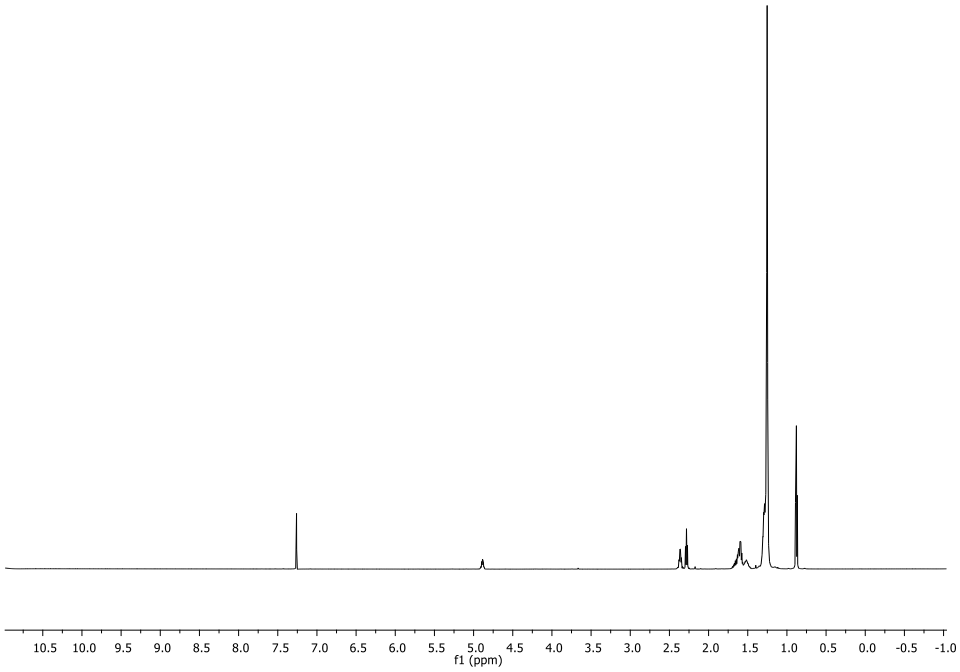
10.5 10.0 9.5 9.0 8.5 8.0 7.5 7.0 6.5 6.0 5.5 5.0 4.5 4.0 3.5 3.0 2.5 2.0 1.5 1.0 0.5 0.0 -0.5 -1.0
f1 (ppm)

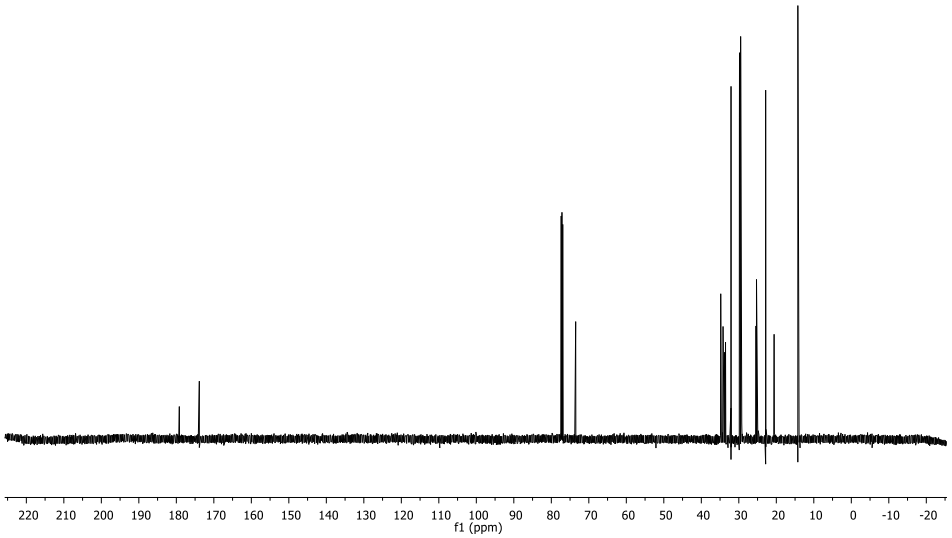
220 210 200 190 180 170 160 150 140 130 120 110 100 90 80 70 60 50 40 30 20 10 0 -10 -20
f1 (ppm)

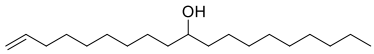
OH

71

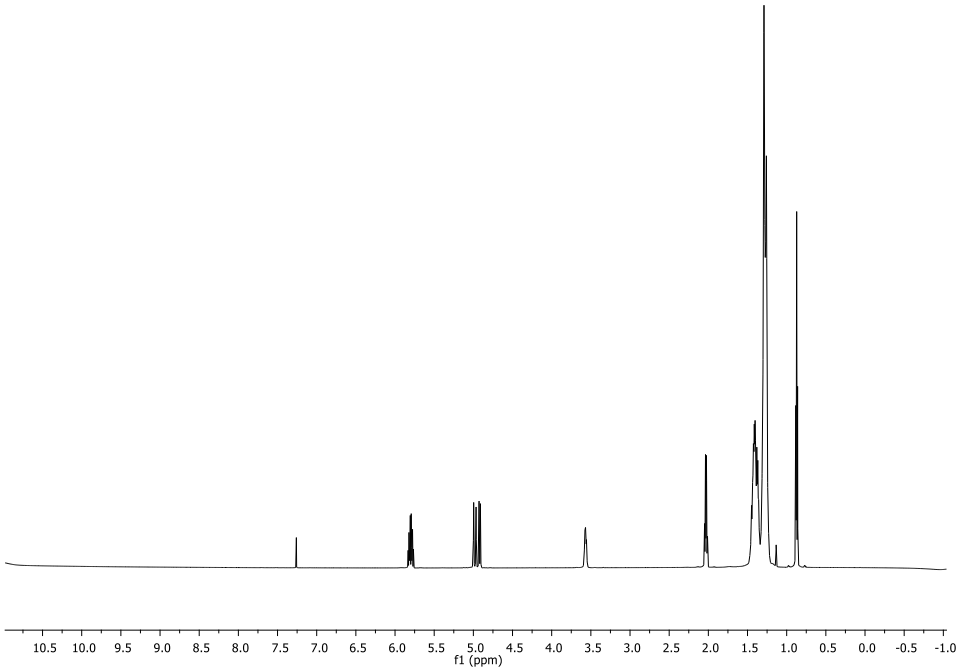
10.5 10.0 9.5 9.0 8.5 8.0 7.5 7.0 6.5 6.0 5.5 5.0 4.5 4.0 3.5 3.0 2.5 2.0 1.5 1.0 0.5 0.0 -0.5 -1.0
f1 (ppm)

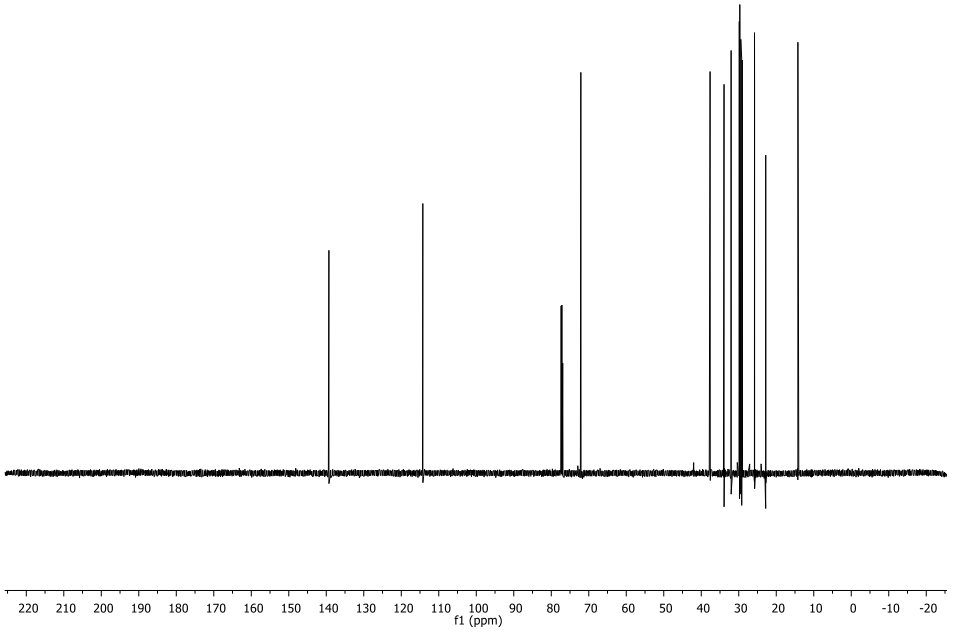
220 210 200 190 180 170 160 150 140 130 120 110 100 90 80 70 60 50 40 30 20 10 0 -10 -20
f1 (ppm)

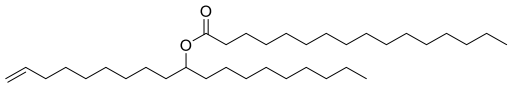

72

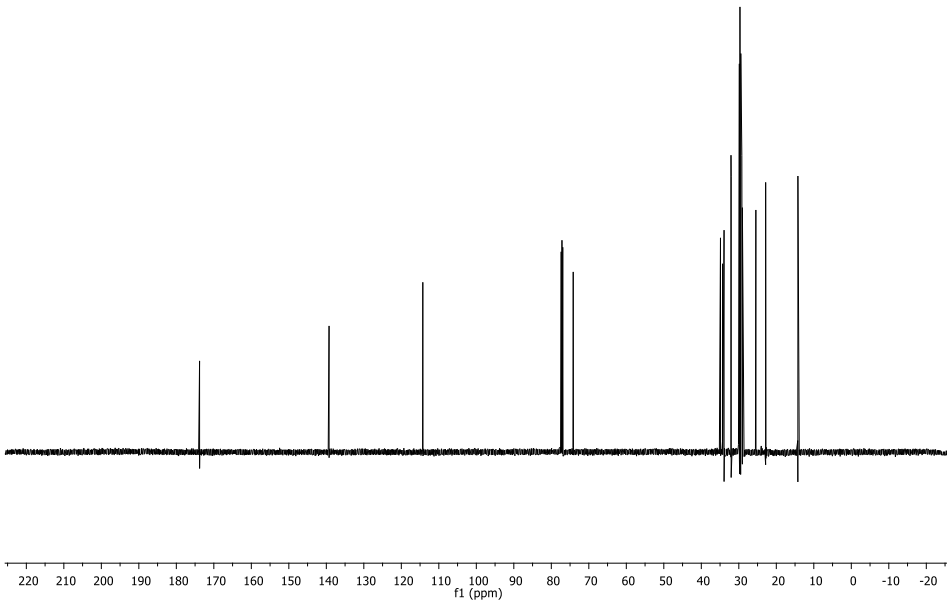
220 210 200 190 180 170 160 150 140 130 120 110 100 90 80 70 60 50 40 30 20 10 0 -10 -20
f1 (ppm)

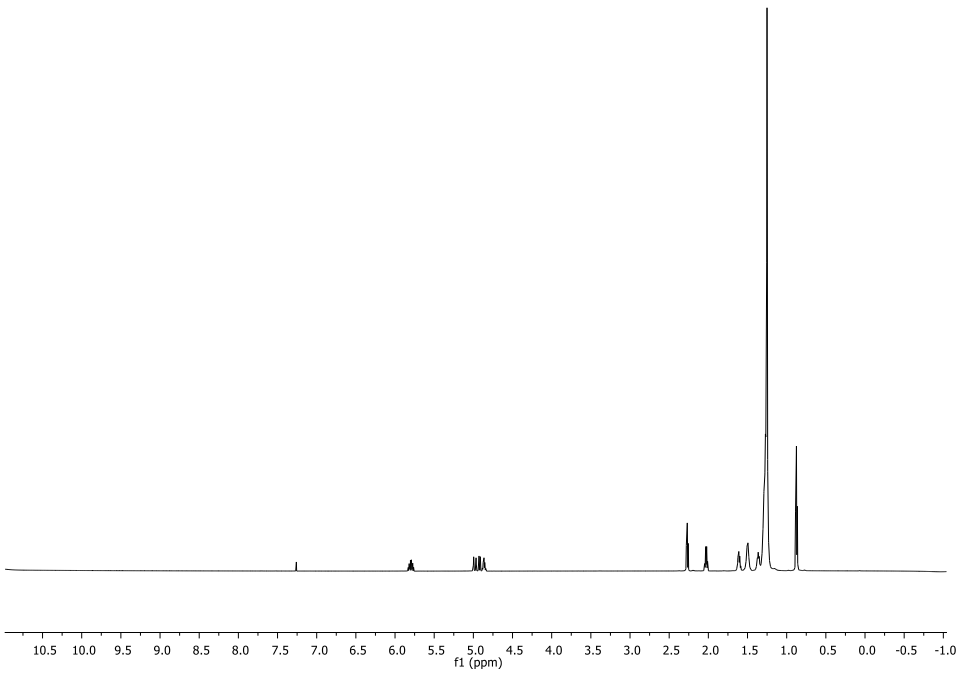
10.5 10.0 9.5 9.0 8.5 8.0 7.5 7.0 6.5 6.0 5.5 5.0 4.5 4.0 3.5 3.0 2.5 2.0 1.5 1.0 0.5 0.0 -0.5 -1.0
f1 (ppm)

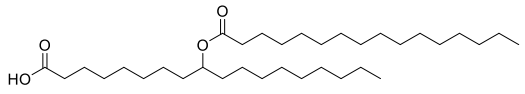

9-PAHSA **13**

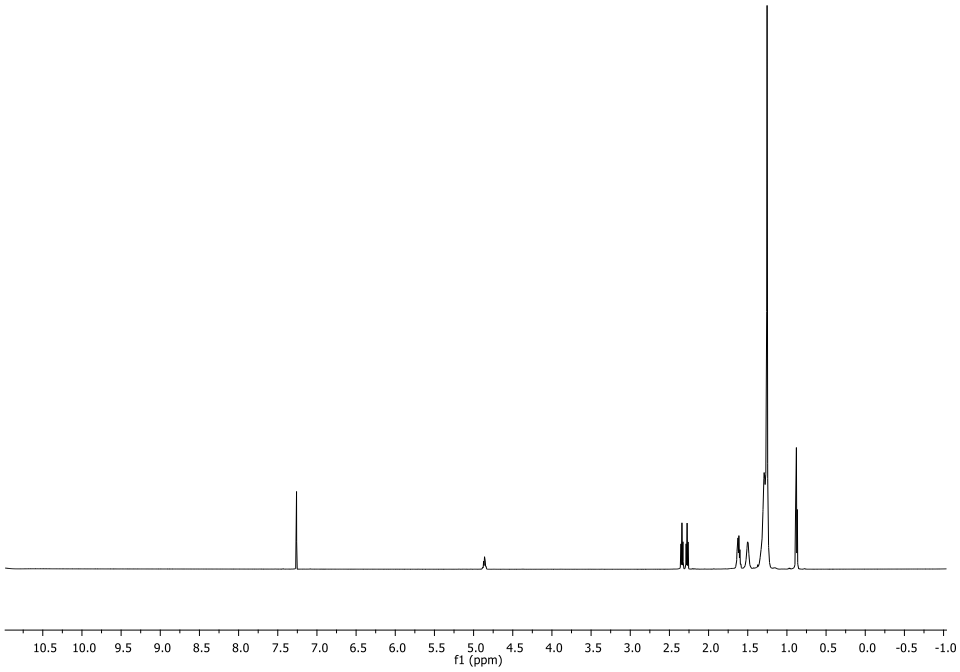
10.5 10.0 9.5 9.0 8.5 8.0 7.5 7.0 6.5 6.0 5.5 5.0 4.5 4.0 3.5 3.0 2.5 2.0 1.5 1.0 0.5 0.0 -0.5 -1.0
f1 (ppm)

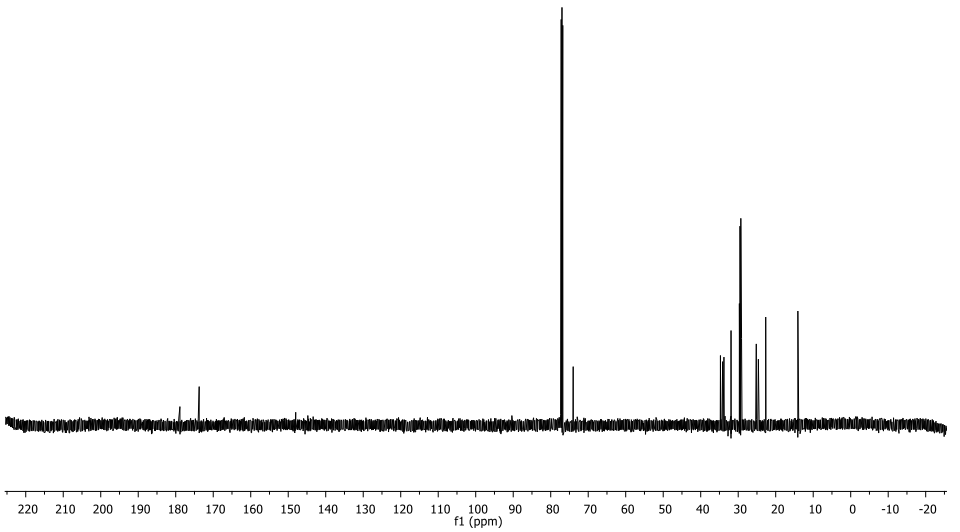
220 210 200 190 180 170 160 150 140 130 120 110 100 90 80 70 60 50 40 30 20 10 0 -10 -20
f1 (ppm)

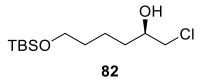
OH
TBSO
Cl

82

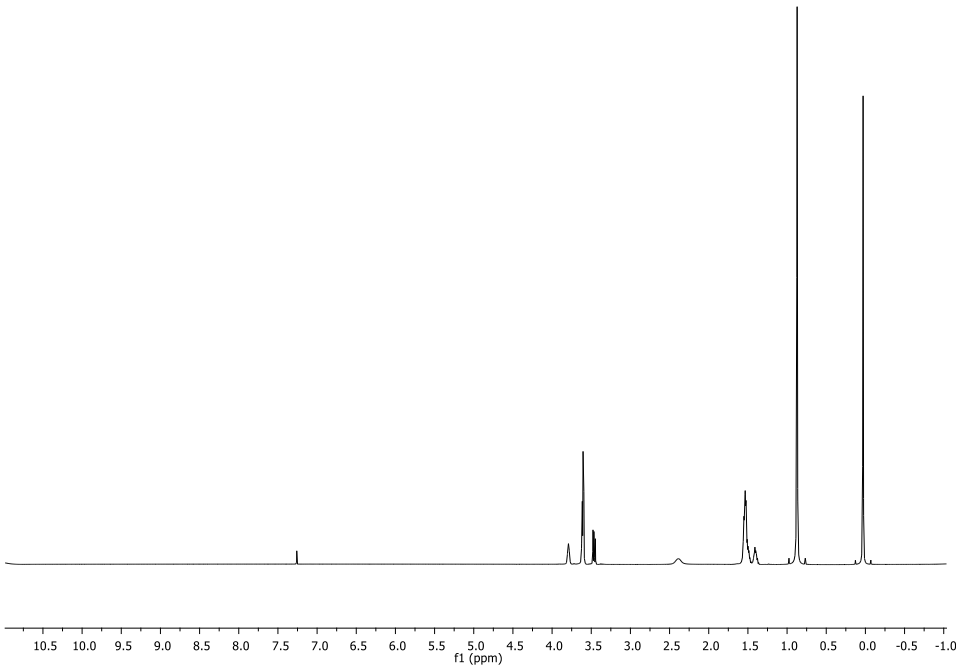
10.5 10.0 9.5 9.0 8.5 8.0 7.5 7.0 6.5 6.0 5.5 5.0 4.5 4.0 3.5 3.0 2.5 2.0 1.5 1.0 0.5 0.0 -0.5 -1.0
f1 (ppm)

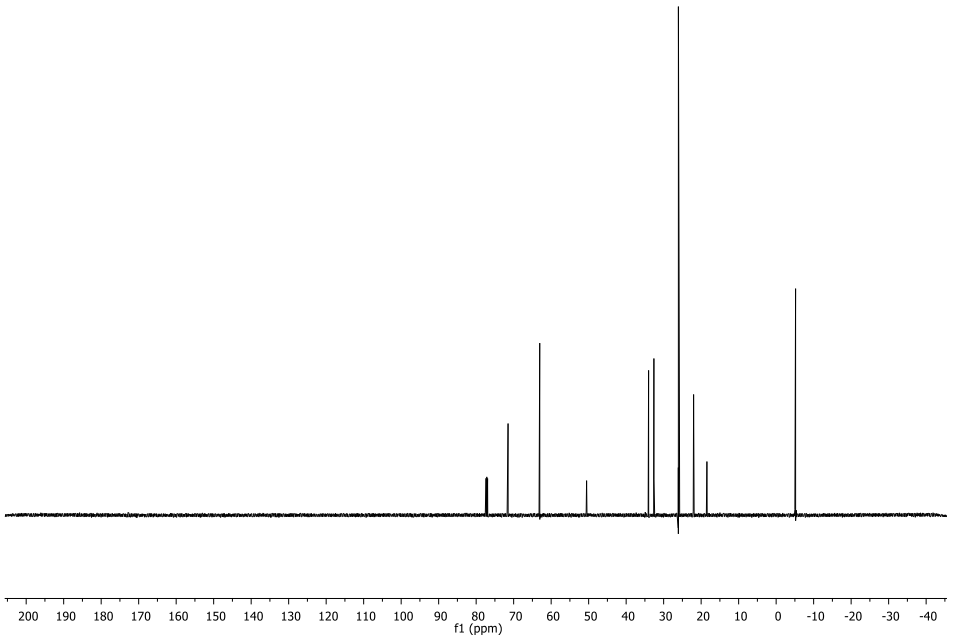
200 190 180 170 160 150 140 130 120 110 100 90 80 70 60 50 40 30 20 10 0 -10 -20 -30 -40
f1 (ppm)

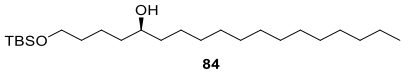
OH
TBSO

84

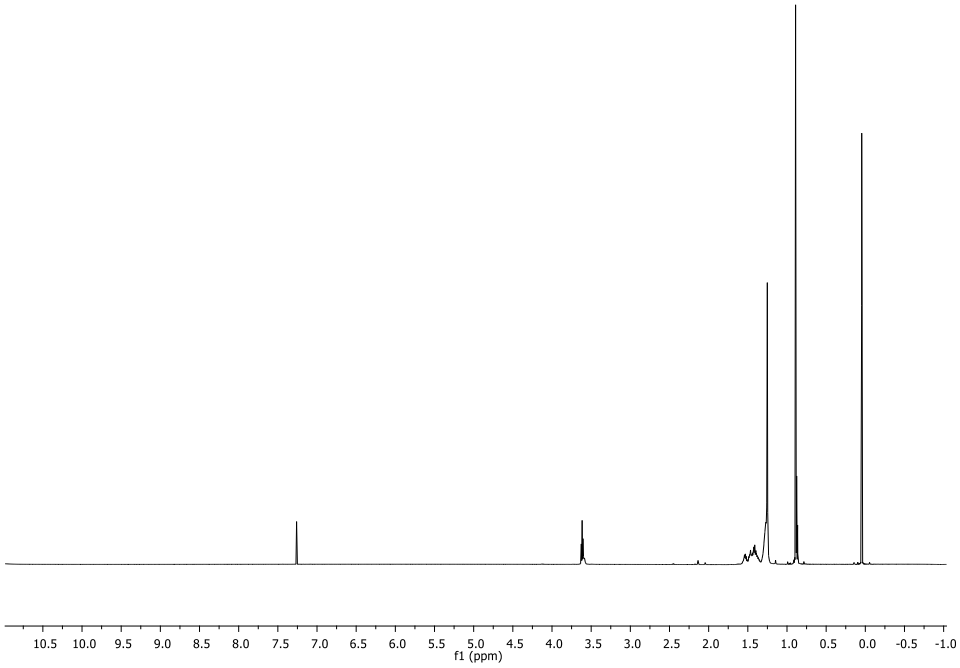
10.5 10.0 9.5 9.0 8.5 8.0 7.5 7.0 6.5 6.0 5.5 5.0 4.5 4.0 3.5 3.0 2.5 2.0 1.5 1.0 0.5 0.0 -0.5 -1.0
f1 (ppm)

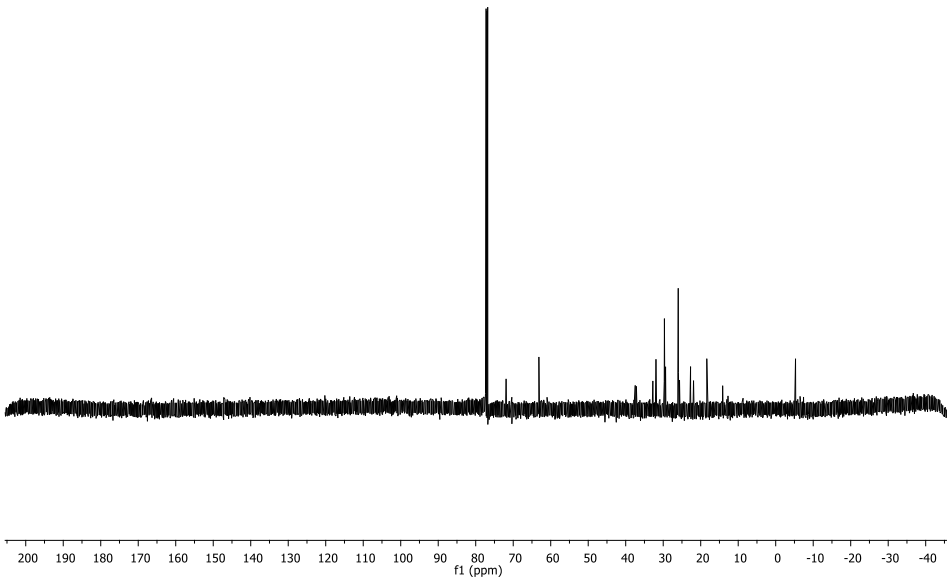
200 190 180 170 160 150 140 130 120 110 100 90 80 70 60 50 40 30 20 10 0 -10 -20 -30 -40
f1 (ppm)

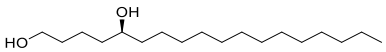
OH
HO

85

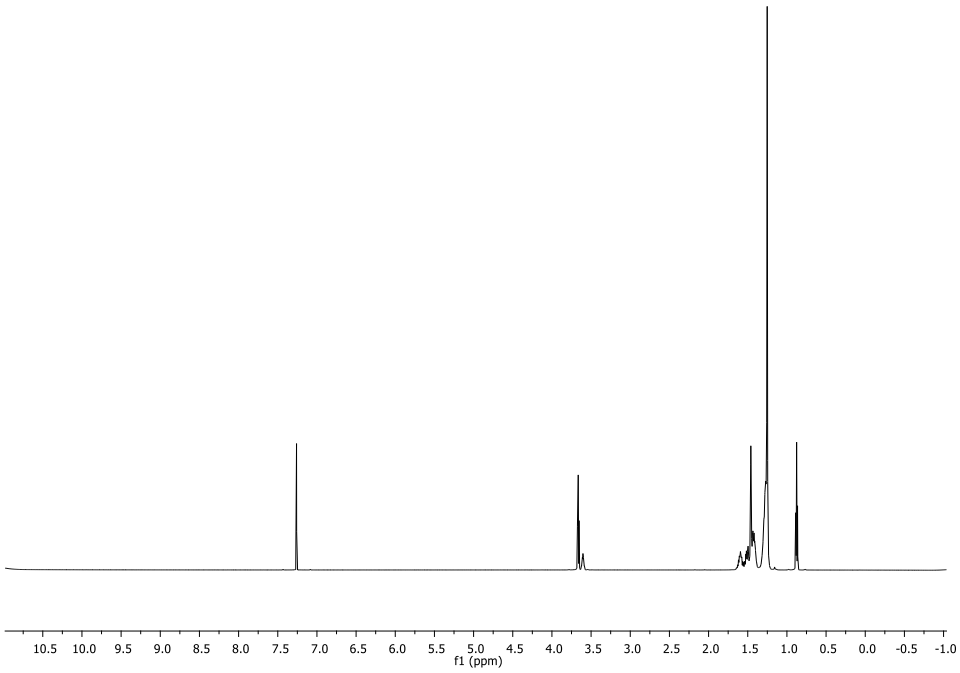
10.5 10.0 9.5 9.0 8.5 8.0 7.5 7.0 6.5 6.0 5.5 5.0 4.5 4.0 3.5 3.0 2.5 2.0 1.5 1.0 0.5 0.0 -0.5 -1.0
f1 (ppm)

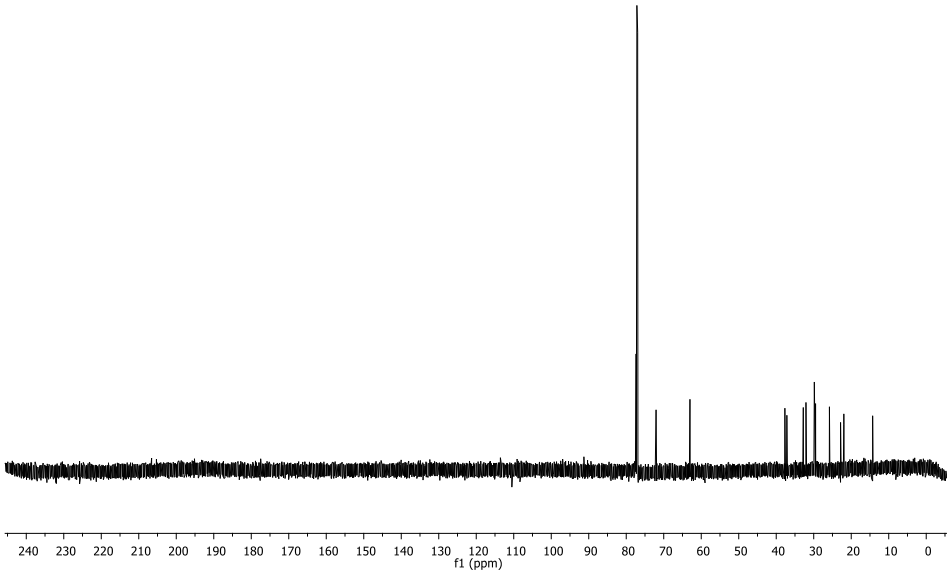
240 230 220 210 200 190 180 170 160 150 140 130 120 110 100 90 80 70 60 50 40 30 20 10 0
f1 (ppm)

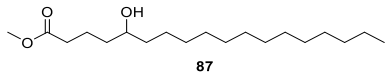
O
OH
O

87

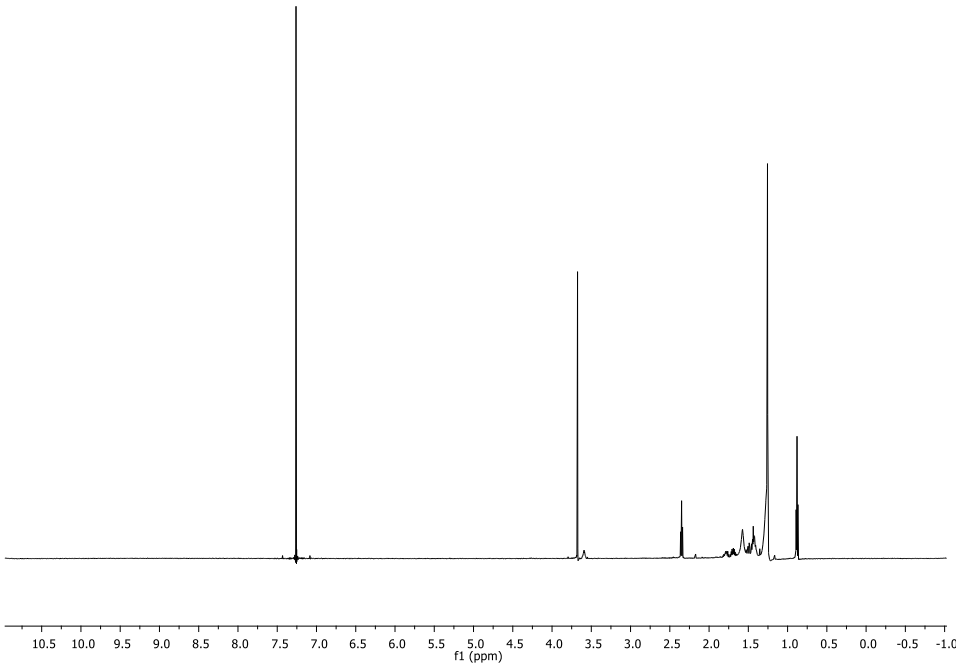
10.5 10.0 9.5 9.0 8.5 8.0 7.5 7.0 6.5 6.0 5.5 5.0 4.5 4.0 3.5 3.0 2.5 2.0 1.5 1.0 0.5 0.0 -0.5
f1 (ppm)

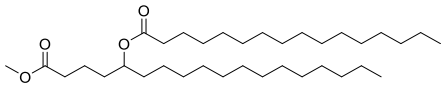

89

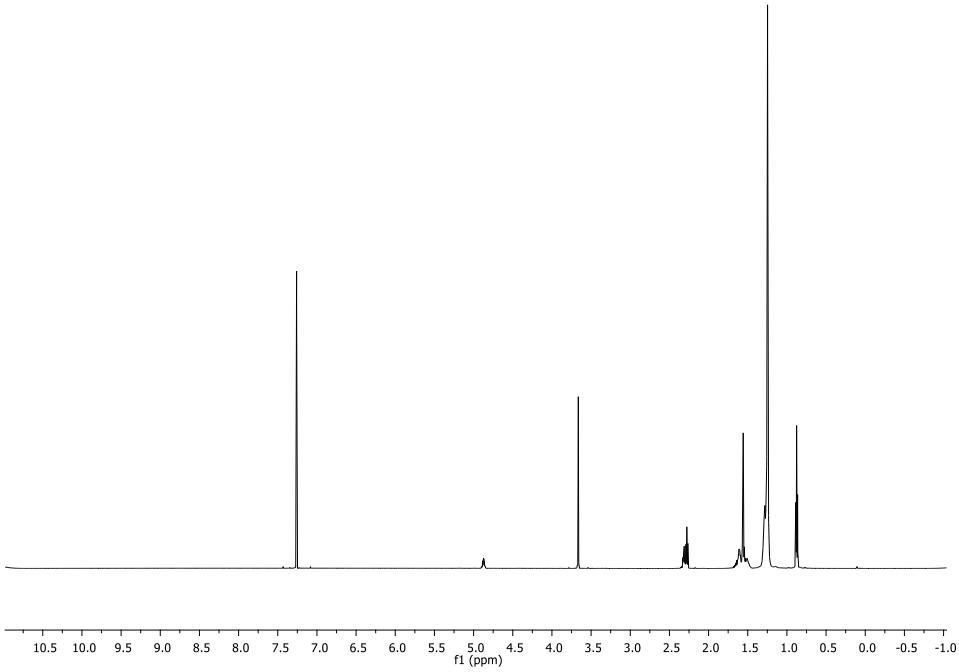
10.5 10.0 9.5 9.0 8.5 8.0 7.5 7.0 6.5 6.0 5.5 5.0 4.5 4.0 3.5 3.0 2.5 2.0 1.5 1.0 0.5 0.0 -0.5 -1.0
f1 (ppm)

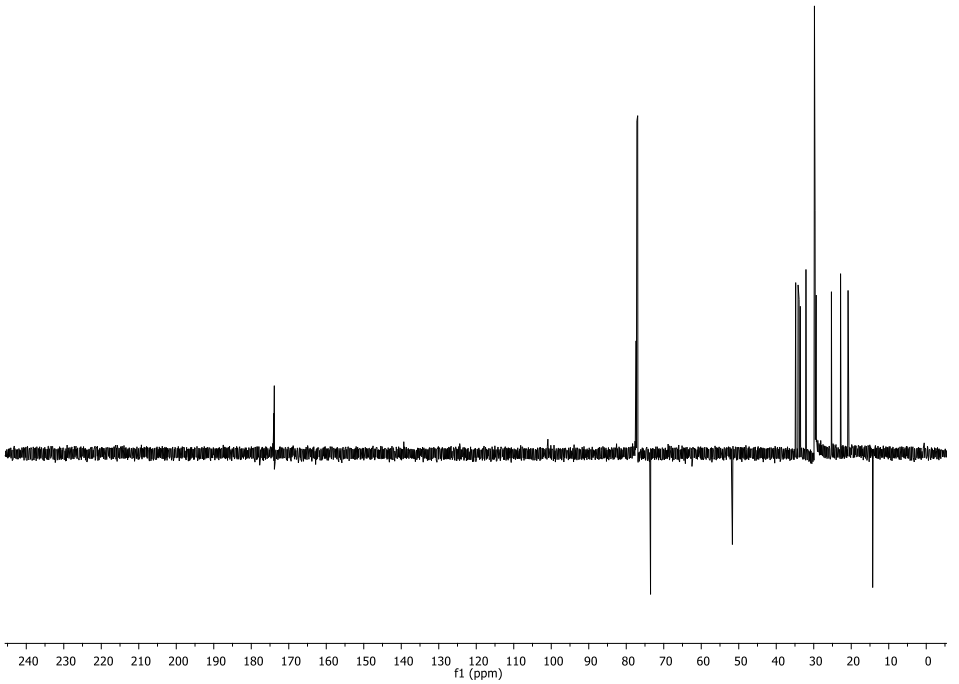
240 230 220 210 200 190 180 170 160 150 140 130 120 110 100 90 80 70 60 50 40 30 20 10 0
f1 (ppm)

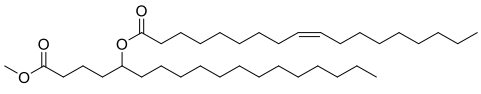

90

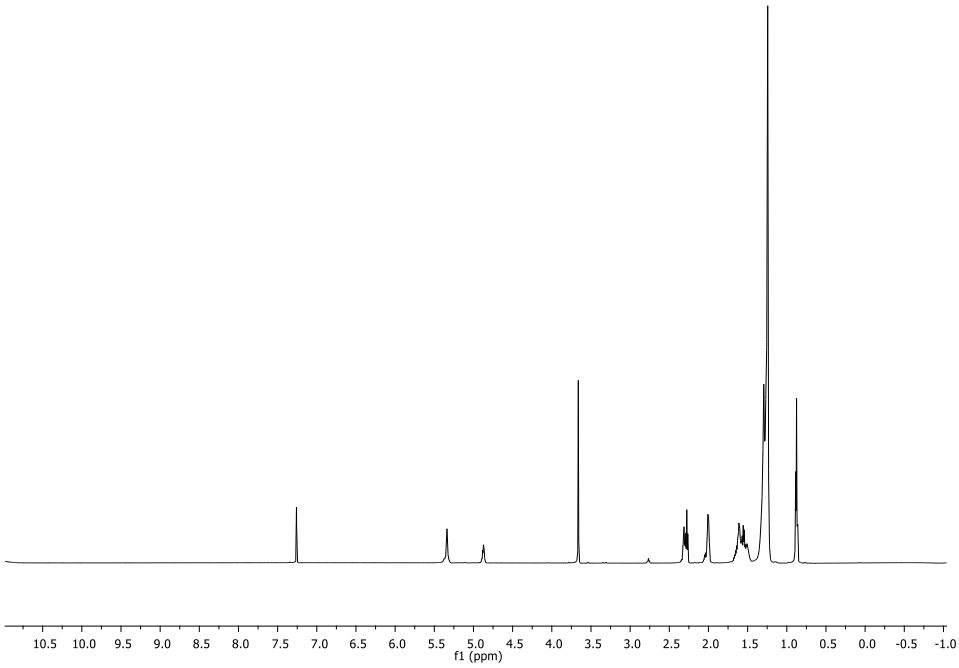
10.5 10.0 9.5 9.0 8.5 8.0 7.5 7.0 6.5 6.0 5.5 5.0 4.5 4.0 3.5 3.0 2.5 2.0 1.5 1.0 0.5 0.0 -0.5 -1.0
f1 (ppm)

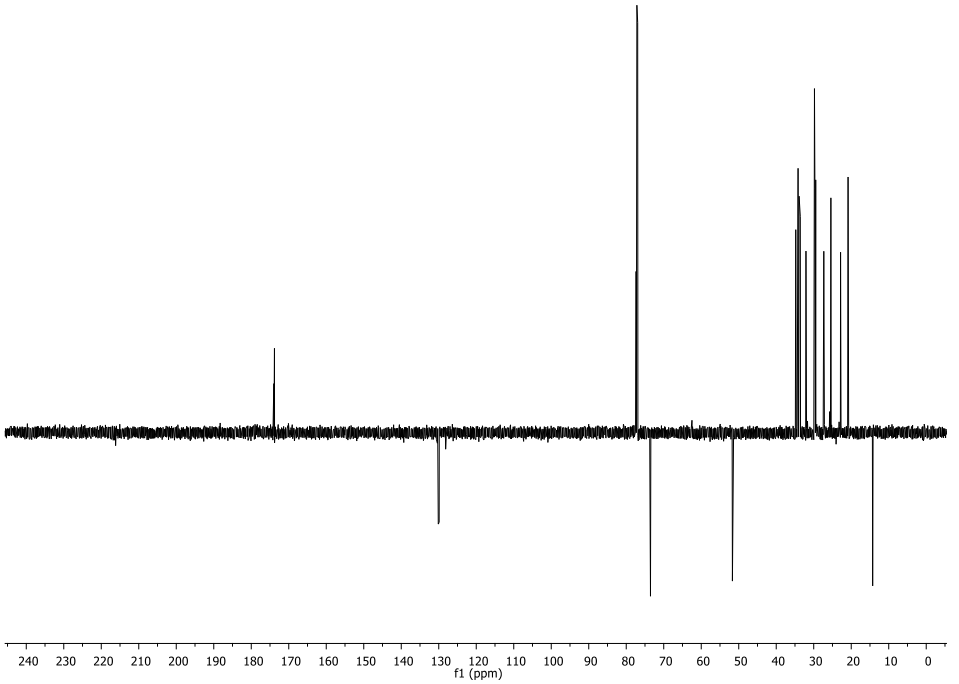
240 230 220 210 200 190 180 170 160 150 140 130 120 110 100 90 80 70 60 50 40 30 20 10 0
f1 (ppm)

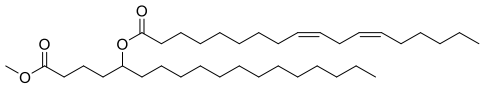

91

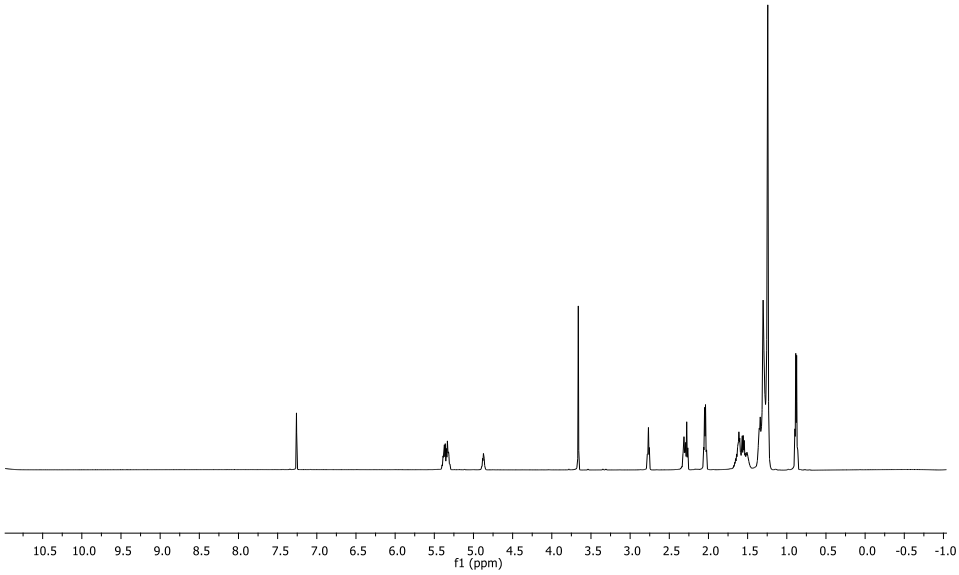
10.5 10.0 9.5 9.0 8.5 8.0 7.5 7.0 6.5 6.0 5.5 5.0 4.5 4.0 3.5 3.0 2.5 2.0 1.5 1.0 0.5 0.0 -0.5 -1.0
f1 (ppm)

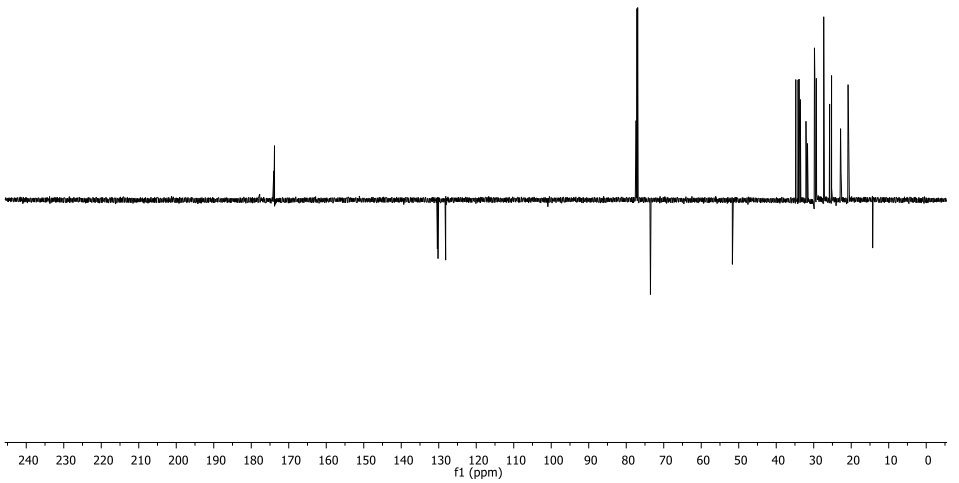
240 230 220 210 200 190 180 170 160 150 140 130 120 110 100 90 80 70 60 50 40 30 20 10 0
f1 (ppm)

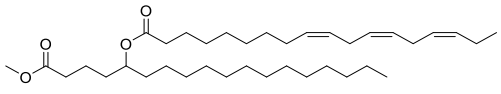

92

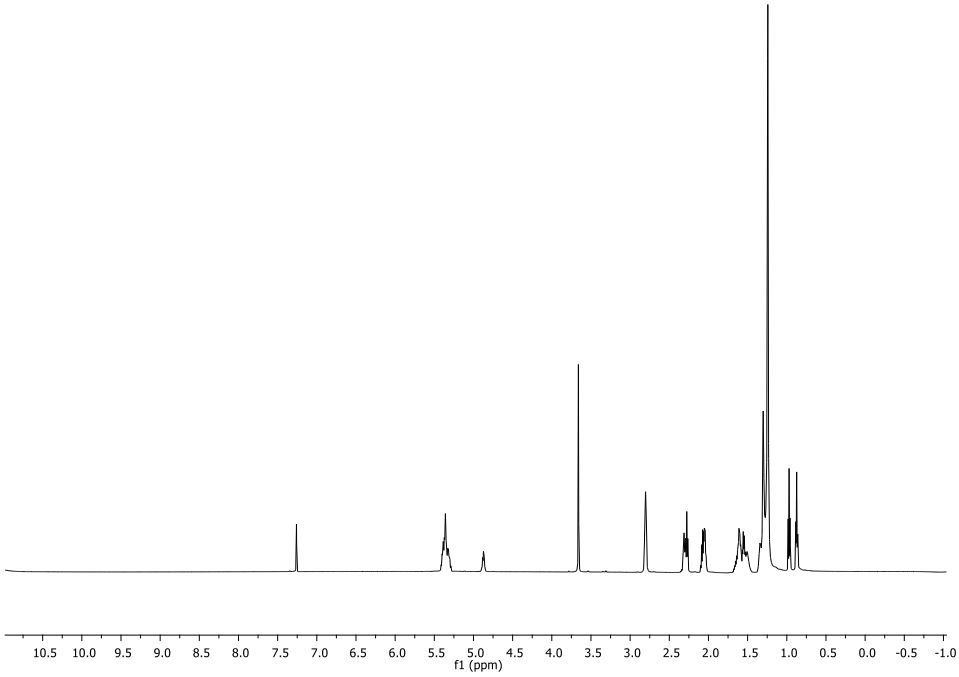
10.5 10.0 9.5 9.0 8.5 8.0 7.5 7.0 6.5 6.0 5.5 5.0 4.5 4.0 3.5 3.0 2.5 2.0 1.5 1.0 0.5 0.0 -0.5 -1.0
f1 (ppm)

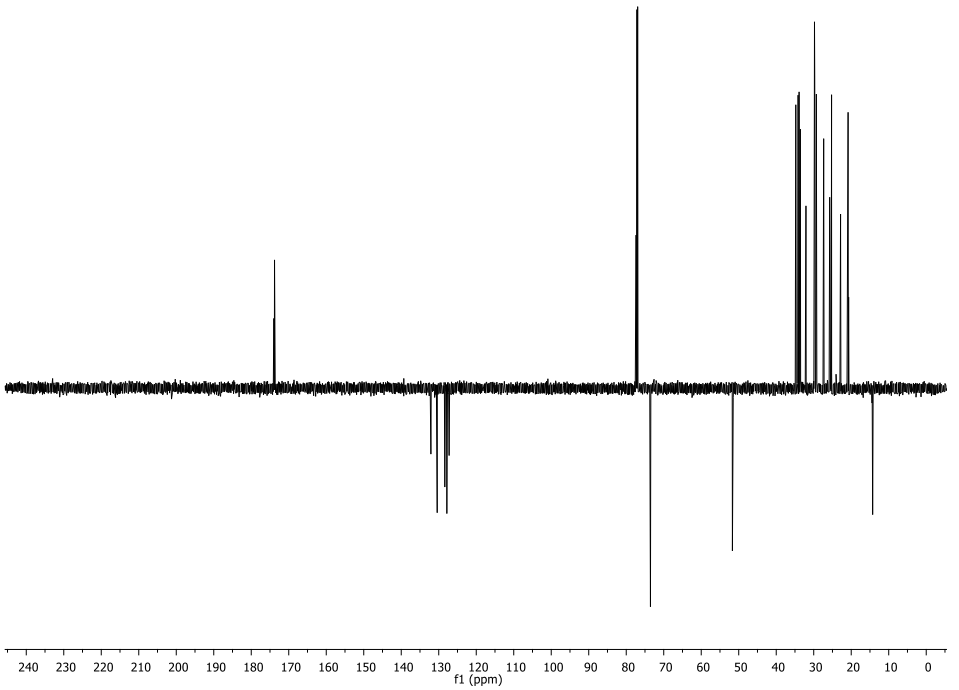
240 230 220 210 200 190 180 170 160 150 140 130 120 110 100 90 80 70 60 50 40 30 20 10 0
f1 (ppm)

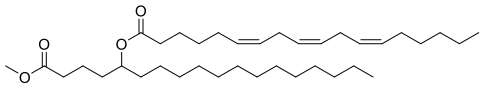

93

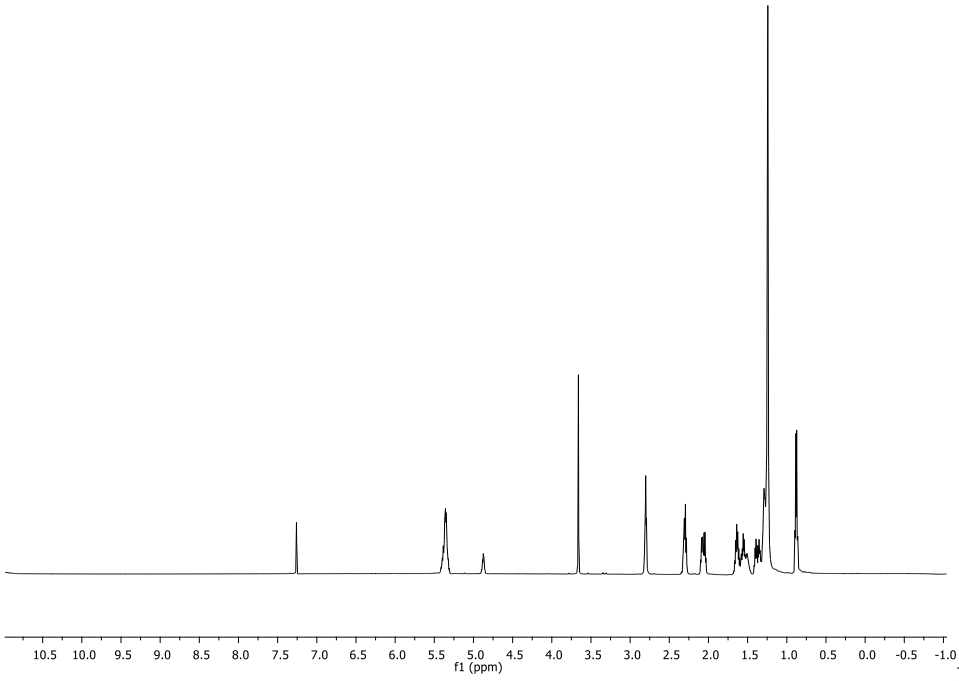
10.5 10.0 9.5 9.0 8.5 8.0 7.5 7.0 6.5 6.0 5.5 5.0 4.5 4.0 3.5 3.0 2.5 2.0 1.5 1.0 0.5 0.0 -0.5 -1.0
f1 (ppm)

f

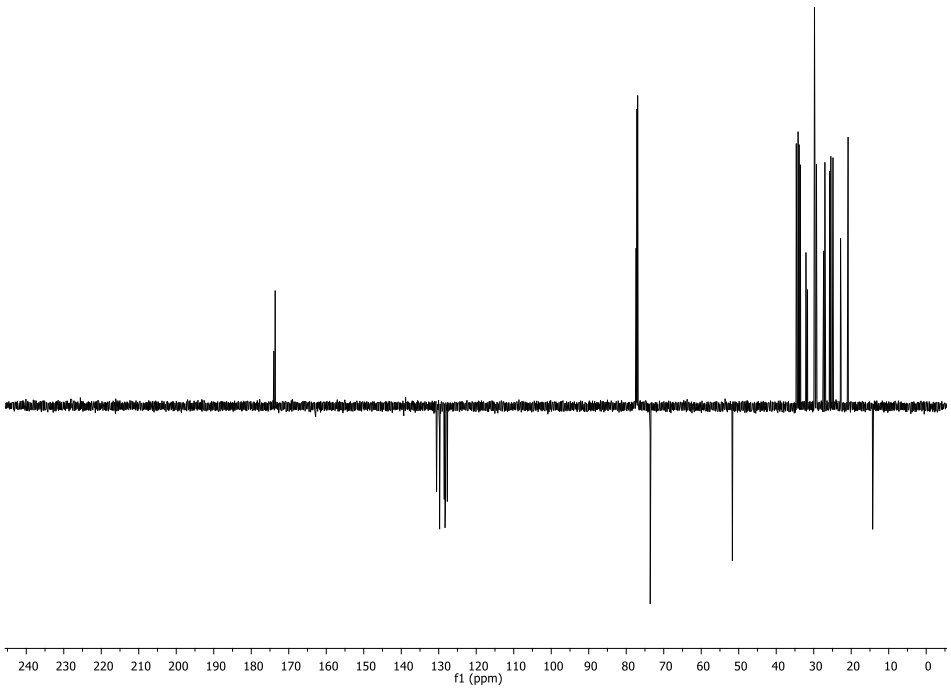
240 230 220 210 200 190 180 170 160 150 140 130 120 110 100 90 80 70 60 50 40 30 20 10 0
f1 (ppm)

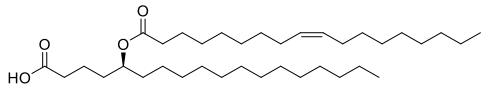
O
O
O
HO

S-5-OAHSA S-95

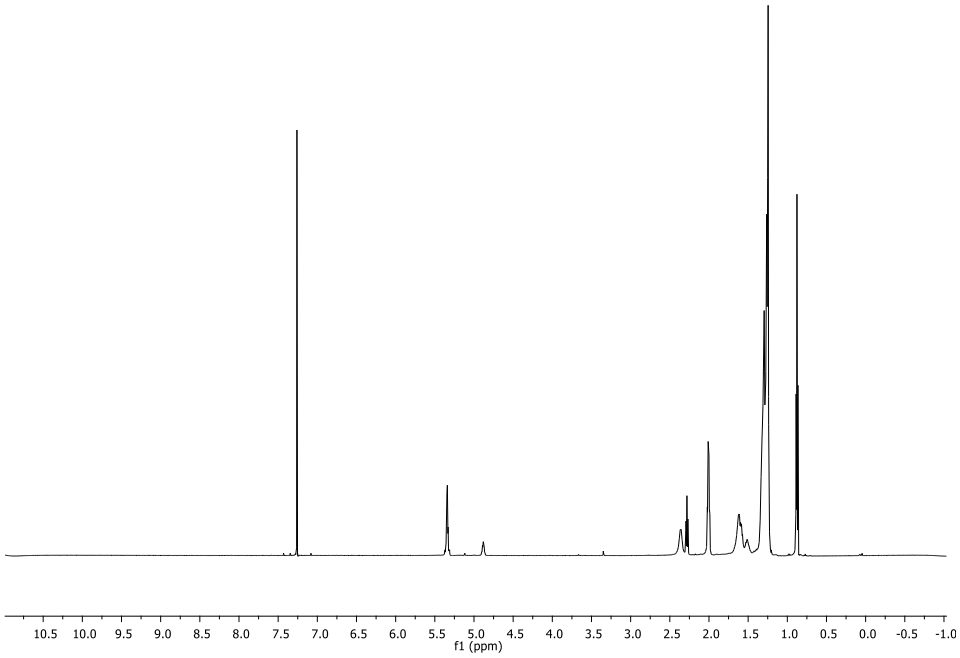
10.5 10.0 9.5 9.0 8.5 8.0 7.5 7.0 6.5 6.0 5.5 5.0 4.5 4.0 3.5 3.0 2.5 2.0 1.5 1.0 0.5 0.0 -0.5 -1.0
f1 (ppm)

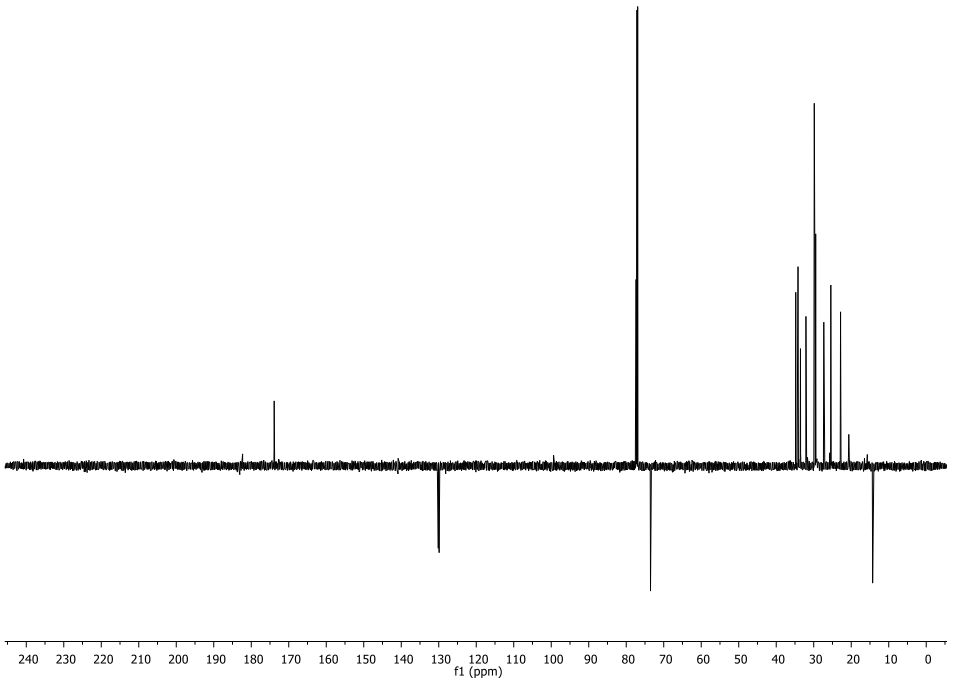
240 230 220 210 200 190 180 170 160 150 140 130 120 110 100 90 80 70 60 50 40 30 20 10 0
f1 (ppm)

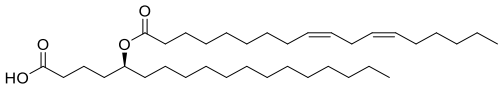
O
O
O
HO

S-5-LAHSA S-96

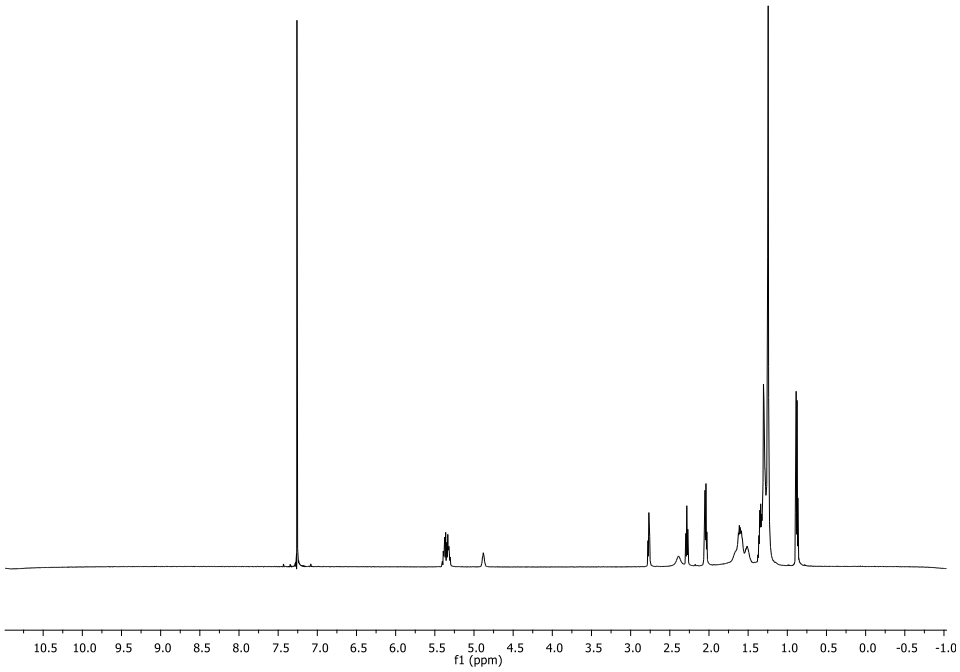
10.5 10.0 9.5 9.0 8.5 8.0 7.5 7.0 6.5 6.0 5.5 5.0 4.5 4.0 3.5 3.0 2.5 2.0 1.5 1.0 0.5 0.0 -0.5 -1.0
f1 (ppm)

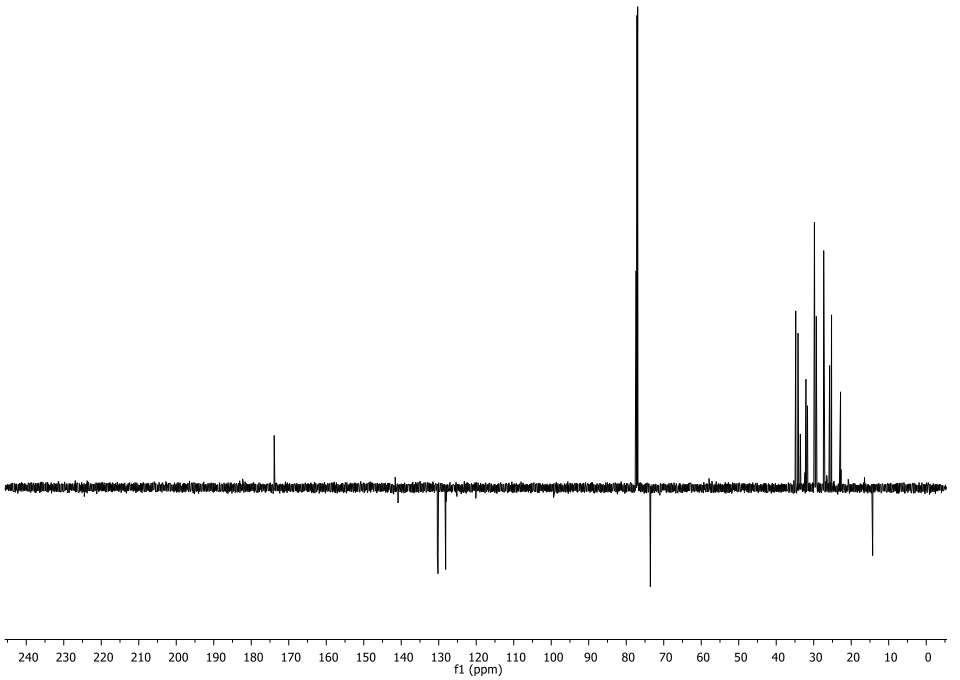
240 230 220 210 200 190 180 170 160 150 140 130 120 110 100 90 80 70 60 50 40 30 20 10 0
f1 (ppm)

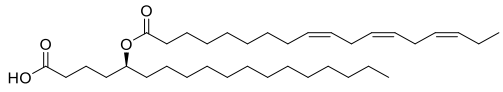

S-5-ALAHSA S-97

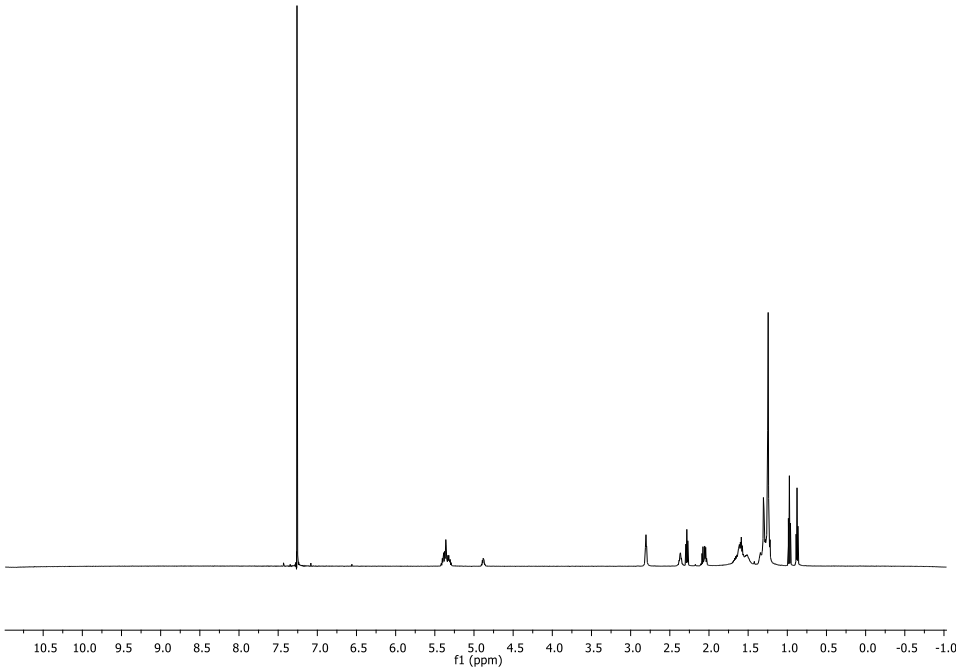

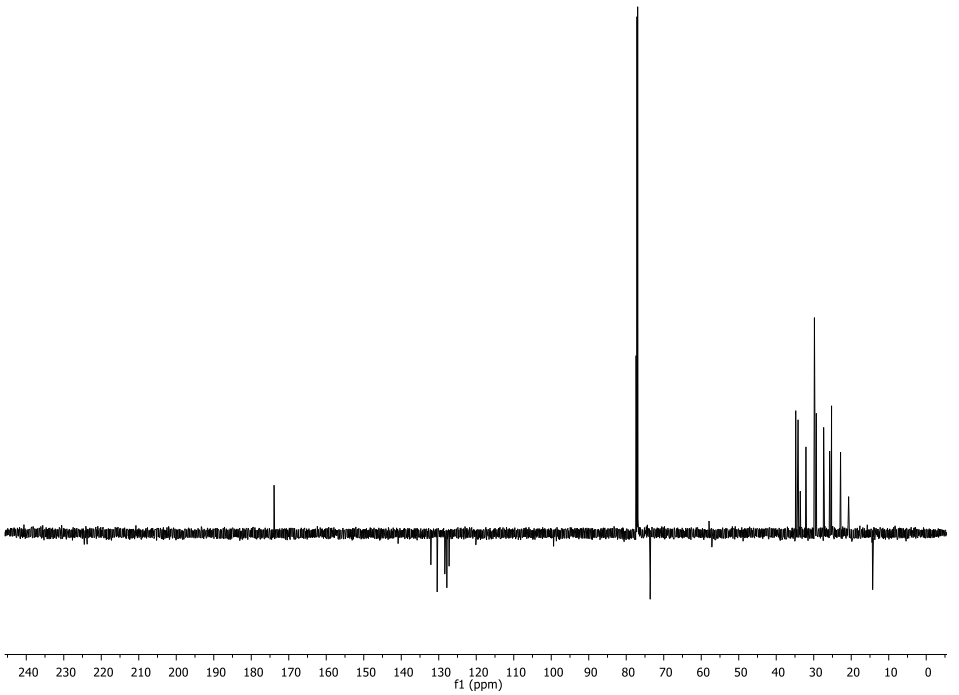

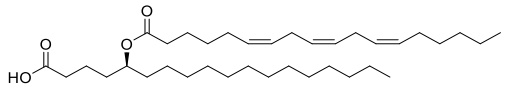

S-5-GLAHSA S-98

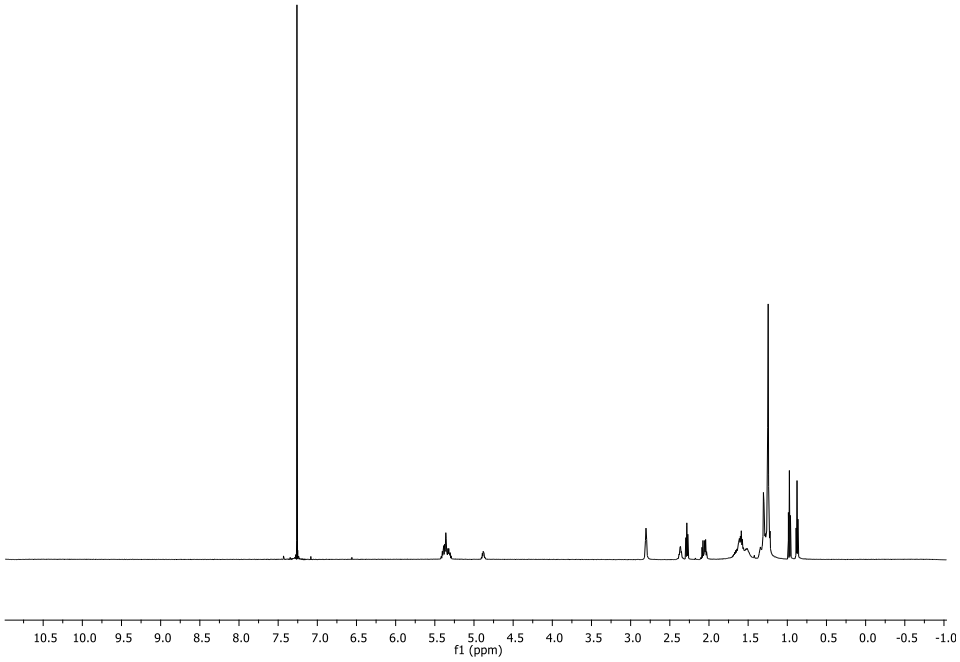

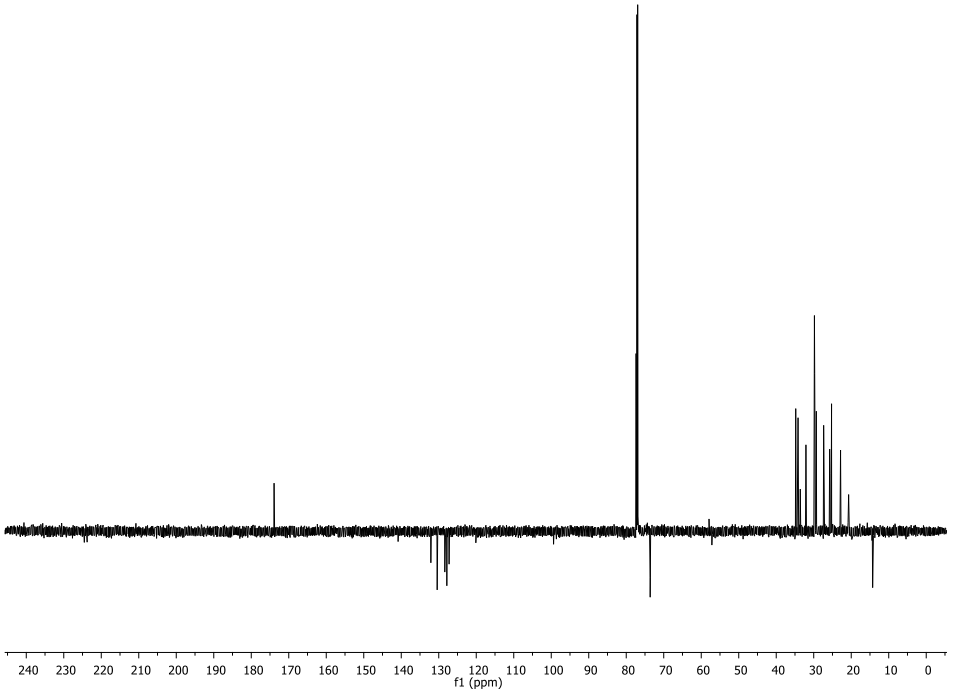

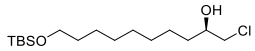
OH
TBSO
Cl

102

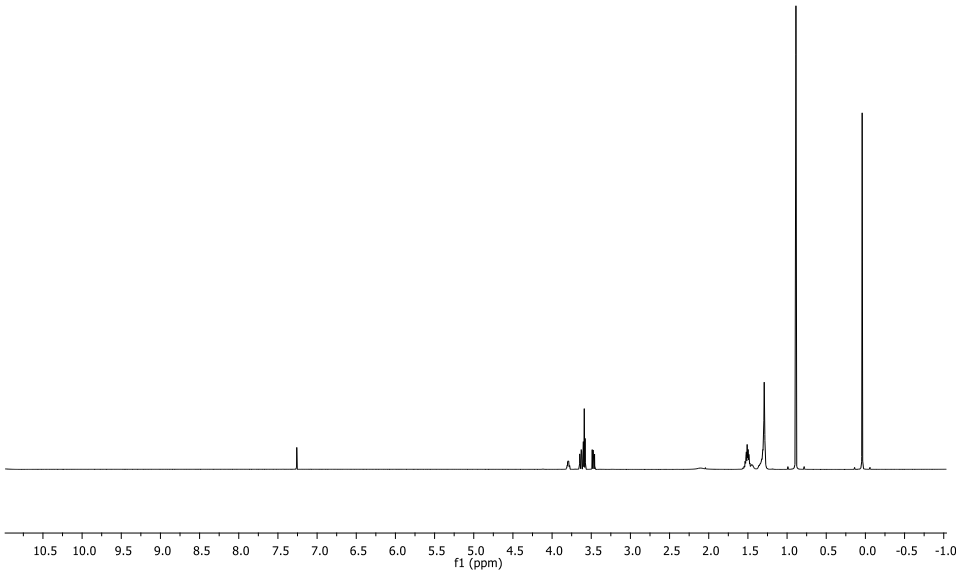
10.5 10.0 9.5 9.0 8.5 8.0 7.5 7.0 6.5 6.0 5.5 5.0 4.5 4.0 3.5 3.0 2.5 2.0 1.5 1.0 0.5 0.0 -0.5 -1.0
f1 (ppm)

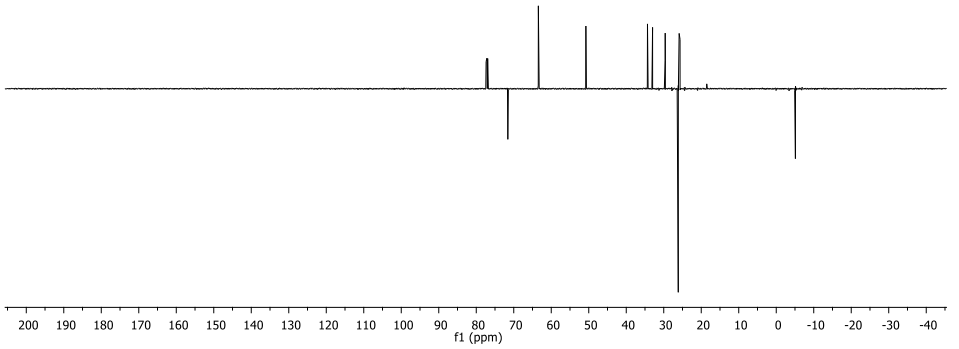
200 190 180 170 160 150 140 130 120 110 100 90 80 70 60 50 40 30 20 10 0 -10 -20 -30 -40
f1 (ppm)

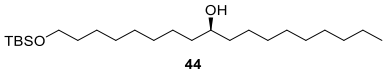
OH
TBSO

44

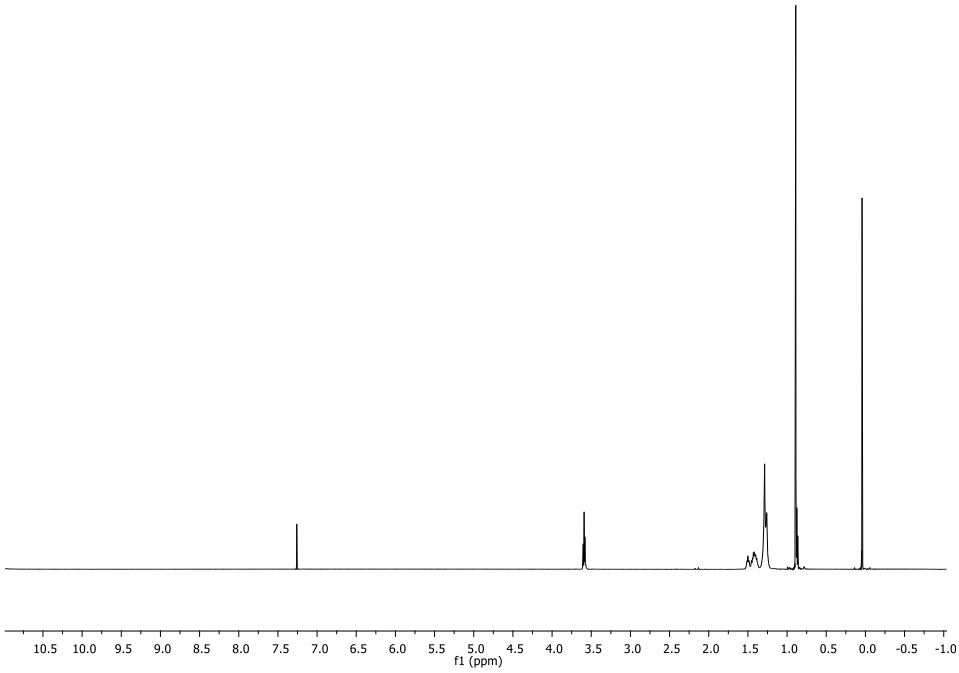
10.5 10.0 9.5 9.0 8.5 8.0 7.5 7.0 6.5 6.0 5.5 5.0 4.5 4.0 3.5 3.0 2.5 2.0 1.5 1.0 0.5 0.0 -0.5 -1.0
f1 (ppm)

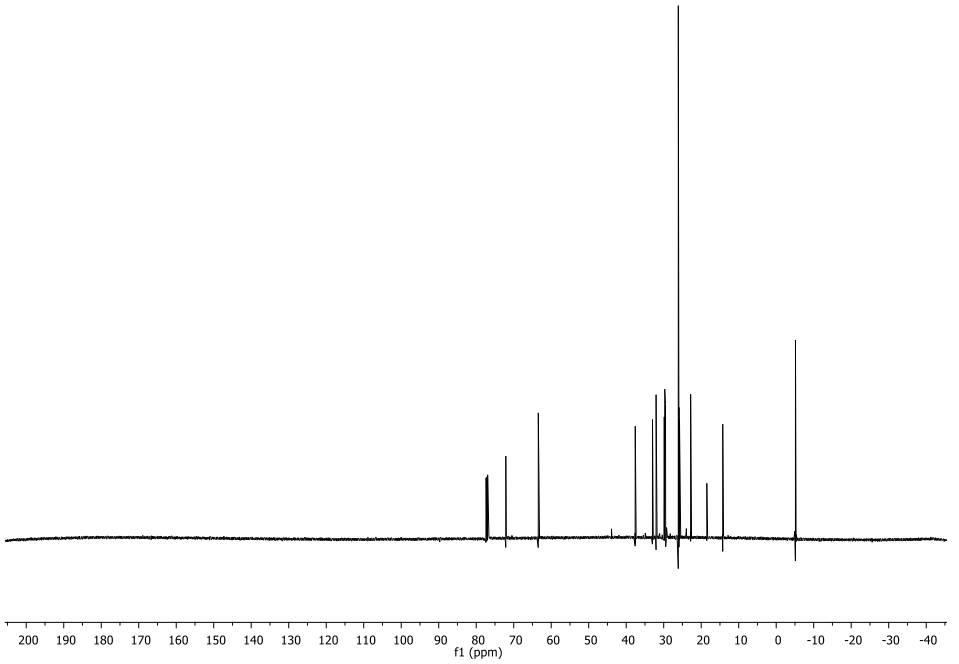
200 190 180 170 160 150 140 130 120 110 100 90 80 70 60 50 40 30 20 10 0 -10 -20 -30 -40
f1 (ppm)

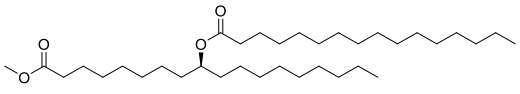

S-105

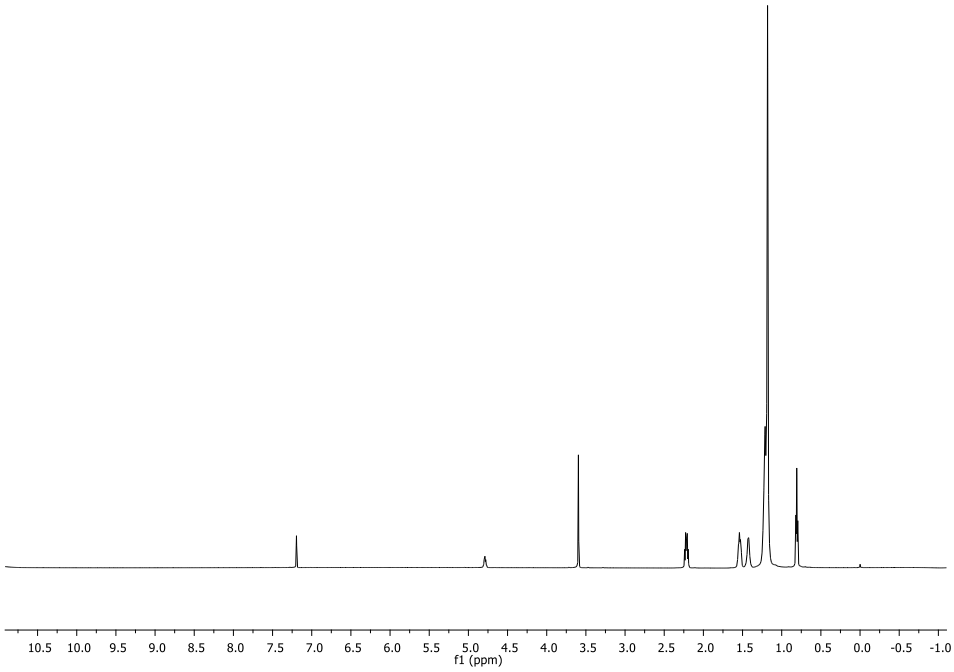
10.5 10.0 9.5 9.0 8.5 8.0 7.5 7.0 6.5 6.0 5.5 5.0 4.5 4.0 3.5 3.0 2.5 2.0 1.5 1.0 0.5 0.0 -0.5 -1.0
f1 (ppm)

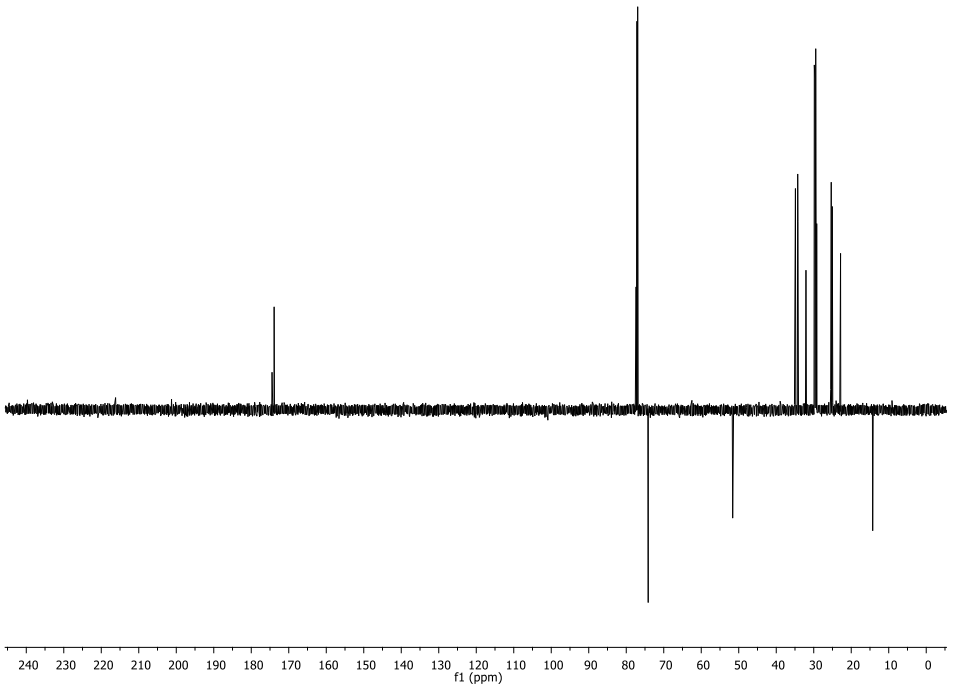
240 230 220 210 200 190 180 170 160 150 140 130 120 110 100 90 80 70 60 50 40 30 20 10 0
f1 (ppm)

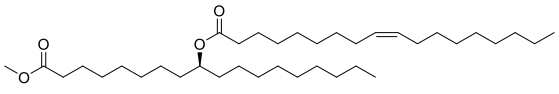

S-106

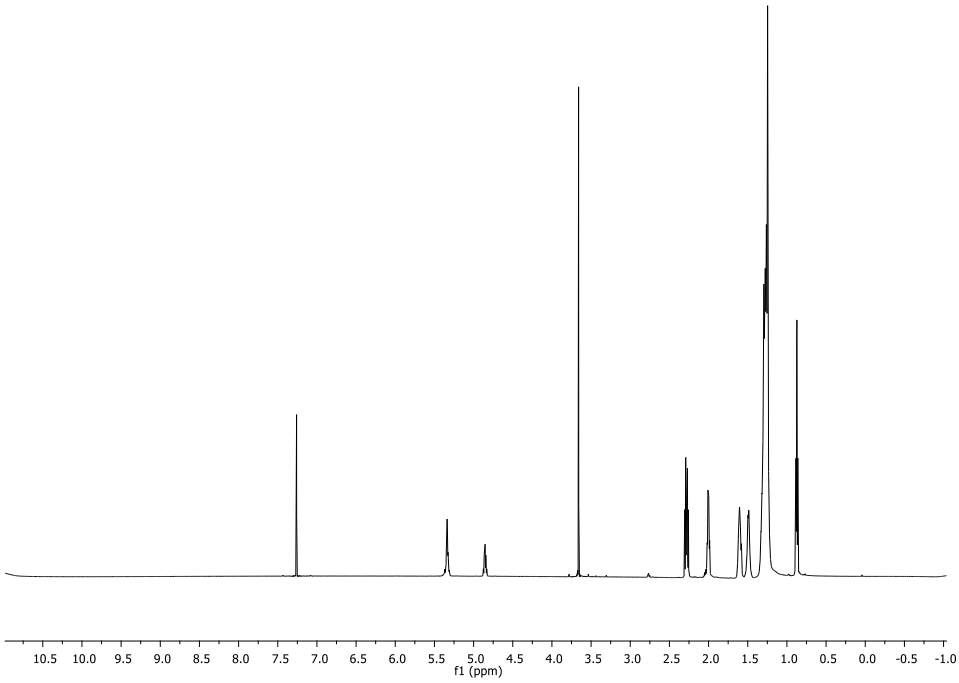
10.5 10.0 9.5 9.0 8.5 8.0 7.5 7.0 6.5 6.0 5.5 5.0 4.5 4.0 3.5 3.0 2.5 2.0 1.5 1.0 0.5 0.0 -0.5 -1.0
f1 (ppm)

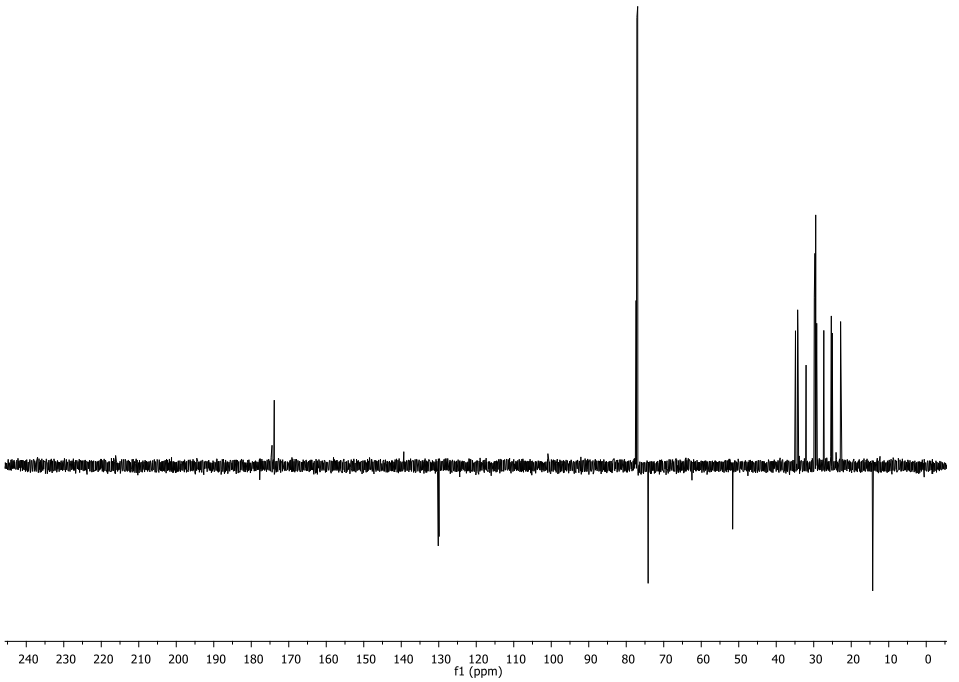
240 230 220 210 200 190 180 170 160 150 140 130 120 110 100 90 80 70 60 50 40 30 20 10 0
f1 (ppm)

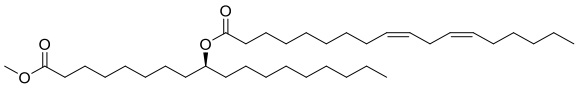

S-107

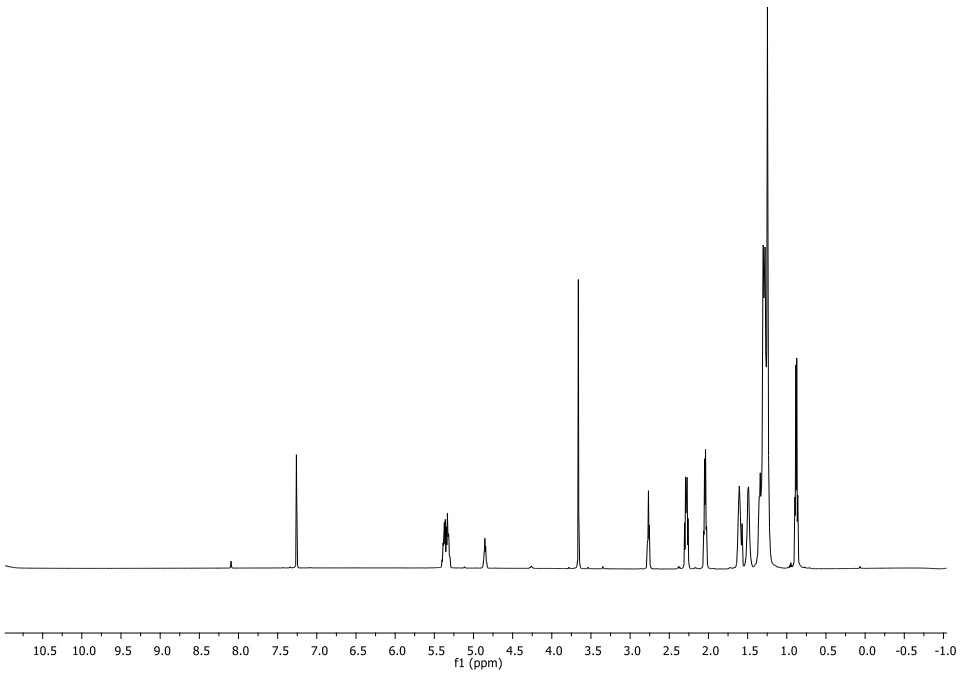
10.5 10.0 9.5 9.0 8.5 8.0 7.5 7.0 6.5 6.0 5.5 5.0 4.5 4.0 3.5 3.0 2.5 2.0 1.5 1.0 0.5 0.0 -0.5 -1.0
f1 (ppm)

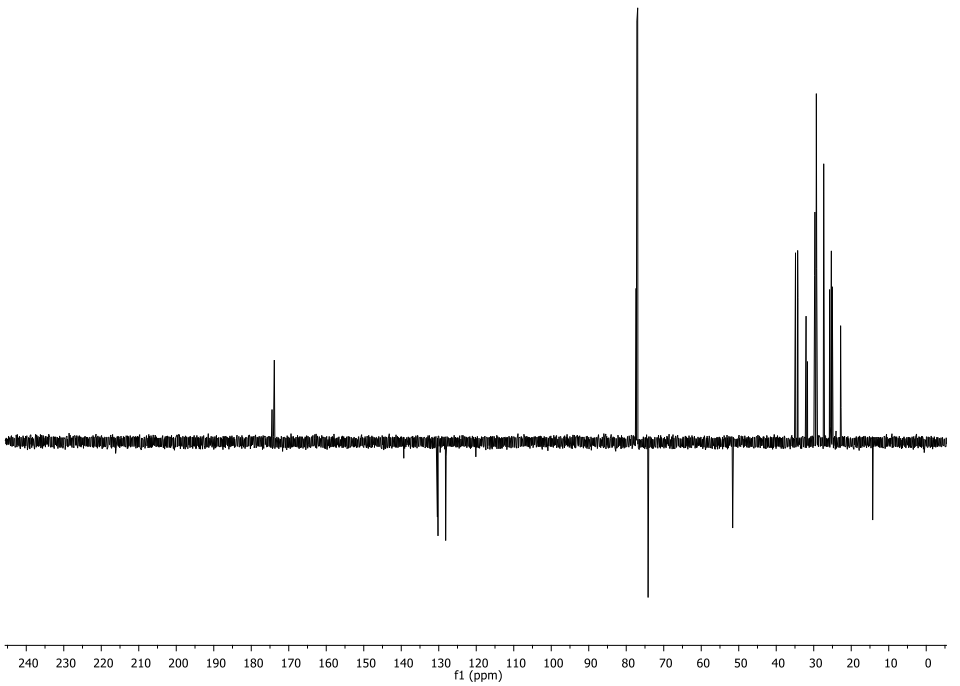
240 230 220 210 200 190 180 170 160 150 140 130 120 110 100 90 80 70 60 50 40 30 20 10 0
f1 (ppm)

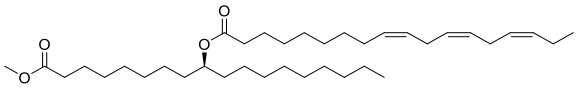

S-108

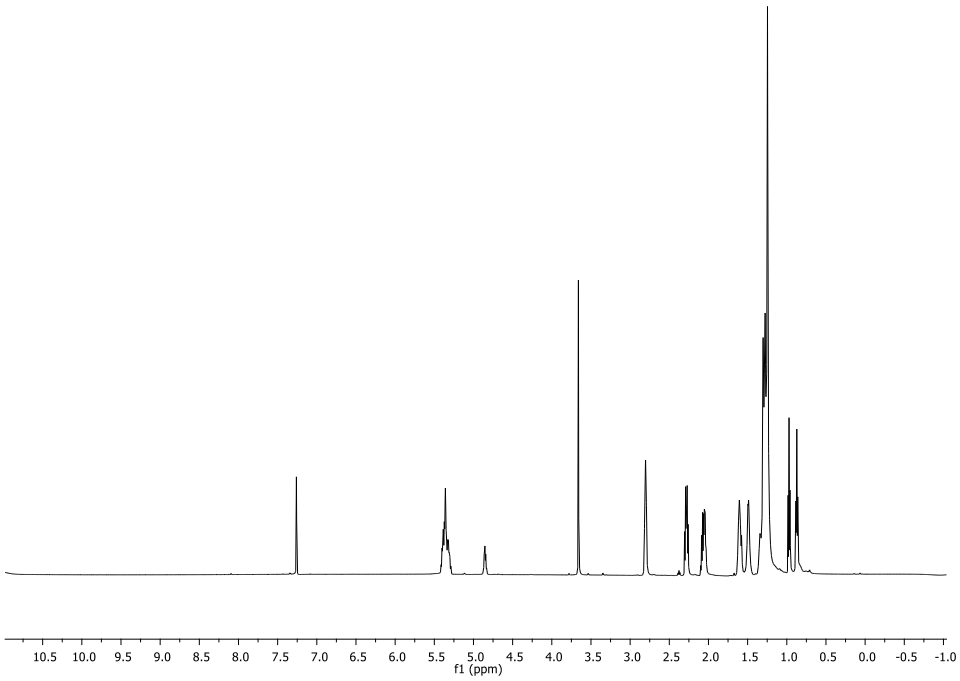
10.5 10.0 9.5 9.0 8.5 8.0 7.5 7.0 6.5 6.0 5.5 5.0 4.5 4.0 3.5 3.0 2.5 2.0 1.5 1.0 0.5 0.0 -0.5 -1.0
f1 (ppm)

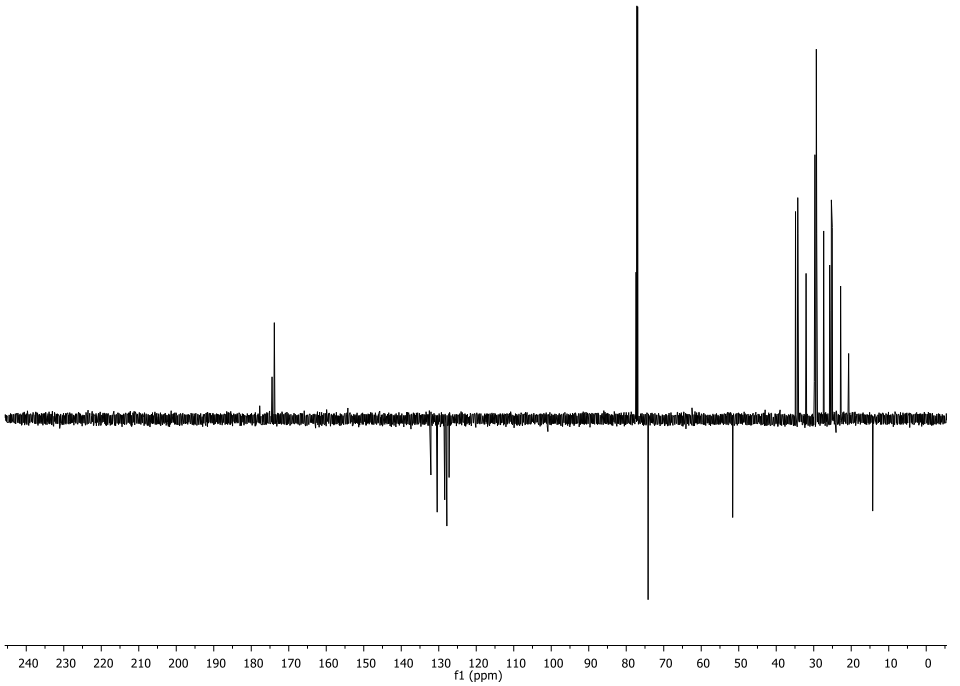
240 230 220 210 200 190 180 170 160 150 140 130 120 110 100 90 80 70 60 50 40 30 20 10 0
f1 (ppm)

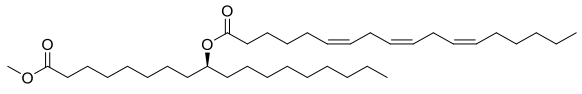

S-109

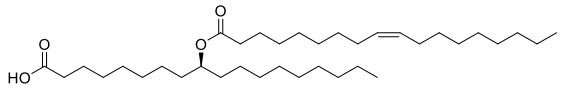

S-9-OAHSA S-111

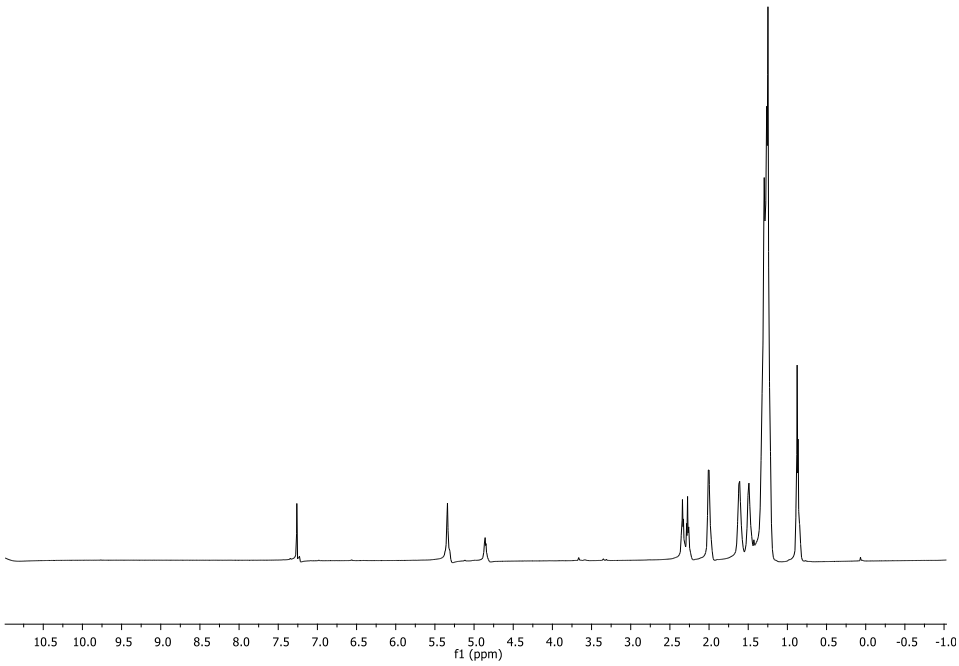

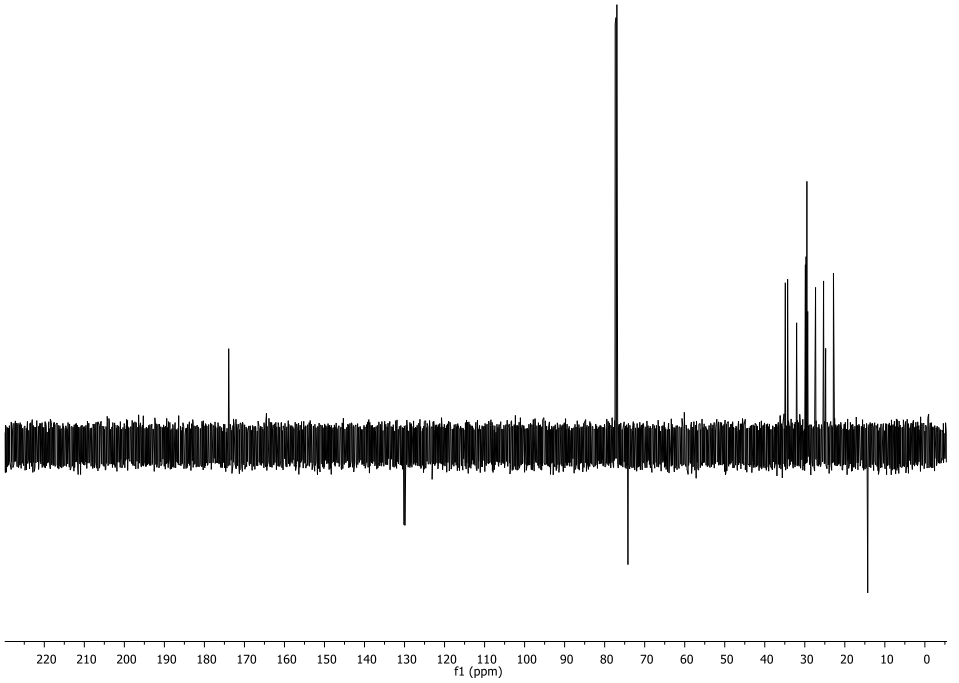

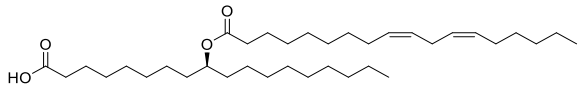

S-9-LAHSA S-112

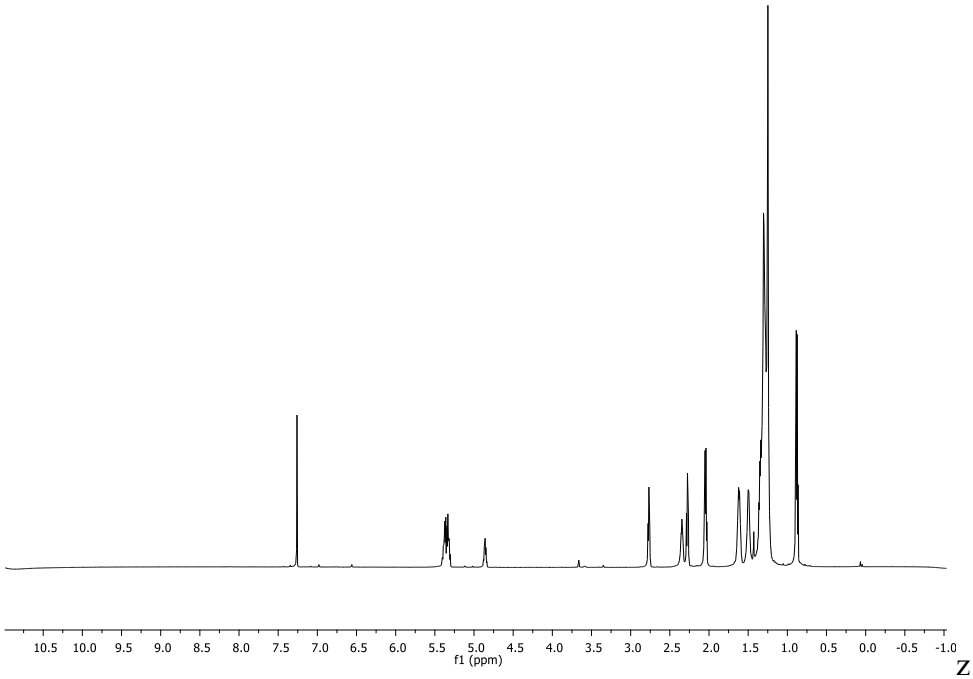

Z

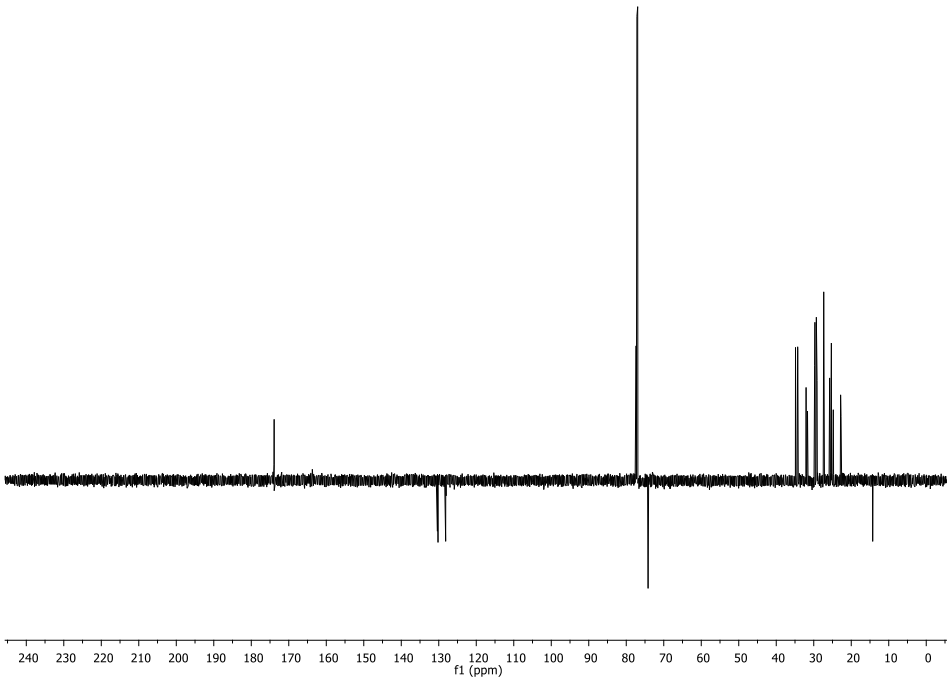

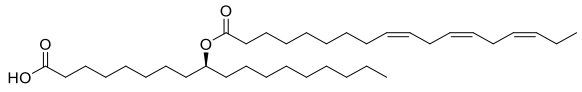

S-9-ALAHSA S-113

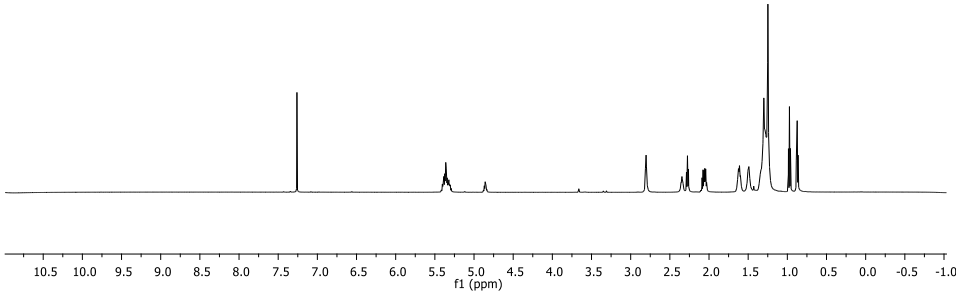

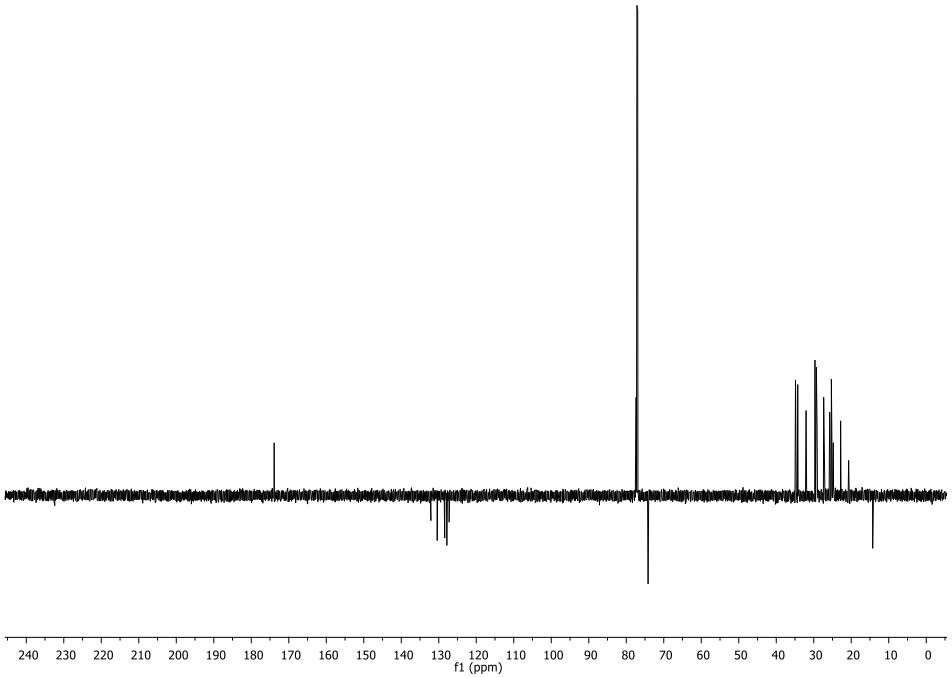

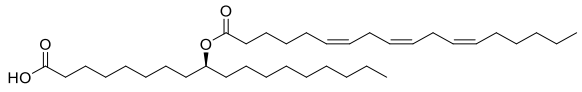

S-9-GLAHSA S-114

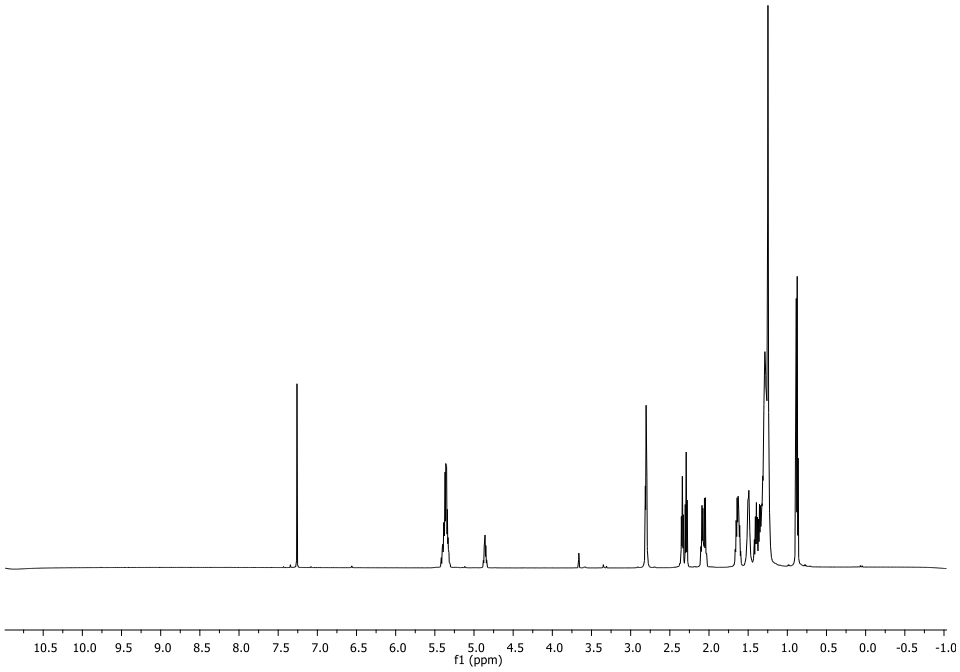

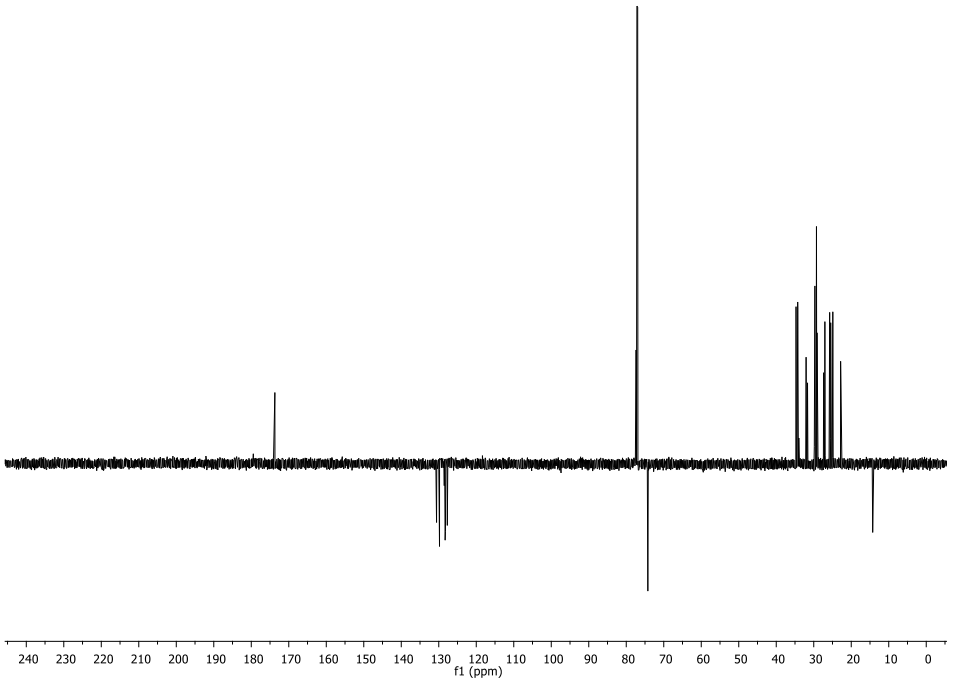

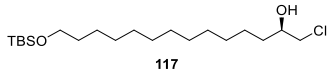
OH
TBSO
Cl

117

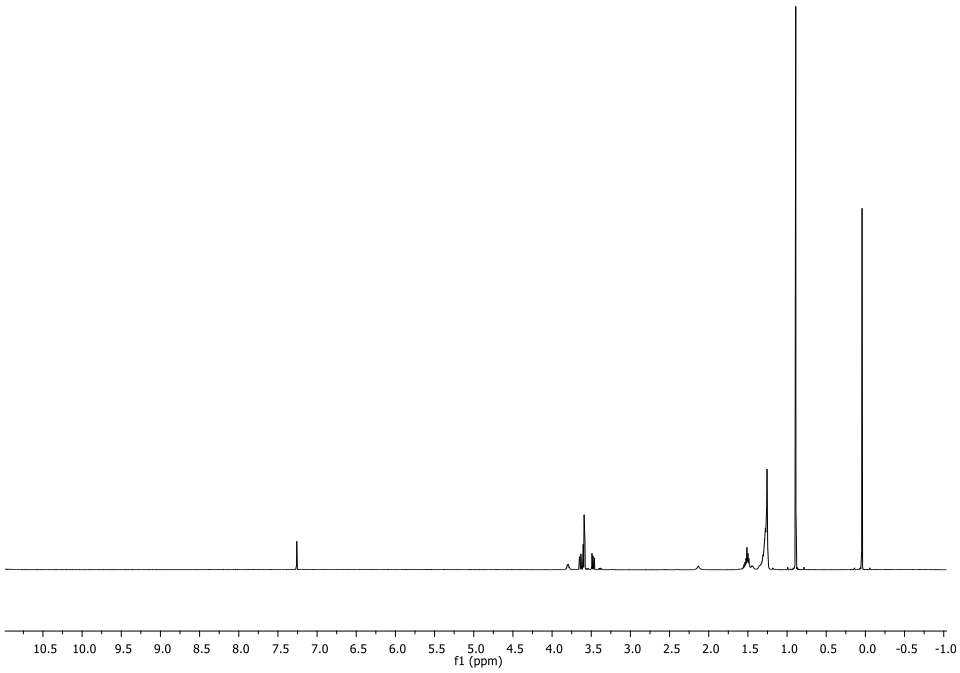
10.5 10.0 9.5 9.0 8.5 8.0 7.5 7.0 6.5 6.0 5.5 5.0 4.5 4.0 3.5 3.0 2.5 2.0 1.5 1.0 0.5 0.0 -0.5 -1.0
f1 (ppm)

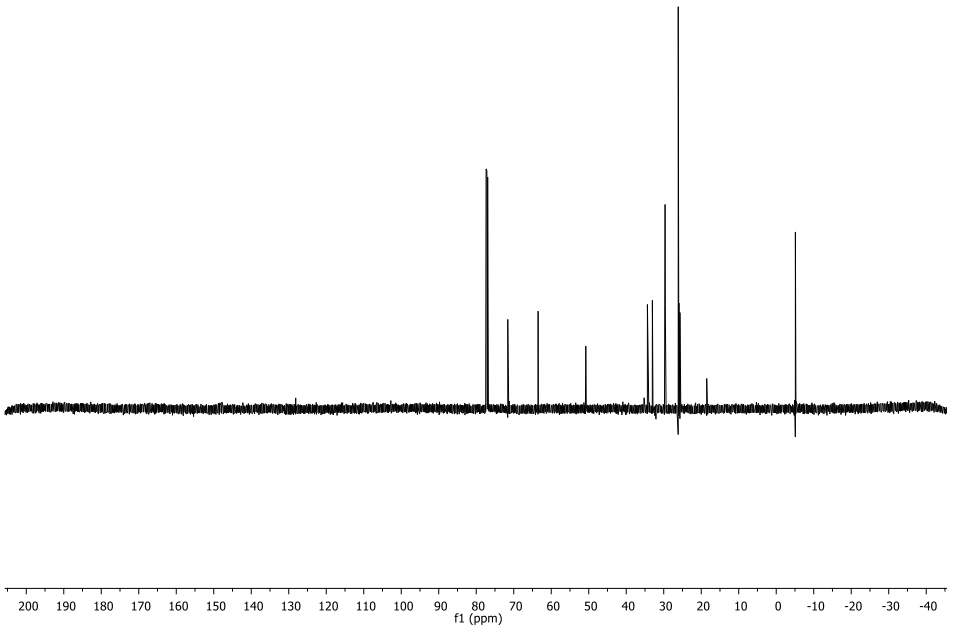
200 190 180 170 160 150 140 130 120 110 100 90 80 70 60 50 40 30 20 10 0 -10 -20 -30 -40
f1 (ppm)

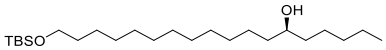
OH
TBSO

119

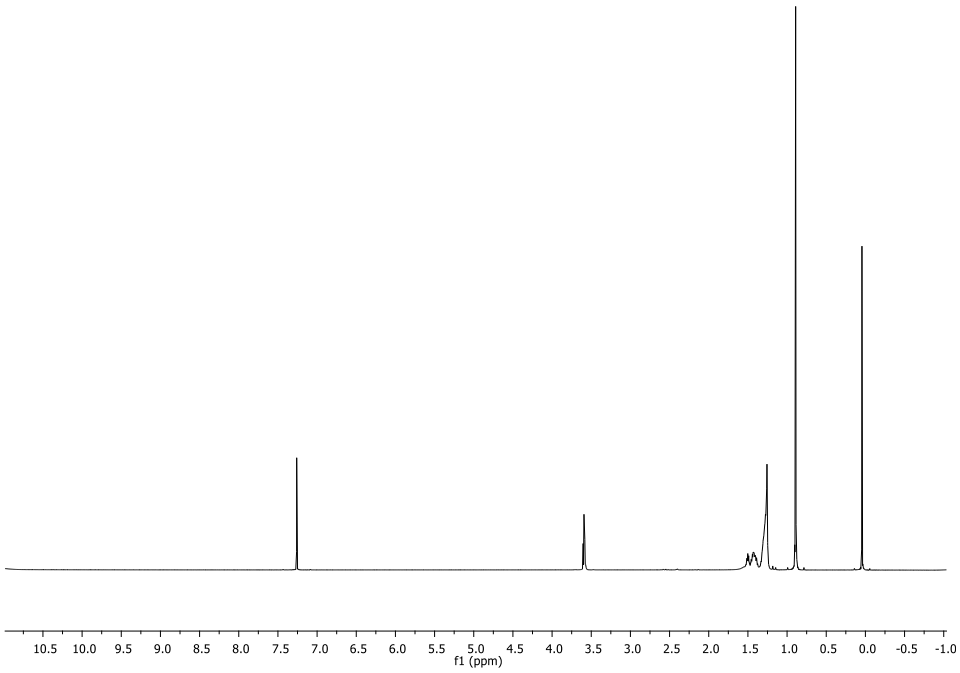
10.5 10.0 9.5 9.0 8.5 8.0 7.5 7.0 6.5 6.0 5.5 5.0 4.5 4.0 3.5 3.0 2.5 2.0 1.5 1.0 0.5 0.0 -0.5 -1.0
f1 (ppm)

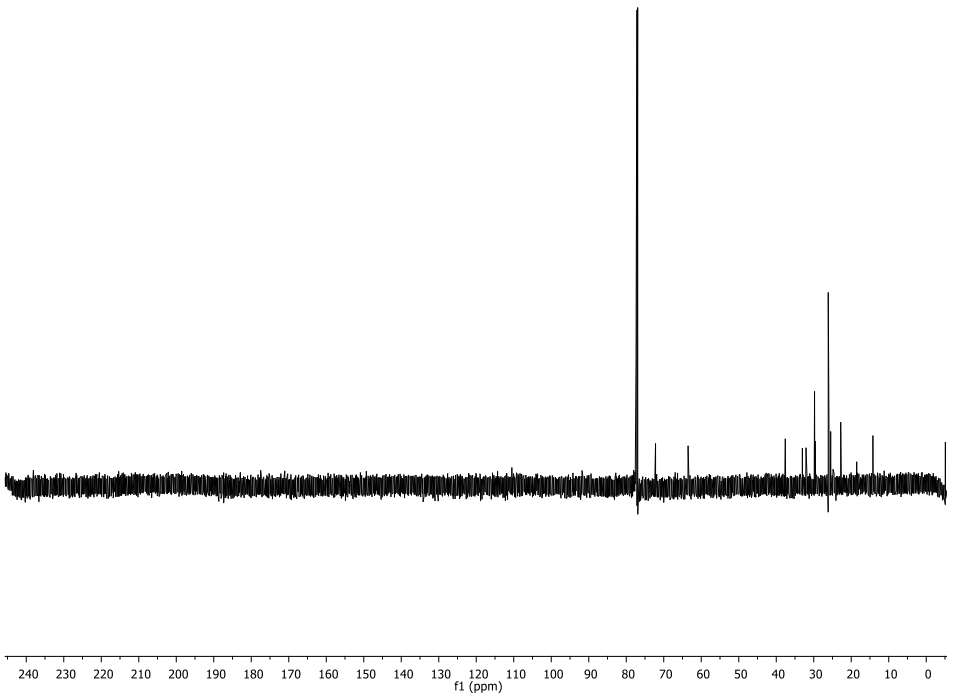
240 230 220 210 200 190 180 170 160 150 140 130 120 110 100 90 80 70 60 50 40 30 20 10 0
f1 (ppm)

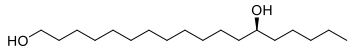
OH
HO

120

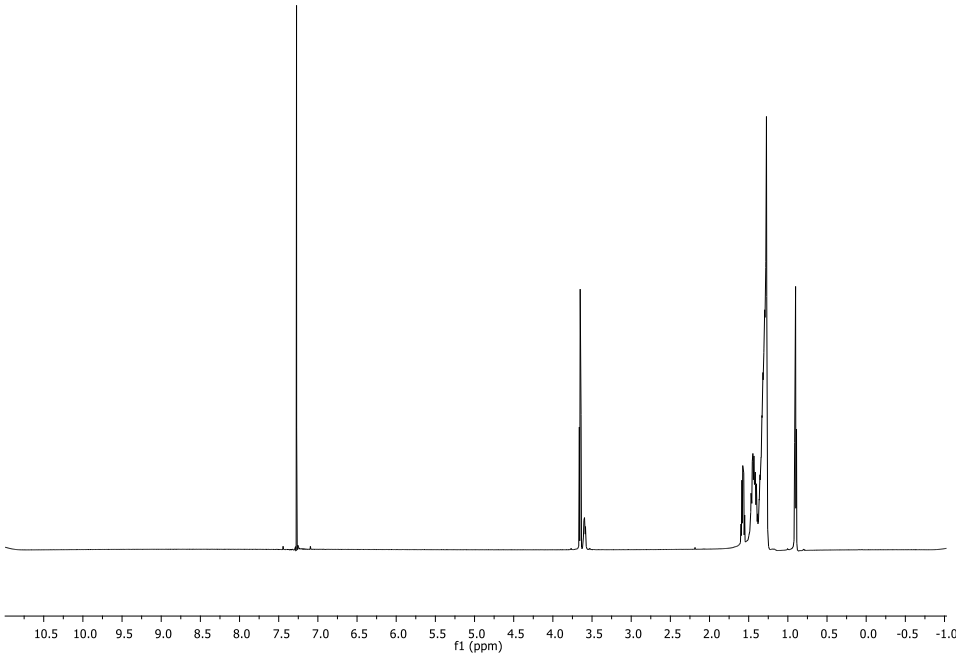
10.5 10.0 9.5 9.0 8.5 8.0 7.5 7.0 6.5 6.0 5.5 5.0 4.5 4.0 3.5 3.0 2.5 2.0 1.5 1.0 0.5 0.0 -0.5 -1.0
f1 (ppm)

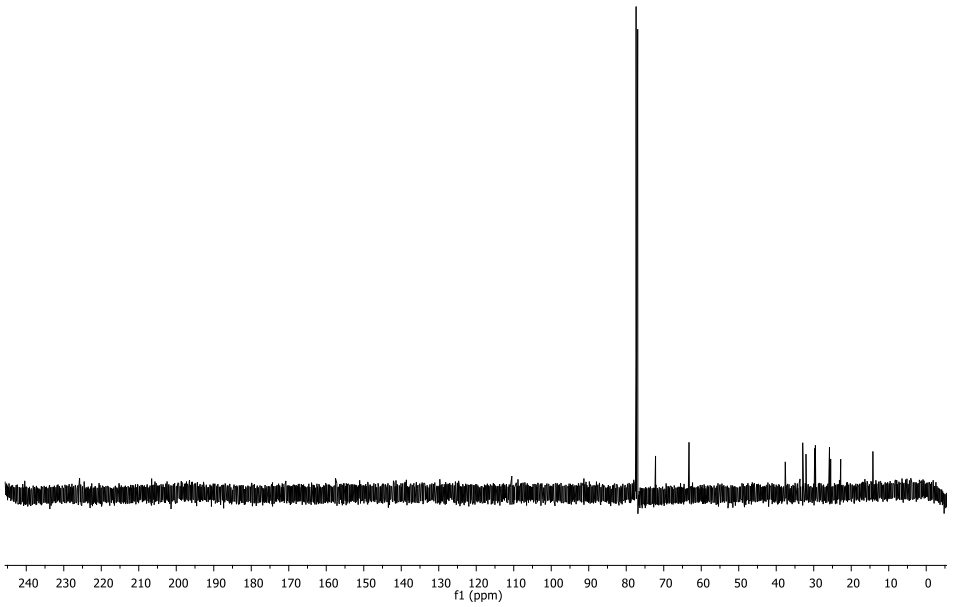
240 230 220 210 200 190 180 170 160 150 140 130 120 110 100 90 80 70 60 50 40 30 20 10 0
f1 (ppm)

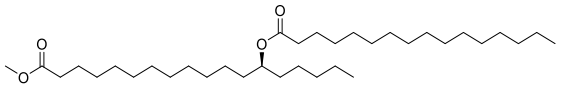

S-122

f

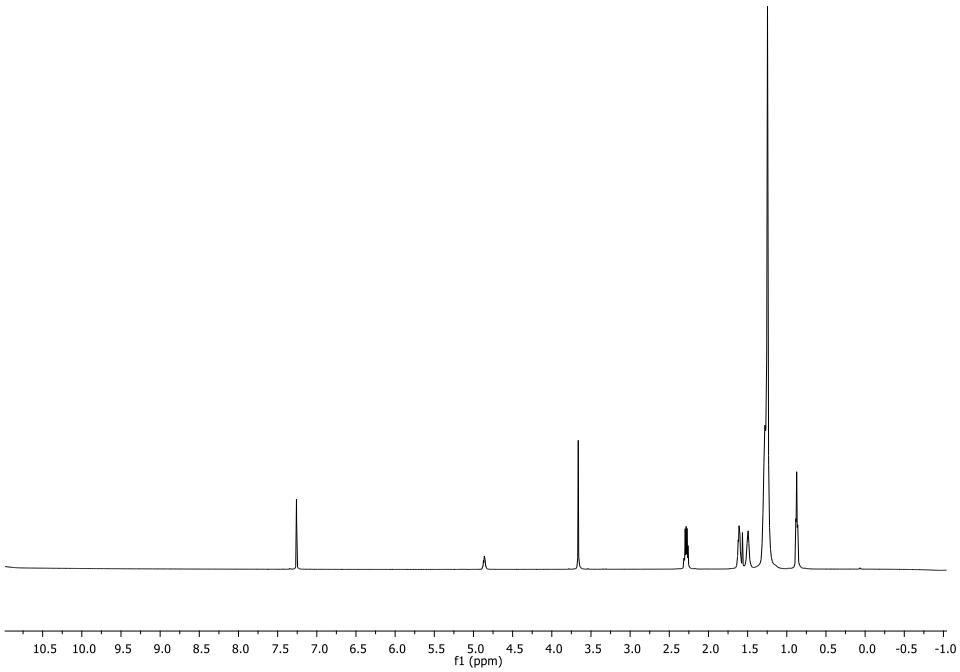
10.5 10.0 9.5 9.0 8.5 8.0 7.5 7.0 6.5 6.0 5.5 5.0 4.5 4.0 3.5 3.0 2.5 2.0 1.5 1.0 0.5 0.0 -0.5 -1.0
f1 (ppm)

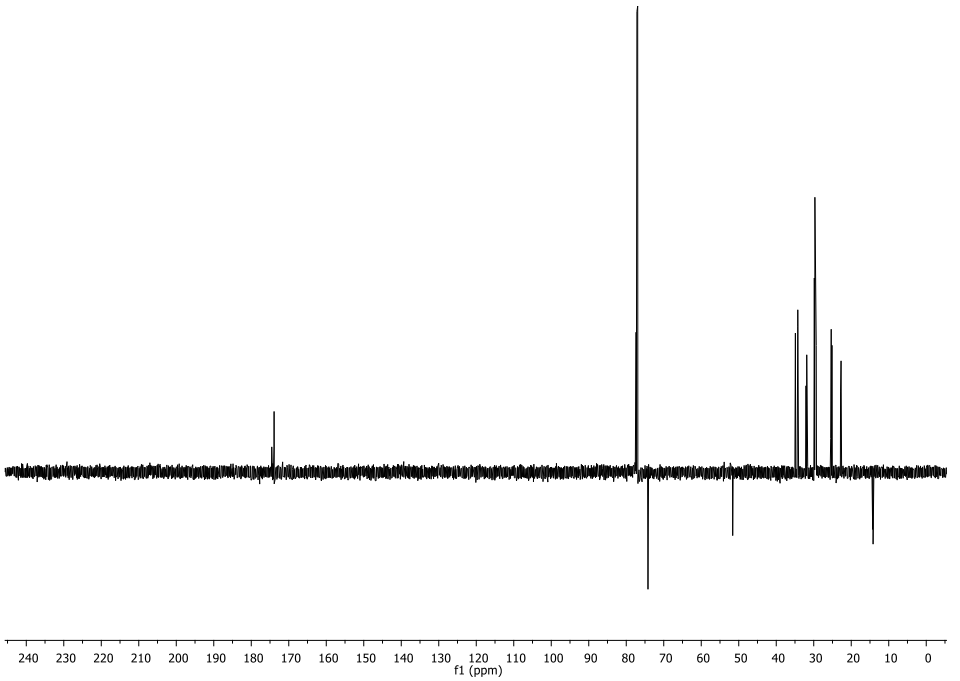
240 230 220 210 200 190 180 170 160 150 140 130 120 110 100 90 80 70 60 50 40 30 20 10 0
f1 (ppm)

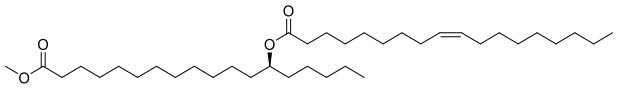

S-123

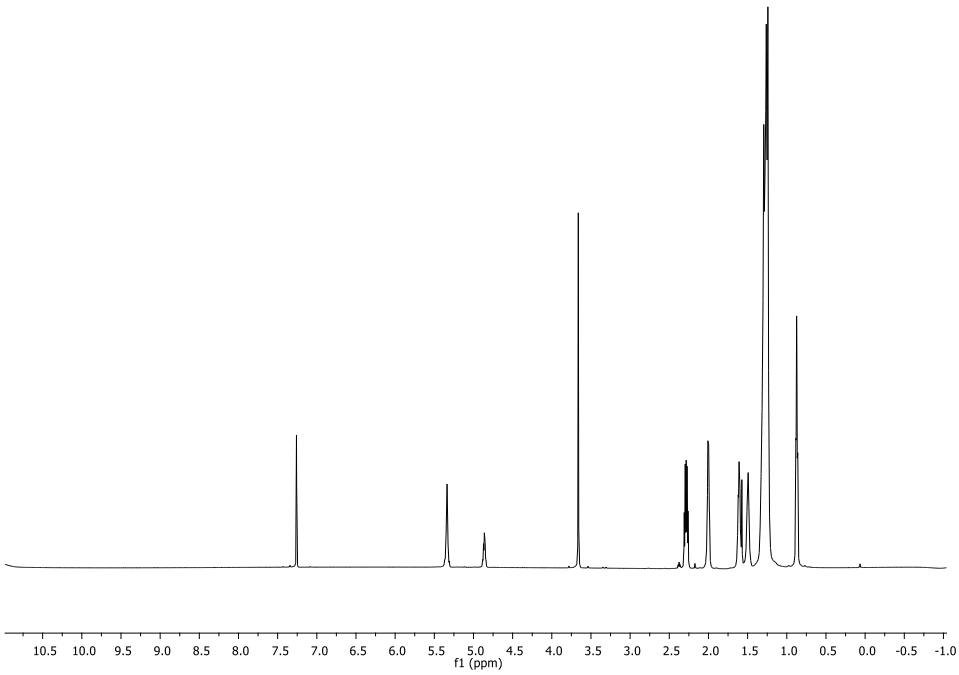
10.5 10.0 9.5 9.0 8.5 8.0 7.5 7.0 6.5 6.0 5.5 5.0 4.5 4.0 3.5 3.0 2.5 2.0 1.5 1.0 0.5 0.0 -0.5 -1.0
f1 (ppm)

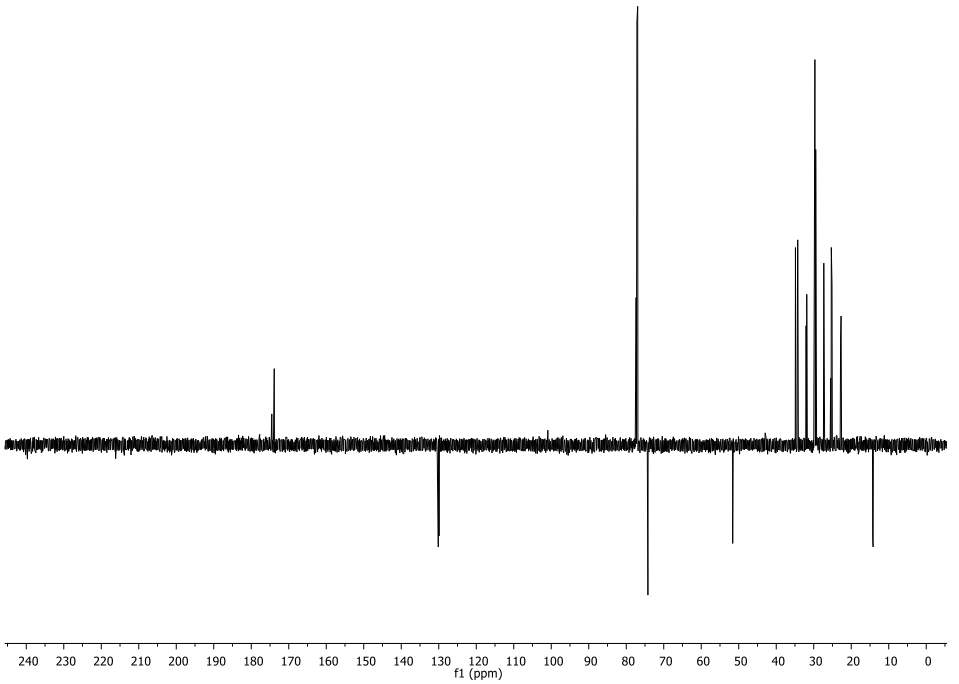
240 230 220 210 200 190 180 170 160 150 140 130 120 110 100 90 80 70 60 50 40 30 20 10 0
f1 (ppm)

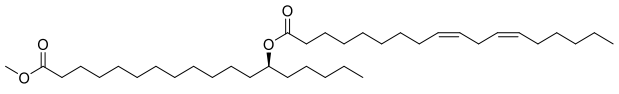

S-124

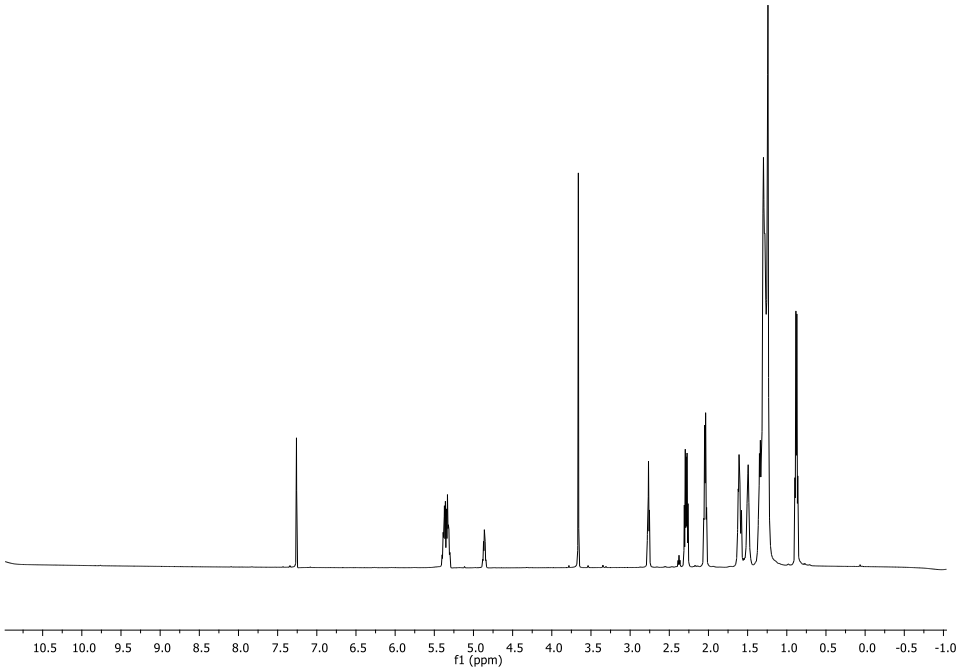
10.5 10.0 9.5 9.0 8.5 8.0 7.5 7.0 6.5 6.0 5.5 5.0 4.5 4.0 3.5 3.0 2.5 2.0 1.5 1.0 0.5 0.0 -0.5 -1.0
f1 (ppm)

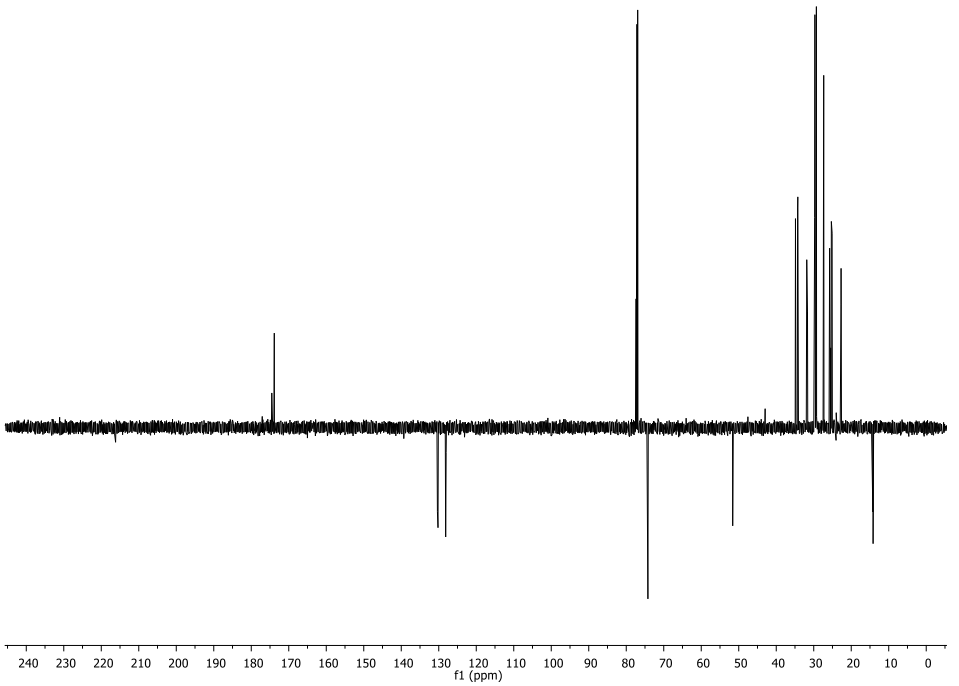
240 230 220 210 200 190 180 170 160 150 140 130 120 110 100 90 80 70 60 50 40 30 20 10 0
f1 (ppm)

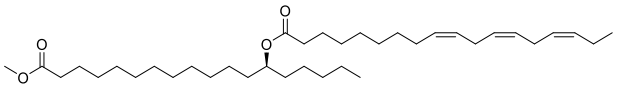

S-125

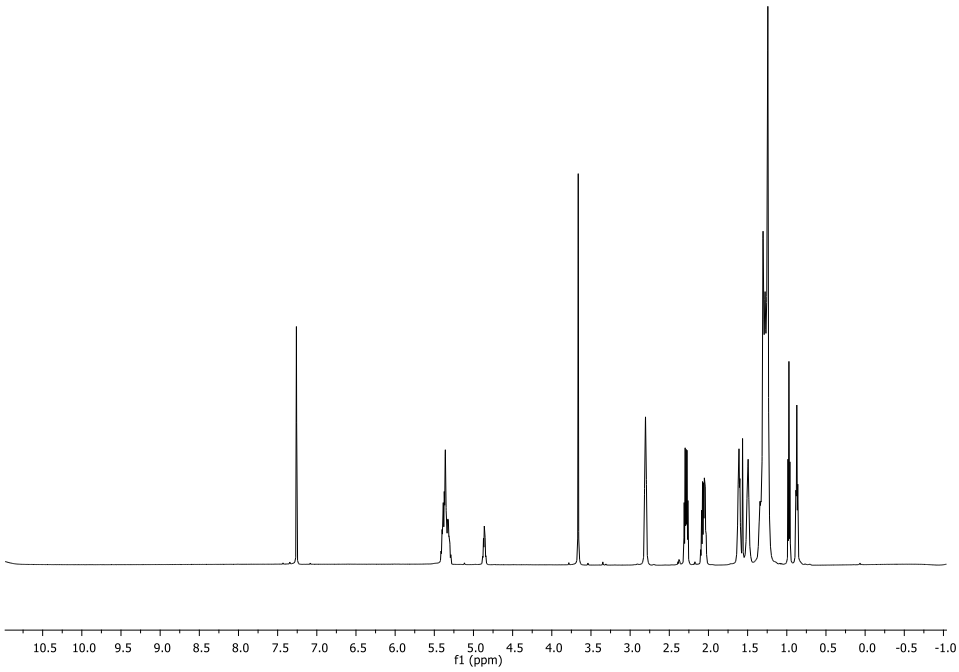
10.5 10.0 9.5 9.0 8.5 8.0 7.5 7.0 6.5 6.0 5.5 5.0 4.5 4.0 3.5 3.0 2.5 2.0 1.5 1.0 0.5 0.0 -0.5 -1.0
f1 (ppm)

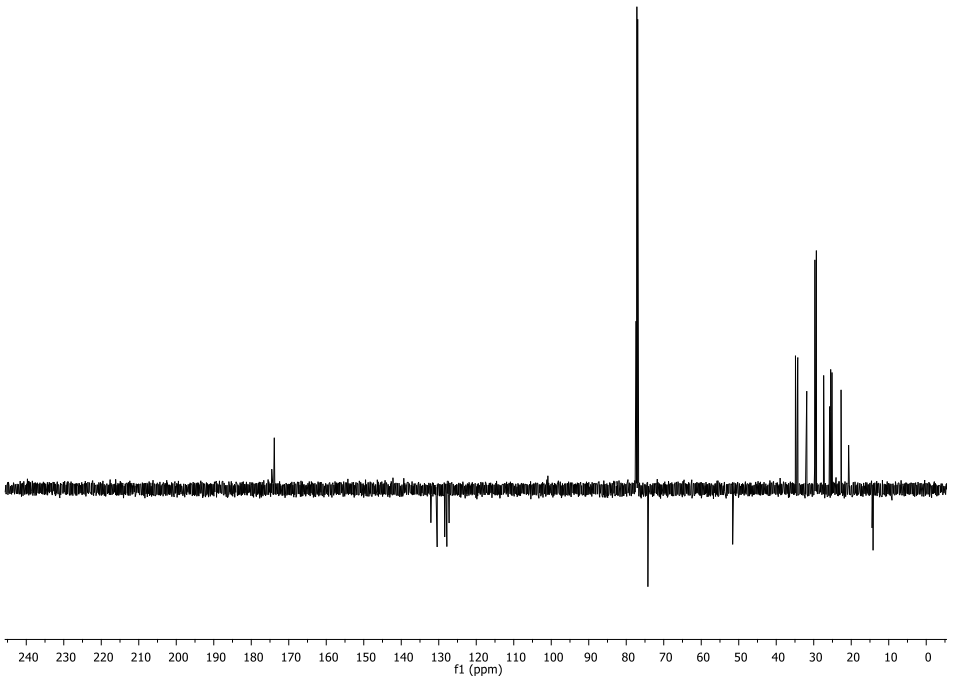
240 230 220 210 200 190 180 170 160 150 140 130 120 110 100 90 80 70 60 50 40 30 20 10 0
f1 (ppm)

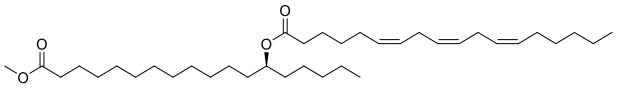

S-126

Z

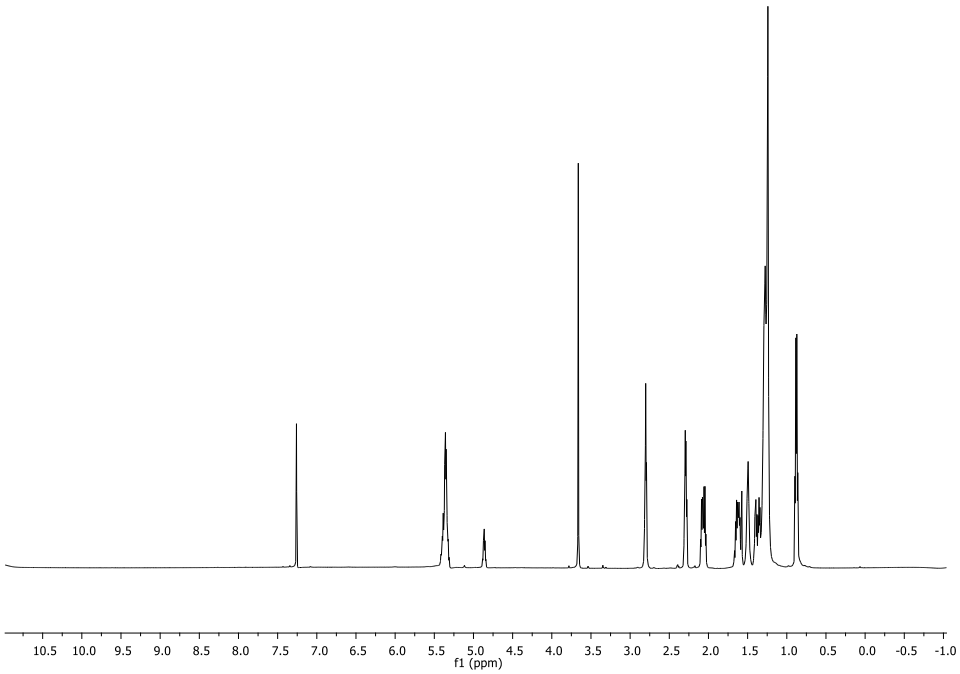
10.5 10.0 9.5 9.0 8.5 8.0 7.5 7.0 6.5 6.0 5.5 5.0 4.5 4.0 3.5 3.0 2.5 2.0 1.5 1.0 0.5 0.0 -0.5 -1.0
f1 (ppm)

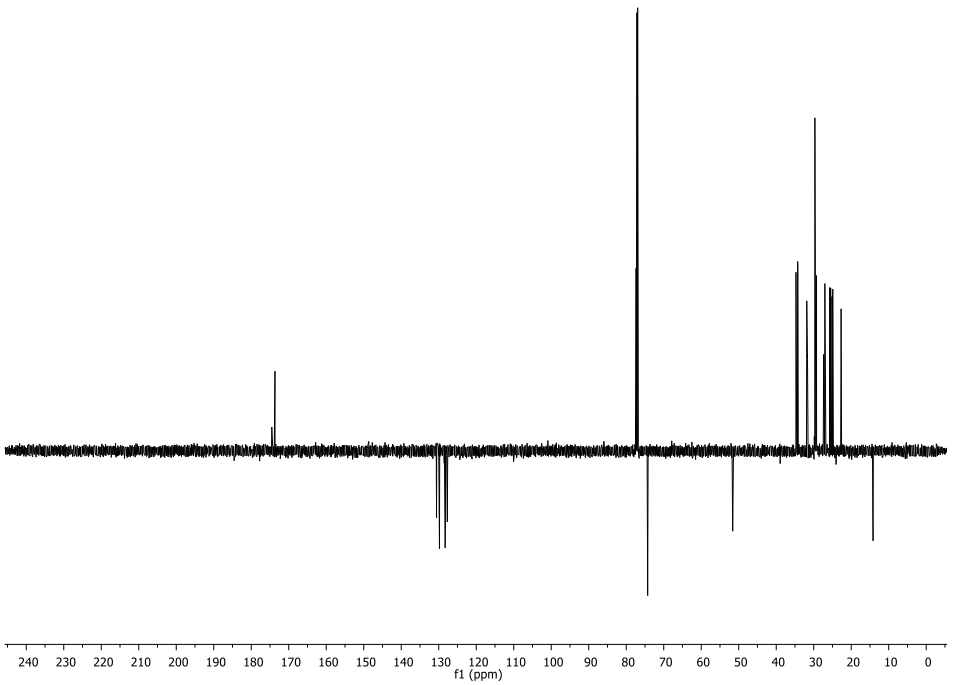
240 230 220 210 200 190 180 170 160 150 140 130 120 110 100 90 80 70 60 50 40 30 20 10 0
f1 (ppm)

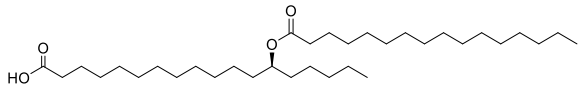

S-13-PAHSA S-127

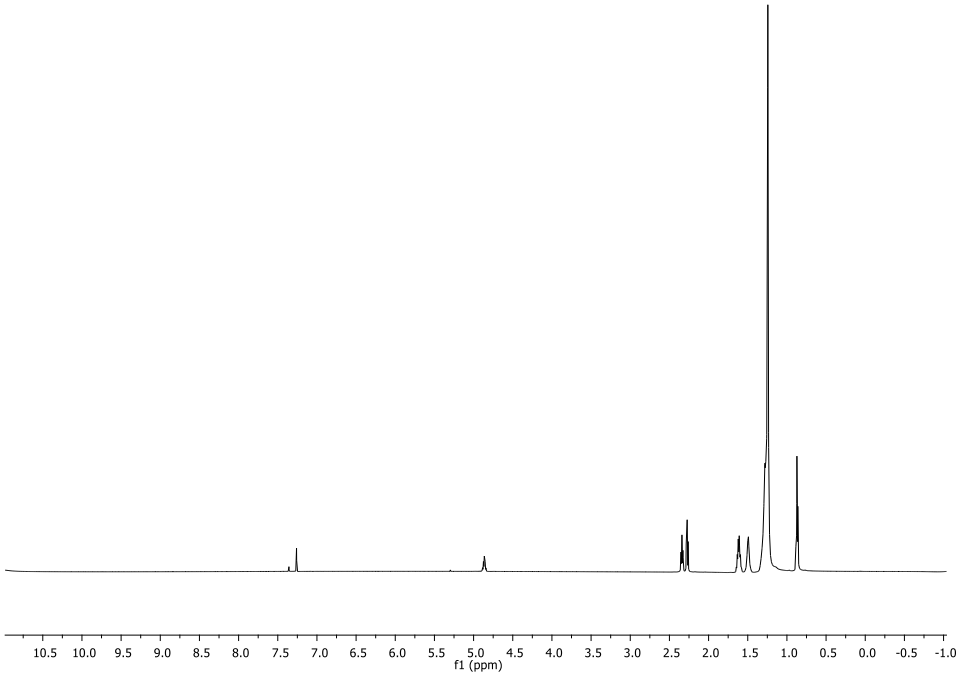

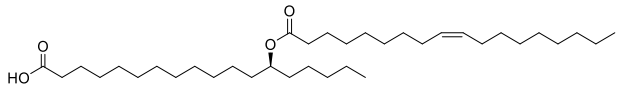

S-13-OAHSA S-128

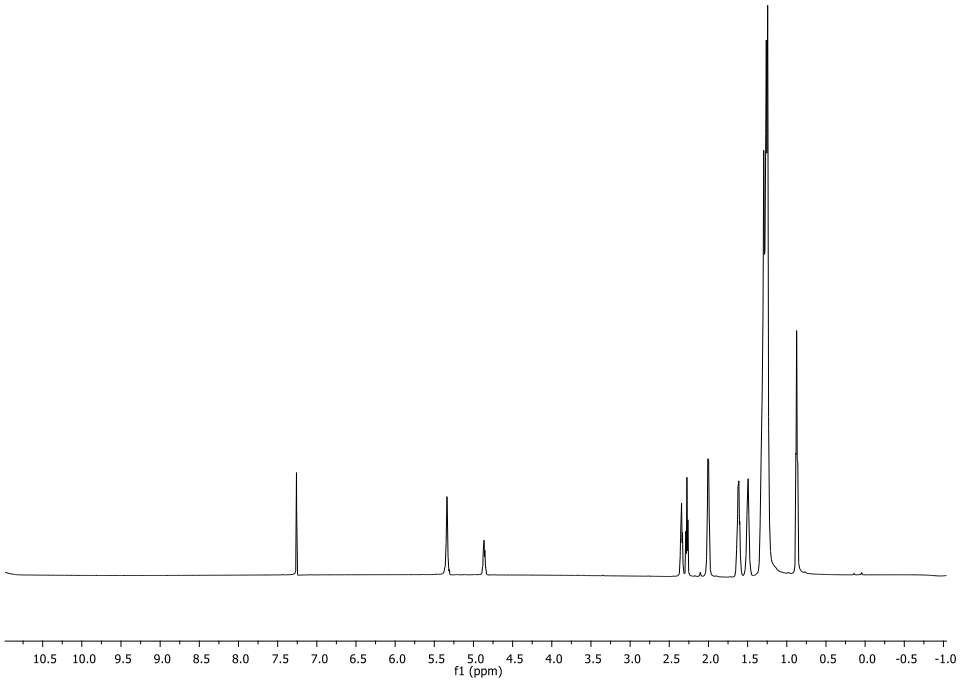

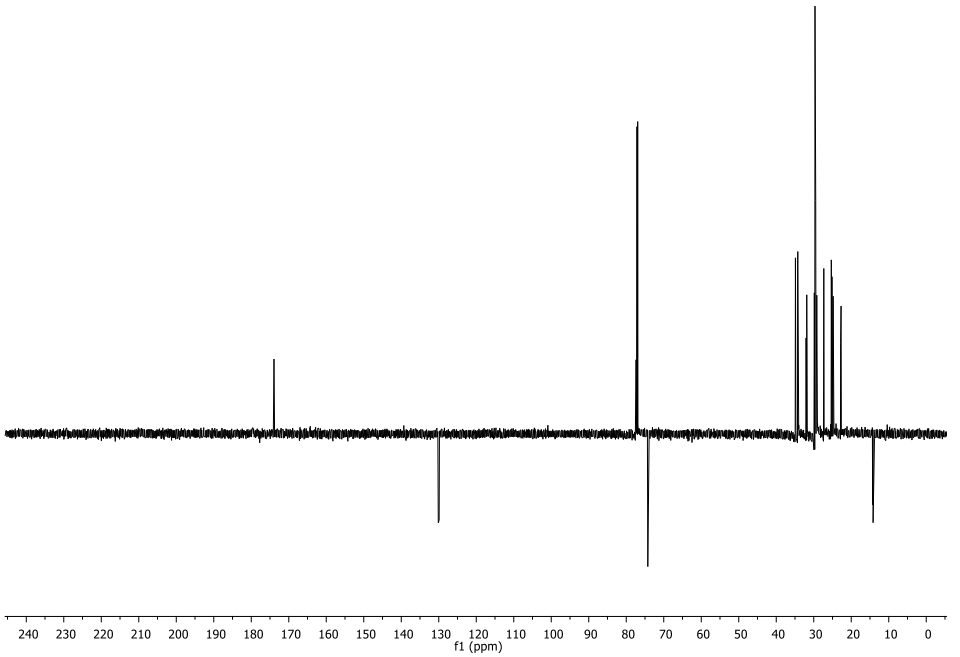

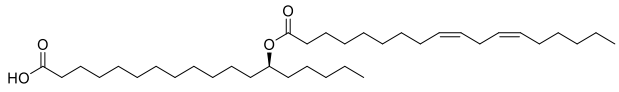

S-13-LAHSA S-129

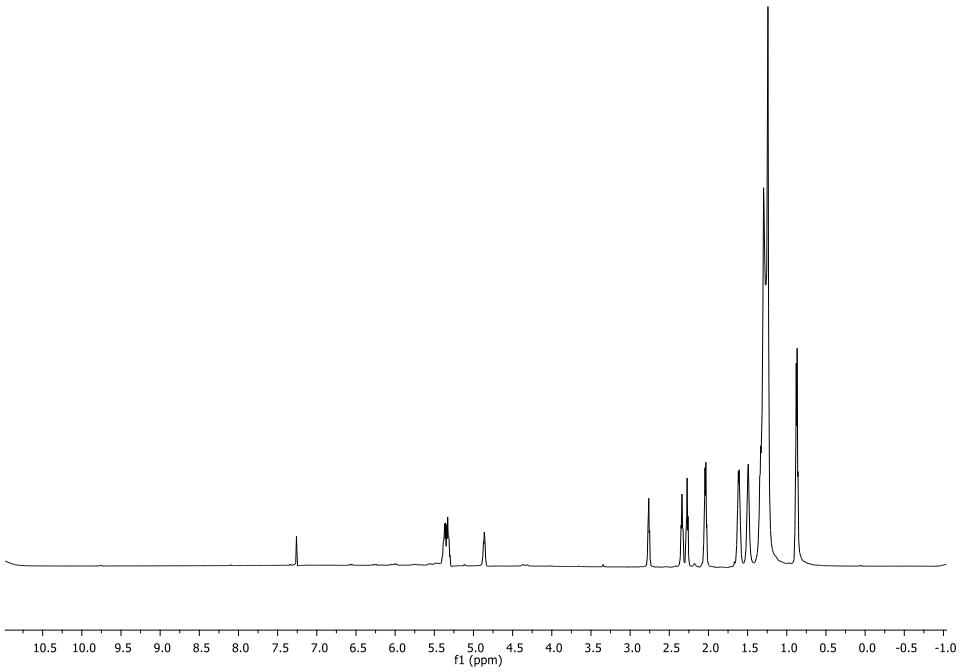

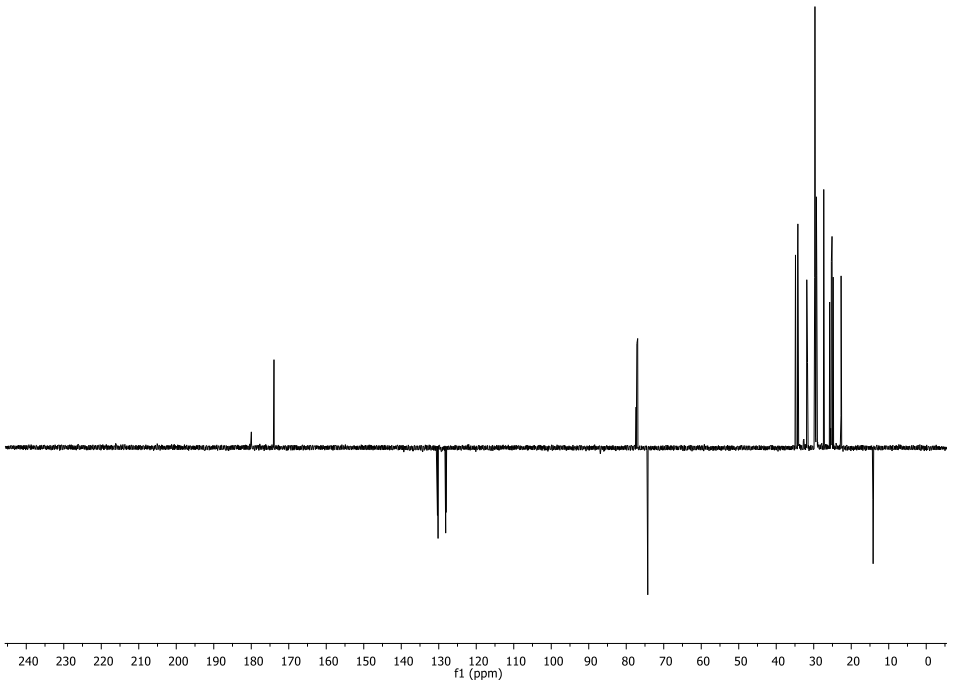

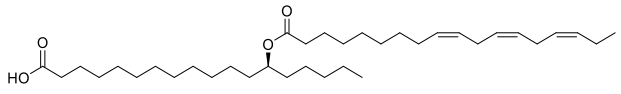

S-13-ALAHSA S-130

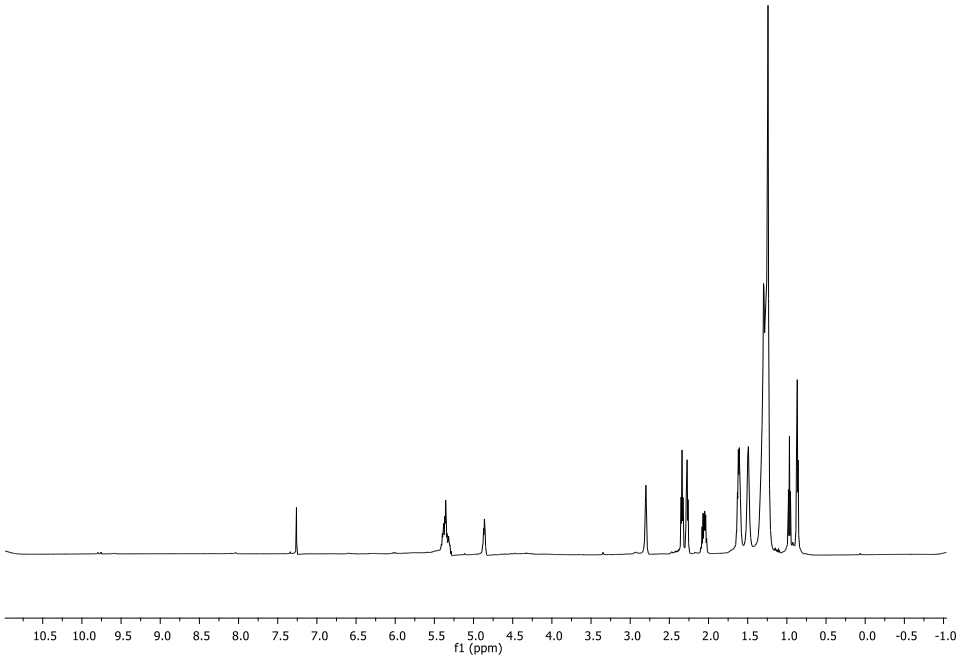

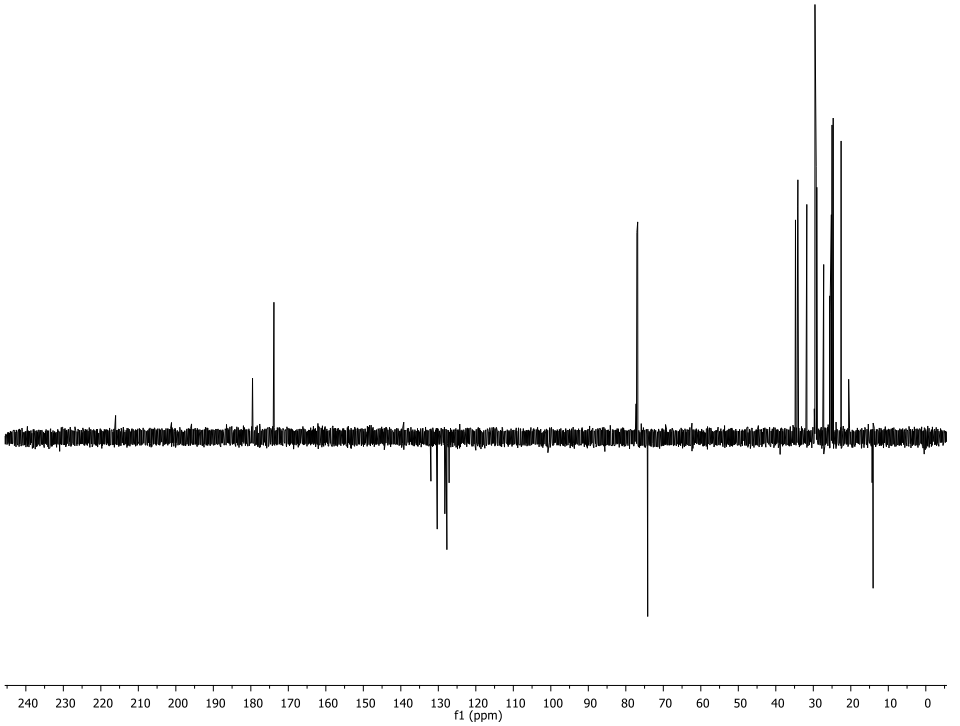

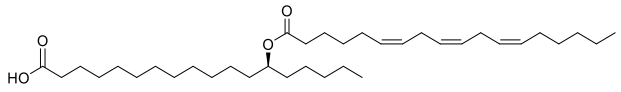

S-13-GLAHSA S-131

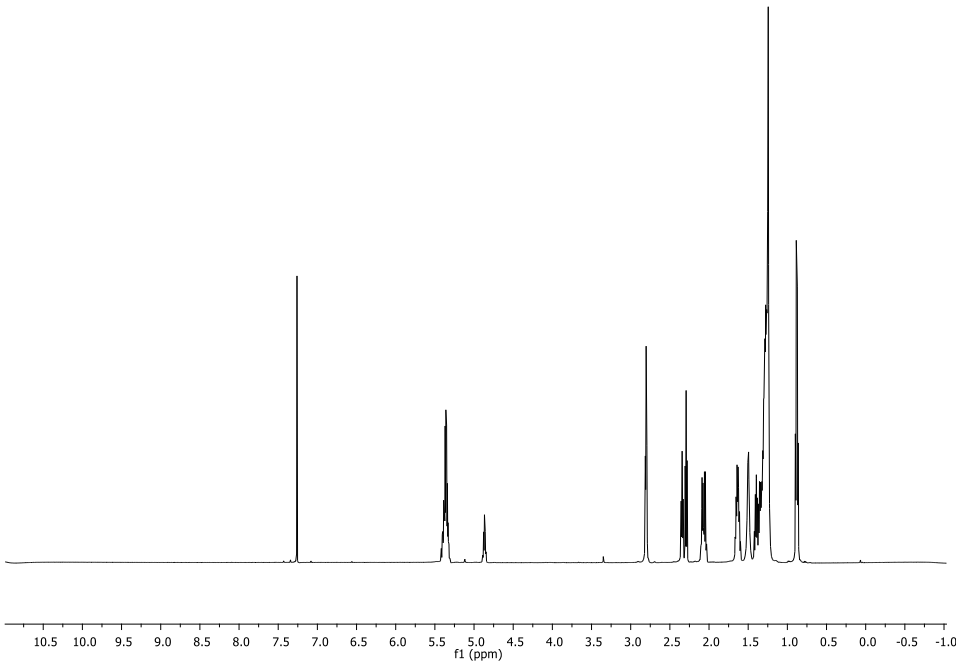

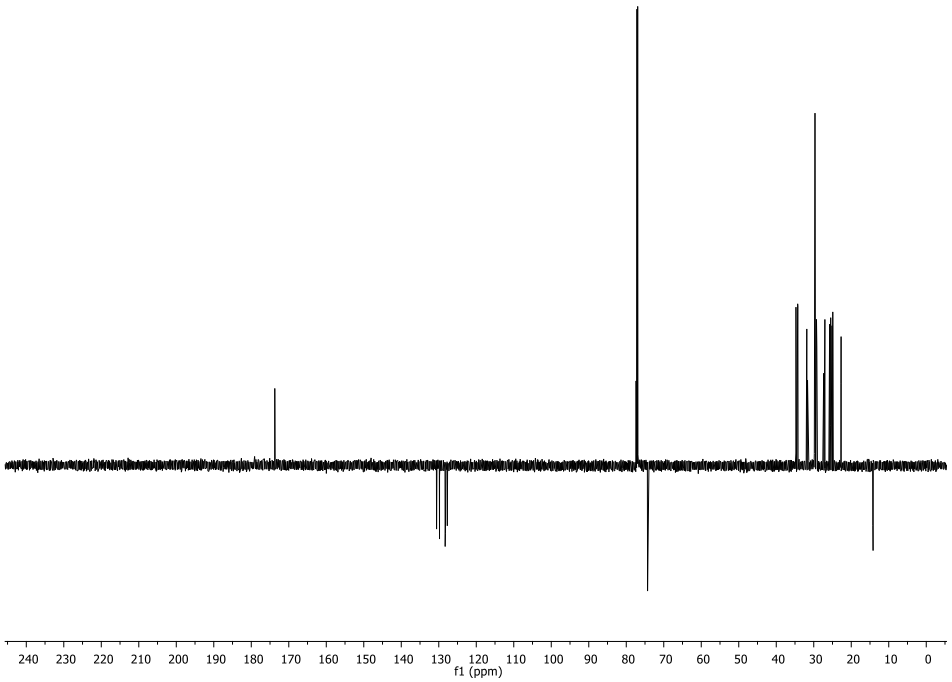

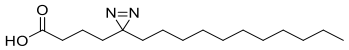
O
HO
N=N

163

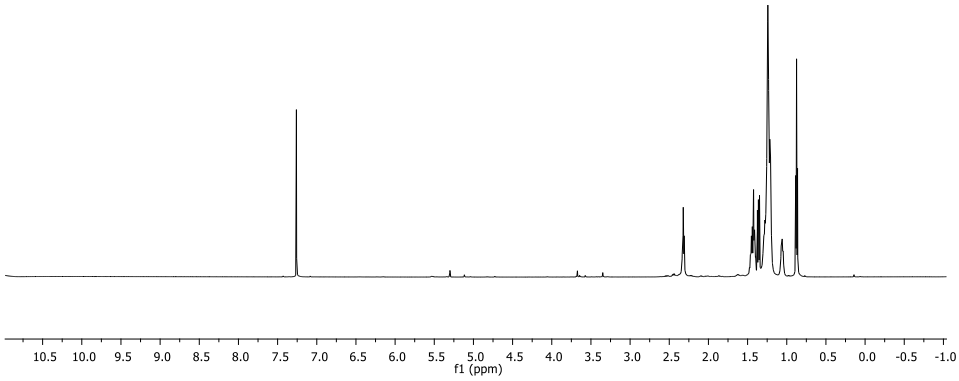
10.5 10.0 9.5 9.0 8.5 8.0 7.5 7.0 6.5 6.0 5.5 5.0 4.5 4.0 3.5 3.0 2.5 2.0 1.5 1.0 0.5 0.0 -0.5 -1.0
f1 (ppm)

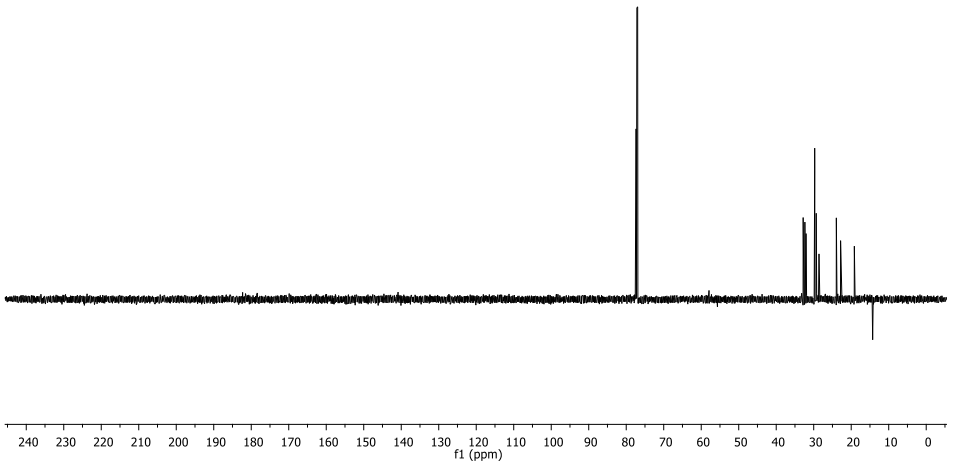
240 230 220 210 200 190 180 170 160 150 140 130 120 110 100 90 80 70 60 50 40 30 20 10 0
f1 (ppm)

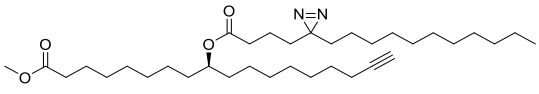

160

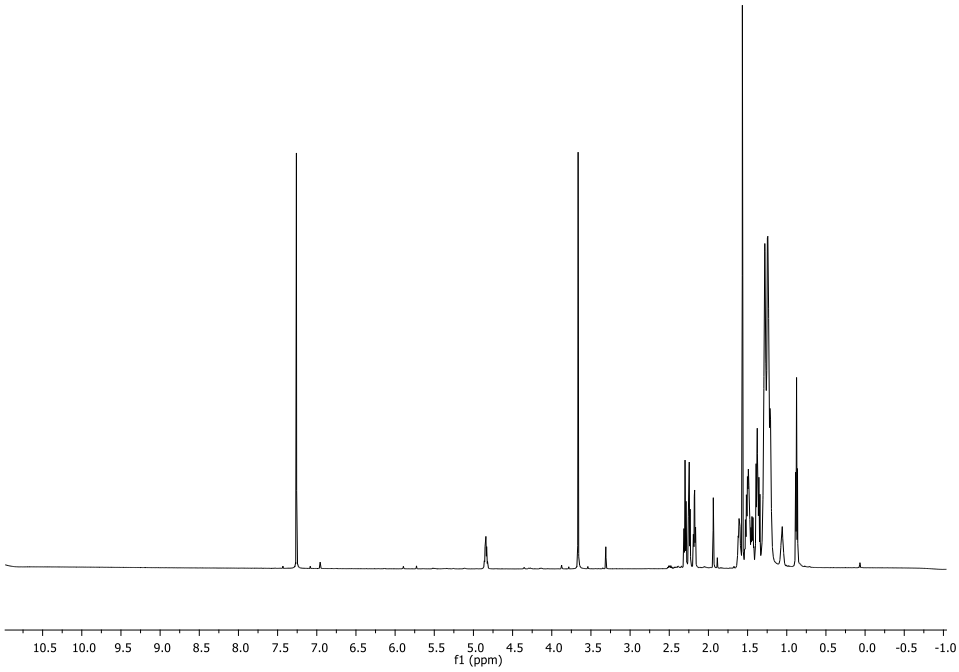
10.5 10.0 9.5 9.0 8.5 8.0 7.5 7.0 6.5 6.0 5.5 5.0 4.5 4.0 3.5 3.0 2.5 2.0 1.5 1.0 0.5 0.0 -0.5 -1.0
f1 (ppm)

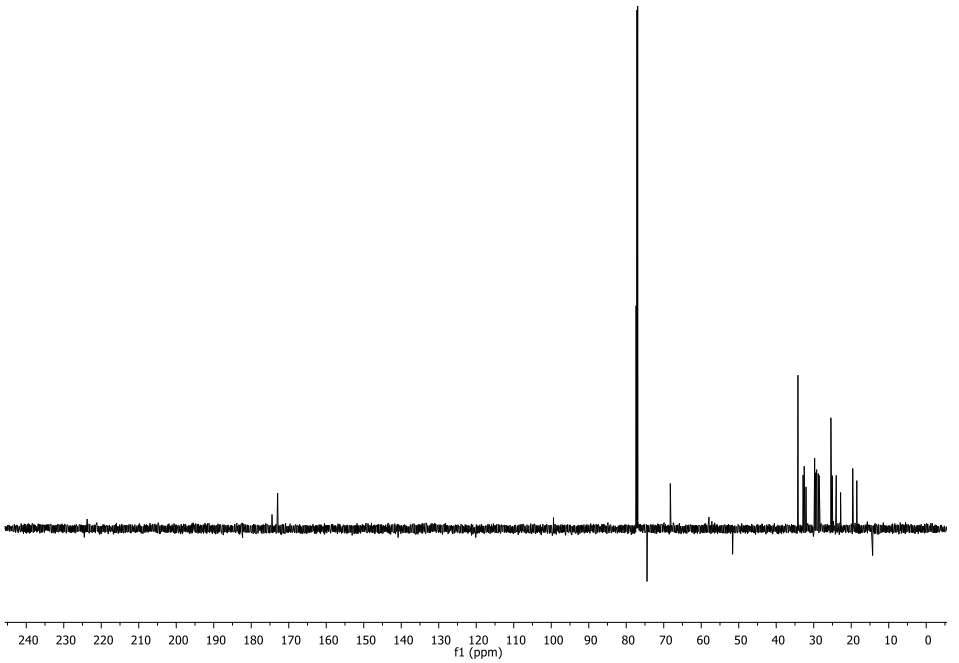
240 230 220 210 200 190 180 170 160 150 140 130 120 110 100 90 80 70 60 50 40 30 20 10 0
f1 (ppm)

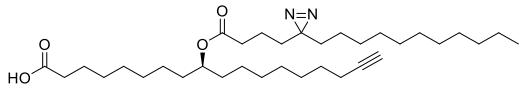
O
N=N
O
O
HO

153

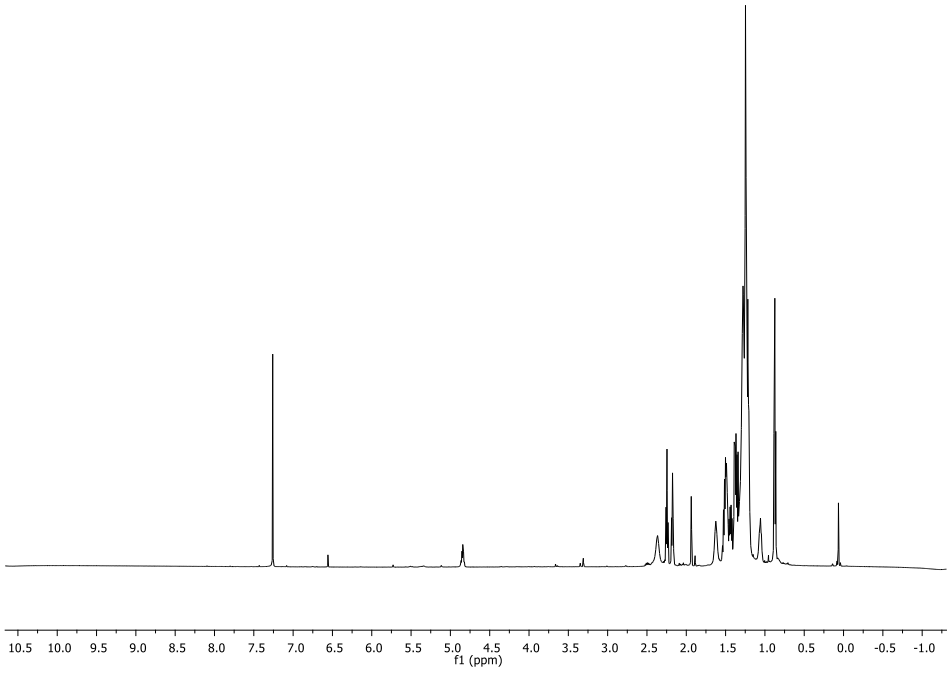
10.5 10.0 9.5 9.0 8.5 8.0 7.5 7.0 6.5 6.0 5.5 5.0 4.5 4.0 3.5 3.0 2.5 2.0 1.5 1.0 0.5 0.0 -0.5 -1.0
f1 (ppm)

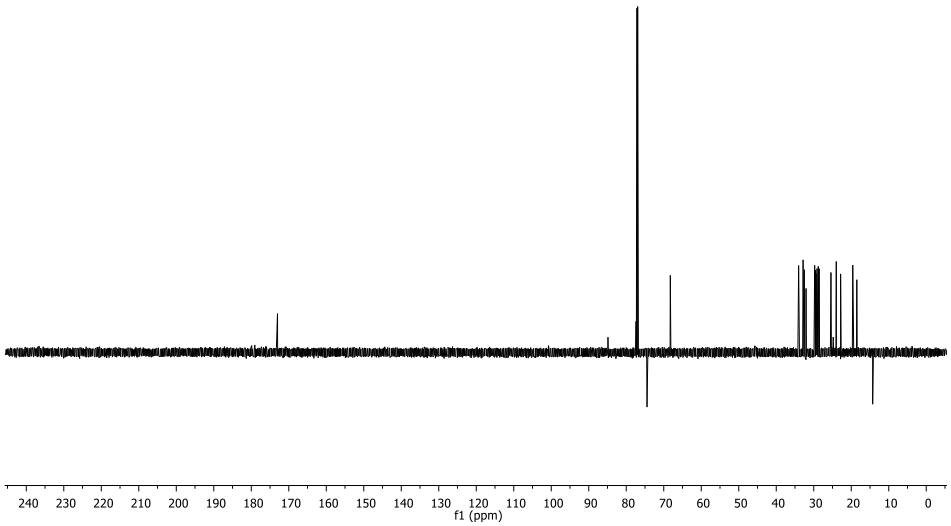
240 230 220 210 200 190 180 170 160 150 140 130 120 110 100 90 80 70 60 50 40 30 20 10 0
f1 (ppm)

References

1. Prevention, C. f. D. C. a., National diabetes statistics report, 2014: estimates of diabetes and its burden in the United States. *Atlanta, GA: US Department of Health and Human Services* **2014**.
2. Association, A. D., Economic Costs of Diabetes in the US in 2017. *Diabetes Care* **2018,** *41* (5), 917-928.
3. Wang, Z.; Liu, M., Life years lost associated with diabetes: an individually matched cohort study using the US National Health Interview Survey data. *Diabetes research and clinical practice* **2016,** *118*, 69-76.
4. Gregg, E. W.; Li, Y.; Wang, J.; Rios Burrows, N.; Ali, M. K.; Rolka, D.; Williams, D. E.; Geiss, L., Changes in diabetes-related complications in the United States, 1990–2010. *New England Journal of Medicine* **2014,** *370* (16), 1514-1523.
5. Cukierman, T.; Gerstein, H.; Williamson, J., Cognitive decline and dementia in diabetes—systematic overview of prospective observational studies. *Diabetologia* **2005,** *48* (12), 2460-2469.
6. Kasper, D.; Fauci, A.; Hauser, S.; Longo, D.; Jameson, J.; Loscalzo, J., Harrison's principles of internal medicine, 19e. **2015**.
7. Mergenthaler, P.; Lindauer, U.; Dienel, G. A.; Meisel, A., Sugar for the brain: the role of glucose in physiological and pathological brain function. *Trends in neurosciences* **2013,** *36* (10), 587-597.
8. Barrett, K. E.; Malley, J.; Naglieri, C., *Gastrointestinal physiology*. Lange Medical Books/McGraw-Hill: 2006.
9. Kumar, V.; Abbas, A. K.; Fausto, N.; Aster, J. C., *Robbins and Cotran pathologic basis of disease, professional edition e-book*. elsevier health sciences: 2014.
10. Baggio, L. L.; Drucker, D. J., Biology of incretins: GLP-1 and GIP. *Gastroenterology* **2007,** *132* (6), 2131-2157.
11. Drucker, D. J., The biology of incretin hormones. *Cell metabolism* **2006,** *3* (3), 153-165.
12. Pederson, R. A.; McIntosh, C. H., Discovery of gastric inhibitory polypeptide and its subsequent fate: Personal reflections. *Journal of diabetes investigation* **2016,** *7* (S1), 4-7.
13. Shepherd, P. R.; Kahn, B. B., Glucose transporters and insulin action—implications for insulin resistance and diabetes mellitus. *New England Journal of Medicine* **1999,** *341* (4), 248-257.
14. Huang, S.; Czech, M. P., The GLUT4 glucose transporter. *Cell metabolism* **2007,** *5* (4), 237-252.

15. Sinha, M. K.; Raineri-Maldonado, C.; Buchanan, C.; Pories, W. J.; Carter-Su, C.; Pilch, P. F.; Caro, J. F., Adipose tissue glucose transporters in NIDDM: decreased levels of muscle/fat isoform. *Diabetes* **1991,** *40* (4), 472-477.

16. Garvey, W.; Maianu, L.; Huecksteadt, T.; Birnbaum, M.; Molina, J.; Ciaraldi, T., Pretranslational suppression of a glucose transporter protein causes insulin resistance in adipocytes from patients with non-insulin-dependent diabetes mellitus and obesity. *The Journal of clinical investigation* **1991,** *87* (3), 1072-1081.

17. Abel, E. D.; Peroni, O.; Kim, J. K.; Kim, Y.-B.; Boss, O.; Hadro, E.; Minnemann, T.; Shulman, G. I.; Kahn, B. B., Adipose-selective targeting of the GLUT4 gene impairs insulin action in muscle and liver. *Nature* **2001,** *409* (6821), 729.

18. Boden, G., Obesity and free fatty acids. *Endocrinology and Metabolism Clinics* **2008,** *37* (3), 635-646.

19. Wellen, K. E.; Hotamisligil, G. S., Inflammation, stress, and diabetes. *The Journal of clinical investigation* **2005,** *115* (5), 1111-1119.

20. Furukawa, S.; Fujita, T.; Shimabukuro, M.; Iwaki, M.; Yamada, Y.; Nakajima, Y.; Nakayama, O.; Makishima, M.; Matsuda, M.; Shimomura, I., Increased oxidative stress in obesity and its impact on metabolic syndrome. *The Journal of clinical investigation* **2017,** *114* (12), 1752-1761.

21. Boden, G., Role of fatty acids in the pathogenesis of insulin resistance and NIDDM. *Diabetes* **1997,** *46* (1), 3-10.

22. Lupi, R.; Dotta, F.; Marselli, L.; Del Guerra, S.; Masini, M.; Santangelo, C.; Patané, G.; Boggi, U.; Piro, S.; Anello, M., Prolonged exposure to free fatty acids has cytostatic and pro-apoptotic effects on human pancreatic islets: evidence that β-cell death is caspase mediated, partially dependent on ceramide pathway, and Bcl-2 regulated. *Diabetes* **2002,** *51* (5), 1437-1442.

23. Shoelson, S. E.; Lee, J.; Goldfine, A. B., Inflammation and insulin resistance. *The Journal of clinical investigation* **2006,** *116* (7), 1793-1801.

24. Boden, G., Obesity and free fatty acids. *Endocrionolgy and Metabolism Clinics* **2008,** *37* (3), 635-646.

25. Robertson, R. P., Chronic oxidative stress as a central mechanism for glucose toxicity in pancreatic islet beta cells in diabetes. *Journal of Biological Chemistry* **2004,** *279* (41), 42351-42354.

26. Houstis, N.; Rosen, E. D.; Lander, E. S., Reactive oxygen species have a causal role in multiple forms of insulin resistance. *Nature* **2006,** *440* (7086), 944.

27. Bhat, S.; Mary, S.; Giri, A. P.; Kulkarni, M. J., Advanced Glycation End Products (AGEs) in Diabetic Complications. In *Mechanisms of vascular defects in diabetes mellitus*, Springer: 2017; pp 423-449.

28. Koya, D.; King, G. L., Protein kinase C activation and the development of diabetic complications. *Diabetes* **1998,** *47* (6), 859-866.

29. Drugs for Type 2 Diabetes. *Treat. Guidel. Med. Lett.* **2014,** *12*, 17-24.

30. Singh, S.; Chang, H.-Y.; Richards, T. M.; Weiner, J. P.; Clark, J. M.; Segal, J. B., Glucagonlike peptide 1–based therapies and risk of hospitalization for acute pancreatitis in type 2 diabetes mellitus: a population-based matched case-control study. *JAMA internal medicine* **2013,** *173* (7), 534-539.

31. Butler, P. C.; Elashoff, M.; Elashoff, R.; Gale, E. A., A critical analysis of the clinical use of incretin-based therapies. *Diabetes care* **2013,** *36* (7), 2118-2125.

32. Hernandez, A. V.; Usmani, A.; Rajamanickam, A.; Moheet, A., Thiazolidinediones and risk of heart failure in patients with or at high risk of type 2 diabetes mellitus. *American Journal of Cardiovascular Drugs* **2011,** *11* (2), 115-128.

33. Nissen, S. E.; Wolski, K., Effect of rosiglitazone on the risk of myocardial infarction and death from cardiovascular causes. *N Engl j Med* **2007,** *2007* (356), 2457-2471.

34. Yore, M. M.; Syed, I.; Moraes-Vieira, P. M.; Zhang, T.; Herman, M. A.; Homan, E. A.; Patel, R. T.; Lee, J.; Chen, S.; Peroni, O. D., Discovery of a class of endogenous mammalian lipids with anti-diabetic and anti-inflammatory effects. *Cell* **2014,** *159* (2), 318-332.

35. Shepherd, P. R.; Gnudi, L.; Tozzo, E.; Yang, H.; Leach, F.; Kahn, B. B., Adipose cell hyperplasia and enhanced glucose disposal in transgenic mice overexpressing GLUT4 selectively in adipose tissue. *Journal of Biological Chemistry* **1993,** *268* (30), 22243-22246.

36. Tozzo, E.; Shepherd, P. R.; Gnudi, L.; Kahn, B. B., Transgenic GLUT-4 overexpression in fat enhances glucose metabolism: preferential effect on fatty acid synthesis. *American Journal of Physiology-Endocrinology And Metabolism* **1995,** *268* (5), E956-E964.

37. Lee, J.; Moraes-Vieira, P. M.; Castoldi, A.; Aryal, P.; Yee, E. U.; Vickers, C.; Parnas, O.; Donaldson, C. J.; Saghatelian, A.; Kahn, B. B., Branched fatty acid esters of hydroxy fatty acids (FAHFAs) protect against colitis by regulating gut innate and adaptive immune responses. *Journal of Biological Chemistry* **2016,** *291* (42), 22207-22217.

38. Kuda, O.; Brezinova, M.; Rombaldova, M.; Slavikova, B.; Posta, M.; Beier, P.; Janovska, P.; Veleba, J.; Kopecky, J.; Kudova, E., Docosahexaenoic acid–derived fatty acid esters of hydroxy fatty acids (FAHFAs) with anti-inflammatory properties. *Diabetes* **2016,** *65* (9), 2580-2590.

39. Parsons, W. H.; Kolar, M. J.; Kamat, S. S.; Cognetta III, A. B.; Hulce, J. J.; Saez, E.; Kahn, B. B.; Saghatelian, A.; Cravatt, B. F., AIG1 and ADTRP are atypical

integral membrane hydrolases that degrade bioactive FAHFAs. *Nature chemical biology* **2016,** *12* (5), 367-372.

40. Kolar, M. J.; Kamat, S. S.; Parsons, W. H.; Homan, E. A.; Maher, T.; Peroni, O. D.; Syed, I.; Fjeld, K.; Molven, A.; Kahn, B. B., Branched fatty acid esters of hydroxy fatty acids are preferred substrates of the MODY8 protein carboxyl ester lipase. *Biochemistry* **2016,** *55* (33), 4636-4641.

41. McLean, S.; Davies, N. W.; Nichols, D. S.; Mcleod, B. J., Triacylglycerol estolides, a new class of mammalian lipids, in the paracloacal gland of the brushtail possum (Trichosurus vulpecula). *Lipids* **2015,** *50* (6), 591-604.

42. Kajikawa, M.; Abe, T.; Ifuku, K.; Furutani, K.-i.; Yan, D.; Okuda, T.; Ando, A.; Kishino, S.; Ogawa, J.; Fukuzawa, H., Production of ricinoleic acid-containing monoestolide triacylglycerides in an oleaginous diatom, Chaetoceros gracilis. *Scientific reports* **2016,** *6*, 36809.

43. Brezinova, M.; Kuda, O.; Hansikova, J.; Rombaldova, M.; Balas, L.; Bardova, K.; Durand, T.; Rossmeisl, M.; Cerna, M.; Stranak, Z., Levels of palmitic acid ester of hydroxystearic acid (PAHSA) are reduced in the breast milk of obese mothers. *Biochimica et Biophysica Acta (BBA)-Molecular and Cell Biology of Lipids* **2018,** *1863* (2), 126-131.

44. Nelson, A. T.; Kolar, M. J.; Chu, Q.; Syed, I.; Kahn, B. B.; Saghatelian, A.; Siegel, D., Stereochemistry of Endogenous Palmitic Acid Ester of 9-Hydroxystearic Acid and Relevance of Absolute Configuration to Regulation. *Journal of the American Chemical Society* **2017,** *139* (13), 4943-4947.

45. Ma, Y.; Kind, T.; Vaniya, A.; Gennity, I.; Fahrmann, J. F.; Fiehn, O., An in silico MS/MS library for automatic annotation of novel FAHFA lipids. *Journal of cheminformatics* **2015,** *7* (1), 53.

46. López-Bascón, M. A.; Calderón-Santiago, M.; Priego-Capote, F., Confirmatory and quantitative analysis of fatty acid esters of hydroxy fatty acids in serum by solid phase extraction coupled to liquid chromatography tandem mass spectrometry. *Analytica chimica acta* **2016,** *943*, 82-88.

47. Zhang, T.; Chen, S.; Syed, I.; Ståhlman, M.; Kolar, M. J.; Homan, E. A.; Chu, Q.; Smith, U.; Borén, J.; Kahn, B. B., A LC-MS-based workflow for measurement of branched fatty acid esters of hydroxy fatty acids. *Nature protocols* **2016,** *11* (4), 747-763.

48. Zhu, Q.-F.; Yan, J.-W.; Gao, Y.; Zhang, J.-W.; Yuan, B.-F.; Feng, Y.-Q., Highly sensitive determination of fatty acid esters of hydroxyl fatty acids by liquid chromatography-mass spectrometry. *Journal of Chromatography B* **2017,** *1061*, 34-40.

49. Kahn, B. B.; Herman, M. A.; Saghatelian, A.; Homan, E., Lipids That Increase Insulin Sensitivity And Methods Of Using The Same. Google Patents: 2015.

50. Balas, L.; Bertrand-Michel, J.; Viars, F.; Faugere, J.; Lefort, C.; Caspar-Bauguil, S.; Langin, D.; Durand, T., Regiocontrolled syntheses of FAHFAs and LC-MS/MS differentiation of regioisomers. *Organic & biomolecular chemistry* **2016,** *14* (38), 9012-9020.

51. De Mico, A.; Margarita, R.; Parlanti, L.; Vescovi, A.; Piancatelli, G., A versatile and highly selective hypervalent iodine (III)/2, 2, 6, 6-tetramethyl-1-piperidinyloxyl-mediated oxidation of alcohols to carbonyl compounds. *The Journal of Organic Chemistry* **1997,** *62* (20), 6974-6977.

52. Einhorn, J.; Einhorn, C.; Ratajczak, F.; Pierre, J.-L., Efficient and highly selective oxidation of primary alcohols to aldehydes by N-chlorosuccinimide mediated by oxoammonium salts. *The Journal of organic chemistry* **1996,** *61* (21), 7452-7454.

53. De Luca, L.; Giacomelli, G.; Masala, S.; Porcheddu, A., Trichloroisocyanuric/TEMPO oxidation of alcohols under mild conditions: A close investigation. *The Journal of organic chemistry* **2003,** *68* (12), 4999-5001.

54. Chen, L.; Lee, S.; Renner, M.; Tian, Q.; Nayyar, N., A Simple Modification to Prevent Side Reactions in Swern-Type Oxidations Using Py⊙ SO3. *Organic process research & development* **2006,** *10* (1), 163-164.

55. Mancuso, A. J.; Huang, S.-L.; Swern, D., Oxidation of long-chain and related alcohols to carbonyls by dimethyl sulfoxide" activated" by oxalyl chloride. *The Journal of Organic Chemistry* **1978,** *43* (12), 2480-2482.

56. Schwartz, C.; Raible, J.; Mott, K.; Dussault, P. H., Fragmentation of carbonyl oxides by N-oxides: An improved approach to alkene ozonolysis. *Organic letters* **2006,** *8* (15), 3199-3201.

57. Criegee, R., Mechanism of ozonolysis. *Angewandte Chemie International Edition in English* **1975,** *14* (11), 745-752.

58. Quermann, R.; Maletz, R.; Schäfer, H. J., Conversion of Fatty Acids and Derivatives, IV. Conversion of Fatty Acid Methyl Esters into Dialkylated Succinic Esters by Oxidative Coupling of their Enolates. *Liebigs Annalen der Chemie* **1993,** *1993* (11), 1219-1223.

59. Nguyen, H.; Oh, S.; Henry-Riyad, H.; Sepulveda, D.; Romo, D., Organocatalytic Enantioselective Synthesis of Bicyclic β-Lactones Via Nucleophile-Catalyzed Aldol-Lactonization (NCAL). *Organic Syntheses*, 121-137.

60. Van Dyke, A. R.; Miller, K. M.; Jamison, T. F., (S)-(+)-Neomenthyldiphenylphosphine in Nickel-Catalyzed Asymmetric Reductive Coupling of Alkynes and Aldehydes: Enantioselective Synthesis of Allylic Alcohols and α-Hydroxy Ketones: [(R)-Butan-2-one, 1-cyclohexyl, 1-hydroxy-]. *Organic Syntheses* **2003,** *84*, 111-119.

61. Willand-Charnley, R.; Fisher, T. J.; Johnson, B. M.; Dussault, P. H., Pyridine is an organocatalyst for the reductive ozonolysis of alkenes. *Organic letters* **2012,** *14* (9), 2242-2245.

62. Schiaffo, C. E.; Dussault, P. H., Ozonolysis in solvent/water mixtures: direct conversion of alkenes to aldehydes and ketones. *The Journal of organic chemistry* **2008,** *73* (12), 4688-4690.

63. Cochran, B. M., One-pot oxidative cleavage of olefins to synthesize carboxylic acids by a telescoped ozonolysis–oxidation process. *Synlett* **2016,** *27* (02), 245-248.

64. Vijayakumar, A.; Aryal, P.; Wen, J.; Syed, I.; Vazirani, R. P.; Moraes-Vieira, P. M.; Camporez, J. P.; Gallop, M. R.; Perry, R. J.; Peroni, O. D., Absence of carbohydrate response element binding protein in adipocytes causes systemic insulin resistance and impairs glucose transport. *Cell reports* **2017,** *21* (4), 1021-1035.

65. Syed, I.; Lee, J.; Moraes-Vieira, P. M.; Donaldson, C. J.; Sontheimer, A.; Aryal, P.; Wellenstein, K.; Kolar, M. J.; Nelson, A. T.; Siegel, D., Palmitic Acid Hydroxystearic Acids Activate GPR40, Which Is Involved in Their Beneficial Effects on Glucose Homeostasis. *Cell metabolism* **2018,** *27* (2), 419-427. e4.

66. Baldwin, J. E., Rules for ring closure. *Journal of the Chemical Society, Chemical Communications* **1976,** (18), 734-736.

67. Hansen, T. M.; Florence, G. J.; Lugo-Mas, P.; Chen, J.; Abrams, J. N.; Forsyth, C. J., Highly chemoselective oxidation of 1, 5-diols to δ-lactones with TEMPO/BAIB. *Tetrahedron letters* **2003,** *44* (1), 57-59.

68. Martin, S. F.; Dodge, J. A., Efficacious modification of the Mitsunobu reaction for inversions of sterically hindered secondary alcohols. *Tetrahedron letters* **1991,** *32* (26), 3017-3020.

69. Dodge, J. A.; Nissen, J. S.; Presnell, M., A General Procedure for M itsunobu Inversion of Sterically Hindered Alcohols: Inversion of Menthol.(1S, 2S, 5R)-5-Methyl-2-(1-Methylethyl) Cyclohexyl 4-Nitrobenzoate: Cyclohexanol, 5-methyl-2-(1-methylethyl)-, 4-nitrobenzoate,[1S-(1α, 2α, 5β)]-. *Organic Syntheses* **2003,** *73*, 110-110.

70. Baldwin, J. E.; Kruse, L. I., Rules for ring closure. Stereoelectronic control in the endocyclic alkylation of ketone enolates. *Journal of the Chemical Society, Chemical Communications* **1977,** (7), 233-235.

71. Baldwin, J. E.; Thomas, R. C.; Kruse, L. I.; Silberman, L., Rules for ring closure: ring formation by conjugate addition of oxygen nucleophiles. *The Journal of organic chemistry* **1977,** *42* (24), 3846-3852.

72. Baldwin, J. E.; Lusch, M. J., Rules for ring closure: application to intramolecular aldol condensations in polyketonic substrates. *Tetrahedron* **1982,** *38* (19), 2939-2947.

73. Alam, M.; Wise, C.; Baxter, C. A.; Cleator, E.; Walkinshaw, A., Development of a Robust Procedure for the Copper-catalyzed Ring-Opening of Epoxides with Grignard Reagents. *Organic Process Research & Development* **2012,** *16* (3), 435-441.

74. Haberkant, P.; Raijmakers, R.; Wildwater, M.; Sachsenheimer, T.; Brügger, B.; Maeda, K.; Houweling, M.; Gavin, A. C.; Schultz, C.; Van Meer, G., In vivo profiling and visualization of cellular protein–lipid interactions using bifunctional fatty acids. *Angewandte Chemie International Edition* **2013,** *52* (14), 4033-4038.

75. Hulce, J. J.; Cognetta, A. B.; Niphakis, M. J.; Tully, S. E.; Cravatt, B. F., Proteome-wide mapping of cholesterol-interacting proteins in mammalian cells. *Nature methods* **2013,** *10* (3), 259.

76. McConnell, H. M.; Hubbell, W. L., Molecular motion in spin-labeled phospholipids and membranes. *Journal of the American Chemical Society* **1971,** *93* (2), 314-326.

77. Dauben, W. G., The synthesis of palmitic acid and tripalmitin labeled with carbon fourteen. *Journal of the American Chemical Society* **1948,** *70* (4), 1376-1378.

78. Ebert, C.; Felluga, F.; Forzato, C.; Foscato, M.; Gardossi, L.; Nitti, P.; Pitacco, G.; Boga, C.; Caruana, P.; Micheletti, G., Enzymatic kinetic resolution of hydroxystearic acids: A combined experimental and molecular modelling investigation. *Journal of Molecular Catalysis B: Enzymatic* **2012,** *83*, 38-45.

79. Ruscoe, R. E.; Fazakerley, N. J.; Huang, H.; Flitsch, S.; Procter, D. J., Copper-Catalyzed Double Additions and Radical Cyclization Cascades in the Re-Engineering of the Antibacterial Pleuromutilin. *Chemistry-A European Journal* **2016,** *22* (1), 116-119.

80. Schlutt, B.; Moran, N.; Schieberle, P.; Hofmann, T., Sensory-directed identification of creaminess-enhancing volatiles and semivolatiles in full-fat cream. *Journal of agricultural and food chemistry* **2007,** *55* (23), 9634-9645.

81. Jiang, C.-S.; Zhou, R.; Gong, J.-X.; Chen, L.-L.; Kurtán, T.; Shen, X.; Guo, Y.-W., Synthesis, modification, and evaluation of (R)-de-O-methyllasiodiplodin and analogs as nonsteroidal antagonists of mineralocorticoid receptor. *Bioorganic & medicinal chemistry letters* **2011,** *21* (4), 1171-1175.

82. Tassignon, P. S.; de Wit, D.; de Rijk, T. C.; De Buyck, L. F., Selective oxidation of primary-secondary diols with methyl hypochlorite in acid buffered medium. *Tetrahedron* **1995,** *51* (43), 11863-11872.

83. Behrouzian, B.; Savile, C. K.; Dawson, B.; Buist, P. H.; Shanklin, J., Exploring the Hydroxylation− Dehydrogenation Connection: Novel Catalytic Activity of Castor Stearoyl-ACP Δ9 Desaturase. *Journal of the American Chemical Society* **2002,** *124* (13), 3277-3283.

84. Peduto, A.; Scuotto, M.; Krauth, V.; Roviezzo, F.; Rossi, A.; Temml, V.; Esposito, V.; Stuppner, H.; Schuster, D.; D'Agostino, B., Optimization of benzoquinone and hydroquinone derivatives as potent inhibitors of human 5-lipoxygenase. *European journal of medicinal chemistry* **2017,** *127*, 715-726.

85. Asai, T.; Fujimoto, Y., Cyclic fatty acyl glycosides in the glandular trichome exudate of Silene gallica. *Phytochemistry* **2010,** *71* (11-12), 1410-1417.